FACULTADE DE BIOLOXÍA

Departamento de Edafoloxía e Química Agrícola

Cuantificación del color en el estudio de la formación de biofilms en rocas graníticas del Patrimonio histórico artístico

Color quantification in the study of biofilm formation on granite stone in historical and artistic heritage

Patricia Sanmartín Sánchez
2012

Este trabajo de investigación doctoral fue financiado por el Ministerio de Ciencia e Innovación (MICINN) dentro del programa de Formación de Personal Investigador (FPI-MICINN). Referencia: BES-2007-16996, en el marco del proyecto de investigación titulado: *Desarrollo de nuevas técnicas no destructivas de cuantificación y estudio de la evolución de la colonización biológica sobre construcciones graníticas.* Referencia: BIA2006-02233. Investigador Principal: Beatriz Prieto Lamas.

This doctoral research was funded by the Spanish Ministry of Science and Innovation (MICINN) as part of the Spanish Scientific program FPI (*Formación de Personal Investigador*)-MICINN. Fellowship reference code: BES-2007-16996. The study was carried out within the framework of a research project entitled *Desarrollo de nuevas técnicas no destructivas de cuantificación y estudio de la evolución de la colonización biológica sobre construcciones graníticas.* Project reference code: BIA2006-02233. Principal Investigator: Beatriz Prieto Lamas.

Departamento de Edafoloxía e Química Agrícola

Tesis Doctoral

PhD Thesis

Cuantificación del color en el estudio de la formación de biofilms en rocas graníticas del Patrimonio histórico artístico

Color quantification in the study of biofilm formation on granite stone in historical and artistic heritage

Patricia Sanmartín Sánchez

2012

Departamento de Edafoloxía e Química Agrícola

Dña. Beatriz Prieto Lamas y **Dña. Benita Silva Hermo**, Profesoras del departamento de Edafoloxía e química agrícola de la Universidade de Santiago de Compostela.

CERTIFICAN:

Que la presente memoria titulada **Cuantificación del color en el estudio de la formación de biofilms en rocas graníticas del Patrimonio histórico artístico (*Color quantification in the study of biofilm formation on granite stone in historical and artistic heritage*)** presentada por **Dña. Patricia Sanmartín Sánchez** para optar al grado de Doctora por la Universidade de Santiago de Compostela, fue realizada bajo nuestra dirección y supervisión, y consideramos que reúne todos los requisitos y condiciones necesarias para ser presentada como trabajo de Tesis doctoral.

Para que así conste, expedimos la presente certificación en Santiago de Compostela el día veintiséis de abril de dos mil doce.

Fdo. Dra. Beatriz Prieto Lamas

Fdo. Dra. Benita Silva Hermo

Contenidos

Contents

Resumen

En la conservación del parque de edificios e infraestructuras, en particular las que constituyen el Patrimonio histórico artístico, es primordial paliar los efectos derivados de la colonización biológica, pues ésta supone no sólo un problema estético sino que puede originar alteraciones físicas, químicas y mineralógicas de los materiales que repercuten en una pérdida del valor de la obra. Puesto que la colonización biológica y la formación de biofilms es inevitable, ya que es consecuencia de la interacción de la propia edificación con el medio ambiente, una detección precoz de esta colonización, y en su caso, el conocimiento de la fase de desarrollo en la que se encuentra, supondría una gran ventaja en la gestión del mantenimiento y rehabilitación de las construcciones, puesto que permitiría atajar el problema desde sus fases iniciales, incluso antes de que dicha colonización pueda ser apreciada visualmente. Además, en el caso de edificaciones con abundante colonización, supondría una herramienta muy útil en el control de la eficacia de los tratamientos empleados para su eliminación y en la detección de la recolonización.

Por lo tanto, esta tesis doctoral tiene por objeto el desarrollo e implementación de una nueva metodología de detección precoz de la formación de biofilms sobre rocas graníticas basada en la medida de su color. Este nuevo método cumple una serie de requisitos indispensables para su aplicación en los bienes del Patrimonio: es no-destructivo, lo que permite subsiguientes análisis sobre una misma muestra, de aplicación *on site*, evitando así la toma de muestra, permite obtener resultados al momento, es barato y fácilmente aplicable, de forma que cualquier operario no especializado con un mínimo de adiestramiento puede realizar las medidas.

La hipótesis de partida que llevó al planteamiento de esta tesis es la idea de que la colonización biológica que soportan las edificaciones puede ser cuantificada determinando el color que generan los organismos que se instalan sobre sus superficies. Esta hipótesis está avalada por trabajos previos en los que por un lado se puso de manifiesto la existencia de una relación directa entre la cantidad y el estado fisiológico de organismos fototróficos presentes y el cambio de color que generan al depositarse sobre una superficie (Prieto *et al.*, 2002; España Patente No. P200002956, 2000), y por otro, al comparar diferentes métodos de cuantificación de biomasa fototrófica sobre rocas, se corroboró que existe una buena correlación entre los

resultados obtenidos con los métodos considerados como los más adecuados (basados en la cuantificación de la clorofila-a) y aquéllos obtenidos a partir de la cuantificación del color (Prieto *et al.*, 2004).

El campo de investigación del proyecto de tesis se acotó a los organismos pioneros en la colonización de sustratos rocosos, en concreto a las cianobacterias por tratarse de los principales constituyentes de los denominados "verdines" o biofilms fototróficos, así como a las rocas graníticas, por constituir un caso complejo en lo que a la determinación de su color se refiere al poseer un color espacialmente heterogéneo formado por las diferentes tonalidades de sus minerales. Para alcanzar el objetivo principal se abrieron tres líneas de actuación diferentes:

1ª. Desarrollo de la metodología de medida y caracterización del color de las rocas graníticas (Prieto *et al.*, 2010a; Sanmartín *et al.*, 2011a).

2ª. Desarrollo de la metodología de medida y caracterización del color de las cianobacterias (Prieto *et al.*, 2010b; Sanmartín *et al.*, 2010a, 2011b).

3ª. Interacción superficies graníticas-cianobacterias: detección y cuantificación de los organismos sobre las construcciones (Fernández-Silva *et al.*, 2011; Sanmartín *et al.*, 2012).

Estas tres líneas acabaron convergiendo en una 4ª línea que investiga la aplicación práctica de la medida del color a otros sustratos inorgánicos naturales de interés en el ámbito de los estudios medioambientales aplicados al Patrimonio natural y cultural, como son el estudio del color en rocas pizarrosas y su importancia como criterio de sustitución en trabajos de restauración (Sanmartín *et al.*, 2010b; Prieto *et al.*, 2011), la caracterización del color en suelos quemados como indicador de la intensidad de un incendio (Sanmartín *et al.*, 2010c) y la medida del color en sedimentos de río para estimar su contenido en fitopigmentos (Sanmartín *et al.*, 2011c).

1ª. Desarrollo de la metodología de medida y caracterización del color de las rocas graníticas

A la primera línea de trabajo de tesis pertenece el **Capítulo 1** que recoge el desarrollo de un protocolo de medida para el estudio del color de las rocas graníticas ornamentales (Prieto *et al.*, 2010a). En este trabajo se determinó por primera vez el área mínima de medida y el número de medidas mínimo necesario para caracterizar objetivamente el color de este tipo de rocas. Para ello se emplearon dos instrumentos de medida del color por reflexión, un espectrofotómetro y un colorímetro, y las medidas de color se analizaron considerando el espacio de color CIELAB teniendo en cuenta el grupo de coordenadas escalares (L*a*b*). Tres

fueron los factores de variación considerados en el estudio: el tipo de roca (color y textura), el acabado superficial (pulido, apomazado, aserrado y flameado) y el cabezal de medida (aberturas circulares de 5, 8, 10 y 50 mm de diámetro). Los resultados obtenidos indican que aunque todos los factores considerados afectan al área de medida mínima y al número de medidas mínimo necesarios, si se trabaja con el número de medidas y área para cada uno de los cabezales de medida recomendados a partir de este estudio, las variaciones de color obtenidas con los distintos cabezales podrán ser obviadas.

Uno de los aspectos más relevantes de esta investigación es que aporta una metodología de estudio para la determinación de las condiciones de medida de color en superficies heterogéneas con diferentes texturas, que puede ser empleada en distintos materiales. Así, fue utilizada con éxito en rocas pizarrosas (Prieto *et al.*, 2011) y en la 2ª línea de investigación de este proyecto de tesis que trata la metodología de medida y caracterización del color de las cianobacterias.

Teniendo en cuenta que todas las rocas ornamentales puestas en obra presentan un acabado superficial, en el **Capítulo 2** se estudió la influencia del tipo de acabado comercial en el color, brillo y rugosidad de las rocas graníticas ornamentales y la relación existente entre estos tres parámetros estéticos (Sanmartín *et al.*, 2011a). Los resultados demostraron que los diferentes acabados sobre una misma roca (pulido, apomazado, aserrado y flameado) dan lugar a cambios casi siempre perceptibles en su color, en especial en su claridad (L*), y que la magnitud de tales cambios depende del color de la roca, siendo mayor en las más oscuras. Sin embargo, la variación de los parámetros de color ($L^*a^*b^*C^*_{ab}h_{ab}$) con los diferentes acabados superficiales no depende de la rugosidad y no se pudo extraer ninguna conclusión en relación a la influencia de la rugosidad en el color de los granitos ornamentales. Se puso de manifiesto que el brillo está afectado por el color de las rocas, pero de forma diferente para acabados pulidos y rugosos, y que, la variación en el brillo también depende de la composición mineral de la roca. Además, brillo y rugosidad están inversamente relacionados, pero sólo dentro del rango de los valores bajos de rugosidad.

En este Capítulo 2 también se analizó la influencia de la inclusión o exclusión del componente especular en el modo de medida. Se comprobó que trabajar con el componente especular excluido (modo SCE) magnifica las diferencias en el color producidas por los distintos acabados superficiales, por lo que cuando se trata de analizar diferencias es preferible este modo en lugar del modo con componente especular incluido (modo SCI).

Los resultados obtenidos en este estudio permitieron además definir la zona tridimensional dentro del espacio de color CIELAB que incluye el color de los granitos ornamentales estudiados, que será de gran utilidad cuando se emplea el criterio estético para la selección

de una roca ornamental y también en la calibración y puesta a punto de cámaras digitales para su uso como colorímetros en el Patrimonio.

2ª. Desarrollo de la metodología de medida y caracterización del color de las cianobacterias

Siguiendo la metodología de estudio desarrollada para la caracterización del color de superficies heterogéneas (Capítulo 1), en la segunda línea de trabajo de tesis se estableció un método de medida del color de biopelículas (biofilms) sobre superficies sólidas (**Capítulo 3**).

Para ello se empleó un cultivo mixto de tres cianobacterias formadoras de biofilms sobre rocas graníticas, *Nostoc* sp. PCC 9104, *Nostoc* sp. PCC 9025 y *Scytonema* sp. CCC 9801, del que se depositaron diferentes volúmenes sobre filtros de celulosa blancos, simulando así la composición y características de un biofilm. El color del área cubierta por los microorganismos fue entonces medido, al igual que en el Capítulo 1, con dos instrumentos de medida del color por reflexión, un espectrofotómetro y un colorímetro, y las medidas se analizaron considerando el espacio de color CIELAB y el grupo de coordenadas escalares (L*a*b*) con el objeto de analizar el efecto del grado de cobertura de los organismos y de su contenido en humedad en la medida de su color.

Los resultados obtenidos pusieron de manifiesto que el número mínimo de medidas necesario para caracterizar el color del biofilm aumenta con el incremento de la heterogeneidad del color de la superficie, que el contenido en humedad provoca cambios en los valores de claridad (L*) y que, como era de esperar, el tamaño del cabezal de medida influye en el número de medidas necesario, que decrece al aumentar éste. Tomando todas las consideraciones en conjunto se propone, realizar 10 medidas/9,62 cm^2 con cualquier tamaño de cabezal, en una superficie, a poder ser completamente cubierta por la película de microorganismos y con un contenido en humedad superior al 50%.

En el **Capítulo 4** se llevó a cabo un estudio de la relación del color de las cianobacterias con la composición y/o abundancia de los pigmentos fotosintéticos y de la influencia de los parámetros medioambientales (luz y nutrientes) en el color de las cianobacterias formadoras de biofilms (Sanmartín *et al.*, 2010a). Para tal fin, se seleccionaron dos cepas de cianobacterias formadoras de biofilms sobre rocas graníticas, *Nostoc* sp. PCC 9104 y *Nostoc* sp. PCC 9025. Ambas cepas fueron aclimatadas en fotobiorreactores tubulares de cultivos aireados en discontinuo (batch) durante dos semanas, con dos intensidades de luz distintas (alta, 170 y baja, 65 µmol fotón m^{-2} s^{-1}), empleando tres medios de cultivo diferentes: con nitrato (BG-11), sin nitrato (BG-11_0), y, sin nitrato y con baja concentración de nutrientes (BG-11_0/10). El contenido en pigmentos (clorofila-a, ficobiliproteínas ficocianinas y carotenoides totales) fue medido a lo largo de todo el experimento junto con el color de las cianobacterias,

que fue representado en el espacio de color CIELAB teniendo en cuenta el grupo de coordenadas escalares (L*a*b*) y el grupo de coordenadas cilíndricas o polares ($L^*C^*_{ab}h_{ab}$).

Los resultados confirmaron que los parámetros de color CIELAB están estrechamente correlacionados con el contenido en pigmentos, de manera que las variaciones de estos últimos se encuentran reflejadas en las variaciones de color siendo sin embargo no todos los parámetros de color CIELAB igualmente sensibles a los cambios en la concentración de pigmentos. Así, L* es el parámetro de color CIELAB más informativo, seguido de a*. Asimismo, h_{ab} se reveló como el parámetro que guarda más relación con la apariencia de los cultivos.

Este estudio supuso además una primera aproximación a la definición de la gama de color de las cianobacterias, lo cual constituye una información esencial para el desarrollo de cualquier metodología de monitorización del crecimiento de este tipo de microorganismos, ya que limita el campo de estudio desde el punto de vista de la colorimetría aplicada. Por primera vez, se establecieron valores objetivos de color de diferentes cepas cianobacterianas creciendo en diferentes condiciones de luz y nutrientes.

Dentro de la segunda línea de trabajo de tesis, el **Capítulo 5** recoge la caracterización del color de las cianobacterias para el análisis de su estado fisiológico después de un tratamiento biocida (Sanmartín *et al.*, 2011b). La eficacia de un biocida en la eliminación de microorganismos fototróficos puede ser probada cuantificando la degradación de su contenido en clorofila. Cuando la clorofila se degrada, se transforma en alguno de los pigmentos de degradación o feopigmentos y la relación entre éstos y la clorofila se puede establecer mediante los índices o cocientes de feofitinización: $A_{435/415}$ y $A_{665/665a}$.

En este Capítulo 5 se demuestra la validez de las medidas de color representadas en el espacio de color CIELAB para el control de la eficacia de un biocida químico, comercial y ampliamente extendido en el campo de la restauración y conservación del Patrimonio cultural pétreo, Biotin T®, sobre una cepa cianobacteriana (*Nostoc* sp. PCC 9104) en sus dos modos de crecimiento: forma planctónica y biofilm.

Ambos índices de feofitinización ($A_{435/415}$ y $A_{665/665a}$) resultaron válidos para estimar la degradación de la clorofila-a en la cepa estudiada. A su vez, los parámetros de color CIELAB se correlacionaron con ambos índices, lo que confirma que se puede conocer la actividad del biocida y el estado fisiológico del organismo a través de la caracterización de su color. Dentro de los parámetros de color CIELAB, L* resultó el más informativo ya que se correlacionó con ambos índices de feofitinización en los dos modos de crecimiento (forma planctónica y biofilm), le siguieron a* y C^*_{ab}, que se correlacionaron con $A_{665/665a}$ en ambos modos de crecimiento.

3ª. Interacción superficies graníticas-cianobacterias: detección y cuantificación de los organismos sobre las construcciones

En las dos primeras líneas de trabajo se trataron los aspectos colorimétricos de las rocas graníticas y las cianobacterias por separado, trabajando siempre en condiciones de laboratorio. Sin embargo, para cubrir el objetivo principal del proyecto de tesis es necesario probar la metodología desarrollada en casos reales de colonización biológica sobre superficies graníticas. Para tal fin, y de forma previa al estudio de la detección y monitorización del crecimiento de biofilms sobre fachadas graníticas empleando la medida del color, fue necesario resolver ciertos problemas metodológicos en el estudio de la interacción roca-microorganismos.

Aunque la cuantificación de la clorofila-a es el método de referencia por excelencia para la cuantificación de biomasa fototrófica, cuando se trata de estimar la cantidad de clorofila-a presente en un material pétreo colonizado, este método presenta algunos problemas ya que la extracción de este pigmento de la roca da lugar a una subestimación en la medida, tal como apuntaban Prieto *et al.* (2004). Estos autores advertían sobre la necesidad de optimizar el método de extracción de la clorofila-a en sustratos rocosos y señalaban que su recuperación no era completa debido a que la propia roca dificultaba la extracción, resultando el límite de detección de este pigmento demasiado alto para la cuantificación de la colonización temprana. La investigación en la mejora del método de extracción de la clorofila-a de biofilms fototróficos sobre sustratos pétreos (**Capítulo 6**) fue necesaria para poder comparar este método con el método basado en la medida del color puesto a punto en esta tesis.

Con este objetivo, se llevó a cabo una optimización del método de extracción de clorofila-a sobre roca granítica usando el método de superficie de respuesta de un diseño factorial incompleto de 3er orden, que predice las condiciones experimentales óptimas para la máxima extracción de clorofila-a (Fernández-Silva *et al.*, 2011).

Se evaluaron tres pretratamientos mecánicos para determinar el mejor procedimiento en la extracción de clorofila-a con dimetil sulfóxido (empleado como solvente) en bloques de granito inoculados con un cultivo mixto de tres cepas cianobacterianas que forman biofilms sobre rocas graníticas, *Nostoc* sp. PCC 9104, *Nostoc* sp. PCC 9025 y *Scytonema* sp. CCC 9801. Dos de ellos, A y B, incluían la trituración de la probeta de granito seguida, en el caso del pretratamiento B de una sonicación de los fragmentos de roca y extracción en baño de ultrasonidos. En el tercer pretratamiento, C, se sustituía la trituración de la probeta por la aplicación de una sonda de ultrasonidos (sonicador) al extractante que baña los bloques enteros.

Para cada pretratamiento se utilizó un diseño de Box-Behnken para 3 factores experimentales o variables de optimización: (1) relación volumen de extractante/volumen de muestra, (2) temperatura durante la extracción y (3) tiempo de extracción, siendo la clorofila-a extraída la

variable dependiente o de respuesta. Tras la incubación en DMSO con las correspondientes condiciones experimentales, se determinó la concentración de clorofila-a por espectrofotometría UV-Vis.

El análisis de los resultados determinó que: (i) la aplicación de ultrasonidos mejora la extracción de clorofila-a de los biofilms desarrollados sobre sustratos rocosos; (ii) la precisión de la medida usando el método de espectrofotometría UV-Vis para el cálculo de la concentración de clorofila-a disminuye cuando las muestras están altamente diluidas, por lo que son más convenientes los métodos que requieren un menor volumen de extractante, y, (iii) la temperatura de extracción es el factor experimental más importante (comparado con los otros dos analizados) en la extracción de clorofila-a de los biofilms desarrollados sobre sustratos rocosos. Con todo ello se propone un método que implica la aplicación de ultrasonidos directamente a la muestra intacta sin necesidad de triturarla (con lo que el método de extracción de clorofila-a deja de ser un método destructivo y pasa a ser un método meramente invasivo) seguido de una incubación en 0,43 ml de DMSO/cm^2 de muestra, a 63ºC durante 40 minutos. Esta mejora fue empleada en un experimento de confirmación en el que se consiguió la recuperación del 90% de la cantidad real (*i.e.* inoculada) de clorofila-a, un incremento sustancial frente al 68% que era el máximo de recuperación en trabajos anteriores.

El **Capítulo 7** se centra en la detección y monitorización del crecimiento de biofilms fototróficos y epilíticos en la fachada de granito de un edificio (Sanmartín *et al.*, 2012). Se trata de un caso real orientado a la conservación preventiva, que proporciona una base para el establecimiento de criterios de detección precoz del verdín y monitorización de su desarrollo en los edificios graníticos, utilizando las variaciones de color registradas mediante un espectrofotómetro portátil y representadas en el espacio de color CIELAB teniendo en cuenta el grupo de coordenadas escalares (L*a*b*).

Con este trabajo se establecen por primera vez los límites de percepción del enverdecimiento (greening) sobre una superficie de granito en términos de incremento de los parámetros de color CIELAB L* (ΔL*), a* (Δa*) y b* (Δb*), cantidad de organismos (en peso seco) y cantidad de clorofila-a extraída. Asimismo, se analiza la evolución de los valores de L*, a* y b* en un caso real de limpieza y recolonización natural de una fachada granítica, con el objetivo de determinar qué parámetro/s CIELAB refleja/n mejor el comienzo del enverdecimiento. Los resultados indican que es el parámetro b* (que define el componente amarillo-azul de un color) el que proporciona mayor información, ya que es el que detecta la colonización más temprana y el que varía en mayor magnitud con el tiempo por lo que condiciona en mayor medida el cambio de color total (ΔE^*_{ab}, $\Delta E^*_{ab} = [(\Delta L^*)^2 + (\Delta a^*)^2 + (\Delta b^*)^2]^{1/2}$).

Además, los resultados expuestos en este Capítulo 7 presentan utilidad práctica en la gestión y mantenimiento de edificaciones con problemas de biodeterioro, al permitir detectar la colonización cuando ésta es aún imperceptible al ojo humano e incluir indicaciones relacionadas con el momento de limpieza y aplicación de tratamientos para detener o revertir la colonización fototrófica en las fachadas.

4ª. Aplicación práctica de la medida del color a otros sustratos inorgánicos naturales: rocas pizarrosas, suelos y sedimentos

La metodología planteada en el Capítulo 1 para el análisis de los factores instrumentales y de superficie que afectan a la determinación del color de cualquier tipo de material heterogéneo en color y textura, fue empleada para el estudio del color de rocas pizarrosas en el **Capítulo 8**. Partiendo de la premisa de que los criterios para la selección de rocas para reemplazar las existentes en edificios históricos deben estar basados en parámetros geológicos, geotécnicos y estéticos, entre los cuales se encuentra el color, en el Capítulo 8 se realizó un exhaustivo y útil estudio colorimétrico de las pizarras de techar de la Península Ibérica (Prieto *et al.*, 2011). Así, se determinó el color de cincuenta variedades comerciales de pizarra de techar, extraídas de doce distritos mineros repartidos entre España y Portugal, con un espectrofotómetro portátil, considerando el espacio de color CIELAB y teniendo en cuenta el grupo de coordenadas escalares (L*a*b*) y el grupo de coordenadas cilíndricas o polares ($L^*C^*_{ab}h_{ab}$).

El análisis de las condiciones de medida indicó que para la determinación del color de este tipo de rocas, el número de medidas mínimo necesario es sustancialmente menor que en las rocas graníticas (Sanmartín *et al.*, 2010b) lo cual es, sin duda, debido a la mayor homogeneidad de color y textura de las rocas pizarrosas con respecto a las graníticas. Asimismo, se definió la zona tridimensional del espacio de color CIELAB en la que se encuadran las pizarras de techar de la Península Ibérica. La delimitación de esta zona ofrece las mismas aplicaciones prácticas que las señaladas en el Capítulo 2 para las rocas graníticas ornamentales.

Por su parte, el tono angular (h_{ab}) resultó el parámetro de color CIELAB más útil en cuanto a la formación de grupos de pizarras para cubierta colorimétricamente similares y el componente especular excluido (SCE) es el modo más sensible para detectar diferencias de color (ΔE^*_{ab}) entre dos variedades de pizarra.

Además, se establecieron las similitudes y diferencias en el color y la microestructura de las diferentes variedades comerciales, así como el grado de aceptación para la sustitución de un tipo de pizarra por otra. Así, cinco variedades de pizarra pueden reemplazar a y ser reemplazadas por prácticamente el resto de las cincuenta variedades y una única variedad no puede reemplazar ni ser reemplazada por ninguna otra pizarra.

El **Capítulo 9** se planteó como una primera aproximación al estudio de la relación existente entre el color que un suelo adquiere tras un incendio y la temperatura que alcanza, con el fin de valorar el uso del color del suelo como indicador de la intensidad de un incendio (Sanmartín *et al.*, 2010c). A pesar de que han sido muchos los casos en los que se han descrito variaciones apreciables en el color del suelo tras un incendio (como el ennegrecimiento debido a carbonización parcial o total de la materia orgánica y el enrojecimiento debido a la deshidratación de los óxidos de hierro), la variación de los parámetros de color y su relación con la intensidad del fuego no habían sido hasta ahora determinados en el contexto de los suelos gallegos. Por este motivo, en este estudio se realizó una quema controlada en el laboratorio de muestras inalteradas del horizonte superficial de un regosol úmbrico empleando lámparas de infrarrojos para alcanzar temperaturas de 200ºC y 400ºC a 1 cm de la superficie. Sobre la superficie de cada una de las muestras quemadas y de las muestras sin quemar (que fueron empleadas como control) se determinó el color en 220 puntos con un colorímetro portátil, considerando los espacios de color CIELAB y Munsell. Los resultados obtenidos mostraron un descenso de la claridad en las muestras quemadas con respecto a las sin quemar, reflejado en los valores de *Value* Munsell y L* CIELAB, así como un descenso del croma, marcado por el *Chroma* Munsell y C^*_{ab} CIELAB, probablemente debidos a la carbonización de la materia orgánica. Además, se produjo un empardecimiento-enrojecimiento del suelo reflejado en los valores de *Hue* Munsell, el descenso de h_{ab} CIELAB, el aumento de a* CIELAB y el descenso de b* CIELAB, que debe atribuirse simplemente a la desaparición de los componentes orgánicos del suelo que enmascaraban el color de los componentes inorgánicos coloreados, principalmente óxidos de hierro.

La comparación entre los valores de los suelos quemados a 200ºC y a 400ºC, temperaturas que se corresponden con incendios de intensidad ligera y moderada respectivamente, muestra que los únicos parámetros que establecen diferencias significativas son aquellos que se refieren al *Hue* Munsell y h_{ab} CIELAB. En este caso, las diferencias pueden ser asignadas principalmente a variaciones en el estado de deshidratación de los compuestos de hierro como el cambio de goethita, de un color anaranjado, a hematite, de color rojo sangre. Esto parece indicar que será el tono el parámetro a tener en cuenta en el uso del color como indicador de la intensidad de incendios en suelos de Galicia.

Para finalizar esta cuarta línea orientada a la aplicación práctica de la medida del color a otros sustratos inorgánicos naturales y concluir así el trabajo de tesis, el último capítulo presenta el uso de las medidas de color en la estimación de los fitopigmentos contenidos en sedimentos de río.

La cuantificación de fitopigmentos en los sedimentos de río recibe la atención de los especialistas porque proporciona información sobre el efecto sinérgico que provocan los nutrientes, en especial nitrógeno y fósforo, en el crecimiento de las algas y por tanto sobre la

eutrofización del río, un descriptor válido del estado trófico y de la calidad de las aguas y sedimentos. El desarrollo de una metodología no-destructiva, rápida, sencilla y económica para la cuantificación del contenido de fitopigmentos en los sedimentos de río, evitando la extracción y análisis químico de los mismos, sería de gran utilidad en este campo. El **Capítulo 10** muestra la validez de las medidas de color realizadas con un espectrofotómetro portátil y representadas en el espacio de color CIELAB en la estimación precisa de los fitopigmentos en sedimentos de río (Sanmartín *et al.*, 2011c).

Se recogieron muestras de sedimentos con cilindros metálicos en tres zonas de baja pendiente, favorables para la deposición de sedimentos, a lo largo del cauce del río Anllóns (Galicia). En ellas se realizaron mediciones de color representadas en el espacio de color CIELAB teniendo en cuenta el grupo de coordenadas escalares (L*a*b*) y el grupo de coordenadas cilíndricas o polares ($L^*C^*_{ab}h_{ab}$), para posteriormente extraer con dimetil sulfóxido y cuantificar por espectrofotometría UV-Vis su contenido en fitopigmentos (clorofila-a, clorofila-b, feopigmentos y carotenoides totales).

Los resultados mostraron que los parámetros de color CIELAB se correlacionaban significativamente con el contenido en fitopigmentos permitiendo el desarrollo de ecuaciones de predicción para el contenido en clorofila-a, clorofila-b, carotenoides totales y contenido total en fitopigmentos a partir del parámetro a* y el parámetro C^*_{ab}. El mejor ajuste se alcanzó en la predicción de clorofila-a (Chl-a): Chl-a = 46,4 – 70,6 $\log_{10}(a^*)$ y Chl-a = –15,7 + 238,1 $(1/C^*_{ab})$ con un valor ajustado de R^2 de 0,84.

Summary

In the conservation of buildings and structures, particularly those of historical and artistic importance, it is essential to mitigate the effects of biological colonization, since this supposes not only an aesthetic problem, but can also cause mineralogical, chemical and physical damage to the materials, with the consequent loss of value. Biological colonization and biofilm formation are unavoidable because they occur as a result of interactions between the building material and the environment. However, early detection of biological colonization, and better knowledge of the developmental stage would suppose a great advantage as regards management of the maintenance and rehabilitation of the buildings, as this would tackle the problem at the first stages, even before the colonization could be assessed visually. Moreover, in the case of heavily colonized structures, early detection would be extremely useful for monitoring the efficacy of the treatments used to eliminate microorganisms and for detecting any recolonization.

Therefore, the overall aim of this doctoral research project was to develop and implement a novel methodology for the early detection of biofilm formation on granite stone in buildings and monuments, based on color measurements. This novel method satisfies various requirements that validate its application to heritage structures: it is non-destructive (allowing further analysis on single samples); it can be applied on site (avoiding sampling and allowing results to be obtained immediately); it is relatively inexpensive and easily applied, so that any unskilled operator with minimal training can perform the measurements.

The hypothesis that led to the approach used in this project is based on the idea that biological colonization on structures can be quantified by determining the color generated by the microorganisms involved. This hypothesis is supported by the findings of previous studies. One of these studies demonstrated the existence of a direct relationship between the quantity and physiological state of phototrophic organisms and the color change generated when they are deposited on a surface (Prieto *et al.*, 2002; Spain Patent No. P200002956, 2000). Another study, which compared different methods of quantifying the phototrophic biomass on rocky substrates, revealed a close correlation between the results obtained with the most appropriate methods (*i.e.* those based on the quantification of chlorophyll-a) and those results obtained from the color quantification (Prieto *et al.*, 2004).

The present research focused on the pioneering microorganisms in the colonization of rocky substrates, specifically cyanobacteria, because these are the main constituents of the phototrophic biofilms that form on building façades. The study specifically evaluated biological colonization on granite stonework, which is a complex case because of the spatially heterogeneous color formed by the different colors of the constituent minerals. Three different aspects were considered in order to achieve the overall aim of the study:

1. Fine-tuning of the methodology for measuring and characterizing the color of granite surfaces (Prieto *et al.*, 2010a; Sanmartín *et al.*, 2011a).

2. Fine-tuning of the methodology for measuring and characterizing the color of cyanobacteria (Prieto *et al.*, 2010b; Sanmartín *et al.*, 2010a, 2011b).

3. Interactions between granite surfaces and cyanobacteria: detection and quantification of microorganisms colonizing the surface of buildings and monuments (Fernandez-Silva *et al.*, 2011; Sanmartín *et al.*, 2012).

These three lines eventually converged in a 4th line of research that addressed the practical application of color measurement in other natural inorganic substrates of interest in the field of environmental studies. Some examples of practical applications include color characterization of roofing slates as a decision-making tool for restoration work (Sanmartín *et al.*, 2010b; Prieto *et al.*, 2011), color characterization of burned soils as an indicator of fire intensity (Sanmartín *et al.*, 2010c) and color measurements in riverbed sediments as an indicator of phytopigment content (Sanmartín *et al.*, 2011c).

1. Fine-tuning of the methodology for measuring and characterizing the color of granite surfaces

The first research line (**Chapter 1**) involves the fine-tuning of a measurement protocol for the color characterization of ornamental granite, originally developed by Prieto *et al.* (2010a). The aim of this study was to determine the minimum area and the minimum number of measurements required for objective characterization of the color of granite rocks. A spectrophotometer and a tristimulus colorimeter were used to measure the color of granite samples, and the reflectance measurements were analyzed with the CIELAB color parameters, using Cartesian (L*a*b*) coordinates. Three parameters were considered as variable factors: the type of rock (color and texture), the surface finish (polished, honed, sawn, and flamed), and the target area of the measurement head (circular apertures of diameter 5, 8, 10, and 50 mm). The results revealed that, although all of the factors considered affected the minimal area and the number of measurements required, the different circular apertures of both instruments can be disregarded if the number of measurements and area recommended in this study are used.

One of the most important findings of this research is that it provides a methodology for determining the conditions for color measurements on heterogeneous surfaces of different textures, and can be used in different materials. The methodology was successfully used with roofing slates (Prieto *et al.*, 2011) and in the 2nd research line in this doctoral research project, in which the methodology for measuring and characterizing the color of cyanobacteria was fine-tuned.

All ornamental stone in built structures has a certain type of surface finish, and **Chapter 2** reports how the effects of the type of commercial finish on the color, gloss and roughness of ornamental granite were studied and a relationship between these three aesthetic parameters was established (Sanmartín *et al.*, 2011a). The results demonstrated that different surface finishes (polished, honed, sawn, and flamed or bush hammered) almost always produce notable differences in color, especially in the lightness parameter (L*); the magnitude of these differences depends on the color of the ornamental granite and is greatest in dark colored rocks. However, the variation in the color parameters ($L^*a^*b^*C^*_{ab}h_{ab}$) with the different surface finishes did not depend on roughness, and no general conclusions could be drawn regarding the influence of the roughness on the color of ornamental granite. Gloss values were affected by the color, but in a different way for smooth and rough surfaces. Variations in gloss also depended on the mineral composition of the rock. Gloss and roughness were inversely related, but only within the range of low roughness values.

The influence of the inclusion or exclusion of the specular component in the measurement mode is also discussed in Chapter 2. It was found that exclusion of the specular component (SCE mode) magnifies the differences in color produced by the different surface finishes, so that this mode is preferred over the specular component included (SCI) mode.

The results obtained also enable identification of the three-dimensional color area of the CIELAB space in which the color of the ornamental granites under study is defined. The information obtained in this study should be taken into account when aesthetic criteria are used to select ornamental granites for building and construction materials, and also to characterize digital cameras for use as colorimeters in studies of cultural heritage monuments.

2. Fine-tuning of the methodology for measuring and characterizing the color of cyanobacteria

Following the methodology developed for measuring color in heterogeneous surfaces (Chapter 1), the second research line in this doctoral research project established a methodology for measuring the color of biofilms on solid surfaces (**Chapter 3**).

For this purpose, samples of a mixed culture of three types of cyanobacteria, *Nostoc* sp. PCC 9104, *Nostoc* sp. PCC 9025 and *Scytonema* sp. CCC 9801, which form biofilms on granite

surfaces, were filtered under vacuum through nitrocellulose filter discs, to simulate the composition and characteristics of a biofilm. The color of the areas coated by the microorganisms was measured, as described in Chapter 1, with two contact-type color measuring devices (spectrophotometer and colorimeter), and the reflectance measurements were analyzed with the CIELAB color parameters, using Cartesian (L*a*b*) coordinates, in order to analyze the effect of the coverage by organisms and their moisture content on their color.

The results showed that the minimum number of measurements required increased with increasing heterogeneity of the color of the measured area, which depended on the concentration of the microorganisms, and decreased with the diameter of the measuring head. To control for the influence of the heterogeneity of the color of the area measured, the color of cyanobacteria should be measured on filters that are completely covered by the microorganisms, so that the color of the filter is totally concealed. The L* values were greatly affected by the moisture content of the samples. Thus, the values of L* decreased exponentially with moisture contents of up to 50%, which can be considered as the point from which a stable asypmtote is reached on the corresponding graph. The color of cyanobacteria should therefore be determined in samples with moisture contents of more than 50%. Considering all of the above, at least 10 consecutive measurements/9.62cm^2 should be made at different randomly selected points on the surface of filters completely covered by films of cyanobacteria in which the moisture contents are higher than 50%.

Chapter 4 describes how the relationship between color and composition and/or abundance of photosynthetic pigments and the efficiency of color measurements was used to evaluate the extent to pigment production is affected by environmental parameters such as light intensity, combined nitrogen and nutrient availability. This was tested with two cyanobacteria, *Nostoc* sp. strains PCC 9104 and PCC 9025, which form biofilms on stone surfaces. Both strains were acclimated, in aerated batch cultures for 2 weeks, to three different culture media, BG-11, BG-11$_0$, and BG-11$_0$/10, at either high or low light intensity. The chlorophyll-a, total carotenoid, and phycocyanin contents were measured throughout the experiment, together with variations in the color of the cyanobacteria, which were represented in the CIELAB color space, using Cartesian (L*a*b*) and cylindrical (L*C*$_{ab}$h$_{ab}$) coordinates.

The results confirmed that the CIELAB color parameters are correlated with pigment content in such a way that variations in the latter are reflected as variations in color. However, not all CIELAB color parameters are equally sensitive to changes in pigment concentrations. Thus, L*, and to a lesser extent a*, is the most informative CIELAB color parameter, and h$_{ab}$, which refers to the dominant wavelength, represents the major color perception attribute.

The color data recorded in Chapter 4 indicate the three-dimensional color area of the CIELAB space in which both strains define their color. This is the first time that objective color values of

different species of cyanobacteria growing in different environmental conditions have been obtained, and is a preliminary step in defining the color gamut of cyanobacteria, which is essential information for the development of any color-based methodology for monitoring cyanobacterial growth.

The second research line (**Chapter 5**) involves the color characterization of phototrophic microorganisms (cyanobacteria) for analysis of their physiological state after treatment with biocides (Sanmartín *et al.*, 2011b). The effectiveness of biocides against phototrophic organisms can be tested by the degree of chlorophyll degradation. When chlorophyll degrades, it forms a series of degradation products or phaeopigments, and the relation between phaeopigments and chlorophyll can be established by the phaeophytination indexes $A_{435/415}$ and $A_{665/665a}$.

Chapter 5 discusses the suitability the CIELAB color measurements as a reliable method for monitoring the effectiveness of the chemical biocide Biotin T® (which is commercially available and widely used in the field of stone cultural heritage materials) against a cyanobacterial strain (*Nostoc* sp. PCC 9104) in both planktonic and biofilm mode of growth. Determination of the phaeophytination indexes ($A_{435/415}$ and $A_{665/665a}$), which have proved useful for describing the degradation of chlorophyll-a to phaeopigments in *Nostoc* sp. PCC 9104 planktonic and biofilm biocide susceptibility assays, could be substituted by color measurements as there is a close relation between these and the color parameters. This confirms that the effectiveness of a biocide and the physiological state of a microorganism can be determined by color characterization. Of the CIELAB parameters, L* appeared to be the best for describing the biocidal activity of Biotin T® against *Nostoc* sp. in both planktonic and biofilm mode of growth. Moreover, a* and C^*_{ab} are correlated with the $A_{665/665a}$ index in both modes of bacterial growth.

3. Interactions between granite surfaces and cyanobacteria: detection and quantification of the microorganisms on the surfaces of buildings and monuments

In the first two research lines of this doctoral study, the colorimetric aspects of granite and cyanobacteria were dealt with separately, always working under laboratory conditions. However, to meet the main objective of the study, the methodology must be tested in real cases of biological colonization on granite surfaces. For this purpose, and prior to the study of the detection and monitoring of the growth of biofilms on granite façades using color measurements, it was necessary to resolve certain methodological problems in the study of granite-microorganism interactions.

Although quantification of chlorophyll-a is considered the reference method of excellence for quantifying phototrophic biomass, in the case of estimating the amount of chlorophyll-a present in colonized rocky substrata, a relatively high value is obtained as the lower limit of detection; this prevents early detection of stone biocolonization below this lower limit, as pointed out by

Prieto *et al.* (2004). These authors suggested that the stone itself impedes total chlorophyll-a extraction, and concluded that optimization experiments carried out on stone samples were necessary.

Further research to improve the method of chlorophyll-a extraction from phototrophic biofilms developed on rocky substrata (**Chapter 6**) was required for comparison of this method with the color measurement method that was fine-tuned during the course of this doctoral research project. With this aim, the method of extracting chlorophyll-a from phototrophic biomass (biofilms) on granite surfaces was optimized, by use of a response surface analysis following a Box–Behnken third order design, which predicts the optimal experimental conditions for maximum extraction of chlorophyll-a (Fernandez-Silva *et al.*, 2011).

Three different mechanical pretreatments were assayed to determine the best procedure for complete extraction of chlorophyll-a with dimethyl sulphoxide (used as solvent) on granite blocks inoculated with a mixed culture of three biofilm-forming cyanobacteria, *Nostoc* sp. PCC 9104, *Nostoc* sp. PCC 9025 and *Scytonema* sp. CCC 9801.

In methods A and B, inoculated blocks were crushed and in method B, the blocks were pretreated by immersing them in an ultrasonic bath to enable application of ultrasound to the whole of each sample. For pretreatment C, the intact blocks were sonicated by inserting the narrow end of an ultrasonic generator into the extractant.

For each pretreatment, a Box–Behnken design was used for three-variable optimization or experimental factors: (1) extractant-to-sample ratio, (2) temperature during the extraction, and (3) time of incubation, considering the chlorophyll-a recovery as the dependent variable or response variable. The samples were incubated in DMSO and then filtered; the concentration of chlorophyll-a in the filtrates was then determined by UV-Vis spectrophotometry.

From the results obtained it can be concluded that: (i) the application of ultrasonic methods improved extraction of chlorophyll-a from biofilms developed on rocky substrata; (ii) the precision of the spectrophotometric method for calculation of the concentration of chlorophyll-a decreases when samples are highly diluted, and thus methods requiring a lower volume of extractant are more convenient; (iii) the temperature of extraction is the most important factor (in comparison with the other two parameters analyzed) in extraction of chlorophyll-a from biofilms on rocky substrata. Therefore, we propose the application of ultrasound directly to uncrushed rock samples (so that the method of extraction of chlorophyll-a ceases to be destructive and becomes merely an invasive method) followed by incubation in 0.43 ml DMSO/cm^2 sample (vol/surface) at 63ºC for 40 min, as an efficient method for extraction of chlorophyll-a from rock materials. Experiments were performed at the predicted optimal conditions to confirm the findings, and 90% of the chlorophyll-a was recovered, which is a substantial improvement with respect to the expected recovery with previous methods (68%).

Chapter 7 addresses the detection and monitoring of the development of epilithic phototrophic biofilms on the granite façade of an institutional building in Santiago de Compostela (NW Spain), and reports a case study of preventive conservation (Sanmartín *et al.*, 2012). The results provide a basis for establishing criteria for the early detection of phototrophic colonization (greening) and for monitoring its development on granite buildings by the use of color changes recorded with a portable spectrophotometer and represented in the CIELAB color space, using Cartesian coordinates (L*a*b*).

This study established the threshold of human perception of greening on granite rock and its value in terms of partial color differences (ΔL*, Δa* and Δb*), amount of phototrophic biomass (dry weight) and chlorophyll-a content extracted. Likewise, the changes in the L*, a* and b* CIELAB coordinates in a real case involving the cleaning and recolonization of a granite façade were analyzed, with the aim of determining the parameter or parameters that best indicate the start of the greening process. The results show that parameter b* (associated with changes in yellowness-blueness) provides the earliest indication of colonization and varies most widely over time, so that it is most important in determining the total color change (ΔE^*_{ab}, $\Delta E^*_{ab} = [(\Delta L^*)^2 + (\Delta a^*)^2 + (\Delta b^*)^2]^{1/2}$).

Moreover, the results outlined in Chapter 7 are of practical use in the management and maintenance of buildings undergoing biodeterioration, even when it is not perceptible to the human eye. The findings enabled development of a methodology for the management and maintenance of buildings. The methodology could be used in making decisions about the frequency of cleaning and biocide treatment required in the case of granite buildings affected by greening.

4. *Practical application of color measurement on other naturally occurring inorganic substrates: slaty rocks, soils and sediments*

The methodology proposed in Chapter 1 for the analysis of the instrumental factors and surface-related features that affect the color determination in any type of heterogeneous material (in terms of color and texture) was used to develop a protocol for characterizing the color of roofing slate, as described in **Chapter 8**. Starting from the premise that the criteria for selecting stones to replace existing stone in historic buildings must be based on geological, geotechnical and aesthetic parameters, among which color is of great importance, a comprehensive colorimetric study of roofing slates from the Iberian Peninsula was carried out, for restoration purposes (Prieto *et al.*, 2011), and is reported in Chapter 8. Thus, the color of fifty commercial varieties of roofing slate mined in quarries from the twelve mining districts in Spain and Portugal was analyzed by spectrophotometry, by considering the CIELAB color space and using Cartesian (L*a*b*) and cylindrical ($L^*C^*_{ab}h_{ab}$) coordinates.

Analysis of the measurement conditions showed that the minimum number of measurements required to determine the color of roofing slates is substantially less than the number required to determine the color of granitic rocks (Sanmartín *et al.*, 2010b). This is undoubtedly due the greater homogeneity of the color and texture of slate than of granite. The three-dimensional color area of the CIELAB space of roofing slate from the Iberian Peninsula was also defined. Delimitation of this area offers the same practical applications as those cited in Chapter 2 for ornamental granite.

The hue angle (h_{ab}) was the most important CIELAB color coordinate in the formation of homogeneous color groups of roofing slate specimens, and the specular component excluded (SCE) mode was the most sensitive for detection of the total color difference (ΔE^*_{ab}) between two varieties of roofing slates.

Moreover, the similarities and differences in color and microstructure of the different commercial varieties were established, as was the degree of acceptance for the replacement of one type of roofing slate by another. Thus, five commercial varieties of slate extracted from the twelve different slate mining districts in the Iberian Peninsula can replace and be replaced by the most of the other fifty varieties, and only one variety cannot replace or be replaced by any other slate.

Chapter 9 describes a preliminary approach in the study of the relationship between color changes in soil and the temperature reached as a consequence of fire, in order to assess the applicability of soil color as an indicator of fire intensity (Sanmartín *et al.*, 2010c). Although many studies have described large variations in the color of the soil after fire (such as the blackening due to partial or total destruction of organic matter and the red color caused by the dehydration of iron oxides), variations in CIELAB color parameters and their relationship with the intensity of the fire have not previously been identified in the context of Galician soils. For this reason, controlled burning of undisturbed soil samples from the surface horizon of an *Umbric Regosol* was conducted in the laboratory, with infrared lamps, until the temperature at a depth of 1 cm reached 200ºC or 400ºC. Unburned samples were used as a control. The color of the surface of the burned and unburned soil samples was determined at 220 points with a portable colorimeter and represented in the CIELAB color space and with Munsell notation. The results showed a decrease in lightness in the burned samples, reflected in the values of Munsell *hue* and CIELAB L*, and a decrease in chroma marked by the *Chroma* Munsell and C^*_{ab} CIELAB, probably due to carbonization of the material organic. There was also slight browning-reddening of the soil, which was reflected in the values of Munsell *Hue*, a decrease in CIELAB h_{ab}, an increase in a* and a decrease in b*, which should be attributed simply to the disappearance of the organic soil components that masked the color of the inorganic components, mainly iron oxides.

Comparison between the values in soils in which different temperatures were reached (200ºC and 400ºC), shows that the parameters that establish significant differences are those refer to the soil hue (Munsell *Hue* and CIELAB h_{ab}). In this case, differences are mainly assigned to variations in the state of dehydration of iron compounds, as goethite (orange color) is converted to haematite (blood-red color). This suggests that soil hue is the parameter that must be taken into account in using color as an indicator of fire intensity in Galician soils.

To end this fourth research line aimed at the practical application of color measurements to other natural inorganic substrates, and therefore conclude this thesis, the final chapter presents a non-destructive method for assessing phytopigments in riverbed sediments. The method described is based on instrumental color measurements without any need for extraction and chemical assay.

Quantification of phytopigments in riverbed sediments deserves further attention because it provides information about eutrophic levels and, therefore, about sediment and water quality. Due to the current interest in the study of eutrophication processes, there is a need to develop a rapid, simple, cost-effective and non-destructive method of quantifying phytopigment content. **Chapter 10** demonstrates that it is possible to determine phytopigment contents in riverbed sediments by means of a non-destructive colorimetric method employing the CIELAB color parameters (Sanmartín *et al.*, 2011c).

Surface riverbed sediment cores were collected in three low sloping areas (*i.e.* which are favourable for sediment deposition) along the course of the Anllóns River (NW Spain). The reflectance color measurements were analyzed with the CIELAB color parameters, using Cartesian (L*a*b*) and cylindrical ($L^*C^*_{ab}h_{ab}$) coordinates. Phytopigments (chlorophyll-a, chlorophyll-b, phaeopigments and total carotenoids) were extracted with dimethylsulphoxide and determined spectrophotometrically.

The CIELAB color parameters were significantly correlated with phytopigment content (involving logarithmic, inverse and simple data). Linear regression equations were used to predict chlorophyll-a, chlorophyll-b and carotenoid contents, as well as the total pigment contents from parameter a* and parameter C^*_{ab}, and values of adjusted R^2 close to 0.9 were obtained. The closest relation between phytopigments and color parameters corresponded to chlorophyll-a (Chl-a), which may be estimated by means of Chl-a = 46.4 – 70.6 $\log_{10}$(a*), and Chl-a = –15.7 + 238.1 ($1/C^*_{ab}$) as predictive equations.

Introducción General

I. Del modo planctónico a la formación y crecimiento del biofilm[1]

El estudio y descripción de los microorganismos se ha venido realizando, desde los comienzos de la microbiología como disciplina, en sus formas planctónicas, es decir como células libres en suspensión creciendo en medios de cultivo nutritivos (Donlan, 2002). Sin embargo, observaciones directas de una amplia variedad de hábitats naturales han permitido comprobar que la mayoría de los microorganismos persisten unidos a las superficies, dentro de un estructurado ecosistema denominado biofilm (Costerton *et al.*, 1987). Esta forma de asociación fue descrita por primera vez a finales del siglo XVII por el microscopista holandés Antonie van Leeuwenhoek (1632-1723) quien, tras observar al microscopio la placa dental de sus propios dientes, afirmó que las bacterias podían adherirse y crecer universalmente sobre superficies expuestas. Ya en el siglo XIX el microbiólogo y edafólogo ruso Sergei N. Winogradsky (1856-1953) desarrolló un sistema que permite reproducir un ecosistema natural, la columna de Winogradsky, y así consiguió aislar asociaciones de microorganismos (biofilms) sobre portas de vidrio. Posteriormente en 1940, Heukelekian & Heller hacen referencia a un incremento sustancial del crecimiento y actividad de las bacterias marinas al adherirse a una superficie predeterminada, definiendo este fenómeno como el "efecto botella", y en 1943 Zobell es el primero en afirmar que el número de bacterias acumuladas en las superficies es mucho más elevado que en el medio circundante (en este caso el agua de mar). En 1978 Costerton *et al.*, basándose en observaciones realizadas en la placa dental y en las comunidades sésiles en arroyos de montaña, plantean una teoría que explica los mecanismos de adherencia de los microorganismos a superficies vivas y a materiales inertes para formar biopelículas, así como el conjunto de ventajas alcanzadas por estos conjuntos vivos en estos nichos ecológicos. Es Costerton quien, ese mismo año (1978), introduce el término biofilm definiéndolo como un agregado de bacterias rodeadas por un "glicocálix" de fibras que permite su adherencia a las superficies inertes y a otras células; lo cual supone un cambio de paradigma en el campo de la microbiología.

[1] El término inglés “biofilm” y su homólogo en español “biopelícula” se emplearán indistintamente a lo largo de todo el texto.

La definición actual de biofilm o biopelícula describe un concepto mucho más complejo según el cual se trata de "comunidades universales de microorganismos (bacterias, hongos, cianobacterias, algas, protozoos), complejas e interdependientes, asociadas a superficies húmedas (vivas o inertes) o a interfases (columnas de agua sujetas a gradientes), mediante una matriz polimérica (EPS) de glicoproteínas extracelulares, de consistencia viscosa, generada *ex profeso* y recorrida por canales de agua, los cuales permiten un intercambio eficiente de agua, nutrientes y gases entre las poblaciones constitutivas y el ambiente exterior" (Costerton, 2007). Así, la capacidad de formación del biofilm no está restringida a ningún grupo específico de microorganismos, considerándose que, bajo condiciones ambientales adecuadas, todos los microorganismos son capaces de formar biofilms. A este respecto, se ha demostrado que muchas células necesitan estar sujetas a las superficies (formando parte de un biofilm) para sobrevivir y proliferar; este requisito de supervivencia es conocido como "dependencia del anclaje" (*anchorage dependence*, Pierres *et al.*, 2002).

La principal característica que distingue las biopelículas del crecimiento planctónico es la existencia de una matriz de sustancia polimérica extracelular (EPS) embebiendo el total de los componentes del biofilm y adhiriendo éste a la superficie. La matriz constituye un medio complejo esencialmente compuesto por agua (hasta un 97%), que contiene además polímeros extracelulares, polisacáridos, proteínas, ácidos nucleicos, lípidos/fosfolípidos, nutrientes absorbidos y metabolitos. Pese a que la matriz extracelular es la característica definitoria de la biopelícula, su papel aún no es totalmente comprendido en la actualidad. A este respecto, la mayoría de los autores defienden que la función primaria de la matriz extracelular es la de proteger la biopelícula de la acción de agentes antimicrobianos, a través de la neutralización química o la creación de una barrera de difusión que impida a los microorganismos ser alcanzados por estos (Lindsay & von Holy, 2006), y de los cambios ambientales adversos en términos de humedad, temperatura, presión osmótica y pH. Así por ejemplo, se sabe que las cianobacterias incrementan la producción de polímeros extracelulares frente a la limitación de luz o de nutrientes (Albertano *et al.*, 2003). Otros autores sin embargo, consideran que el papel más relevante de los productos poliméricos extracelulares (EPS) ocurre durante las etapas iniciales de la formación del biofilm al facilitar la unión de las células al sustrato (Decho, 2000; Barranguet *et al.*, 2005), dar cohesión al biofilm incipiente y facilitar la interacción entre sus distintos componentes (Flemming & Wingender, 2001).

Los microorganismos que forman un biofilm también se diferencian de sus homólogos en suspensión en que presentan comportamientos fenotípicos particulares que los diferencian de sus formas libres en su modo de ubicación, agrupación y organización colonial, movilidad, adaptación metabólica y ambiental, y en su forma y tasa de crecimiento (Donlan, 2002). Durante el complejo proceso de adhesión, los microorganismos alteran sus características fenotípicas como respuesta a la proximidad a una superficie. Además, durante los estados iniciales de la formación de la biopelícula, los microorganismos sésiles se encuentran en una

yuxtaposición estable con microorganismos de la misma especie y de otras especies, formando de esta manera microcolonias. La interrelación que se produce en estas microcolonias hace posible el intercambio de material genético, que resulta en un cambio global en el fenotipo de la biopelícula (Stolz, 2000), así como la creación de ambientes heterogéneos desde el punto de vista físico-químico en los cuales los microorganismos asociados a la biopelícula presentan características fisiológicas distintas de las planctónicas. Muchos microorganismos alteran sus procesos fisiológicos para adaptarse a estos nichos particulares, por ejemplo creciendo anaeróbicamente (Stoodley *et al.*, 2002). Además, los diferentes microorganismos contenidos en la biopelícula responden a las condiciones de sus microambientes específicos, presentando diferentes patrones de crecimiento. La cooperación fisiológica es el factor principal que ayuda a conformar la estructura y establecer la eventual yuxtaposición, haciendo de las biopelículas maduras, adheridas a las superficies, comunidades microbianas muy eficientes (Costerton *et al.*, 1994).

En un contexto amplio, la formación de un biofilm (**Figura 1**) implica que los microorganismos constituyentes, al dejar su condición de células móviles (planctónicas), conforman poblaciones no estratificadas de microorganismos, con una estructura y una interacción multiespecie, así como un metabolismo concreto con tasa de crecimiento controlada y una ubicación relativa concreta. En la formación del biofilm se distinguen varios pasos o fases (O'Toole *et al.*, 2000; Boonaert *et al.*, 2001). En primer lugar, macromoléculas y moléculas orgánicas de distintos orígenes se fijan al sustrato por adsorción, acondicionándolo para una eventual colonización (Paso 1, Figura 1). A continuación, los microorganismos se aproximan al sustrato mediante movimientos propios y brownianos, y entonces se producen interacciones físico-químicas con las moléculas adsorbidas que conducen a una adhesión primaria de las células (Paso 2, Figura 1). Esta adherencia al sustrato, como paso fundamental de la formación del biofilm, es un proceso complejo, regulado por el medio circundante, la superficie del sustrato y los microorganismos (Ophir & Gutnick, 1994; O'Toole *et al.*, 2000; Donlan, 2002). Tras ella, el anclaje de los microorganismos se provoca mediante la excreción de productos poliméricos extracelulares (EPS) (Paso 3, Figura 1). A partir de este punto la multiplicación celular lleva a la proliferación de las comunidades microbianas y a su adhesión permanente al sustrato. La maduración de la biopelícula corresponde al crecimiento tridimensional e involucra la generación de una arquitectura específica y compleja del biofilm con canales y poros, así como una redistribución de los microorganismos lejos del sustrato (Paso 4, Figura 1). La “arquitectura del biofilm” (*biofilm architecture*, Lawrence *et al.*, 1991) y en particular la disposición espacial de las microcolonias (grupos de microorganismos) en relación con otras, tiene profundas implicaciones para la función de estas complejas comunidades (Donlan, 2002). La arquitectura de la matriz del biofilm no es sólida y presenta canales que permiten el flujo de agua, nutrientes y oxígeno incluso hasta las zonas más profundas del biofilm. La existencia de estos canales no evita sin embargo, que dentro del biofilm se encuentren ambientes con diferentes

concentraciones de nutrientes, pH y oxígeno (Pasos 5 y 6, Figura 1). Tras la maduración del biofilm, la última fase es de retorno de los microorganismos del biofilm a un modo de crecimiento planctónico, provocado por una reducción en la producción de exopolímeros (Paso 7, Figura 1. O'Toole *et al.*, 2000). Por consiguiente, los microorganismos que abandonan la biopelícula cierran el ciclo de vida de la misma (Costerton, 2007).

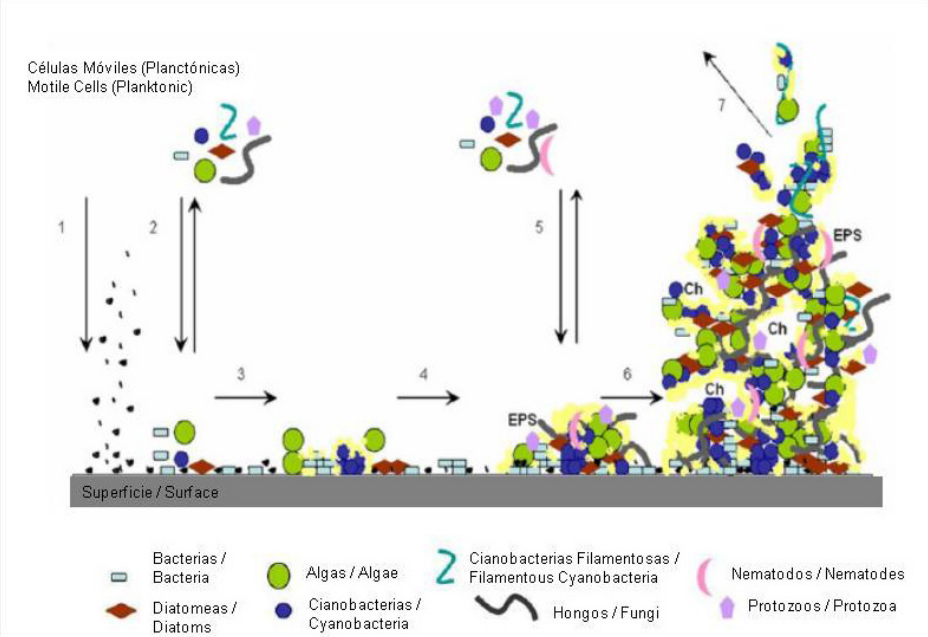

Figura 1. Representación esquemática de la formación de un biofilm. Adaptado de Cuzman (2009). (1) Establecimiento de las macromoléculas y moléculas orgánicas sobre la superficie a colonizar, (2) adhesión reversible de los colonizadores primarios, (3) transición a la adhesión irreversible, multiplicación y comienzo de la producción de EPS (sustancia polimérica extracelular), (4) comienzo del desarrollo tridimensional de la estructura del biofilm, (5) adhesión de colonizadores secundarios y desarrollo continuo del biofilm, (6) maduración del biofilm con una estructura expresa (arquitectura del biofilm) formando un micro-ecosistema específico, (7) fase/estado de homeostasis que mantiene en equilibrio al biofilm, con un crecimiento continuo de la estructura dotada de canales (Ch "channel"), y a los microorganismos que se desprenden y retornan a un modo de crecimiento planctónico.

El reconocimiento de la importancia de los biofilms constituye un fenómeno reciente y aunque sólo hace un par de decenios que se viene investigando la fisiología de estas comunidades, se ha puesto de manifiesto la existencia de importantes mecanismos de comunicación microbiana que afectan a la estabilidad de la biopelícula permitiendo la organización/desorganización de la actividad y el asentamiento/desprendimiento de su soporte. Así, existe un mecanismo de comunicación bacteriana de efecto positivo (*Quorum Sensing*) y otro negativo (*Quorum Quenching*). Las proteínas responsables de estos mecanismos de comunicación bacteriana o *Quorum Sensing* (QS) y de bloqueo de comunicación bacteriana o *Quorum Quenching* (QQ) fueron descubiertas a comienzos de los noventa (Fuqua *et al.*, 1994). Según los trabajos publicados por Otero *et al.* (2004) y Otero & Romero (2010), la detección del quórum o *Quorum*

Sensing (QS) describe la capacidad de un microorganismo para percibir y responder a la densidad poblacional mediante la regulación de la expresión génica, siendo así capaz de desarrollar un comportamiento social coordinado mediante la producción de pequeñas moléculas señal. Si estas moléculas señal son eliminadas del medio, es decir, si cortamos la comunicación entre los organismos se produce el proceso contrario denominado interceptación del quórum o *Quorum Quenching* (QQ).

II. Interacción biofilm-sustrato: colonización biológica de superficies expuestas al exterior

La formación de un biofilm requiere la presencia de un sustrato y son pocos los sustratos que no se ven afectados por biofilms, ocupando los biofilms subaéreos la mayor parte de la superficie terrestre (Krumbein *et al.*, 2003). En ciertos casos su presencia resulta beneficiosa, ya que estabilizan y fertilizan suelos (Acea *et al.*, 2001, 2003), sedimentos (Liess & Francoeur, 2010) y rocas (Prieto *et al.*, 2005, 2006). En otros casos su aparición, que suele producirse desde las primeras etapas de exposición de prácticamente cualquier superficie a la intemperie (**Figura 2**, Silva *et al.*, 1997; Gaylarde & Morton, 1999; Warscheid & Braams, 2000), provoca no sólo un cambio estético derivado de la presencia de pigmentos biológicos (Urzì *et al.*, 1992) sino también un problema evidente en términos de biodeterioro ("cualquier cambio indeseable en las propiedades de un material, originado por la actividad vital de los organismos", Hueck, 1965) y envejecimiento acelerado (Warscheid & Braams, 2000). El desarrollo de los biofilms degrada activamente los materiales al producir condiciones ácidas/alcalinas, retener la humedad y absorber el calor de forma diferencial en función de la coloración que presenten (Krumbein, 1988; Garty, 1990; Warscheid *et al.*, 1991, 1996), por lo que su desarrollo resulta especialmente dañino al producirse sobre superficies valiosas desde un punto de vista artístico e histórico (Figura 2, Dornieden *et al.*, 2000).

El sustrato representa para los microorganismos formadores del biofilm un espacio o superficie donde desarrollar su actividad biológica, así como la fuente de energía para su desarrollo (Gorbushina & Krumbein, 2000). Por esta razón, en el caso de superficies inertes es necesario un proceso de colonización secuencial en el que el sustrato en cuestión se va convirtiendo poco a poco en el ecosistema adecuado para los colonizadores implicados. Así, la secuencia de colonización no es caprichosa sino que responde a la propia estrategia de los organismos. Los colonizadores primarios del sustrato son por lo general los microorganismos autotróficos tales como diatomeas, algas, bacterias fotoautotróficas *sensu lato* y cianobacterias, que sólo necesitan agua y una mínima cantidad de sales minerales para asentarse y poder desarrollarse sobre el sustrato (Saiz-Jimenez & Ariño, 1995). Su crecimiento por lo general provoca el denominado verdín (*greening*) que raramente es uniforme formando manchas de tonalidad verdosa en áreas húmedas y con una presencia mayor en los lugares sombreados que en los

expuestos, debido a que los últimos se secan más rápidamente (Barberousse *et al.*, 2006; Smith *et al.*, 2011). Es la duración del período de humedad, más que la frecuencia, lo que resulta crucial para predisponer un sustrato a su colonización por este tipo de organismos, que resulta favorecida además, cuando existe vegetación adyacente (Saiz-Jimenez & Ariño, 1995; Smith *et al.*, 2011). En el caso concreto de las cianobacterias (bacterias oxigénicas fotoautotróficas), éstas poseen una serie de capacidades como: tolerancia a la desecación y al estrés hídrico, a altos niveles de sales, resistencia a altas temperaturas y uso eficiente de radiaciones de baja intensidad de la luz solar, que explican su presencia generalizada en ciertos sustratos soportando las condiciones ambientales más extremas (*e.g.* Friedmann, 1980). La presencia de los organismos pioneros da paso a la formación evolutiva de consorcios microbianos más complejos al permitir el asentamiento de otras especies (microorganismos heterótrofos) con el consecuente crecimiento del biofilm, en el que se incluyen ahora líquenes, bacterias heterótrofas, hongos, briófitos *sensu lato* e incluso plantas superiores (Ortega-Calvo *et al.*, 1991a; Saiz-Jimenez, 1992; Tiano, 1993; Tomaselli *et al.*, 2000; Crispim *et al.*, 2003; Sterflinger, 2010). Estos nuevos organismos son más deteriorantes para el sustrato, ya que la mayor parte (bacterias heterótrofas, hongos y líquenes) metabolizan la materia orgánica producida por los fotoautótrofos y secretan ácidos orgánicos que degradan químicamente el sustrato (Warscheid & Braams, 2000). Además, provocan un daño físico causado por la penetración de las estructuras filamentosas de anclaje, particularmente las hifas de los hongos, dentro de las cavidades porosas de la superficie (Hirsch *et al.*, 1995; Prieto *et al.*, 2000; Silva & Prieto, 2004), que al humectarse se expanden ejerciendo presión en el interior del poro y abriendo fisuras que pueden derivar en la formación de ampollas y el desprendimiento del material (*detachment*/*spalling*). También, la superficie mucosa y por lo general cargada negativamente (Costerton *et al.*, 1978) del biofilm favorece la adsorción de cationes y de moléculas orgánicas, y la adherencia de partículas transportadas por el viento (polvo, polen, partículas de carbón elemental, cenizas volantes, etc.) dando lugar a una pátina oscura más consistente y difícil de eliminar, que recibe el nombre de pátina negra (*black crust*) (Camuffo, 1995). Estas pátinas además del origen biogénico en ambientes contaminados, pueden presentar otros orígenes, como el biogénico en ambientes no contaminados (Aira, 2007; Gaylarde *et al.*, 2007; Prieto *et al.*, 2007; Silva *et al.*, 2009) y el no-biogénico (Del Monte *et al.*, 2001; Aira, 2007; Prieto *et al.*, 2007; Silva *et al.*, 2009).

Debido a que provoca un cambio estético de los elementos sobre los que se asienta, el aspecto del biofilm debe ser tenido muy en cuenta. En lo que se refiere a su coloración, ésta varía según el tipo de organismos y partículas que lo conforman. El color de los organismos está determinado por el tipo y abundancia de pigmentos biológicos que poseen, que a su vez varían en función de las condiciones ambientales, tales como cambios en nutrientes, luz, temperatura, radiación ultravioleta y pH (*e.g.* Tandeu de Marsac, 1977; Collier & Grossman, 1992; Soltani *et*

al., 2006). De modo general, los pigmentos biológicos presentan tonalidades: rojizas (carotenoides y ficobiliproteínas ficoeritrinas), amarillentas (carotenoides), verdosas (clorofilas y

Figura 2. Diversidad de biofilms subaéreos (terrestres). (a) "La casa de esquí", también llamada "La casa del futuro" o "Futuro", diseñada por el arquitecto finlandés Matti Suuronen en 1965 en Múnich (Baviera, Alemania). Su exterior, compuesto por plástico y fibra de vidrio reforzada con poliéster, poliuretano-poliéster y polimetacrilato de metilo (plexiglás), presenta una visible colonización biológica. Se trata de un ejemplo de la presencia de biofilms en objetos de arte contemporáneo. (Imagen extraída de Cappitelli *et al.*, 2006). (b) Detalle del exterior de "Futuro", mostrando una zona de crecimiento del biofilm formado esencialmente por cianobacterias y arqueas (Cappitelli *et al.*, 2006). (c) Detalle de la fachada este (donde se encuentra ubicada la Puerta Santa) de la Catedral de Santiago de Compostela (A Coruña, España), construida en su totalidad en roca granítica. La colonización biológica en esta zona es variada con presencia de briófitos, líquenes, algas y cianobacterias. (d) Detalle de la pared con un abundante verdín en la parte superior del claustro del monasterio de San Martín Pinario situado en Santiago de Compostela (A Coruña, España). (e) Detalle de pared y suelo con visible colonización biológica de una de las construcciones de la villa romana de Chedworth, una de las mayores villas romanas en Gran Bretaña, situada en Gloucestershire (Inglaterra).

ficobiliproteínas aloficocianinas) y azuladas (ficobiliproteínas ficocianinas), así como pardas-oscuras-negras debidas a las melaninas y scytoneminas (García-Pichel & Castenholz, 1991; Proteau *et al.*, 1993). Los pigmentos biológicos no son comunes a todos los microorganismos, las ficobiliproteínas por ejemplo son exclusivas de cianobacterias y algas rojas (Glazer, 1977) y las scytoneminas sólo aparecen en cianobacterias (García-Pichel & Castenholz, 1991), por lo

que en ciertas ocasiones el color del biofilm puede orientar acerca del tipo de microorganismo que lo forma. Sin embargo, es difícil determinar visualmente a qué tipo de pigmento y microorganismo es debida la coloración de la biopelícula; así por ejemplo, una biopelícula rosada cubriendo una de las superficies de piedra caliza de las ruínas mayas de Edzná (Campeche, México) debía su color a una concentración alta de carotenoides pertenecientes al alga *Trentepohlia umbrina* (Gaylarde *et al.*, 2006), mientras que una coloración similar presente en los frescos realizados por Luca Signorelli en la Capilla de San Brizio (Catedral de Orvieto, Umbría, Italia) era debida a las ficobiliproteínas rojizas (ficoeritrinas) pertenecientes a organismos cianobacterianos (Cappitelli *et al.*, 2009). En otros casos, sobre todo cuando el biofilm es de escaso grosor y su coloración no es la más habitual, como es el caso de los colores azulados y rosados, resulta difícil a simple vista determinar si el color es propio del sustrato o se debe a la colonización biológica (**Figura 3**, Gaylarde *et al.*, 2006). Existen algunos trabajos en los que el color del biofilm (determinado cualitativamente) se relaciona con el tipo de pigmento y/o microorganismo; algunos ejemplos son las biopelículas de color naranja debidas a algas y bacterias y las películas de color grisáceo producidas principalmente por hongos que se encontraban en la roca calcárea de la torre barroca de Noto en Siracusa (Sicilia, Italia) (Urzì & Realini, 1998) y las biopelículas de color negro de las piedras del exterior del templo de Bayón (Angkor, Camboya) formadas por especies del género *Dematiáceous* (ascomicetos) que producían un alto contenido en melanina (Sterflinger, 2000). A este respecto, sin embargo, cabe señalar que el conocimiento de la magnitud de la diversidad microbiana que se encuentra en los biofilms subaéreos está lejos de ser completo, ya que mediante las técnicas tradicionales de cultivo se aíslan, y por tanto identifican, menos del 1% de la diversidad total (Ward *et al.*, 1990). En los últimos años, se han desarrollado diversos métodos moleculares para permitir la identificación de microorganismos en muestras ambientales (Amann *et al.*, 1995). Técnicas de biología molecular como la electroforesis en gel con gradiente desnaturalizante (EGGD), el análisis de polimorfismo conformacional de un solo filamento o de cadena sencilla (PCCS) y la hibridación fluorescente *in situ* (HISF) apuntan la posibilidad de que bacterias halófilas o halotolerantes, alcalófilas y también arqueas formen parte de los biofilms subaéreos que se encuentran en superficies del Patrimonio histórico artístico (Saiz-Jiménez & Laiz, 2000; McNamara *et al.*, 2003; Ortega-Morales *et al.*, 2004; Cappitelli *et al.*, 2007; Piñar *et al.* 2009).

Por lo general, los materiales sintéticos (Figura 2a, b) se consideran más resistentes a los daños químicos, físicos y biológicos producidos por la presencia del biofilm que los materiales naturales (Figura 2c, d, e) (Cappitelli *et al.*, 2006). En cualquier caso, la disponibilidad de agua y nutrientes en el sustrato es el principal factor limitante de la colonización biológica y del consiguiente desarrollo del biofilm, y las condiciones ambientales junto a las características del sustrato determinan el tipo de biofilm así como su velocidad de crecimiento (Silva *et al.*, 1997). En este sentido, el conjunto de las propiedades de un sustrato que determina su capacidad

para ser colonizado por microorganismos se ha denominado biorreceptividad (Guillitte, 1995). Características como una alta porosidad y rugosidad superficial favorecen *a priori* la colonización biológica y formación del biofilm, al facilitar la adhesión de los microorganismos al sustrato, aumentando por tanto su biorreceptividad (Caneva *et al.*, 1991; Silva *et al.*, 1997; Warscheid & Braams, 2000; Prieto & Silva, 2005; Miller *et al.*, 2006). Sin embargo, la influencia exacta de las propiedades del sustrato en el crecimiento microbiano y resultante biorreceptividad no está aún completamente clara (Miller *et al.*, 2012).

Figura 3. Columnas de mármol en el interior de una iglesia de la costa mediterránea. La columna de la derecha presenta una coloración rojo anaranjada que a simple vista parece propia del material y en realidad es debida a una biopelícula.

Ciñéndonos al ámbito litológico, la presencia de biofilms también supone uno de los principales problemas que atañen a la conservación del parque de edificios, tanto a aquellos que pertenecen al Patrimonio histórico-artístico como a los de reciente construcción (Herrera & Videla, 2004; Crispim & Gaylarde, 2005; Gorbushina, 2007; Scheerer *et al.*, 2009). La mayor parte de los monumentos elaborados por la humanidad están construidos con piedra natural o la incluyen como elemento auxiliar. Entre las rocas más utilizadas para este fin se encuentran las de mayor durabilidad, es decir, de alta resistencia a la meteorización como son los mármoles y las rocas graníticas. La aparición de biofilms sobre este tipo de construcciones suele ser epilítica (sobre la superficie) debido en parte a la baja porosidad de este tipo de rocas (Prieto *et al.*, 1999, 2000; Silva *et al.*, 1999). Rocas más porosas como calizas y areniscas presentan en muchos casos un crecimiento endolítico (en el interior de la roca) del biofilm

(Saiz-Jimenez *et al.*, 1990; Miller *et al.*, 2010). Los biofilms endolíticos han sido clasificados en más detalle por Golubic *et al.* (1981) en función de su presencia en grietas (chasmoendolíticos), en poros (criptoendolíticos), o si muestran una verdadera capacidad de perforación de la matriz de piedra (euendolíticos). El clima de la zona también influye en este aspecto, Warscheid *et al.* (1996) consideran que mientras en los climas templados los microorganismos tienden a colonizar la superficie de las rocas, en los climas tropicales y subtropicales prefieren penetrar en el interior del sustrato con el fin de protegerse de la luz del sol y la desecación. Matthes-Sears *et al.* (1997), sin embargo, sugieren que los microorganismos se ven obligados a convertirse en endolíticos no por protección frente a las condiciones ambientales adversas sino en la búsqueda de mayores nutrientes y un mayor espacio. Según la mayoría de los autores, las poblaciones endolíticas son extremadamente difíciles de eliminar y altamente deteriorantes, al contribuir a la disminución de la cohesión entre los granos minerales a profundidades de hasta varios milímetros (*e.g.* Ascaso *et al.*, 1998; Miller *et al.*, 2010), aunque Hoppert *et al.* (2004) a este respecto apuntan que, dado que sus tasas de crecimiento en el interior de la roca son bajas, las poblaciones endolíticas rara vez están asociadas a procesos de biodeterioro. En el caso de biofilms epilíticos, el biodeterioro está provocado en primera instancia por la decoloración a la que dan lugar en la superficie, que ocasiona no sólo un problema estético sino también un problema físico ya que en las áreas oscuramente coloreadas decrece el albedo, absorbiendo más radiación solar, lo que repercute en un aumento de los ciclos frío/calor y humectación/secado, que termina causando un estrés físico en el biofilm y un estrés mecánico en el interior de la roca (Warke *et al.*, 1996; Warscheid & Braams, 2000; Sand *et al.*, 2002). Las temperaturas que se alcanzan en las superficies pétreas colonizadas por organismos oscuros fueron registradas por Garty en 1990, mostrando una diferencia en más de 8ºC con respecto a las áreas sin colonizar. Una variación muy similar de temperatura fue obtenida por Carter & Viles (2004) en bloques de roca calcárea con y sin cobertura liquénica, mostrando además los mayores gradientes de temperatura justo por debajo del biofilm liquénico.

Diversos estudios han demostrado que las cianobacterias constituyen la biomasa mayoritaria que se desarrolla sobre las superficies de piedra natural (Ortega-Morales *et al.*, 2000; Gaylarde *et al.*, 2001). Existen dos teorías sobre el efecto concreto de biodeterioro que provocan este tipo de organismos, junto con los organismos fotoautotróficos en general, sobre las superficies pétreas. Mientras algunos autores consideran despreciable la acción agresiva de las cianobacterias y algas sobre el sustrato, otros reportan datos que apuntan a un mecanismo de deterioro directo en el que en primer lugar se produce un deterioro físico llevado a cabo por el biofilm, que emplea la masa de filamentos entrecruzados reunidos en la matriz mucosa de las vainas de cianobacterias y algas para extraer los granos minerales de la roca y las partículas de la superficie (Ortega-Calvo *et al.*, 1991a, 1991b). En contra de lo que pueda parecer muchas cianobacterias, no necesariamente filamentosas, presentan esta dañina habilidad (Scheerer *et*

al., 2009). A partir de ahí mediante contracciones y expansiones, la biopelícula hace que se desprendan los granos minerales y partículas, contribuyendo a la desagregación gradual del material (Ortega-Calvo *et al.*, 1991a, 1991b). Además, la formación de biofilms de cianobacterias y algas produce una mayor retención de agua en la superficie del material, incrementando los procesos de hidrólisis y otros mecanismos de meteorización.

Una conclusión común a todos los estudios relativos al biodeterioro de los materiales pétreos provocado por la aparición de biopelículas, es la necesidad de invertir esfuerzos en la detección precoz de la colonización biológica, es decir cuando el biofilm aún se encuentra en las primeras etapas de su formación, ya que en ese momento la intervención sería mínima y se enmarcaría en el campo de la conservación preventiva, que se define como "todas aquellas medidas y acciones que tienen como objetivo evitar o minimizar futuros deterioros o pérdidas" (ICOM-CC, 2008). Una intervención mayor para la eliminación de biofilms ya formados debe ser cuidadosamente evaluada, ya que en muchos casos supone un deterioro importante de la superficie tras la eliminación de la biopelícula (**Figura 4**). Además, en el caso de aplicar a continuación algún tratamiento, incluido la simple limpieza con agua, éste puede exacerbar una futura colonización biológica (Young, 1997). A finales de los años noventa Young (1997) apuntaba que tras la limpieza de las fachadas de edificios en Escocia (Reino Unido), la reaparición de partículas inorgánicas en superficie tardaba varios años en producirse, sin embargo, el crecimiento de las algas verdes (*greening*) ocurría en pocos meses. Dos ejemplos de la aplicación de tratamientos de restauración que han llevado a un aumento de la colonización microbiana, son el empleo de un consolidante a base de extractos de plantas locales utilizado en las ruinas mayas de Joya de Cerén (El Salvador), el cual favoreció el crecimiento de hongos y actinomicetos (Caneva & Nugari, 2005), y los consolidantes sintéticos de polilaurilmetacrilato y poliisobutilmetacrilato empleados en la catedral de Milán (Italia) en los años setenta que favorecieron también el crecimiento de hongos (Cappitelli *et al.*, 2007).

Las acciones contra la colonización biológica y el desarrollo de biofilms se pueden dividir en cuatro grandes categorías (Scheerer *et al.*, 2009): (1) control indirecto mediante la modificación de las condiciones ambientales, generando condiciones que resulten adversas para los microorganismos, (2) eliminación mecánica, (3) empleo de productos químicos (biocidas), y, (4) métodos físicos de erradicación, como el uso de un campo electromagnético o el uso de ultrasonidos. La primera de las acciones resulta la más recomendable, sin embargo en pocas ocasiones se puede aplicar debido a la gran adaptabilidad de los microorganismos, en especial bacterias y cianobacterias, a los cambios externos, no pudiendo aplicarse nunca por razones obvias en casos de superficies expuestas a la intemperie. Según las dimensiones de la superficie a tratar, en la eliminación mecánica se puede emplear el bisturí o chorros de aire, agua o diversos abrasivos a presión. El principal inconveniente de este tipo de técnicas es que pueden dañar el sustrato por microabrasión debido al contacto directo entre los agentes

Figura 4. Escultura en mármol en Villa Dosi Delfino situada cerca de Pontremoli (Massa-Carrara, Italia). En la fotografía de la izquierda se observa el estado de la escultura antes de realizar las labores de limpieza. A la derecha aparece un detalle de la misma escultura tras haber eliminado los biofilms que la recubrían, en esta fotografía se aprecia el daño causado por los organismos a la superficie.
Imágenes cedidas por el Dr. Piero Tiano, presentadas en "International conference on microbiology and conservation: of microbes and art". Florencia (Italia), 16-19 June 1999 y publicadas por Kluwer Academic en "Of microbes and art: the role of microbial communities in the degradation and protection of cultural heritage" (2000).

abrasivos y la superficie. A pesar de esto, la limpieza de las fachadas de piedra de edificios colonizados es una intervención frecuente que supone un gasto económico considerable puesto que debe realizarse de forma periódica ya que, aunque se consiga eliminar el total de los biofilms visibles, éstos vuelven a aparecer en un plazo de tiempo más o menos corto. Una medida de mantenimiento útil a este respecto es realizar la limpieza en las fases incipientes de la formación de los biofilms, de manera que el área a tratar sea menor y la limpieza más fácil y eficaz, lo que repercutirá también en un menor coste económico. Los biocidas, por su parte, son un tratamiento frecuente, en especial en el caso de la rehabilitación de edificios antiguos por lo general profusamente colonizados. Sin embargo, en ocasiones presentan efectos perjudiciales sobre la piedra como por ejemplo la decoloración u oxidación/reducción de algunos componentes como el hierro y la formación sales en superficie (Caneva *et al.*, 1991; Kumar & Kumar, 1999; Warscheid & Braams, 2000). La ecotoxicidad de algunos biocidas

comerciales también los vuelve débiles candidatos para su uso en ambientes externos, y la presencia de nitrógeno en algunas formulaciones puede servir de nutriente para los microorganismos (Warscheid & Braams, 2000). Pero sin duda el aspecto más negativo de la aplicación de un biocida es que la eliminación de la comunidad microbiana habitual pueda dar lugar a una sucesión de nuevos microorganismos más perjudiciales para el sustrato, debido a que la inhibición de grupos específicos de microorganismos favorece el crecimiento de otros (Webster *et al.*, 1992; Warscheid & Braams, 2000). La última de las estrategias, los métodos físicos, se vuelve peligrosa y muy costosa al querer aplicarla sobre grandes superficies.

III. Detección y cuantificación de la colonización biológica y desarrollo del biofilm. Medida instrumental del color y sistema CIELAB

Partiendo de la base de que todas las superficies pétreas, más tarde o más temprano, van a ser colonizadas por organismos vivos (con la correspondiente formación de biopelículas) y que dicha colonización supone no sólo un daño estético, sino también químico y físico que aumenta a medida que la colonización avanza, la detección precoz de la formación del biofilm constituiría un importante progreso en lo que atañe a la conservación preventiva de edificios, monumentos y esculturas construidos en piedra.

En la detección temprana de estos procesos de colonización biológica, algas y cianobacterias son clave ya que debido a su carácter autótrofo suelen ser pioneras en la colonización de superficies pétreas. Por ello, las investigaciones desarrolladas en este campo han ido dirigidas principalmente a la detección y cuantificación de este tipo de microorganismos. Martín (1990) realizó una recopilación de la metodología tradicional utilizada en el estudio de la agresión biológica en obras de piedra de interés histórico artístico; dicho autor clasifica los métodos empleados para la cuantificación de la presencia de microorganismos en métodos morfológicos, microbiológicos, histoquímicos y bioquímicos, químicos y fisicoquímicos. En la presente introducción para una mejor compresión se considera una clasificación distinta, diferenciando tres clases de métodos: morfológicos y estructurales, microbiológicos y extractivos.

Los métodos morfológicos y estructurales son utilizados por la mayoría de los autores para el reconocimiento de las especies colonizadoras. Implican técnicas de visualización del material pétreo en campo, con observaciones macroscópicas (Urzì *et al.*, 1992; Krumbein, 1993), o en laboratorio donde la microscopía permite conocer de manera más detallada las características del microorganismo y por tanto su identificación y clasificación. Para este fin se realizan observaciones directas con el estereomicroscopio, que permite el reconocimiento de las estructuras fisiológicas específicas de los organismos (Prieto *et al.*, 1995; Shirakawa *et al.*, 2003); el microscopio óptico (MO), que permite el reconocimiento de la morfología y estructura

celular específica de cada grupo de microorganismos con una preparación de muestra muy sencilla (Ariño, 1996); los colorantes vitales fluorescentes junto con el uso del microscopio de fluorescencia (Tayler & May, 1991) y la bioluminiscencia (Ranalli *et al.*, 2000), aportando cada una de estas técnicas un tipo de información, en muchos casos complementaria a la ofrecida por el resto. Técnicas aparecidas más recientemente para el mismo fin, son las observaciones directas con microscopio electrónico de barrido (Ortega-Calvo *et al.*, 1991a; Prieto *et al.*, 1997), en modo de electrones retrodispersados (MEB-ERD), microscopia de barrido a bajas temperaturas (MEB-CRIO), microscopia láser confocal (MLC) y microscopia electrónica de transmisión (MET) (De los Ríos *et al.*, 2008), que permite la observación tridimensional del microorganismo con una ampliación de hasta 10.000 aumentos.

Los métodos microbiológicos por su parte, se basan en el recuento de colonias después de un periodo largo de incubación en medios específicos y condiciones adecuadas de luz y temperatura (ICR-CNR, 1988); de esta manera se conoce el número de unidades formadoras de colonias por gramo de muestra (UFC/g). Si la incubación se realiza en medio líquido se emplea el estadístico de McCrady (Hurley & Roscoe, 1983) para determinar el número más probable de organismos por gramo de muestra (NMP/g). Dos ejemplos de la aplicación de estos métodos en muestras tomadas sobre monumentos son los estudios realizados por Ortega-Calvo *et al.* (1993) y Hyvärinen *et al.* (2002).

Con los métodos extractivos la biomasa se estima a partir de la cantidad extraída de diversos componentes celulares presentes en los microorganismos (Bartolini & Monte, 2000), como determinadas proteínas (Schwenzfeier *et al.*, 2011), ATP (Tiano *et al.*, 1989), ADN (Saiz-Jimenez & Laiz, 2000; Tomaselli *et al.*, 2000), lípidos y polisacáridos (Di Pippo *et al.*, 2009). En el caso de microorganismos fototróficos el contenido de pigmentos fotosintéticos en general, y en particular el contenido en clorofila-a (Bell & Sommerfeld, 1987; Nagarkar & Williams, 1997; Prieto *et al.*, 2004; Schumann *et al.*, 2005; Eggert *et al.*, 2006), es un buen indicador de la presencia y cantidad de microorganismos, resultando probablemente el método más prolijo y uno de los más fiables. Asociados a estos métodos extractivos suelen emplearse los métodos fisiológicos, en los que la biomasa fotoautotrófica se estima a partir del aumento inicial de la tasa de respiración (Bartolini & Monte, 2000). Por otro lado, a través de la medida de las actividades enzimáticas tales como la actividad deshidrogenasa y la actividad enzimática total, medida a partir de la hidrólisis del diacetato de fluoresceína (DAF), también se puede estimar la actividad microbiana; así lo han hecho autores como Tayler & May (2000) que emplearon la medida de la actividad deshidrogenasa en monumentos antiguos de piedra arenisca y Prieto *et al.* (2004) que utilizaron la medida de DAF en experimentos de laboratorio realizados con roca granítica.

Si bien todas las técnicas anteriormente citadas presentan ventajas y su uso está ampliamente difundido en investigación, también muestran ciertos inconvenientes. Así, además de ser todas

ellas costosas y lentas en su ejecución, la mayor parte son destructivas y deben ser llevadas a cabo en el laboratorio lo que implica la necesidad de realizar una toma de muestra previa, lo cual en el caso de estudios realizados sobre superficies del Patrimonio monumental supone un gran inconveniente, resultando en muchos casos imposible. Para solventar estos problemas una posibilidad es recurrir a técnicas basadas en metodologías ópticas que, debido al pequeño tamaño de los organismos en cuestión deben tener un alto poder de magnificación y de resolución. A este respecto dos de las características físicas de los microorganismos fototróficos pueden ser empleadas: la fluorescencia emitida por su clorofila y el color al que dan lugar al acumularse sobre una superficie sólida. De cada una de estas características surge una técnica de detección y monitorización del crecimiento de biofilms en superficie: (i) la medida de la emisión de fluorescencia de la clorofila *in vivo* y (ii) la medida instrumental del color empleando un espectrofotómetro o un colorímetro triestímulo. En ambos casos es posible realizar una monitorización de la superficie, incluso de gran tamaño como la fachada de un edificio, ya que ambas técnicas son no-destructivas (no-invasivas) y de aplicación *on site*, evitando así la toma de muestra.

Son varios los trabajos donde se ha aplicado el método de detección *in vivo* de la presencia de clorofila mediante espectrofluorimetría y la cuantificación del área colonizada como porcentaje del área total (Guillite & Dreesen, 1995; Brechet *et al.*, 1996, 1997; McStay *et al.*, 2001; Miller *et al.*, 2006, 2010). Sin embargo, la medida de fluorescencia presenta algunas desventajas frente a la medida de color, como son que la señal de fluorescencia se produce en un corto espacio de tiempo, que depende de las condiciones fisiológicas de los organismos (no tomando en cuenta las células muertas) y, principalmente, que es muy difícil abordar el análisis de los espectros con características desconocidas, es decir, la técnica requiere un conocimiento básico de las características espectrales de los parámetros investigados con el fin de elegir las bandas correctamente y separar contribuciones de fluorescencia debidas a factores externos a los microorganismos, como son la fluorescencia de algunos minerales (Lognoli *et al.*, 2003). El carbonato cálcico, la fluorita, la scheelita y los minerales de uranio son algunos de los componentes minerales que pueden presentar fluorescencia, que por lo general consiste en una amplia banda de emisión en la región azul del espectro, por ejemplo en el caso del carbonato cálcico con un máximo de emisión alrededor de 420 nm (Cecchi *et al.*, 2000).

En lo que respecta a la medida instrumental del color para la cuantificación de la colonización biológica sobre fachadas de edificios, Newby *et al.* (1991) fueron de los primeros autores en relacionar la medida de la reflectancia, que puede obtenerse a través de un espectrofotómetro o un colorímetro triestímulo, con el cambio de color provocado por la acumulación de partículas sobre una superficie sólida. Basándose en un trabajo previo de Ball (1989), Newby *et al.* (1991) definieron el ensuciamiento (*soiling*) de un edificio como “un efecto óptico, un oscurecimiento de la superficie que se puede medir como un cambio en la reflectancia de la luz, y que generalmente está relacionado con la deposición de partículas procedentes del aire sobre la

superficie del edificio". Años después y tomando en cuenta esta definición, Gorbushina & Krumbein (2000) afirmaron que muchos, si no la mayoría, de estos cambios espectrales están relacionados con el crecimiento de las biopelículas coloreadas; dichos autores consideran que las partículas transportadas por el viento (polvo, polen, partículas de carbón elemental, etc.) y los microorganismos a menudo actúan concomitantemente para producir el ensuciamiento del edificio, apuntando que, ya en 1853 Ehrenberg había llegado a la conclusión de que los microorganismos, en parte debido a sus productos extracelulares viscosos, podían atrapar partículas del aire de manera más eficiente que la superficie de la roca limpia, *i.e.* sin biopelícula (Krumbein, 1995).

El empleo de colorímetros triestímulo y espectrofotómetros portátiles para cuantificar el color generado por microorganismos fototróficos que se desarrollan de forma epilítica sobre sustratos pétreos, no empezó a difundirse hasta finales de los noventa. Así, como parte de un programa de investigación más amplio financiado por Historic Scotland (http://www.historic-scotland.gov.uk/), investigadores de la Robert Gordon University (Aberdeen, Escocia. Reino Unido) realizaron una serie de experimentos en edificios de piedra arenisca, en los que se monitorizaba mediante un colorímetro portátil triestímulo el cambio de color en sus fachadas provocado por la colonización biológica (algas) tras la aplicación de varios tratamientos biocidas (Urquhart *et al.*, 1995; Young *et al.*, 1995; Young, 1997). En esa misma época, Urzì & Realini (1998) publicaron un estudio donde correlacionaban el color naranja o gris, determinado instrumentalmente con un colorímetro portátil triestímulo, de las pátinas biológicas en la roca calcárea de la torre barroca de Noto en Siracusa (Sicilia, Italia) con los microorganismos responsables, algas y bacterias u hongos respectivamente. Por su parte, Viles y colaboradores trabajaron entre 1987 y 1995 en el *British National Materials Exposure Programme* (N.M.E.P.) en el que la colonización microbiana, el ensuciamiento (*soiling*) y el deterioro (*decay*) de muestras de piedra caliza emplazadas en más de 20 sitios de Gran Bretaña (Reino Unido) fueron monitorizados por un periodo de 1, 2, 4 u 8 años dependiendo de las condiciones climáticas y de contaminación de la ubicación. Para ello emplearon un espectrofotómetro portátil además de técnicas de caracterización, como la microscopia electrónica de barrido (Viles *et al.*, 2002). Posteriormente, el estudio se centró en las construcciones de piedra caliza localizadas junto a las carreteras con diferentes flujos de tráfico de Oxford (Inglaterra, Reino Unido) que fueron monitorizadas durante un periodo de tres años (Viles & Gorbushina, 2003). Viles siguió trabajando en esa misma línea en años posteriores, tras haberse aplicado en 1999 la *Oxford Transport Strategy* (OET) con el fin de restringir el acceso, en particular de los vehículos privados, al centro histórico de la ciudad; registrando los cambios en las pautas de crecimiento de organismos y en el ensuciamiento de las construcciones de Oxford (Thornbush & Viles, 2004, 2006).

Por otra parte, la validez del uso del color como estimador de la biomasa de organismos fototróficos sobre superficies pétreas fue demostrada por Prieto *et al.* (2004), a partir de

comparaciones entre los métodos más usuales de cuantificación de biomasa fototrófica, como es la medición de la clorofila-a *in vitro* y la actividad enzimática total medida a partir de la hidrólisis del diacetato de fluoresceína (DAF); demostrando además, a partir de experimentos de laboratorio, que existe una relación directa entre la cantidad de organismos fototróficos depositados sobre una superficie y el color que generan (Prieto *et al.*, 2002). Estos mismos autores realizaron a continuación un trabajo de campo, en el que empleaban un espectrofotómetro portátil para sólidos para monitorizar el crecimiento de biofilms inducidos en varios frentes de una cantera de cuarzo a cielo abierto (Prieto *et al.*, 2005). El crecimiento de los biofilms tenía como finalidad enmascarar el color blanco brillante del mineral reduciendo así el imparto visual de la explotación minera. De estos últimos trabajos se concluye, que una de las principales ventajas de la medida instrumental de color para la cuantificación de la biomasa fototrófica sobre sustratos de una coloración mayormente clara y homogénea, es que permite detectar la colonización biológica de forma precoz, incluso antes de que ésta sea percibida por el ojo humano (Prieto *et al.*, 2002, 2005). Esto supone una importante ventaja en la gestión y mantenimiento de superficies recién expuestas a la intemperie, así como en superficies tratadas en las que se ha eliminado la biopelícula existente, ya que en muchos casos aunque aparentemente la superficie tratada quede limpia, una observación más rigurosa deja patente que algunas de las estructuras biológicas permanecen entre los granos de la piedra, facilitando así la re-instalación de los organismos (Prieto *et al.*, 1995).

En lo que se refiere al análisis de las medidas instrumentales de color, en prácticamente la totalidad de los estudios realizados en este campo es el espacio de color CIELAB (CIE Publication 15-2, CIE, 1986) el que se emplea para representar y analizar los valores obtenidos. El espacio CIELAB ó CIE 1976 L*a*b* intenta reproducir un espacio de color que sea más "perceptivamente lineal" que otros espacios de color como RGB o CMYK. Perceptivamente lineal significa que un cambio de la misma cantidad o magnitud en un valor de color debe producir un cambio casi de la misma importancia visual. Específicamente con este propósito fue desarrollado este espacio por la *Commission Internationale d'Eclairage* (Comisión Internacional de la Iluminación: CIE), y está basado en el espacio de color CIE 1931 XYZ (CIE, 1932) y fuertemente influenciado por el espacio de color Munsell (Munsell, 1905). Considerando que el color depende de tres factores: la fuente luminosa, el objeto iluminado y el observador que capta la imagen, la CIE establece este espacio sobre la base de cuatro puntos fundamentales: fuente estándar de iluminación, condiciones exactas de observación, unidades matemáticas apropiadas y curvas del observador estándar (Wyszecki & Stiles, 1982).

El espacio CIELAB (**Figura 5**), que suele representarse como una esfera, un clindro o un cubo aunque esto no se ajuste a la realidad, está basado en el modelo de los colores opuestos y cada color se localiza dentro de un espacio tridimensional de tres ejes (L*a*b* ó $L^*C^*_{ab}h_{ab}$). Así, cada color está definido por tres coordenadas cartesianas, escalares o lineales, L*a*b*, donde L* es una medida de la claridad que varía de 100 (blanco absoluto) a 0 (negro absoluto), y a* y

b* definen las componentes de color rojo-verde y amarillo-azul, respectivamente. Así, un valor negativo de a* define un color más verde que rojo, mientras que un valor positivo de b* define un color más amarillo que azul. Además de este grupo de coordenadas escalares (L*a*b*) el espacio CIELAB puede ser representado mediante otro sistema de coordenadas cilíndricas o polares que sustituye a* y b* por,

croma $C^*_{ab} = \sqrt{a^{*2} + b^{*2}}$

y, tono angular $h_{ab} = \text{arco - tangente}(b^*/a^*)$.

En la percepción humana del color se distinguen tres características principales que corresponden a los tres parámetros básicos del color: claridad, croma y tono. La consideración de las coordenadas cilíndricas ($L^*C^*_{ab}h_{ab}$) en lugar de las escalares (L*a*b*) permite cuantificar el color del mismo modo en que es percibido, es decir teniendo en cuenta estos tres atributos de apreciación visual: claridad (su análogo en CIELAB es L*), croma (su análogo en CIELAB es C^*_{ab}) y tono (su análogo en CIELAB es h_{ab}).

Una de las ventajas del espacio de color CIELAB frente a otros es que permite cuantificar la diferencia de color entre dos muestras mediante la combinación de las diferencias de sus tres coordenadas, tanto escalares como cilíndricas, en un espacio euclidiano. Este es el fundamento de la fórmula clásica de 1976 de diferencia de color CIELAB (Wyszecki & Stiles, 1982), que asume la uniformidad del espacio de color:

$$\Delta E^*_{ab} = \sqrt{(\Delta L^*)^2 + (\Delta a^*)^2 + (\Delta b^*)^2} \quad \text{ó} \quad \Delta E^*_{ab} = \sqrt{(\Delta L^*)^2 + (\Delta C^*_{ab})^2 + (\Delta H^*_{ab})^2}$$

Esta fórmula de distancia euclídea para medir la diferencia de color ha sido progresivamente revisada y mejorada debido al reconocimiento de la falta de uniformidad de este espacio. La mayoría de las fórmulas de diferencia de color utilizadas en la actualidad parten de las coordenadas del espacio CIELAB, introduciendo factores de ponderación (*weighting functions*), indicados por S (en otros textos, W), que consiguen una más estrecha relación entre las diferencias de color calculadas y percibidas respecto a CIELAB; y los números k, factores paramétricos (*parametric factors*) que representan variables dependientes de las condiciones de observación. Estos factores de ponderación (S) y factores paramétricos (k) se introducen sobre las diferencias CIELAB de claridad, croma y tono para corregir la falta de uniformidad perceptual del espacio, y así surgen las fórmulas de diferencia de color CIE94 (CIE Publication 116-1995, 1995):

$$\Delta E^*_{94}(k_L : k_C : k_H) = \sqrt{\left(\frac{\Delta L^*}{k_L S_L}\right)^2 + \left(\frac{\Delta C^*_{ab}}{k_C S_C}\right)^2 + \left(\frac{\Delta H^*_{ab}}{k_H S_H}\right)^2}$$

y CIEDE2000 (CIE Publication 142-2001, 2001), que incluye además un factor denominado término de rotación (R_T) y una transformación específica de la coordenada a*, que afecta principalmente a los colores con bajo croma (colores neutros):

$$\Delta E_{00}(k_L : k_C : k_H) = \left\{ \left(\frac{\Delta L'}{k_L S_L} \right)^2 + \left(\frac{\Delta C'}{k_C S_C} \right)^2 + \left(\frac{\Delta H'}{k_H S_H} \right)^2 + R_T \left(\frac{\Delta C' \cdot \Delta H'}{k_C S_C k_H S_H} \right) \right\}^{1/2}$$

Em ambas ecuaciones los factores paramétricos: los valores k_L, k_C, k_H sirven para ajustar las contribuciones relativas de claridad, croma y tono, y así, adoptando los valores k_L=1, k_C=1, k_H=1, las fórmulas que se obtienen son CIE94(1:1:1) y CIEDE2000(1:1:1); mientras que aumentando la contribución relativa a la diferencia de claridad, k_L=2, k_C=1, k_H=1, las fórmulas son CIE94(2:1:1) y CIEDE2000(2:1:1). En cuanto a la importancia relativa de estas correcciones (CIE94 y CIEDE2000), los autores destacan que la mejora de CIE94 sobre CIELAB es notablemente superior a la mejora de CIEDE2000 sobre CIE94 (Melgosa *et al.*, 2004).

El espacio de color CIELAB intenta linealizar las diferencias de color perceptibles por el ojo humano, usando la métrica de diferencias de color descritas por las elipses de MacAdam (MacAdam, 1942). Las relaciones no lineales para L*, a* y b* pretenden emular la respuesta no lineal del ojo humano. Además, los cambios uniformes de los componentes en el espacio de color L*a*b* tienen por objeto corresponder a cambios uniformes en el color percibido, por lo que las diferencias relativas de percepción entre dos colores en el espacio L*a*b* se pueden aproximar tratando cada color como un punto en un espacio tridimensional, con tres componentes: L*, a*, b* y tomando la distancia euclídea entre ellos.

Son varias las causas que podrían justificar la aceptación generalizada de CIELAB en los estudios científicos, así como en las aplicaciones industriales. Entre esas causas cabría citar el carácter oponente de sus coordenadas L*a*b*, la asociación de su otra terna de coordenadas $L^*C^*_{ab}h_{ab}$ con los tres atributos clásicos del color (claridad, croma y tono) o incluso su analogía respecto al espacio de color Munsell (Munsell, 1905), con el que mucha gente está bien familiarizada.

La instrumentación para la medida del color disponible en la actualidad muestra fundamentos similares, diferenciándose normalmente en el grado de sofisticación y en la configuración que presenta el aparato, la cual depende de la aplicación concreta a la que se destina (Capilla *et al.*, 2002). Las medidas instrumentales de color están sujetas a las condiciones de medida del espectrofotómetro o del colorímetro como son la configuración óptica y geometría de medida o de iluminación-observación (0/45, 45/0, d/0, …), el iluminante (A, C, D65, F11, …) y el observador (observadores estándar CIE 1931 - 2º y CIE 1964 - 10º), pudiendo estos dos últimos, iluminante y observador, prefijarse para generalizar el proceso de medida obteniendo

así medidas fiables y reproducibles que resultan comparables entre sí. La configuración óptica y geometría de medida de un colorímetro o un espectrofotómetro es propia del aparato y viene determinada por dos valores, X/Y, donde X es el valor que indica la dirección del haz que ilumina la muestra, e Y, la dirección de medición del haz reflejado. Según cómo se ilumine la muestra (X) y cómo se coloque el detector de luz reflejada con respecto a ésta (Y), los resultados pueden mostrar alguna discrepancia, por lo que, cuando se vaya a emplear más de un instrumento en la medida es recomendable comparar los resultados de las mediciones para poner de manifiesto esas diferencias instrumentales (*e.g.* Campos Acosta *et al.*, 2004). Entre las geometrías de medida más comunes están 0/45 y 45/0, que corresponden respectivamente a la situación en la que la muestra y el blanco de referencia son iluminados normalmente, es decir con 0º de inclinación, mientras que el detector está colocado de forma que registra la radiación reflejada a 45º y viceversa. También existen aparatos cuya configuración óptica o geometría es de esfera integradora, en estos casos la geometría se indica con una "d" que indica o que la muestra se ilumina difusamente, esto es con luz proveniente de todos lados (d/Y), o que en el detector se mide la componente total difusa (X/d). Así, si la iluminación es difusa y el detector se encuentra colocado normalmente a la muestra, la geometría es d/0, si se encuentra desplazado 8º, d/8, si se encuentra desplazado sólo 6º, d/6, etc. Si la iluminación está colocada en la normal a la muestra y al detector llega la componente total difusa, la geometría es 0/d, si la iluminación se encuentra desplazada 8º, 8/d, si se encuentra desplazada sólo 6º, 6/d, etc.

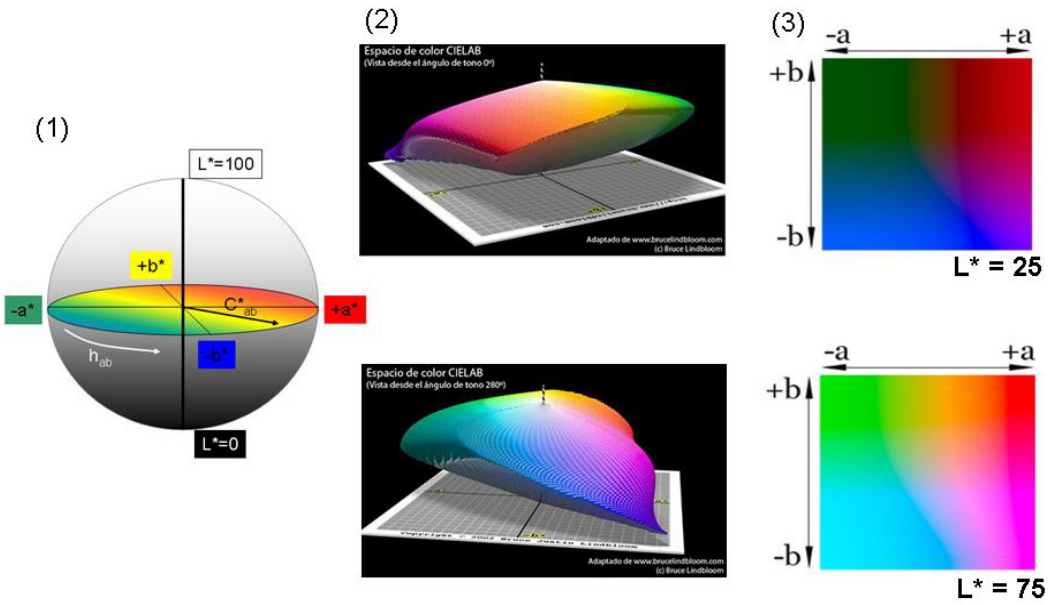

Figura 5. Espacio de color CIELAB. (1) Representación clásica del espacio de color CIELAB en una esfera, donde aparecen reflejados los dos grupos de coordenadas, escalares (L*a*b*) y polares ($L^*C^*_{ab}h_{ab}$); (2) Representación real del espacio de color CIELAB, que no es ni una esfera, ni un cilindro, ni un cubo, sino un cuerpo sólido de límites irregulares. (Adaptado de: http://www.brucelindbloom.com/index.html?ColorCheckerRGB.html); (3) Planos de color a*–b* con un valor de claridad (L*) constante.

Cuando se mide con las geometrías 0/45 y 45/0, se excluye automáticamente la componente especular de la reflectancia, es decir “aquélla que viene de una dirección concreta y se refleja con un angulo igual de salida”. Por esta razón en materiales lisos y brillantes éstas son unas geometrías recomendables. Cuando la geometría es de esfera integradora con luz difusa (X/d ó d/Y), cuyo uso es recomendable para los materiales heterogéneos en textura, es preciso ajustar en el aparato la inclusión (SCI) o exclusión (SCE) de la reflectancia especular, lo cual se consigue mediante lo que se llama una trampa óptica (tapón blanco). En el modo SCE, con componente especular excluida, la reflectancia especular está excluida de la medición y sólo se mide la reflectancia difusa. Cuando se utiliza el modo SCI ambas reflectancias están incluidas. Precisamente dada la necesidad de excluir la componente especular de las mediciones con la esfera integradora, muchos instrumentos emplean una geometría 8/d ó 6/d en lugar de 0/d.

Figura 6. Izquierda: Instrumentos de medida del color por contacto. Arriba: Colorímetro portátil triestímulo Minolta con procesador de datos DP-310 y cabezal de lectura CR-300. Medio: Espectrofotómetro portátil GretagMacbeth CE-XTH. Abajo: Espectrofotómetro portátil Konica Minolta CM-700d. Derecha: Realización de la medida instrumental de color *on site*.

Teniendo en cuenta tales premisas antes de comenzar la medición, las medidas obtenidas por un espectrofotómetro o por un colorímetro triestímulo (**Figura 6**) serían completamente equivalentes aunque ambos aparatos no son instrumentalmente iguales. La diferencia fundamental entre un espectrofotómetro y un colorímetro consiste en que el colorímetro trabaja

únicamente en el espectro de luz visible y selecciona una longitud de onda determinada mediante filtros fijos, mientras que un espectrofotómetro es capaz de trabajar en otras regiones del espectro electromagnético (ultravioleta e infrarroja) y posee un monocromador para seleccionar la longitud de onda deseada. Además, el colorímetro funciona como una cámara digital RGB, cuyos canales de color se ajustan espectralmente a las funciones de igualación CIE combinando las sensibilidades espectrales del sensor, la lente y los filtros coloreados RGB. Por esta razón los colorímetros dan valores triestímulo relativos mientras que los espectrofotómetros proporcionan mediciones espectrales.

Con todo lo expuesto hasta el momento, parece posible en principio medir el color en cualquier situación que se presente. Sin embargo, las aplicaciones prácticas de la medida del color son tan extensas y variadas que en algunas situaciones es necesario definir una serie de conceptos particulares asociados al objeto concreto de estudio. En ciertas áreas como la alimentaria, dental y textil, la medida instrumental del color posee una amplia tradición, por lo que el desarrollo e implementación de los métodos de medida se encuentran muy avanzados, existiendo incluso en ciertos casos, como el vino y el aceite, métodos oficiales para la determinación de su color. Sin embargo en otras áreas, como la que recoge el objetivo principal de esta tesis, así como áreas afines relacionadas con sustratos inorgánicos naturales, tales como rocas, suelos y sedimentos, la medida instrumental del color apenas ha sido aplicada, lo que lleva a la necesidad de determinar un procedimiento de medida previo a la aplicación de la técnica (Artigas *et al.*, 2002).

General Introduction

I. From a planktonic lifestyle to formation and growth of biofilms

Historically, microorganisms were considered as free-living unicellular life forms and characterized on the basis of their growth in different culture media (Donlan, 2002). However, advances in microscopic and molecular techniques have made possible the direct observation of a wide variety of natural habitats, and it has been established that most microorganisms live attached to surfaces within a structured biofilm and not as free-floating organisms (Costerton *et al.*, 1987). The discovery of microbial biofilms, in the late seventeenth century, can be attributed to the Dutch microscopist Antonie van Leeuwenhoek (1632-1723), who, after observing the "animalcules" in plaque from his own teeth, affirmed that bacteria could adhere and grow universally on exposed surfaces. In the nineteenth century, the Russian microbiologist and soil scientist Sergei N. Winogradsky (1856-1953) developed a system of simulating natural ecosystems (the Winogradsky column), and thus managed to isolate associations of microorganisms (biofilms) on glass slides. In 1940, Heukelekian & Heller observed the "bottle effect" in marine microorganisms, whereby bacterial growth and activity were substantially enhanced by the incorporation of a surface to which these organisms were able to attach. In 1943, Zobell observed that the number of bacteria on surfaces was much higher than in the surrounding medium (in this case, seawater). On the basis of observations of dental plaque and sessile communities in mountain streams, Costerton *et al.* (1978) proposed a theory of biofilms that explained the mechanisms whereby microorganisms adhere to living and nonliving materials, as well as the benefits afforded by this ecologic niche. The term biofilm was coined by Costerton in 1978, in an article in *Scientific American*, in which he stated that, "in nature (but not in laboratory cultures) bacteria are covered by a "glycocalyx" of fibres that adhere to surfaces and to other cells". This supposed a paradigm shift in the way microbiologists viewed the growth and ecology of microorganisms.

The current definition of a biofilm describes a more complex concept: "a universal community of microorganisms (bacteria, fungi, cyanobacteria, algae, protozoa), complex and interdependent, linked to wet surfaces (biotic or abiotic) or interfaces (subject to water column gradients) by a polymeric matrix (EPS) of extracellular glycoproteins with viscous texture, generated *ex profeso*

and travelled by water channels, which allow an efficient water, nutrients and gas exchange between constituent populations and the outside environment "(Costerton, 2007).

The capacity for biofilm formation is not restricted to any specific group of microorganisms; under suitable environmental conditions all microorganisms can form biofilms. In this regard, it has been shown that many cells must attach to solid surfaces (forming part of a biofilm) to survive and proliferate, a requirement for survival known as "anchorage dependence" (Pierres *et al.*, 2002).

The main feature that distinguishes sessile biofilm cells from their motile or free-floating planktonic counterparts is the existence of a matrix of extracellular polymeric substance (EPS) that embeds all components of the biofilm and enables it to adhere to surfaces. The biofilm matrix is a complex milieu, comprising mainly water (up to 97%) and a mixture of EPS such as polysaccharides, proteins, nucleic acids, lipids/phospholipids, absorbed nutrients and metabolites. Although the extracellular matrix is the defining characteristic of the biofilm, its role is not yet fully understood. Most authors believe that the primary function of the extracellular matrix is to protect the biofilm from antimicrobial action and from adverse changes in humidity, temperature, osmotic pressure and pH. The extracellular matrix acts via chemical neutralization or the creation of a diffusion barrier that prevents antimicrobial agents reaching the microorganisms (Lindsay & von Holy, 2006). It is also known that cyanobacteria increase their production of extracellular polymers under light- and nutrient-limiting conditions (Albertano *et al.*, 2003). However, other authors consider that the most important role of the matrix occurs during the initial stages of biofilm formation when it facilitates cell attachment to the substrate (Decho, 2000; Barranguet *et al.*, 2005); this gives cohesion to the nascent biofilm and facilitates interaction between its various components (Flemming & Wingender, 2001).

It has also been established that sessile cells are physiologically distinct from planktonic microorganisms and that biofilms exhibit a distinct phenotype from their free-floating counterparts. The main phenotypic differences are related to location, grouping and colonial organization, mobility, metabolic and environmental adaptation, and form and growth rate (Donlan, 2002). During the complex process of adhesion, microorganisms alter their phenotypic characteristics in response to their proximity to a surface. During the initial stages of biofilm formation, sessile microorganisms form microcolonies within which they are in stable juxtaposition with microorganisms of the same and other species. Interactions within these microcolonies enable exchange of genetic material, which results in an overall change in the phenotype of the biofilm (Stolz, 2000). This also creates physico-chemically heterogeneous environments in which microorganisms associated with biofilm have different physiological characteristics than the planktonic cells. Many microorganisms alter their physiological processes to adapt to these particular niches (*e.g.* by growing anaerobically) (Stoodley *et al.*, 2002). In addition, the different micro-organisms in the biofilm respond to the conditions of their specific micro-environments by presenting different growth patterns. Physiological cooperation

is the main factor that helps form the structure and establish equilibria, so that mature biofilms (*i.e.* attached to surfaces) are highly efficient microbial communities (Costerton *et al.*, 1994).

During biofilm formation, the constituent microorganisms usually leave their status of motile cells (planktonic) to form unstratified populations of microorganisms within which several species of microorganisms interact; each species has its own metabolic rate, with a controlled growth rate and specific, relative location within the biofilm (**Figure 1**). Several stages of biofilm formation can be distinguished (O'Toole *et al.*, 2000; Boonaert *et al.*, 2001). In the first stage, macromolecules and organic molecules from different sources are adsorbed onto the substrate and thus prepare it for possible colonization (Step 1, Figure 1). The microorganisms then approach the substrate by self-propulsion and Brownian motion; physicochemical interactions with the adsorbed molecules lead to initial adhesion of cells (Step 2, Figure 1). Adherence to the substrate, which is a key step in biofilm formation, is a complex process regulated by the surrounding medium, the surface of the substrate and the microorganisms themselves (Ophir & Gutnick, 1994; O'Toole *et al.*, 2000; Donlan, 2002). The subsequent attachment of the microorganisms is caused by excretion of EPS (Step 3, Figure 1). From this moment, cell division leads to the proliferation of microbial communities and their continued adherence to the substrate. Maturation of the biofilm involves three-dimensional growth via the generation of a specific and complex 3D structure of channels and pores, often referred to as biofilm architecture (Lawrence *et al.*, 1991) and redistribution of microorganisms away from the substrate (Step 4, Figure 1). The architecture of the biofilm, in particular the spatial arrangement of microcolonies (clusters of microorganisms) in relation to others, has important implications for the function of these complex communities of microorganisms attached to surfaces or associated with interfaces (Donlan, 2002). The architecture of the biofilm matrix is strongly substrate dependent; it is not solid, but has channels that allow the flow of water, nutrients and oxygen to even the deepest parts of the biofilm. However, the existence of these channels does not preclude the existence of environments in which the pH and concentrations of nutrients and oxygen will differ within the biofilm (Steps 5 and 6, Figure 1). Once the biofilm is mature, some of the microorganisms will return to a planktonic mode of growth, as a result of a decrease in exopolymer production (Step 7, Figure 1. O'Toole *et al.*, 2000). The microorganisms leave the biofilm, thus completing the life cycle (Costerton, 2007).

Recognition of the importance of the biofilm phenomenon is recent, and therefore a concerted effort to study microbial biofilms began only two decades ago. However, study of these communities has already revealed the existence of important mechanisms of microbial communication that affect the stability of the biofilm and enable organization/disorganization and settlement/release. Thus, some bacterial communication mechanisms have positive effects (Quorum Sensing), and others have negative effects (Quorum Quenching). The proteins responsible for bacterial communication (Quorum Sensing) and blockage of communication (Quorum Quenching) were discovered in the early 1990s (Fuqua *et al.*, 1994). According to

studies published by Otero *et al.* (2004) and Otero & Romero (2010), Quorum sensing (QS) refers to the ability of microorganisms to regulate their gene expression according to population density and thus develop a type of social behaviour coordinated by producing small signal molecules. If these signal molecules are removed from the environment, the communication between organisms will break down; this is known as Quorum Quenching (QQ).

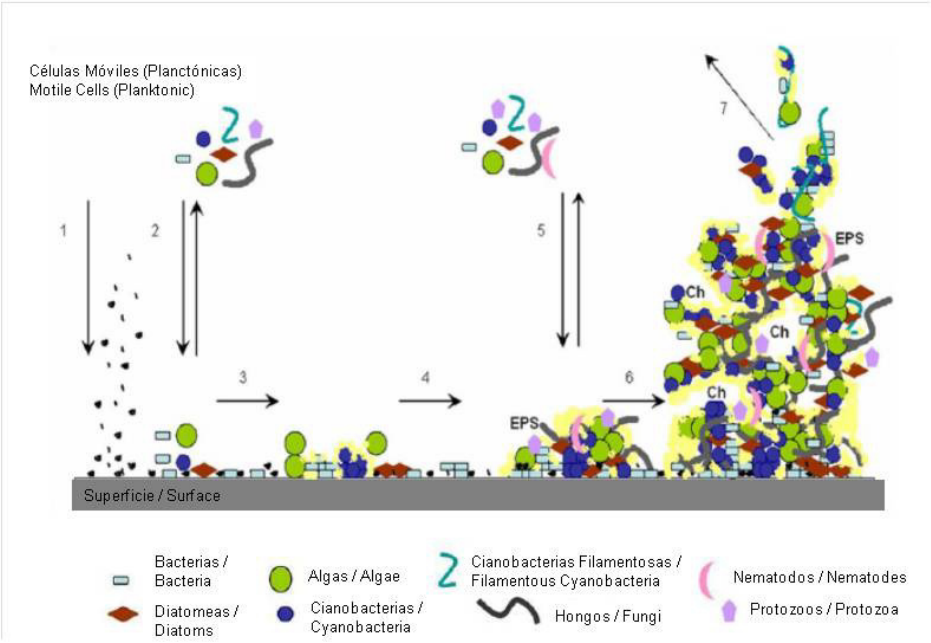

Figure 1. Schematic model of the phases involved in biofilm formation on a solid surface. Adapted from Cuzman (2009). (1) Establishment of macromolecules and organic molecules on the surface being colonized; (2) Reversible adhesion of primary colonizers; (3) Transition to irreversible adhesion, followed by multiplication and start of production of extracellular polymeric substance (EPS); (4) Start of three-dimensional development of the biofilm structure; (5) Adhesion of secondary colonizers and continuous development of the biofilm; (6) Mature biofilm with an expressed structure (biofilm architecture) and forming a specific micro-ecosystem; (7) Biofilm homeostasis during which continuous growth of the structure with channels (Ch "channel") takes place and some microorganisms break off and return to a planktonic mode of growth.

II. Biofilm-substrate interaction: biological colonization of surfaces exposed to outdoor conditions

Biofilm formation requires the presence of a substrate, and as very few substrates are not affected by biofilms, all of the earth's surface is covered by subaerial biofilms (Krumbein *et al.*, 2003). Moreover, biofilms usually appear from the early stages of exposure of almost all outdoor surfaces under all types of environmental conditions (**Figure 2**, Silva *et al.*, 1997; Gaylarde & Morton, 1999; Warscheid & Braams, 2000). In some cases, the presence of biofilms is beneficial as it stabilizes and fertilizes soils (Acea *et al.*, 2001, 2003), sediments (Liess & Francoeur, 2010) and rocks (Prieto *et al.*, 2005, 2006). However, the presence of biofilms

sometimes leads to aesthetic deterioration of the surface, which is associated with staining by biogenic pigments (Urzì *et al.*, 1992), and is an important problem in terms of biodeterioration ("the undesirable change in the properties of a material caused by the activities of organisms"; Hueck, 1965) and accelerated aging (Warscheid & Braams, 2000). The presence of biofilms actively degrades materials because the films produce acidic/alkaline conditions, retain moisture and absorb heat differently depending on the coloration (Krumbein, 1988; Garty, 1990; Warscheid *et al.*, 1991, 1996). From the viewpoint of cultural heritage, the development of biofilms on valuable surfaces is particularly detrimental (Figure 2, Dornieden *et al.*, 2000).

For biofilm-forming microorganisms, substrates provide a surface for development of biological activity and also supply the energy required for development (Gorbushina & Krumbein, 2000). Therefore, for inert surfaces, a sequential process of colonization is required in which the substrate in question gradually becomes suitable for the colonizers. Thus, the sequence of colonization is not random, but responds to the microorganisms' own strategies. The primary colonizers of the substrate are generally autotrophic microorganisms such as diatoms, algae, photoautotrophic bacteria *sensu lato* and cyanobacteria (*e.g.* Grant, 1982), which only need water and a minimal supply of mineral salts to settle and grow on the substrate (Saiz-Jimenez & Ariño, 1995). Growth of these microorganisms often leads to the formation of greenish patches in damp areas, in a phenomenon often referred to as greening; this is more apparent in shaded areas than in exposed sites because the latter dry out more readily (Barberousse *et al.*, 2006; Smith *et al.*, 2011). The duration of the dampness (rather than the frequency of wetting) is crucial in predisposing a substrate to colonization by these types of microorganisms, and colonization is more rapid in sites with adjacent or overhanging vegetation (Saiz-Jimenez & Ariño, 1995; Smith *et al.*, 2011). Cyanobacteria (oxygenic photoautotrophic bacteria) have several characteristics that enable them to withstand extreme environmental conditions, such as tolerance to desiccation and water stress, tolerance to high levels of salts, high temperature resistance and efficient use of low-intensity sunlight radiation; these features explain the widespread presence of cyanobacteria on certain substrates (*e.g.* Friedmann, 1980). The presence of photoautotrophic microorganisms, cyanobacteria and algae (primary colonizers) leads to the formation of more complex microbial associations, which in turn enables settlement of other species (heterotrophic microorganisms) and the concomitant growth of a biofilm, which now includes lichens, heterotrophic bacteria, fungi, bryophytes *sensu lato* and sometimes even higher plants (Ortega-Calvo *et al.*, 1991a; Saiz-Jimenez, 1992; Tiano, 1993; Tomaselli *et al.*, 2000; Crispim *et al.*, 2003; Sterflinger, 2010). Heterotrophic microorganisms (bacteria, fungi and lichens) may have more severe effects on substrates because most of them metabolize organic matter produced by photoautotrophs, and they secrete organic acids that chemically degrade the substrate (Warscheid & Braams, 2000). Heterotrophic microorganisms also cause physical damage because their filaments (particularly the hyphae of fungi) penetrate the porous cavities on the substrate surface (Hirsch *et al.*, 1995; Prieto *et al.*, 2000; Silva & Prieto, 2004). When wet, the filaments expand and exert pressure

within the pore; this causes fissures to open up, which can cause blistering and detachment (or spalling) of the material. The slimy, usually anionic, surface of the biofilm (Costerton *et al.*, 1978) also favours cation adsorption. The adsorption of organic molecules and the adherence of airborne particles (dust, pollen, particulate elemental carbon (PEC), fly ash, etc.) give rise to the formation of hard crusts and patinas (also called black crusts), which are more difficult to remove (*e.g.* Camuffo, 1995). Black crusts may have different origins from the biogenic crusts observed in polluted atmospheres, as well as from the biogenic crusts observed in pollution-free environments (Aira, 2007; Gaylarde *et al.*, 2007; Prieto *et al.*, 2007; Silva *et al.*, 2009) and from crusts that are non-biogenic in origin (Del Monte *et al.*, 2001; Aira, 2007; Prieto *et al.*, 2007; Silva *et al.*, 2009).

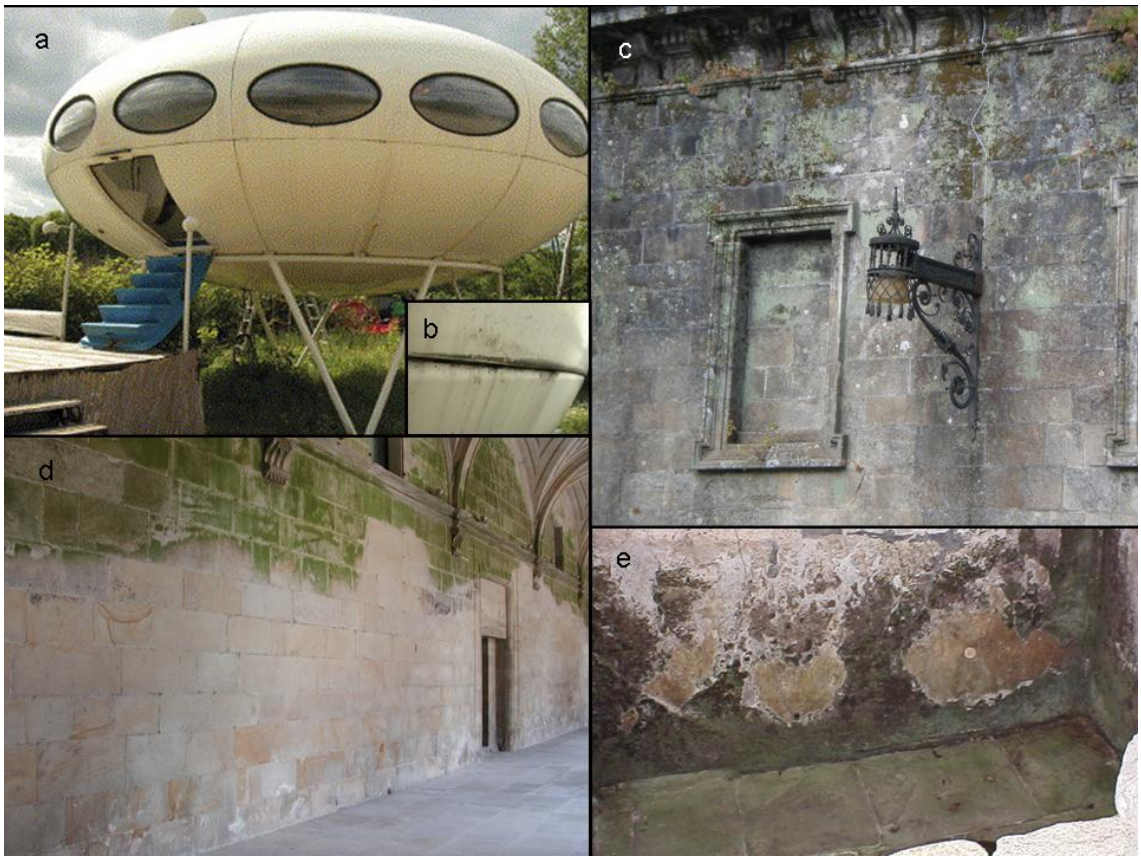

Figure 2. Diversity of subaerial (terrestrial) biofilms: (a) The plastic ski-cabin known as “Futuro” (also “Futuro House” or “The UFO house”) was designed by the Finnish architect Matti Suuronnen in 1965 in Munich (Bavaria, Germany). The exterior, which consists of glass fibre-reinforced polyester filled with polyester-polyurethane foam, and the poly(methylmethacrylate) (Perspex) windows display clear signs of microbial growth. This is an example of the presence of biofilms in a contemporary work of art (Image extracted from Cappitelli *et al.*, 2006); (b) Detail of the exterior of "Futuro", showing an area of biofilm growth mainly formed by cyanobacteria and archaea (Cappitelli *et al.*, 2006); (c) Detail of the Eastern façade (where the “Holy Door”, which is only opened during “Holy Years”, is located) of the Cathedral of Santiago de Compostela (A Coruña, Spain); the Cathedral is built entirely of granite. Biological colonization in this area is by biofilms comprising bryophytes, lichens, algae and cyanobacteria; (d) Detail of “greening” at the top of one of the granite walls of the cloister of San Martiño Pinario monastery, also located in Santiago de Compostela (A Coruña, Spain); (e) Detail of wall and floor significantly degraded by conspicuous growth of microorganisms in part of the Chedworth Roman Villa, one of the largest Roman villas in Britain, located at Chedworth, Gloucestershire (England).

The presence of microorganisms discolors substrates and causes aesthetic damage. The color of the biofilm depends on the microorganisms and abiotic particles that form the film. The color of the microorganisms is determined by the composition and/or abundance of their biological pigments, which differ greatly depending on environmental conditions such as type and concentration of nutrients, light intensity and quality, temperature, ultraviolet radiation and pH (*e.g.* Tandeu de Marsac, 1977; Collier & Grossman, 1992; Soltani *et al.*, 2006). In general, biological pigments are reddish (carotenoids and phycobiliproteins, phycoerythrins), yellowish (carotenoids), greenish (chlorophylls and phycobiliproteins, allophycocyanins) and bluish (phycobiliproteins, phycocyanins) in color, although dark-brown-blackish coloration may also occur as the result of the presence of melanins and scytonemin (García-Pichel & Castenholz, 1991; Proteau *et al.*, 1993). Biological pigments are not common to all of microorganisms; for example, the phycobiliproteins are exclusive to cyanobacteria and red algae (Glazer, 1977), and scytonemin only appears in cyanobacteria (García-Pichel & Castenholz, 1991). Thus, the color of the biofilm may indicate the type of microorganism involved, although this is difficult to determine visually. For example, the color of a pink-stained limestone surface at the Mayan site of Edzna (Campeche, Mexico) is caused by a high concentration of carotene-packed cells of the alga *Trentepohlia umbrina* (Gaylarde *et al.*, 2006), whereas the rosy discoloration of the frescoes in the St. Brizio Chapel (Orvieto Cathedral, Umbria, Italy), painted by Luca Signorelli, is probably caused by the presence of the phycobiliprotein phycoerythrin (a cyanobacterium) (Cappitelli *et al.*, 2009). In other instances, especially when the biofilm is thin and is not aesthetically disagreeable (*e.g.* pinkish or bluish staining), it is difficult to determine by naked eye whether the color is intentional or it has been altered by biological colonization (**Figure 3**, Gaylarde *et al.*, 2006). Some studies have related the color of the biofilm (determined qualitatively) to the type of pigment and/or microorganism. Thus, the orange and grey patinas on the calcarenite stone used to build the Baroque town of Noto in Syracuse (Sicily, Italy) have been associated with algae and bacteria and fungi, respectively (Urzì & Realini, 1998), and black biofilms on the exterior surfaces of the Bayon Temple Sandstone (Angkor, Cambodia) have been found to caused by the *Dematiaceous* fungus (also called black fungus, an ascomycete), which produces dark brown melanin pigmentation (Sterflinger, 2000). However, knowledge of the extent of the diversity of the microbial microflora in subaerial biofilms is far from complete, since traditional culture techniques isolate less than 1% of the microbial community (Ward *et al.*, 1990). Molecular methods that allow the identification and, to some extent, enumeration of microorganisms in environmental samples have been developed in recent years (Amann *et al.*, 1995). The use of techniques such as denaturing gradient gel electrophoresis (DGGE), single strand conformational polymorphism (SSCP) and fluorescent *in situ* hybridization (FISH) has shown that halophilic or alkanophilic eubacteria and archaea may also be present in the subaerial biofilms found on surfaces of art and cultural heritage (Saiz-Jimenez & Laiz, 2000; McNamara *et al.*, 2003; Ortega-Morales *et al.*, 2004; Cappitelli *et al.*, 2007; Piñar *et al.* 2009).

In general, synthetic materials (Figure 2a, b) are considered to be more resistant than natural materials (Figure 2c, d, e) to the chemical, physical and biological damage produced by the biofilm (Cappitelli *et al.*, 2006). However, the availability of water and nutrients in the substrate is the main limiting factor for biological colonization and biofilm development, and environmental conditions, together with the characteristics of the substrate, determine the type of biofilm formed and its growth rate (Silva *et al.*, 1997). The combination of properties that determine the ability of a substrate to be colonized by microorganisms has been termed bioreceptivity (Guillitte, 1995). Properties such as high porosity and surface roughness favour biological colonization and biofilm formation because they facilitate adhesion of microorganisms to the substrate and thus increase its bioreceptivity (Caneva *et al.*, 1991; Silva *et al.*, 1997; Warscheid & Braams, 2000; Prieto & Silva, 2005; Miller *et al.*, 2006). However, is not yet clear how the properties of the substrate affect microbial growth and the subsequent bioreceptivity (Miller *et al.*, 2012).

Figure 3. Marble columns in the interior of a church on the Mediterranean coast. The column on the right hand side has a pinkish-orange color that appears to be due to the material, but is actually due to the presence of a biofilm.

Focusing on the field of lithology, the presence of biofilms is one of the main problems concerning the conservation of new structures as well as historically and artistically important structures (Herrera & Videla, 2004; Crispim & Gaylarde, 2005; Gorbushina, 2007; Scheerer *et al.*, 2009). From the beginning of civilization, important structures and monuments have been built from, or based on, natural stone. Marble and granite, which are highly resistant to weathering, are among the most commonly used types of stone. The biofilms that appear on

structures built with this type of stone are usually epilithic (on the surface), partly because of the low porosity of this material (Prieto *et al.*, 1999, 2000; Silva *et al.*, 1999). In more porous stone, such as limestone and sandstone, endolithic growth (inside of the rock) of the biofilm is more common (Saiz-Jimenez *et al.*, 1990; Miller *et al.*, 2010). Endoliths have been further classified into chasmoendoliths (present in cracks), cryptoendoliths (present in pores) and euendoliths (when they show a true ability to bore into the stone matrix) (Golubic *et al.*, 1981). The local climate also affects the depth of penetration of the organisms. Warscheid *et al.* (1996) considered that although microorganisms in moderate climates tend to colonize the surface of stones, their tropical and subtropical counterparts prefer to penetrate deeper into the rock profile for protection against sunlight and desiccation. However, Matthes-Sears *et al.* (1997) suggested that organisms do not become endolithic as a protective measure, but rather as a result of the search for nutrients and space. According to most authors, endolithic populations are extremely difficult to remove and are highly deleterious as they contribute to disrupting the cohesion of mineral grains at depths of up to several millimeters (*e.g.* Ascaso *et al.*, 1998; Miller *et al.*, 2010). However, Hoppert *et al.* (2004) reported that the growth rate of endolithic populations within the rock is slow and that these populations are rarely associated with biodeterioration processes. In the case of epilithic biofilms, biodeterioration is caused in the first instance by the change in color of the surface, which causes aesthetic damage. The presence of this type of biofilm also leads to physical problems because the albedo decreases in darker areas of the stone surface (*i.e.* those covered by biofilm), so that more sunlight is adsorbed and the stone experiences an increase in heating/cooling and wetting/drying cycles, which causes physical stress on the biofilm and mechanical stress within the rock (Warke *et al.*, 1996; Warscheid & Braams, 2000; Sand *et al.*, 2002). Temperatures on darkly colonized areas of stone have been shown to differ by as much as 8ºC relative to uncolonized areas (Garty, 1990). The above effect has been demonstrated experimentally in limestone blocks with and without a lichen covering as changes in surface temperature and thermal gradients were greater in the area below the lichen (Carter & Viles, 2004).

Several studies have shown that cyanobacteria constitute most of the biomass on external surfaces of natural stone structures (Ortega-Morales *et al.*, 2000; Gaylarde *et al.*, 2001). The aggressive action of cyanobacteria (and photoautotrophic microorganisms *sensu lato*) in relation to the substratum where they develop has been considered negligible by some authors, although this is controversial. Apart from the unaesthetic appearance, there are references in the literature that indicate that decay occurs directly as a result of biofilm formation. Such decay is mainly attributed to the mucilage formed by the cyanobacterial and algal sheaths that enable the microorganisms to adhere to the substratum; the mucilage undergoes large changes in volume owing to its water retaining properties (Ortega-Calvo *et al.*, 1991a, 1991b). The mineral grains and particles are removed by the mass of entangled filaments held in a slimy matrix (the mucilage) in which particles of different sizes are embedded. Many cyanobacteria (not

necessarily filamentous types) have been shown to have this ability (Scheerer *et al.*, 2009). Grains may be lost from stone surfaces as a result of the contraction and expansion of biofilms, and this contributes to the gradual destruction of the materials (Ortega-Calvo *et al.*, 1991a, 1991b). In addition, the formation of photoautotrophic biofilms results in moisture being retained for longer at the surface, which increases the mechanical damage produced by the freezing and thawing of water present in the pores of the building materials.

The need to invest efforts in early detection (*i.e.* during the first stages of formation of biofilm: Figure 1) is often suggested in studies on the detrimental effects of stone-colonizing microorganisms. Intervention to remove biological colonization at this moment would be minimal and would be considered as preventive conservation, which is defined as "all measures and actions aimed at avoiding and minimizing future deterioration or loss" (ICOM-CC, 2008). Intervention for the removal of mature biofilms (Figure 1) should be carefully evaluated as it often leads to significant deterioration of the surface (**Figure 4**). Furthermore, the application of treatments after biofilm removal, including simple cleaning with water, may exacerbate future microbial growth; for example, it was found that although re-soiling from inorganic material does not occur for several years after cleaning building façades in Scotland (UK), re-soiling in the form of green algal growth (greening) occurred within only a few months (Young, 1997). The following are examples of restoration treatments that have led to an increase in microbial colonization: the use of a consolidant made from mucilaginous carbohydrate-like extracts from a local plant (*Escobilla*) at the Mayan site of Joya de Ceren (El Salvador), which favoured fungal growth, particularly of actinomycetes (Caneva & Nugari, 2005); the use of acrylic resins (poly-isobutylmethacrylate) as synthetic consolidants on the façade of the Milan cathedral (Italy) in the 1970s, which promoted development of melanin-producing fungi (Cappitelli *et al.*, 2007).

Action against microbial growth and the development of biofilms can be divided into four major categories (Scheerer *et al.*, 2009): (1) indirect control by changing environmental conditions so that they are adverse to the microorganisms, (2) mechanical removal of biodeteriogens, (3) use of chemicals (biocides), and (4) physical eradication methods, such as the use of an electromagnetic field or the use of ultrasound. The first action is the most recommendable, but can rarely be applied because of the high adaptability of microorganisms, especially bacteria and cyanobacteria, to external change; for obvious reasons it can never be applied to outdoor exposed surfaces. Depending on the dimensions of the surface to be treated, biofilm can be removed mechanically with the aid of a scalpel or a high-pressure jet of abrasive dust or stream of fluid. The main drawback with these techniques is that the surface may be damaged by microabrasion caused by direct contact between the abrasive and the surface. The stone façades of colonized buildings are often cleaned in this way, despite the damage caused and the fact that the treatment is expensive and must be repeated periodically because microorganisms re-appear quickly. In this respect, it is advisable to carry out cleaning at the early stages of biofilm formation, so that the treatment area is smaller and the cleaning is

easier, more efficient and thus less expensive than with older biofilms. Microbial abatement is commonly achieved with biocides, especially in the case of rehabilitation of old buildings, which are often profusely colonized. However, biocides often have detrimental effects on stone as they can cause discoloration, oxidation/reduction of stone compounds and formation of salts, which may crystallize on drying and lead to exfoliation (Caneva *et al.*, 1991; Kumar & Kumar, 1999; Warscheid & Braams, 2000). The ecotoxicity of commercial biocides may make them poor candidates for use in outdoor environments, and many countries have forbidden the use of some of the previously most common (and effective) biocides. Furthermore, nitrogen-containing biocides may serve as nutrients for surviving or newly attaching microorganisms (Warscheid & Braams, 2000). The most negative aspect of the application of biocides is the fact that removal of the existing microbial community may favour the growth of other harmful microorganisms (Webster *et al.*, 1992; Warscheid & Braams, 2000). Finally, physical methods of applying biocides become dangerous and expensive when large areas are involved.

Figure 4. Marble sculpture at the Villa Dosi Delfino near Pontremoli (Massa-Carrara, Italy). The photograph on the left shows the state of the sculpture before cleaning. The photograph on the right shows a detail of the sculpture after removal of the biofilm, revealing the extensive damage caused by the microorganisms.
These images are included courtesy of Dr. Piero Tiano, and were presented at the "International conference on microbiology and conservation of microbes and art". Florence (Italy), 16-19 June 1999 and published by Kluwer Academic in "Of microbes and art: the role of microbial communities in the degradation and protection of cultural heritage" (2000).

III. Detection and quantification of biological colonization and biofilm development. Instrumental color measurements and the CIELAB color system

It can be assumed that all stone surfaces will be colonized at some stage by living organisms (leading to biofilm formation) and that the settlement involves not only aesthetic damage, but also physical and chemical damage, which increase as the colonization spreads. Therefore, the early detection of biofilm formation would constitute significant progress as regards preventive conservation of stone buildings, monuments and sculptures.

Identification of autotrophic microorganisms is a key step in the early detection of the biological colonization processes as these organisms are often pioneers in the colonization of stone surfaces (*e.g.* Grant, 1982). For this reason, research in this field has mainly focused on the detection and quantification of these types of microorganisms. Martín (1990) reviewed the traditional methods used to study biological damage in stoneworks of cultural heritage and classified the methods used to quantify the presence of microorganisms as follows: morphological, microbiological, histochemical and biochemical, and chemical and physicochemical methods. A slightly different classification is considered here, and three types of methods are distinguished: structural and morphological, microbiological and extractive methods.

Structural and morphological methods are the most commonly used to identify and classify pioneer species. These methods involve macroscopic observations of stone material in the field (Urzì *et al.*, 1992; Krumbein, 1993) and/or microscopic observations in the laboratory. Use of the stereomicroscope enables recognition of specific physiological structures of microorganisms (Prieto *et al.*, 1995; Shirakawa *et al.*, 2003); use of the optical microscope (OM) enables recognition of specific cellular morphology and cellular structure of each group of microorganisms with a very simple sample preparation (Ariño, 1996). Fluorescent probes (vital dyes and fluorescent proteins) can also be used with the fluorescence microscope (Tayler & May, 1991) and bioluminescence techniques (Ranalli *et al.*, 2000) to enhance the fluorescent signal. Each of these techniques provides a particular type of information, which is often complementary to that offered by the other techniques. Direct observations can also be made by conventional scanning electron microscopy (SEM) (Ortega-Calvo *et al.*, 1991a; Prieto *et al.*, 1997), SEM in backscattered electron mode (SEM-BSE), low temperature SEM (LTSEM), confocal laser scanning microscopy (CLSM) and transmission electron microscopy (TEM) (De los Ríos *et al.*, 2008), all of which allow three-dimensional observations of the microorganism at 10,000x magnification.

Microbiological methods for biofilm quantification are based on counting colonies (number of colony forming units per gram of sample, CFU/g) after a long incubation period in specific media and suitable conditions of temperature and light (ICR-CNR, 1988). If the biofilm is incubated in

liquid medium, the statistical approach originally suggested by McCrady (Hurley & Roscoe, 1983) is used to determine the most probable number of organisms per gram of sample (MPN/g). The studies carried out by Ortega-Calvo *et al.* (1993) and Hyvärinen *et al.* (2002) are examples of the application of these methods in samples taken from stone monuments.

In extractive methods, the biomass is estimated from the amount of various cell components present in microorganisms (Bartolini & Monte, 2000), such as certain proteins (Schwenzfeier *et al.*, 2011), ATP (Tiano *et al.*, 1989), DNA (Saiz-Jimenez & Laiz, 2000; Tomaselli *et al.*, 2000), lipids and polysaccharides (Di Pippo *et al.*, 2009). In the case of phototrophic microorganisms, the content of photosynthetic pigments in general, and the content of chlorophyll-a in particular (Bell & Sommerfeld, 1987; Nagarkar & Williams, 1997; Prieto *et al.*, 2004; Schumann *et al.*, 2005; Eggert *et al.*, 2006), is a good indicator of the presence and amount of microorganisms, and is probably the most prolific and one of the most reliable methods. Physiological methods, in which the biomass is estimated from the initial increase in respiratory rate (Bartolini & Monte, 2000), are often used in combination with extractive methods. Furthermore, microbial activity can be estimated by measuring enzymatic activities, such as dehydrogenase activity and total enzyme activity, via the hydrolysis of fluorescein diacetate (FDA). Tayler & May (2000) measured dehydrogenase activity on sandstone from ancient monuments, and Prieto *et al.* (2004) measured FDA in laboratory experiments carried out with granitic rock.

Although the above techniques have certain advantages and their use is widespread in research, they also have some disadvantages. The main disadvantages are the associated costs and the length of time they take. Moreover, most of the techniques are destructive and require prior sample preparation and acquisition, which is always difficult or even impossible task in the case of cultural heritage monuments. Techniques based on optical methods can be used to overcome these problems. Because of the small size of the organisms in question, the methods must use a high magnification and resolving power. In this respect two of the physical characteristics of phototrophic microorganisms can be made use of: the fluorescence emitted by their chlorophyll, and the color that they form when they accumulate on solid surfaces. Each of these characteristics has enabled development of a technique for detecting and monitoring the growth of biofilm on surfaces: (i) measurement of the fluorescence emitted by chlorophyll *in vivo* and, (ii) instrumental color measurement with a spectrophotometer or a tristimulus colorimeter. Large surfaces such as building façades, can even be monitored as both techniques are non-destructive (non-invasive) and they are applied on site, so that sampling is not required.

Several studies have investigated the use of chlorophyll-a fluorescence *in vivo* for direct quantification and monitoring of phototrophic colonization of lithotypes (Guillite & Dreesen, 1995; Brechet *et al.*, 1996, 1997; McStay *et al.*, 2001; Miller *et al.*, 2006, 2010). However, fluorescence measurements have some disadvantages relative to color measurement: the fluorescence signal occurs within a short time, depending on the physiological conditions of the

organisms (not taking into account the dead cells), and moreover, it is very difficult to analyze spectra with unknown characteristics. In other words, the technique requires basic knowledge of the spectral features of the parameters investigated so that the bands are chosen correctly to enable contributions from factors other than the microorganisms, such as the fluorescence of certain minerals within in the same spectral region (Lognoli *et al.*, 2003). Calcium carbonate, fluorite, scheelite and uranium ores are some of the mineral components that may emit fluorescence, which usually consists of a broad emission band in the blue region of the spectrum. Carbonate calcium, for example, has an emission maximum at about 420 nm (Cecchi *et al.*, 2000).

In relation to the quantification of biological colonization on building façades by instrumental color measurements, Newby *et al.* (1991) were the first authors to relate measurements of reflectance (which can be obtained with a spectrophotometer or tristimulus colorimeter) to the color change caused by deposition of particles (from natural sources as well as pollutants) on a solid surface. On the basis of a previous study by Ball (1989), Newby *et al.* (1991) defined soiling of building materials as "an optical effect, a darkening of the surface that can be measured as a change in light reflectance, and is generally related to the deposition of airborne particulate matter onto the building surface". Several years later and taking this definition into account, Gorbushina & Krumbein (2000) stated that many of the spectral changes are related to the growth of massively pigmented biofilms. Krumbein (1995) considered that airborne particles (dust, pollen, particulate elemental carbon (PEC), fly ash, etc.) and microorganisms often act concurrently to fouling (soiling) of the building, and noted that as early as 1853, Ehrenberg had came to the conclusion that microorganisms can trap airborne particles, in their slimy extracellular products, more efficiently than the rock surface itself.

The use of portable tristimulus colorimeters and portable spectrophotometers to measure the color generated by phototrophic microorganisms developed epilithically on stony substrates came into common use in the late 1990s. As part of a larger research programme funded by Historic Scotland (http://www.historic-scotland.gov.uk/), researchers at Robert Gordon University (Aberdeen, Scotland. United Kingdom) conducted a series of experiments on sandstone buildings in Scotland. These researchers used a portable tristimulus colorimeter to monitor the color change brought about on building façades by biological growth (algae) after application of various treatments biocides (Urquhart *et al.*, 1995; Young *et al.*, 1995; Young, 1997). Around the same time, Urzì & Realini (1998) published a study in which the color of orange and grey patinas developed on the calcarenite stone from which the Baroque town of Noto is built (Syracuse, Sicily, Italy) was determined with a portable tristimulus colorimeter and correlated with the associated microflora (respectively algae, and bacteria and fungi). As part of the *British National Materials Exposure Programme* (NMEP), Viles and colleagues monitored (between 1987 and 1995) microbial colonization, soiling and decay of limestone tablets located over 20 sites around the UK for periods of 1, 2, 4 and 8 years (depending on the climate and

pollution conditions of the location), using a portable spectrophotometer and characterization techniques such as scanning electron microscopy (SEM) (Viles *et al.*, 2002). The study subsequently focused on limestone buildings located along roads, in Oxford (England, UK), with different levels of traffic, and the buildings were monitored for a period of three years (Viles & Gorbushina, 2003). In addition, after access to vehicles (particularly private vehicles) was restricted in the centre of the historic city of Oxford, in 1999, as part of the Oxford Transport Strategy (OTS), Thornbush & Viles (2004, 2006) recorded the changing patterns changes of microbial growth and soiling on building stone in Oxford.

Furthermore, the reliability of color measurements for estimating the biomass of phototrophic organisms in biofilms on stone surfaces was demonstrated by Prieto *et al.* (2004) in a comparative study of the most common methods of quantifying phototrophic biomass, such as as the *in vitro* measurement of chlorophyll-a and fluorescein diacetate (FDA) hydrolysis. Moreover, Prieto *et al.* (2002) carried out laboratory experiments that demonstrated a direct relationship between the amount of phototrophic organisms deposited on a surface and the color generated. The same authors subsequently conducted a field study in which they used a portable spectrophotometer to monitor growth of a biofilm that was induced on quartz surfaces to mask the brilliant white color and thus mitigate the visual impact (Prieto *et al.*, 2005). The latter studies concluded that one of the major advantages of instrumental color measurement for the quantification of phototrophic biomass on surfaces that are largely homogeneous in color is that it enables early detection of biological colonization, even before it is visible to the human eye (Prieto *et al.*, 2002, 2005). This is an important advantage for the management and maintenance of surfaces recently exposed to outdoor conditions. It is also advantageous in treated surfaces in which the biofilm has been removed, as careful examination has shown that, despite cleaning efforts, some biological structures remain between the grains of the stone, which facilitates the re-establishment of microorganisms (Prieto *et al.*, 1995).

The CIELAB color space (CIE Publication 15-2, CIE, 1986) is used in most studies involving analysis of the instrumental color measurement, to represent and analyze the color values obtained. CIELAB or CIE 1976 L*a*b* attempts to produce a color space, that is perceptually more linear or uniform than other color spaces, such as RGB or CMYK. The term perceptually linear or uniform is used to indicate that similar changes in the amount of a color value should produce change of similar visual importance. This CIELAB color space was specifically developed for this purpose by the International Commission on Illumination (usually abbreviated to CIE for its French name, *Commission Internationale d'Eclairage*). The CIELAB or CIE 1976 L*a*b* is based on the CIE 1931 color space XYZ (CIE, 1932) and is strongly influenced by the Munsell color space (Munsell, 1905). Color depends on the interaction between three factors: the light source, the illuminated object and the observer who captures the image, and therefore the CIE established the CIELAB space on the basis of four key points: standard light source,

exact conditions of observation, appropriate mathematical units and standard observer curves (Wyszecki & Stiles, 1982).

The CIELAB color space (**Figure 5**), which can be visualized inside a sphere, a cylinder or a cube (although this does not conform to reality), uses three values to determine each color (L*a*b* or $L^*C^*_{ab}h_{ab}$) and is based on the opponent-colors theory of color vision, which states that one color cannot be both green and red at the same time, nor blue and yellow at the same time. As a result, single values can be used to describe the red/green and the yellow/blue attributes. Thus, one color can be expressed with Cartesian coordinates L*a*b*, where L* defines lightness ranging from 100 (absolute white) to 0 (absolute black), a* denotes the red/green value and b* the yellow/blue value. A movement of color measurement in a positive a* direction depicts a shift towards red. Along the b* axis, a positive b* movement represents a shift towards yellow. The CIELAB space can also be represented by another coordinate system, by using polar coordinates ($L^*C^*_{ab}h_{ab}$) that replace a* and b* with

chroma $C^*_{ab} = \sqrt{a^{*2} + b^{*2}}$

and, hue angle $h_{ab} = \text{arc tangent}(b^*/a^*)$.

The human perception of color appears to correspond to three attributes: hue, chroma and value (lightness) (Wyszecki & Stiles, 1982). The use of polar coordinates ($L^*C^*_{ab}h_{ab}$) rather than Cartesian coordinates (L*a*b*) leads to quantification of a color's similarity to it is perceived color, *i.e.* by taking into account the three attributes of visual assessment: value or lightness (L*), chroma (C^*_{ab}) and hue (h_{ab}).

One advantage of the CIELAB color space is that allows the color difference between two samples to be quantified by combining the differences in their three coordinates, both Cartesian and polar, in a Euclidean space. This is the basis of the classical color difference formula of 1976 CIELAB (Wyszecki & Stiles, 1982), which assumes a uniform color space:

$$\Delta E^*_{ab} = \sqrt{(\Delta L^*)^2 + (\Delta a^*)^2 + (\Delta b^*)^2} \text{ or } \Delta E^*_{ab} = \sqrt{(\Delta L^*)^2 + (\Delta C^*_{ab})^2 + (\Delta H^*_{ab})^2}$$

The CIELAB color difference has been progressively revised and improved since the lack of uniformity of the CIELAB color space was recognized. Currently, most color difference formulae are based on the classical CIELAB color formula. They are therefore considered as CIELAB-based formulae and have a common structure. The lightness, chroma, and hue differences are always computed from CIELAB, and each is weighted by two different types of variables: the weighting functions (designated by the letter *S*, also *W* in other texts), which are intended to improve the perceptual uniformity of CIELAB, and the parametric factors (designated by the

letter *k*), which are meant to account for the influence of specific experimental conditions on perceived color differences. This leads to the CIELAB-based color-difference formulae, CIE94 (CIE Publication 116-1995, 1995):

$$\Delta E^*_{94}(k_L : k_C : k_H) = \sqrt{\left(\frac{\Delta L^*}{k_L S_L}\right)^2 + \left(\frac{\Delta C^*_{ab}}{k_C S_C}\right)^2 + \left(\frac{\Delta H^*_{ab}}{k_H S_H}\right)^2}$$

and CIEDE2000 (CIE Publication 142-2001, 2001), which also incorporates a rotation term (R_T) that accounts for the interaction between chroma and hue differences in the blue region and a modification of the a* coordinate of CIELAB, which mainly affects colors with low chroma (neutral colors):

$$\Delta E_{00}(k_L : k_C : k_H) = \left\{\left(\frac{\Delta L'}{k_L S_L}\right)^2 + \left(\frac{\Delta C'}{k_C S_C}\right)^2 + \left(\frac{\Delta H'}{k_H S_H}\right)^2 + R_T\left(\frac{\Delta C' \Delta H'}{k_C S_C k_H S_H}\right)\right\}^{1/2}$$

The parametric factors can be set to k_L=1, k_C=1 and k_H=1 for CIE94(1:1:1) and CIEDE2000(1:1:1), and to k_L=2, k_C=1, k_H=1 (to increase the relative contribution of the lightness term) for CIE94(2:1:1) and CIEDE2000(2:1:1). As for the relative importance of CIELAB-based formulae, Melgosa *et al.*, (2004) found that the improvement of CIE94 over CIELAB was considerably greater than that of CIEDE2000 over CIE94.

The CIELAB color space attempts to linearize the perceptibility of color differences, by use of the color difference metric described by the MacAdam ellipses (MacAdam, 1942). The nonlinear relations for L*, a*, and b* are intended to mimic the nonlinear response of the human eye. Furthermore, uniform changes in components of the L*a*b* color space should correspond to uniform changes in perceived color, so that the relative perceptual differences between any two colors in L*a*b* can be approximated by treating each color as a point in a three dimensional space (with three components: L*, a*, b*) and measuring the Euclidean distance between them.

There are several reasons for the widespread acceptance of CIELAB in scientific and industrial applications, including the opposing character of the coordinates L*a*b*, the association of another set of coordinates, $L^*C^*_{ab}h_{ab}$, with the three color attributes (lightness, chroma and hue), and even its analogy relative to the Munsell color space (Munsell, 1905), with which many people are familiar.

The instrumentation for color measurement available nowadays has a similar basis, but usually differs in the degree of sophistication and configuration of the device, which depends on the particular application for which it is intended (Capilla *et al.*, 2002).

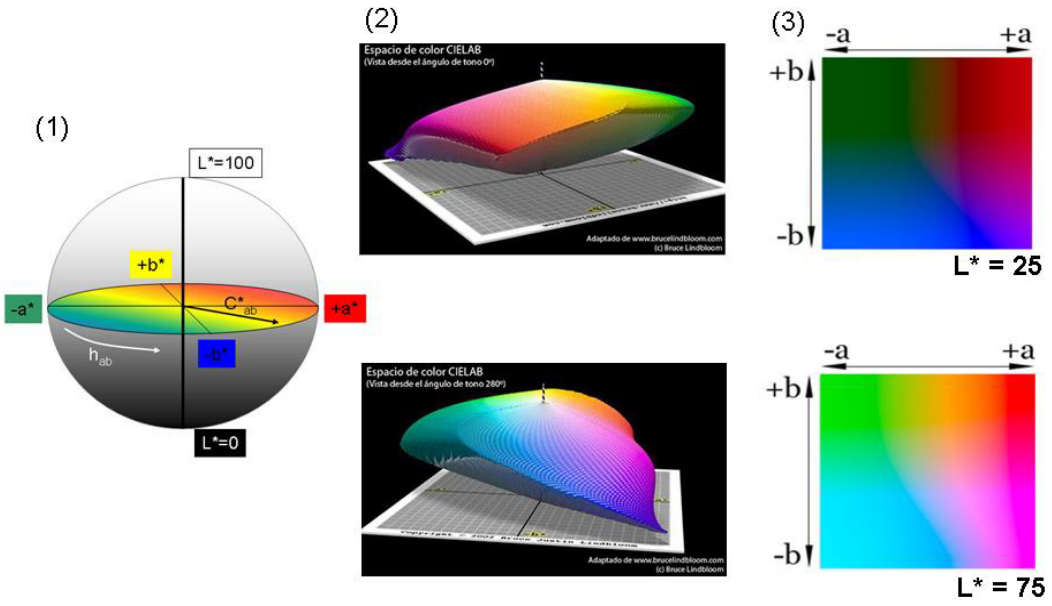

Figure 5. CIELAB color space. (1) Classical representation inside a sphere of CIELAB color space in which the two groups of coordinates are represented, Cartesian (L*a*b*) and polar ($L^*C^*_{ab}h_{ab}$), (2) Real representation of the CIELAB color space, which is neither a sphere, cylindar nor a cube, but a solid body of irregular boundaries (adapted from http://www.brucelindbloom.com/index.html?ColorCheckerRGB.html), (3) a* - b* color planes with a constant value of lightness (L*).

Instrumental color measurements are subject to the conditions of measurement of the spectrophotometer or colorimeter, such as the optical configuration, measuring geometry or illumination/observation geometry (0/45, 45/0, d/0, …), the illuminant (A, C, D65, F11, …), and the observer (standard observers CIE 1931 - 2º and CIE 1964 - 10º). Illuminant and observer can be preset in order to generalize the measurement process and thus obtain reliable, reproducible and comparable measures. The illumination/observation geometry of a colorimeter or spectrophotometer is characteristic of the measuring device and it is determined by two values, X/Y, where X is the value that indicates the direction in which the specimen surface is illuminated, and Y is the value that indicates the direction of the reflected beam, where the detector is located. The results may differ depending on how the sample is illuminated (X) and on how the detector is positioned relative to the sample (Y). Therefore, when more than one color measuring instrument is used, it is advisable to compare the results of the measurements to highlight these instrumental differences (*e.g.* Campos Acosta *et al.*, 2004). The most common measuring geometries are 0/45 and 45/0. With 0/45 geometry, the specimen surface is illuminated from the normal line direction (0 degrees) and the light is received at an angle of 45 degrees from the normal line. With 45/0 geometry, the specimen surface is illuminated from an angle of 45 degrees to the normal line and the light is received in the normal direction (0

degrees). Some devices also use an integrating sphere for illuminating or viewing a sample uniformly from all directions. An integrating sphere is a spherical device in which the internal surfaces are coated with a white material such as barium sulphate, so that the light is uniformly diffused. In such cases, the geometry is indicated by a "d", which indicates a diffuse illumination integrating sphere system. An instrument with X/d optical geometry illuminates the sample in the X degrees direction and collects the light reflected in all directions. An instrument with d/Y optical geometry illuminates the sample diffusely and detects the light in the Y degrees direction. Thus, if the sample is diffusely illuminated and the detector is placed at the normal direction relative to the sample, the optical geometry is d/0, if the detector is displaced 8 degrees, the optical geometry is d/8; if it is displaced only 6 degrees, d/6, etc. On the contrary, if the sample is illuminated at the normal angle (0 degrees) and the reflected light collected in all directions the optical geometry is 0/d, if the lighting beam is displaced 8 degrees, the optical geometry is 8/d, if it is displaced only 6 degrees, 6/d, etc.

When the measuring geometries are 0/45 and 45/0, the specular component of reflectance, *i.e.* the reflected light from the surface such that the angle of reflection equals the angle of incidence, is automatically excluded. These geometries are therefore recommended in smooth and shiny materials. For integrating sphere-based geometries (X/d or d/Y), the use of which is recommended for heterogeneous materials, the specular component of reflectance can be included or excluded mechanically by opening and closing an optical trap provided inside the integrating sphere. If the specular reflectance is included in the color measurement, by completing the sphere with a specular plug, it is referred to as Specular Component Included (SCI). In Specular Component Excluded (SCE) mode, the specular reflectance is excluded from the measurement and only the diffuse reflectance is measured. Because of the need to exclude the specular component, many devices with integrating sphere based geometries use 8/d or 6/d geometry instead of 0/d geometry.

Taking into account the previous premises, the measurements obtained with a spectrophotometer and with a tristimulus colorimeter (**Figure 6**) should be equivalent, although both devices are not instrumentally equal. The fundamental difference between a spectrophotometer and a colorimeter is that a colorimeter only works in the visible light spectrum and at a wavelength selected by fixed filters, while a spectrophotometer works in other regions of the electromagnetic spectrum (ultraviolet and infrared) and has a monochromator to select the required wavelength. In addition, the colorimeter works as a digital camera RGB, whose color channels spectrally fit the CIE matching functions by combining the spectral sensitivities of the sensor, lens and RGB colored filters. For this reason, colorimeters provide tristimulus relative values, while spectrophotometers provide spectral measurements.

Figure 6. Left: Contact color-measuring instruments. Top: Minolta portable tristimulus colorimeter with CR-300 measuring head. Middle: GretagMacbeth (now XRite) portable spectrophotometer CE-XTH. Bottom: Konica Minolta's CM-700d spectrophotometer. Right: On site instrumental color measurement.

From all of the above, it appears possible *a priori* to measure the color in any situation. However, the practical applications of color measurement are so extensive and varied that in some situations it is necessary to define a particular set of concepts associated with the particular object of study. Instrumental color measurement has a long tradition in certain fields of study such as those related to food, dentistry and textiles, so that the development and implementation of measurement methods are highly advanced; some official methods for determination of color have even been developed, *e.g.* for wine and oil. However, in other areas, such as that including the overall scientific aim of this doctoral thesis and those related to natural inorganic substrates such as rocks, soils and sediments, instrumental color measurement has scarcely been applied, so that a measurement procedure must be established prior to application of the technique (Artigas *et al.*, 2002).

Investigación / *Research*

1ª línea de trabajo

Desarrollo de la metodología de medida y caracterización del color de las rocas graníticas

1st line of research

Fine-tuning of the methodology for measuring and characterizing the color of granite surfaces

Chapter 1. Measuring the color of granite rocks: A proposed procedure

Prieto, B.; Sanmartín, P.; Silva, B.; Martínez-Verdú, F.

Color Research and Application 35 (5): 368-375 (2010)

JCR index (IF) 2010 = 0.753 (77/134, 57 percentile in Engineering Chemical)

Total number of times cited: 11

Measuring the Color of Granite Rocks: A Proposed Procedure

Beatriz Prieto,[1]* Patricia Sanmartín,[1] Benita Silva,[1] Francisco Martínez-Verdú[2]

[1]Departamento Edafología y Química Agrícola, Facultad Farmacia, Universidade de Santiago de Compostela, 15782-Santiago de Compostela, Spain

[2]Departamento Óptica, Farmacología y Anatomía, Universidad de Alicante, San Vicente del Raspeig, 03690-Alicante, Spain

Received 12 January 2009; revised 13 April 2009; accepted 10 May 2009

Abstract: In spite of color being one of the physicochemical parameters most commonly used to characterize ornamental stone, there is yet no standardized protocol for measuring this parameter. Such a protocol is of particular importance for characterizing the color of heterogeneous surfaces, as in the case of granite. The aim of the present study was to determine the minimum area and the number of measurements required to characterize the color of granite rocks. A spectrophotometer and a tristimulus colorimeter, were used to measure the color of granite samples, and the measurements were expressed in CIE L*a*b* *color system units. Three parameters were considered as variable factors: the type of rock (Labrador Claro, Grissal, Rosa Porriño, and Blanco Cristal), surface finish (polished, honed, sawn, and flamed), and target area (circular apertures of diameter 5, 8, 10, and 50 mm). The results of the application of multivariate analysis of variance and of the classical CIELAB formula and CIE* L*a*b**-based color-difference formulae (i.e., CIE94 and CIEDE2000) to the data revealed that, although all considered factors affected the minimal area and the number of measurements required, the different circular apertures of both the instruments can be disregarded if the number of measurements and area recommended in this study are used.* © 2010 Wiley Periodicals, Inc. Col Res Appl, 35, 368–375, 2010; Published online 22 January 2010 in Wiley InterScience (www.interscience.wiley.com). DOI 10.1002/col.20579

Key words: color measurement; granitic rocks; minimum area of measurement; minimum number of measurements; CIELAB

*Correspondence to: Beatriz Prieto (e-mail: beatriz.prieto@usc.es).

Contract grant sponsor: Science and Education Ministry of Spain (MEC); contract grant number: BIA2006-02233/BES-2007-16996.

INTRODUCTION

Although color is frequently determined in studies involving the conservation and restoration of historical stone artworks, no standardized protocol for measuring color has yet been established for ornamental stones. Such a protocol is particularly necessary for measuring the color of stones constituted by minerals of very different colors, such as granite rocks. The measuring instruments used at present—colorimeters, spectrophotometers, and telespectroradiometers—have some limitations in terms of measuring the color of heterogeneous surfaces, because the required integration of the field of view may produce an unrealistic color.[1] Furthermore, in the case of colorimeters and spectrophotometers, the target area is always circular and of a size determined by the diameter of the measurement head (<60 mm), and therefore color measurements must be made sequentially, i.e., point-by-point, and the representative color of the whole nonhomogeneous surface cannot be determined by a single measurement.

Prior determination of the number of measurements must therefore be made because of these limitations, so that the results can be reproducible and the results of diverse types of studies can be compared, such as those involving measurement of the color of granite rock to characterize the material,[2,3] the color changes produced by consolidation and/or hydrofugation treatments,[4–6] the ageing and weathering effects caused by environmental agents,[3,7,8] and the change in color produced by biological colonization.[9]

Moreover, although the International Commission on Illumination (CIE) has explicitly recommended the study of the color of surfaces of different texture,[10] so far relatively few studies have been focused on the methodology of study.[11,12] In some studies, the color changes produced by different mechanical surface treatments applied to ornamental rocks have been quantified and the importance

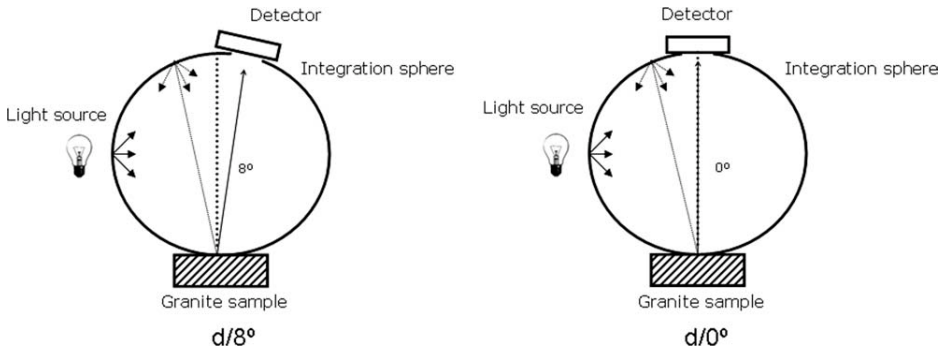

FIG. 1. Schematic view of a diffuse illumination geometry 0° (*d*/0°) right and diffuse illumination geometry 8° (*d*/8°) left.

of these types of measurements were stressed.[3] However, as there is no standardized protocol, aspects such as the number of measurements and the area of measurement vary from study to study and therefore it is impossible to compare the results obtained by different authors and instruments.

For all of the above reasons, the aims of the present study were to determine the minimum number of measurements and the minimum area of measurement required to quantify the color of a granite sample, in relation to the dimensions of the measuring head, and to establish a methodology applicable to the determination of these parameters in other types of ornamental stone.

EXPERIMENTAL

Two different instruments were used to measure the color, a GretagMacbeth (now XRite) portable spectrophotometer (CE-XTH), with two diameter viewing apertures of 5 and 10 mm, and a Konica Minolta colorimeter, which has two measuring heads: CR-300 with 8-mm-diameter viewing area and CR-310 with 50-mm-diameter viewing area. A wide range of measurement areas was thus achieved with the two devices (circular areas of 5, 10, 8, and 50 mm diameter).

The same measuring conditions were fixed in both the devices so that the measurements were comparable. The following were therefore selected: illuminant D65, which represents a phase of daylight, with a CCT of approximately 6500 K, including the ultraviolet region spectrum, and 2° observer (CIE 1931). The measurements were made by spectral reflectance, using the diffuse illumination geometry with an integration sphere, covered with a white material, so that the light is uniformly diffuse in all directions illuminating the sample, and is observed with the specular component included in 8° in relation to normal (*d*/8°) in the case of the spectrophotometer and 0° (*d*/0°) in the case of the colorimeter (Fig. 1).

The color measurements were plotted in the CIELAB color space. The CIELAB system is since 1976, the most widely used system for calculating color differences for most practical applications. Use of the CIELAB system enables estimation of three classical color parameters: L^*, a^*, and b^*, where L^* represents lightness, a^* represents the position between red and green on the redness (+) to greenness (−) axis, and b^* represents the position between yellow and blue on the yellowness (+) to blueness (−) axis. The three parameters are plotted on three orthogonal axes in a Cartesian coordinate system. In addition, the classical CIELAB formula (ΔE^*_{ab}) and two CIELAB-based color-difference formulae (ΔE^*_{94} and ΔE_{00}) were applied.

Four varieties of ornamental granite with very different characteristics in terms of color and texture were selected: Labrador Claro, a bluish-black, coarse-grained granite; Grissal, a grey, medium-grained granite; Rosa Porriño, a pinkish, coarse-grained granite; and Blanco Cristal, a white, fine-grained granite. Samples of all varieties were prepared with four different types of finish, i.e., of increasing degree of roughness: polished, honed, sawn, and flamed, except in Labrador Claro whose flamed finish is not easy to obtain. This set of samples was denominated Granite Training group because it comprised the reference samples (Fig. 2).

To determine the number of measurements required, five square specimens (surface area, 36 cm^2) of each variety of granite and type of finish were used. A total of 20 measurements with each of the four measurement heads of 5, 8, 10, and 50 mm diameter were made consecutively with replacement at different points selected randomly on the surface of each square specimen.

To determine the minimum area that must be measured, the same conditions were used on five square specimens of the same and larger surface area (36, 54, 72, and 90 cm^2) of each variety of granite and type of finish.

Once the minimum area and number of measurements were determined, the validity of the results was tested with other ornamental granite commonly used as a building material, but of a different color from the four test varieties. The variety chosen for this was Silvestre, a fine-grained, lightly weathered granite, which has a brownish-gold color due to weathering of its minerals (Fig. 2). The Silvestre variety of granite does not allow flamed or polished finish, therefore, they were substituted by bush hammered and polished without glow, respectively.

FIG. 2. Granite specimens used in the study. Granite training group: specimens in the same row are of the same type, from above to below: Blanco Cristal, Grissal, Rosa Porriño, and Labrador Claro. Specimens in the same column have the same finish, from left to right: polished, honed, sawn, and flamed. Granite test group: Silvestre, from above to below: polished without glow, honed, sawn, and bush hammered.

Color measurements were made on specimens of this granite, denominated Granite Test group (Fig. 2), in the same way as for the specimens in the Granite Training group.

All of the data were subjected to multivariate analysis of variance (MANOVA) by use of the SPSS statistical programme (version 15.0).

RESULTS AND DISCUSSION

For each of the specimens in the Granite Training group, the cumulative averages of the CIELAB color system coordinates: L^*, a^*, and b^* were plotted. The general shape of the graphics obtained was an inverted exponential decay with a horizontal asymptote, this steady section corresponds to the number of measurements from which the mean become constant; consequently, the first point of this section of the curve represents the minimum number of measurements required to characterize the coordinates L^*, a^*, and b^* for each specimen. By way of example, the plots obtained for one of the specimens are shown in Fig. 3. In each of the three graphs the number of measurements, from which the horizontal asymptote is reached and the mean become constant, is indicated by a marked segment. It can be seen that the number of measurements is different for each of the coordinates (L^*, a^*, and b^*); in general the value of lightness coordinate L^* is the first to stabilize, whereas for the other two coordinates, a^* and b^*, more measurements are generally required.

The data were subjected to a MANOVA with the minimum number of measurements determined for L^*, a^*, and b^* as dependent variables, and the type of rock, surface finish, and diameter of the instrument measurement head as independent variables. The results of the analysis revealed that the type of rock, the surface finish, and the diameter of the measurement head and their interactions produced significantly different results in terms of the minimum number of measurements required to characterize L^*, a^*, and b^*. The results of the analysis, including Wilks' lambda, the F-factor, the level of significance, and the number of degrees of freedom are shown in Table I.

The largest number obtained for each measurement head was therefore taken as the minimum number required to characterize the color of the specimens. Thus, according to the values shown in Table II, in which the number of measurements required to define the color of the specimens is shown in relation to the measurement head, the finish, and type of rock, it was established that for textured samples the smaller the measured head the larger the number of measures are needed. So, for a measurement head of 50 mm diameter, 6 measurements/36 cm^2 are required, for measurement heads of 8 and 10 mm diameter, 14 measurements/36 cm^2 are required; and for a measurement head of 5 mm diameter, 17 measurements/36 cm^2 are required (Table II).

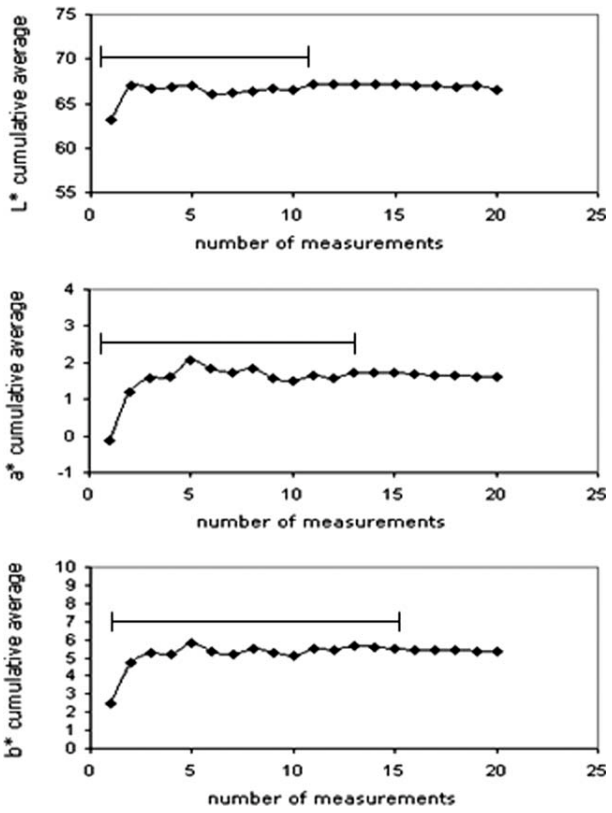

FIG. 3. Example of the graphs used to determine the minimum number of measurements required. Cumulative averages for parameters L^*, a^*, b^* in relation to the number of measurements made in one specimen of the Rosa Porriño granite with the 8 mm measurement head. The marked segment indicates the minimum number of measurements required.

TABLE I. Three-way multivariate analysis of variance (MANOVA) for the number of measurements.

Source	Wilk's lambda	*F*-value	*df*	Significance
Type of rock (granite)	0.625	13.663	9	0.000
Surface finish	0.678	11.093	9	0.000
Diameter of the measurement head	0.123	87.715	9	0.000
Type of rock × surface finish	0.594	5.645	24	0.000
Type of rock × diameter of the measurement head	0.637	4.282	27	0.000
Surface finish × diameter of the measurement head	0.729	2.933	27	0.000
Type of rock × surface finish × diameter of the measurement head	0.487	2.681	72	0.000

Dependent: L^*, a^*, and b^*.

Once the minimum number of measurements required to characterize the color of granite rocks was established, the minimum area of measurement was determined. For this, five specimens of each type of granite and surface finish were prepared with different areas (36 cm^2, 54 cm^2, 72 cm^2, and 90 cm^2), on which the corresponding number of measurements were made for each area and measurement head, according to the results obtained in the previous paragraph and by using the four different measurement heads (5, 8, 10, and 50 mm).

To determine whether the color varied with the measurement area, the data were subjected to MANOVA for each type of rock and measurement head (Table III), with the mean values of L^*, a^*, and b^* for each specimen as dependent variables and the measurement area (36, 54, 72, and 90 cm^2) as independent variables. As shown in Tables III and IV, there were statistically significant differences between the color obtained with the 50-mm diameter measurement head for an area of 36 cm^2 and the other areas. According to these results, to characterize the color of granite, a measurement area of 36 cm^2 and 14 measurements with random replacement is sufficient only if measurement heads of diameter $\leq$10 mm are used.

To determine the minimum area of measurement required with a 50 mm diameter measurement head, the statistical analysis was repeated with only the values of L^*, a^*, and b^* obtained for areas greater than 36 cm^2, i.e., with those corresponding to areas of 54, 72, and 90 cm^2 and with those obtained for areas greater than 54 cm^2, i.e., with areas of 72 and 90 cm^2.

Comparison of the values obtained for areas larger than 36 cm^2 revealed statistically significant differences for Grissal, Blanco Cristal, and Labrador Claro between the values obtained in an area of 54 cm^2 and those obtained in the other two areas (72 and 90 cm^2). However, there were no statistically significant differences between the values obtained for areas of 72 and 90 cm^2 (Table V), and therefore it can be concluded that to characterize the color of granite when working with a 50 mm diameter measurement head, a minimum surface area of 72 cm^2 is required.

Once the number and area of measurement were established in relation to the dimensions of the measurement head, the color determined by each head was compared to establish whether the results obtained are comparable. Considering the previous results, only the data obtained for an area of 72 cm^2 were used, and the number of measurements required was 12, 28, 28, and 34 for measurement heads of 50 mm, 10 mm, 8 mm, and 5 mm, respectively.

The results of a MANOVA, with L^*, a^*, and b^* as dependent variables and the diameter of the measurement head as the independent variable revealed statistically significant differences between the values obtained with the different measurement heads (Wilks' lambda: 0.949; *F*: 44 739; *df*: 9; significance: 0.000) with the 50 mm measurement head producing the greatest differences (Table VI).

TABLE II. Minimum number of measurements in relation to the measurement head, surface finish, and type of granite.

		Diameter of the measurement head (mm)			
Type of rock (granite)	Surface finish	50	10	8	5
Grissal	Flamed	4	11	12	14
	Sawn	1	10	11	15
	Honed	2	14	14	17
	Polished	1	6	12	17
Rosa Porriño	Flamed	3	13	14	15
	Sawn	2	9	13	16
	Honed	6	13	9	10
	Polished	3	13	13	17
Blanco crystal	Flamed	1	14	14	17
	Sawn	5	11	12	15
	Honed	1	12	13	17
	Polished	4	13	14	17
Labrador claro	Sawn	4	8	12	14
	Honed	4	11	13	17
	Polished	5	13	11	15

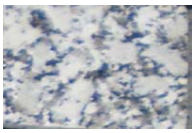

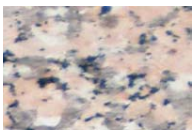

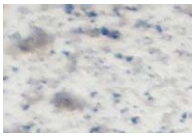

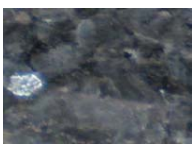

TABLE III. Three-way multivariate analysis of variance (MANOVA) for the measurement area in relation to the size of the measurement head.

Type of rock (granite)	Diameter of the measurement head (mm)	Wilk's lambda	*F*-value	*df*	Significance
Grissal	5	0.996	0.032	9	1.000
	8	1.000	0.003	9	1.000
	10	1.000	0.004	9	1.000
	50	0.004	172.529	9	0.000
Rosa Porriño	5	0.984	0.133	9	0.999
	8	0.998	0.013	9	1.000
	10	0.998	0.013	9	1.000
	50	0.009	118.037	9	0.000
Blanco Cristal	5	0.984	0.130	9	0.999
	8	1.000	0.003	9	1.000
	10	0.999	0.006	9	1.000
	50	0.427	8.378	9	0.000
Labrador Claro	5	0.999	0.006	9	1.000
	8	0.998	0.011	9	1.000
	10	0.999	0.007	9	1.000
	50	0.473	5.265	9	0.000

Dependent: L^*, a^*, and b^*.

With the aim of analyzing the real significance, rather than the statistical significance, of the differences in color obtained with the 5, 8, 10, and 50 mm diameter measurement heads, the total color differences (ΔE) for pairs of measurement heads (Fig. 4) were calculated with the classical CIELAB formula (ΔE^*_{ab}) and the CIELAB-based color-difference formulae (ΔE^*_{94} and ΔE_{00}) and they were expressed in CIELAB units[13,14] and the more recent CIE94 and CIEDE2000 units,[10] respectively. The differences in color were calculated with the Granite Training group, to obtain generalized results. The results obtained (Fig. 4) show that the differences in color expressed in CIEDE2000 and CIE94 units, which clearly improve on the CIELAB units[15–17] and are more appropriate for evaluating samples with low chromaticity values,[18] were the same as or lower in magnitude than the CIELAB color differences. It was also found that there was no equivalence of scale factor among the values produced with the three formulae considered. The visual color difference threshold or just noticeable difference (jnd), which constitutes the lower limit of perception in an individual with normal color vision[19–21] and that it can be established as 0.73 CIELAB units,[22,23] is also shown in the Fig. 4. Below this value, the differences in color are inappreciable and therefore the colors determined with the 8 and 10 mm measurement heads would be considered identical by an observer. However, if the suprathreshold color-difference, which is approximately 1.75 CIELAB units,[15] is taken into account, all of the values of the total color differences (ΔE) for pairs of measurement heads are below this value and are only outshined in the case of the color differences for the 8 and the 50 mm measurement heads, which were measured with the same device (the Minolta colorimeter). These two measurement heads provided the greatest differences in the total color differences (ΔE) from the three formulae used: ΔE^*_{ab}, ΔE^*_{94}, and ΔE_{00}.

On the other hand, if we take into account the color tolerances or units of color differences applied in the industrial field, where larger color differences are used, all of the values of ΔE obtained for the different measurement head were lower than 3 CIELAB units, the value considered as the upper limit of rigorous color tolerance.[14,24]

With the aim of standardizing the results obtained with the granites included in the Granite Training group, a test

TABLE IV. Tukey-b test for the 50-mm-diameter measurement head.

Type of rock (granite)	Area (cm^2)	L^*	a^*	b^*
Grissal	36	57.02^a	3.88^a	-8.49^a
	54	64.07^b	-0.75^b	0.86^b
	72	64.08^b	-0.54^c	0.79^b
	90	63.48^b	-0.54^c	0.78^b
Rosa Porriño	36	57.45^a	5.91^a	-3.67^a
	54	63.89^b	2.20^b	5.63^b
	72	63.91^b	2.33^b	5.68^b
	90	63.93^b	2.34^b	5.70^b
Blanco Cristal	36	68.05^a	2.75^a	-3.42^a
	54	72.38^b	-0.28^b	3.13^b
	72	71.96^b	-0.11^b	2.72^b
	90	71.34^b	-0.10^b	2.72^b
Labrador Claro	36	48.28^a	-0.49^a	-1.32^a
	54	$48.05^{a,b}$	$-0.40^{a,b}$	-1.34^a
	72	47.75^b	-0.28^b	-1.42^a
	90	47.74^b	-0.28^b	-1.42^a

Superscript letters a–c in each column for each granite indicate significant differences (α: 0.05).

was performed to determine whether these were applicable to other granites. For this, the color of one of the granites most commonly used at present in the building industry for cladding and for constructing monuments—a brownish gold granite denominated Silvestre—was determined.

The values obtained for this granite (for an area of 72 cm^2 and number of measurements depending on the measurement head used: 34/5 mm head, 28/8 and 10 mm head, 12/50 mm head) were subjected to MANOVA, with

TABLE V. Three-way multivariate analysis of variance (MANOVA) comparing the different areas measured.

Type of rock (granite)	Areas (cm^2)	Wilk's lambda	*F*-value	*df*	Significance
Grissal	54–72–90	0.511	7.313	6	0.000
	72–90	0.981	0.227	3	0.877
Rosa Porriño	54–72–90	0.958	0.396	6	0.880
Blanco Cristal	54–72–90	0.581	5.712	6	0.000
	72–90	0.969	0.388	3	0.762
Labrador Claro	54–72–90	0.615	3.662	6	0.003
	72–90	0.999	0.002	3	0.999

Dependent: L^*, a^*, b^*.

TABLE VI. Tukey-b test for the four measurement heads.

Diameter of the measurement head (mm)	L^*	a^*	b^*
50	62.87^a	0.39^a	2.17^a
10	64.45^b	0.08^b	2.84^b
8	64.32^b	0.06^b	3.43^c
5	62.76^a	0.18^b	3.17^c

Superscript letters a–c in each column indicate significant differences (α: 0.05).

L^*, a^*, and b^* as dependent variables and the diameter of the measurement head (5, 8, 10, and 50 mm) as the fixed factor. The results were similar to those obtained with the Granite Training group; there were statistically significant differences in relation to the measurement head (Wilks' lambda: 0.865, *F*: 33.843; *df*: 9; significance: 0.000) for each of the parameters considered (Table VII). The total color differences (ΔE) were calculated for the different measurement heads (Fig. 5) and a rigorous color tolerance (i.e., <3 CIELAB units) was obtained. Again, the greatest difference was between the color measurements made with the measurement heads of 50 mm and 8 mm diameter. The total color difference ΔE^*_{ab} comparing small heads (5–10 and 5–8 mm) decreased by ~0.5 CIELAB units in relation to the results obtained with the Granite Training group, whereas any comparison (ΔE^*_{ab}, ΔE^*_{94}, and ΔE_{00}) between the 50 mm and the 5 mm measurement heads caused an increase in the difference of 0.5 units and of 1 unit when the comparison was between the 50 mm and the 8 or 10 mm measurement heads.

It must be stressed that the chromatic appearance of heterogeneous surfaces, and in particular their chromatic discrimination, should be based not only on conventional colorimetric measures but on visual correlations with real observers. In this regard, although there are some recent contributions combining both the methods,[25–28] all of them are related to textured materials having well delimited contours which makes dubious their application to other kind of materials. In the case of granite, it has been

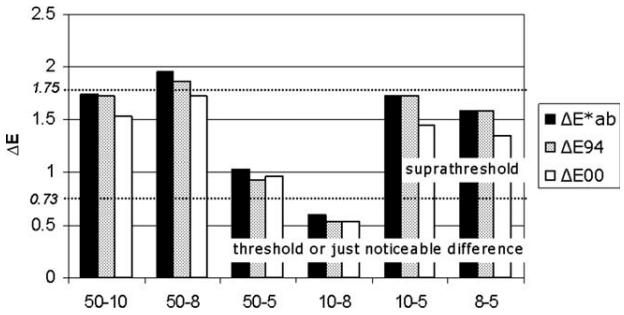

FIG. 4. Total color differences for granite training group, in CIELAB units (ΔE^*_{ab}), CIE94 units (ΔE^*_{94}), and CIEDE2000 units (ΔE_{00}), obtained with different pairs of measurement heads.

one attempt to combine colorimetric measures and visual assessment to analyze changes in the appearance of the surface of granite rocks when they are colonized by microorganisms[29] and it has been established that the minimum increment in color that observers can appreciate is $\Delta E^*_{ab} = 3.17$, which is bigger than the tolerance above commented. However, owing to that value has been determined in a very specific experiment it cannot be considered as a definitive value and future research in this field would be focussed on performing visual experiments using psychophysical techniques with the aim of defining the granitic rocks threshold. Therefore, in a sense and awaiting progress in granite visual assessment, the reader should be careful with the interpretation of differences in total color data as two granite samples could have identical average CIELAB color and could be judged as different images by an observer.

CONCLUSIONS

This work provides an adaptable and affordable methodology of study supported by statistical analysis, which has been successful in examination of the factors affecting the color measurements on granite rocks and demonstration that color may be affected by both material and instruments properties. In this way, the methodology used enabled the determination of the minimum number of measurements and the minimum measuring area required to characterize the representative color of the whole nonhomogeneous surface of granite rocks. However, it should be noted that although the application of the present color-difference formulae to heterogeneous surfaces has not yet been validated, they have been employed in this study as a tool for comparison assuming a correlation between spatial averaging of CIELAB and visual judgment of granite.

In relation to the minimum number of measurements required to characterize the color of granite rocks, it was found that it is affected by the type of rock, surface finish, and independently of the rock, by the diameter of the measurement head of the device. By use of a wide variety of granite rocks that differ in terms of color, texture, and surface finish, it was determined that the minimum number of measurements required to characterize the color of granitic rocks is higher the smaller measurement head. Thus, the number of measurements required is 6/36 cm^2 surface area for a 50 mm diameter measurement head, 14/36 cm^2 for 8 and 10 mm diameter measurement heads, and 17/36 cm^2 for a 5 mm measurement head.

TABLE VII. Tukey-b test for the four measurement heads and Silvestre granite.

Diameter of the measurement head (mm)	L^*	a^*	b^*
50	70.02^a	-0.04^a	3.48^a
10	72.56^b	-0.11^b	4.37^b
8	72.56^b	-0.24^c	4.68
5	71.41^c	0.02^d	4.41^b

Superscript letters a–d in each column indicate significant differences (α: 0.05).

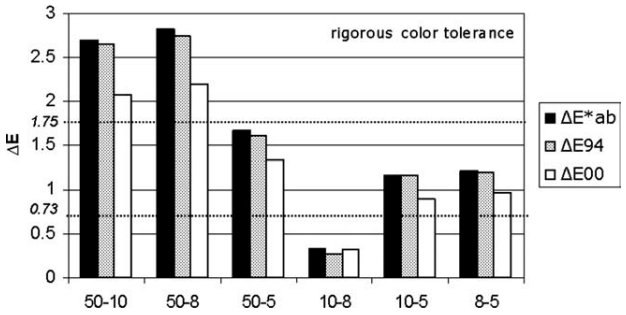

FIG. 5. Total color differences for granite test group (Silvestre), in CIELAB units (ΔE^*_{ab}), CIE94 units (ΔE_{94}), and CIEDE2000 units (ΔE_{00}), obtained with different pairs of measurement heads.

As regards the minimum measuring area, the results showed that an area of 36 cm^2 is sufficient when measurement heads of diameter $\leq$10 mm are used. A surface area equal to or larger than 72 cm^2 is required for measurement heads of larger diameters.

The validity of the above results was tested with other ornamental granite (Granite Test group) allowing to conclude that if and when the number of measurements considered corresponds to those established in this study for the measurement head diameter and the measurement area, any results thus obtained will be comparable.

As granite rocks can be considered as a complicated case of surface heterogeneity due to the complexity of their mineral distribution, it could be hypothesized that the methodology here proposed can be extrapolated to other types of rocks.

1. Capilla P, Artigas JM, Pujol J. Fundamentos de Colorimetría. Valencia: Universitat de València; 2002.
2. Calvo B, Menduina J, Parra JL. Ensayo metodológico para el estudio de las propiedades de granitos meteorizados. Boletín Geológico y Minero 1991;102:295–307.
3. Benavente D, Martínez-Verdú F, Bernabeu A, Viqueira V, Fort R, García del Cura MA, Illueca C, Ordóñez S. Influence of surface roughness on color changes in building stones. Color Res Appl 2003;28:343–351.
4. Íñigo AC, Vicente-Tavera S, Rives V, Vicente MA. Color changes in the surface of granitic materials by consolidated and/or water repellent treatments. Color Res Appl 1997;22:133–141.
5. Rivas T, Silva B, Prieto B. Medida de la eficacia de dos hidrofugantes aplicados a rocas graníticas. Materiales de Construcción 1998;249:5–21.
6. Sanmartín P, De los Santos DM, Rivas T, Prieto B, Mosquera MJ, Silva B. Different behaviour of TEOS-based consolidant applied to granite and biocalcareous sandstone. Proceedings of the International Symposium on Stone Consolidation in Cultural Heritage Research and Practice, Lisbon, 2008.
7. Grossi CM, Esbert RM, Díaz-Pache F, Alonso FJ. Soiling of buildings stones in urban environments. Build Environ 2003;38:147–159.
8. Grossi C, Brimblecombe P, Esbert RM, Alonso FJ. Color changes in architectural limestones from pollution and cleaning. Color Res Appl 2007;32:320–331.

9. Prieto B, Rivas T, Silva B. Rapid quantification of phototrophic microorganisms and their physiological state through their color. Biofouling 2002;18:229–236.
10. CIE Publ. 15:2004. Colorimetry, 3rd edition. Vienna: CIE Central Bureau; 2004.
11. Montag ED, Berns RS. Lightness dependencies and the effect of texture on suprathreshold lightness tolerances. Color Res Appl 2000;25: 241–249.
12. Chorro E, Perales E, de Fez D, Luque MJ, Martínez-Verdú FM. Application of the S-CIELAB color model to processed and calibrated images with a colorimetric dithering method. Opt Express 2007;15:7810–7817.
13. Wyszecki G, Stiles WS. Color Science. Concepts and Methods, Quantitative Data and Formulae. New York: Wiley; 1982.
14. Berns RS. Billmeyer and Saltzman's Principles of Color Technology, 3rd edition. New York: Wiley; 2000.
15. Melgosa M, Hita E, Poza AJ, Alman DH, Berns RS. Suprathreshold color-difference ellipsoids for surface colors. Col Res Appl 1997;22:148–155.
16. Melgosa M, Huertas A, Berns RS. Relative significance of the terms in the CIEDE2000 and CIE94 color-difference formulas. J Opt Soc Am A 2004;21:2269–2275.
17. Kim D-H, Cho EK, Kim JP. Evaluation of CIELAB-based colour-difference formulae using a new dataset. Color Res Appl 2001;26: 369–375.
18. Johnson G, Fairchild MD. A top down description of S-CIELAB and CIEDE2000. Color Res Appl 2003;28:425–435.
19. Brown WRJ, MacAdam DL. Visual sensitivities to combined chromaticity and luminance differences. J Opt Soc Am 1949;39:808–834.
20. Brown WRJ. Color discrimination of twelve observers. J Opt Soc Am 1957;47:137–143.
21. Wyszecki G, Fielder G. New color matching ellipses. J Opt Soc Am 1971;61:1135–1152.
22. MacAdam DL. Visual sensitivities to color differences in daylight. J Opt Soc Am 1942;32:247–274.
23. Melgosa M, Hita E, Pérez MM, El Moraghi A. Sensitivity differences in chroma, hue, and lightness from several classical threshold datasets. Color Res Appl 1995;20:220–225.
24. Völz HG. Industrial Color Testing. Weinheim: Wiley–VCH; 2001.
25. Day EA, Berns RS, Taplin LA, Imai FH. A psychophysical experiment evaluating the color and spatial image quality of several multispectral image capture techniques. J Imaging Sci Technol 2004;48: 93–104.
26. Kuriki I. Testing the possibility of average-color perception from multicolored patterns. Opt Rev 2004;11:249–257.
27. Xin JH, Shen HL, Lam CC. Investigation of texture effect on visual colour difference evaluation. Color Res Appl 2005;30:341–347.
28. Ariño I, Johansson S, Kleist U, Liljenström-Leander E, Rigdahl M. The effect of texture on the pass/fail colour tolerances of injection-molded plastics. Color Res Appl 2007;32:47–54.
29. Prieto B, Silva B, Aira N, Álvarez L. Toward a definition of a bioreceptivity index for granitic rocks: Perception of the change in appearance of the rock. Int Biodeter Biodeg 2006;58:150–154.

Chapter 2*. Effect of surface finish on roughness, color, and gloss of ornamental granites

Sanmartín, P.; Silva, B.; Prieto, B.

Journal of Materials in Civil Engineering 23 (8): 1239-1248 (2011)

JCR index (IF) 2010 = 0.677 (19/53, 36 percentile in Construction & Building Technology; 54/115, 47 percentile in Engineering Civil)

Total number of times cited: 3

* Selected as *Research Highlight* by the journal during the months of August, September, October, November and December 2011.

Effect of Surface Finish on Roughness, Color, and Gloss of Ornamental Granites

P. Sanmartín[1]; B. Silva[2]; and B. Prieto[3]

Abstract: The effects of four of the most common types of surface finish on the appearance of five varieties of ornamental granite, all widely used in building construction and selected for their different colors, were analyzed by means of roughness, color, and gloss measurements. The results demonstrated that different surface finishes produce differences in color, especially in the lightness parameter (L^*), and that the magnitude of these differences depends on the color of the ornamental granite and is greatest in dark colored rocks. However, the variation in the color parameters with the different surface finishes did not depend on roughness, and no general conclusions could be drawn regarding the influence of the roughness on the color of ornamental granite. Gloss values were affected by the color of the ornamental granite, but in a different way for smooth and rough surfaces. Variation in gloss also depended on the mineral composition of the rock. Gloss and roughness were inversely related, but only within the range of low roughness values. In addition, the color gamut of the studied ornamental granites was defined within the CIELAB color space. These results will contribute to providing a standardized, objective method of characterizing the color of granite that will be useful for different workers in the field of building construction. **DOI: 10.1061/(ASCE)MT.1943-5533.0000285.**

CE Database subject headings: Surface roughness; Stones; Color; Coating.

Author keywords: Color assessment; Gloss; Ornamental granite; Roughness; Surface finishes.

Introduction

Many of the most impressive monuments and buildings in the world are built from granite because this is one of the oldest, most durable, and most respected of building materials. The popularity of granite in the building, construction, monument, and tombstone industries is attributable not only to its resistance to weathering but also to its appearance. Selection of ornamental granites for new constructions is primarily based on their aesthetic properties because these define the architectural harmony of the construction with the surroundings and enhance the visual perception of the building. Several types of surface finish, such as polished, flamed, and sawn, have been developed to produce different appearances and thus increase the decorative potential of the granite. Surfaces finishes differ in surface roughness and affect slab aesthetics because they induce variations in the perceived texture, color, and gloss. Therefore, when appearance is the main selection criterion, aesthetic properties such as texture, color, and gloss must be taken into account.

Texture is defined as the visual characteristic and tactile quality of the surface of a material, although the term is also used in geology to refer to the degree of crystallinity, grain size, and fabric (geometrical relationships) of the constituents of a rock. Two terms were therefore used in the present study: surface texture and petrographic texture. Obviously, the petrographic texture affects the surface texture. However, in the case of ornamental rocks, other surface properties such as the surface finish of the rock, which is not related to the petrographic texture because it is induced by humans, must be considered because it is very important from an aesthetic point of view. Surface roughness is a measure of the surface texture, and the parameter most frequently used to describe roughness is the average roughness (Ra or ΔRa), defined as the integral of the absolute value of the roughness profile over an evaluation length and measured with a profilometer (ISO 1984).

Although color is the aesthetic property most often used in selecting building material, objective colorimetric characterization of different granitic rocks is not usually carried out in the granite industry, and operators must trust in their skill to differentiate colors. This leads to misunderstandings between architects and builders. This problem is reflected in the colorimetric terms used to classify granite. Terms such as "champagne cream" and "golden yellow" may suggest different colors to different people. One clear example, granites commercialized as *Rosa Porriño* and *Rosabel* are classified as pink granites in some catalogs and as red granites and gray granites, respectively, in others.

Likewise, despite the great acceptance of contact color-measurement devices for objective measurement of the color of granite (Grossi et al. 2007a; Iñigo et al. 2004, 1997) and other more homogeneous rocks (Durán-Suárez et al. 1995; García-Talegón et al. 1998; Grossi et al. 2007b), a standardized protocol enabling comparison of the results obtained by different authors and instruments has only recently been published (Prieto et al. 2010). In that work, which took into account the high heterogeneity in color and texture of this plutonic rock, a protocol for characterization of color and a methodology for the analysis of instrumental and surface factors that may affect the determination of color were proposed by using statistical tools and colorimetric criteria.

[1]Ph.D. Student, Departamento Edafología y Química Agrícola, Facultad Farmacia, Universidad de Santiago de Compostela, 15782-Santiago de Compostela, Spain. E-mail: patricia.sanmartin@usc.es

[2]Full Professor, Departamento Edafología y Química Agrícola, Facultad Farmacia, Universidad de Santiago de Compostela, 15782-Santiago de Compostela, Spain. E-mail: benita.silva@usc.es

[3]Full Professor, Departamento Edafología y Química Agrícola, Facultad Farmacia, Universidad de Santiago de Compostela, 15782-Santiago de Compostela, Spain (corresponding author). E-mail: beatriz.prieto@usc.es

Note. This manuscript was submitted on September 23, 2010; approved on January 27, 2011; published online on January 29, 2011. Discussion period open until January 1, 2012; separate discussions must be submitted for individual papers. This paper is part of the ***Journal of Materials in Civil Engineering***, Vol. 23, No. 8, August 1, 2011. ©ASCE, ISSN 0899-1561/2011/8-1239–1248/$25.00.

Gloss is an optical phenomenon related to the appearance of a surface and represents the capacity of a surface to reflect directed light (ASTM 1995). According to Hunter (1937), six different visual criteria relate to the perception of gloss: (1) specular gloss, (2) sheen, (3) contrast gloss or luster, (4) absence-of-bloom gloss, (5) distinctness-of-image gloss, and (6) surface-uniformity gloss. In the particular case of ornamental rocks, the specular gloss is often used to monitor surface quality because it is related to the surface roughness (Huang et al. 2002; ASTM 1997).

Several studies analyzed the relationships among these three aesthetic properties (roughness, color, and gloss) in different materials (Ignell et al. 2009; Shih et al. 2008; Briones et al. 2006; Ariño et al. 2005; Eliades et al. 2004; Keyf and Etikan 2004; Simonot and Elias 2003; Dalal and Natale-Hoffman 1999; Thomas 1999; Barnett 1973). Thus, it has been demonstrated that (1) an inverse relationship exists between roughness and gloss; (2) lightness (L^* CIELAB coordinate) and chroma (C^*_{ab} CIELAB coordinate) of the color vary with roughness and gloss; (3) lightness (L^* CIELAB coordinate) affects gloss; and (4) the magnitude of the change in color with superficial texture is governed by the color of the material. However, all these studies were carried out with homogeneous surfaces from the point of view of color and composition rather than from arbitrary heterogeneous samples such as granite rocks.

In this sense, none of the aforementioned studies included ornamental rocks. To date, only one study examining the influence of the induced surface roughness on the color change of ornamental rocks has been published (Benavente et al. 2003). These authors demonstrated that the color variations caused by acid attack on building stones basically depend on variations in surface roughness and the type of rock.

In the present study, the effect of four of the most common surface finishes on the appearance of five varieties of ornamental granite, all widely used in building construction and selected for their different colors, was analyzed by means of roughness, color, and gloss measurements to provide an objective standardized method of aesthetic characterization useful for the different workers in the fields of construction and building materials.

Experimental

Rocks and Mechanical Surface Finishes

Five varieties of ornamental rocks of very different color were selected: *Grissal*, a gray coarse-grained granite; Rosa Porriño, a pinkish coarse-grained granite; *Blanco Cristal*, a white medium-grained granite; *Silvestre*, a white medium-grained with some ochre spots owing to biotite weathering; and *Labrador Claro*, a bluish-black coarse-grained rock although classified petrographically as a diorite-gabbro, was included in this study because its dark (almost black) color increased the color gamut of the rocks under study. Labrador Claro is one of the most commercialized of the darkest rocks and is also referred to as granite in the ornamental stone industry (Fig. 1). Each variety was petrographically and

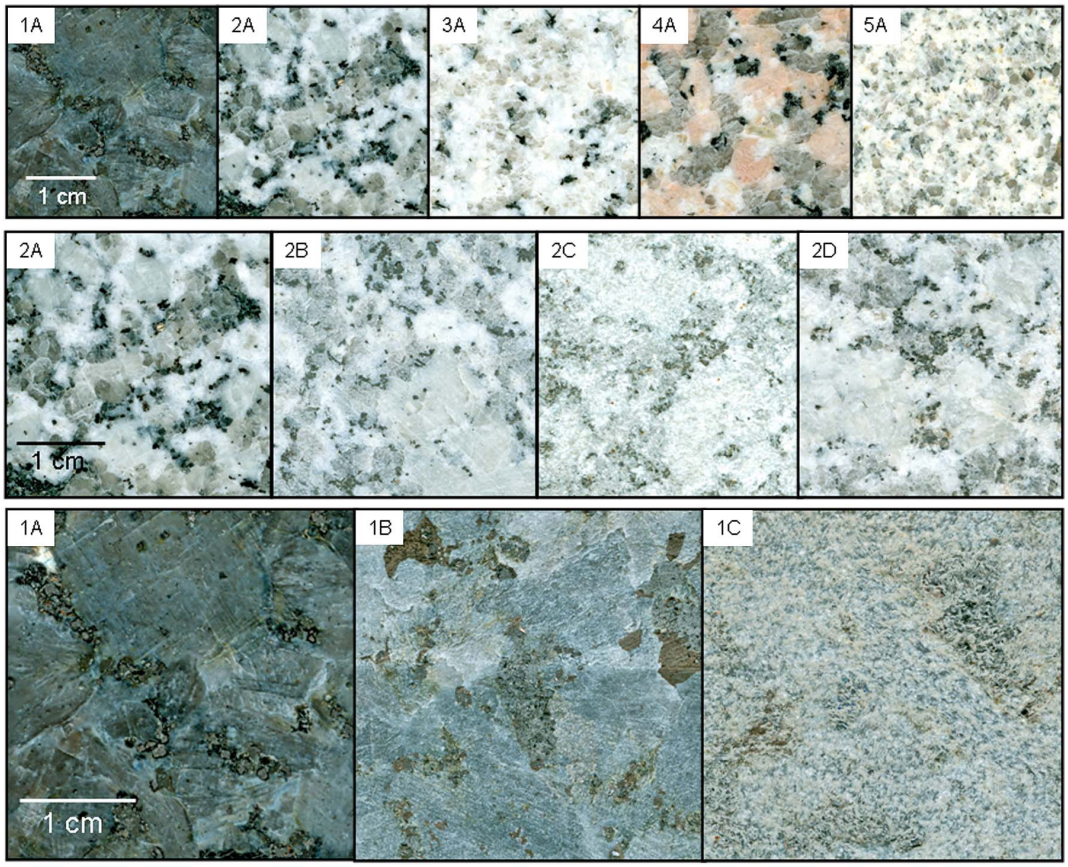

(1) Labrador Claro; (2) Grissal; (3) Blanco Cristal; (4) Rosa Porriño; (5) Silvestre. (A) Polished finish (B) Honed finish, (C) Sawn finish, (D) Flamed finish.

Fig. 1. Macroscopic appearance of the studied ornamental granites

mineralogically characterized by optical microscopy. Information relating to petrographic classification, petrographic texture, mineral composition, and mineral size grain of the studied rocks is shown in Table 1.

Five square specimens (36 cm^2) of each granitic rock were prepared with different types of surface finish. Four types of finish were applied to four of the granites (in order of increasing roughness): polished, honed, sawn, and flamed (López Jiménez 1996). Flamed and polished finishes cannot be applied to the Silvestre variety of granite, which is more weathered than the others, and these finishes were therefore substituted by bush hammered and polished without glow, respectively.

Table 1. Petrographic Classification, Petrographic Texture, Mineral Composition and Mineral Grain Size of the Studied Ornamental Granites

		Mineral size (mm)		
Mineral	%	Mean	Maximum	Minimum
Blanco cristal (biotite adamellitic granite; texture: heterogranular-panallotriomorphic of medium grain)				
Quartz	26	1.7 ± 1.0	5.4	0.3
Feldspar-K	29	3.2 ± 1.7	5.5	0.6
Plagioclases	27.5	1.6 ± 0.9	3.7	0.7
Biotite	9	0.9 ± 0.3	1.6	0.6
Moscovite	2	0.4 ± 0.1	0.5	0.2
Chlorite	4.5	0.5 ± 0.2	0.4	0.3
Grissal (alcaline granite; texture: porphyritic-panallotriomorphic of coarse grain)				
Quartz	30.5	2.6 ± 0.9	4.2	1.1
Feldspar-K	34.5	7.0 ± 6.0	17.6	1.3
Plagioclases	20.75	2.0 ± 1.4	4.2	0.3
Biotite	8.5	0.6 ± 0.3	1.0	0.3
Moscovite	0.5	0.2 ± 0.1	0.3	0.1
Chlorite	3.5	0.7 ± 0.4	1.3	0.3
Rosa porriño (biotite adamellitic granite; texture: porphyritic-panallotriomorphic of coarse grain)				
Quartz	30	3.6 ± 2.3	8.2	0.8
Feldspar-K	33	5.7 ± 5.2	14.4	1.3
Plagioclases	21	3.3 ± 2.5	8.0	0.6
Biotite	9	1.4 ± 0.9	3.2	0.3
Chlorite	3.5	0.8 ± 0.5	1.6	0.3
Labrador claro (diorite-gabbro with labradorite feldspar; texture: phaneritic-hipidiomorphic of coarse grain)				
Feldspar	48	8.7 ± 4.1	15.3	3.5
Pyroxene	16.5	3.9 ± 3.0	9.6	1.0
Olivine	6.5	0.8 ± 0.5	1.4	0.4
Biotite	3.5	1.6 ± 1.7	4.8	0.3
Amphiboles	5.5	1.8 ± 1.5	4.6	0.5
Opaques	15	0.5 ± 0.3	1.0	0.3
Apatite	4.0	0.5 ± 0.2	0.6	0.2
Silvestre (two mica adamellitic granite; texture: equigranular-panallotriomorphic of medium grain)				
Quartz	29	2.0 ± 0.6	2.9	0.5
Feldspar-K	26	2.2 ± 1.0	3.8	1.0
Plagioclases	24	1.9 ± 0.8	3.2	1.0
Biotite	8	1.0 ± 0.3	1.6	0.4
Moscovite	8	1.2 ± 0.6	2.0	0.3
Chlorite	3.5	0.5 ± 0.2	1.0	0.3

Polishing is a surface treatment often used in granite stones, because it highlights all the colors and petrographic textures of the material. The polishing process is carried out with particles of different grain size, i.e., successively finer particles. The process can close the rock pores because during the polished process, the voids are filled with crushed material from the rock itself or from the abrasive materials used; the process makes the material more resistant to external aggressions because it reduces its water absorbing capacity (Rojo et al. 2003). The resulting surface is flat and glossy with a perceptually darker tone than achieved with other treatments. Honing is very similar to polishing, but the stone does not acquire the characteristic gloss. The honing process is similar to polishing, but only coarse-grained grinding particles are used, and a matte finish is achieved. Polishing without glow, an intermediate finish between polishing and honed, was also used. Sawing is a finish resulting from cutting the granite with steel sheets or diamond disks. This is usually carried out before applying another finish. The resulting appearance is even, matte, and slightly rough, sometimes with small undulations caused by the cut. Flaming is carried out by heating the granite surface with a blowtorch. The thermal shock causes some mineral grains to be shed from the surface, particularly those fragmented by the saw. The result is a rough surface with a glassy appearance. This finish cannot be achieved in brownish, moderate, or highly weathered granite (e.g., Silvestre) because it would modify the aspect of the surface unevenly as a result of chemical alterations. Bush hammering is one of the most commonly used finishes; in earlier times, it was carried out by beating the stone manually with a bush hammer. Nowadays, the system is mechanized so that it produces a more homogeneous rough finish.

Roughness Measurements

Roughness measurements were performed to quantify the surface texture achieved on the granite specimens with the different surface finishes. Roughness was characterized with a noncontact laser profilometer (UBM microfocus measurement system, UBM Messtechnik GmbH, Ettlingen, Germany) with a measurement range of ± 500 μm. The noncontact laser profilometer was equipped with a 780 nm wavelength laser triangulation sensor with a spot diameter of 1 μm and an axis and sensor resolution of 0.06 μm. One specimen of each studied rock and surface finish (except flamed and bush hammered finishes, which produce roughness above the threshold of 500 μm) was analyzed. To take into account the surface anisotropy of the ornamental granites, the laser profilometer was driven in a horizontal $(X - Y)$ plane by a two-dimensional (2D) positioning system with two linear motor actuators. A total of six lines of 17.50 mm long, three on longitudinal axis (X) and three on transverse axis (Y), were scanned. The average roughness (Ra) is defined as the integral of the absolute value of the roughness profile over an evaluation length (12.50 mm) and was determined from the six measurements with a resolution or point density of 150 points/mm.

Color Measurements

The color was measured with a GretagMacbeth (now XRite; Eibar, Spain) portable spectrophotometer CE-XTH equipped with OptiviewSilver/i QC Basic software. The measuring conditions fixed in the device were: diameter viewing aperture of 10 mm, illuminant D65, and observer 2° (CIE 1932) with a $d/8^{\circ}$ illumination viewing geometry (Prieto et al. 2010). Because the surface of granite samples is not totally reflective or matte, inclusion or exclusion of the specular component may be important for color measurements. Thus, the measurements were made in both specular component

included (SCI) and specular component excluded (SCE) modes. The SCI mode, in which the gloss trap of the spectrophotometer is closed, includes the total reflectance (considering both specular and diffuse reflections); whereas the SCE mode, with an open gloss trap, includes the diffuse reflectance and excludes most of the specular component and is therefore more sensitive to differences in color owing to differences in surface roughness (Wyszecki and Stiles 1982). It is generally accepted in the field of color science that the SCE mode approximates the view with the naked eye and the SCI mode is adequate for analyzing the intrinsic color of objects.

Following the protocol recently described by Prieto et al. (2010) for measuring the color of granite rocks, 14 readings were taken with substitution in random zones of the surface of each of the five square specimens (36 cm^2) of each variety of granite and type of finish.

The CIELAB (CIE 1986) color space was selected to represent the color measurements by use of two different sets of coordinates, Cartesian coordinates, CIEL$^*a^*b^*$ and cylindrical coordinates, CIEL$^*C^*_{ab}h_{ab}$. The first coordinates consider the lightness of the color L^* (which varies from 0 black to 100 white), the redness-greenness changes a^* (red (+) to green (−) axis), and the yellowness-blueness changes b^* (yellow (+) to blue (−) axis). The other set of coordinates is defined by two cylindrical coordinates, the chroma of the color C^*_{ab} and the hue of the color h_{ab}, in addition to the lightness L^*; C^*_{ab} and h_{ab} are related to a^* and b^* as $C^*_{ab} = (a^{*2} + b^{*2})^{1/2}$ and $h_{ab} = \arctan(b^*/a^*)$.

The CIEL$^*a^*b^*$ coordinates are preferred for achromatic colors, whereas the CIEL$^*C^*_{ab}h_{ab}$ coordinates are recommended for stronger colors (Catalina and Bruna 1997). Because this study attempted to cover the full range of granite colors and chromatic and achromatic rocks were studied, both sets of coordinates were used.

The partial color differences (ΔL^*, Δa^*, Δb^*, ΔC^*_{ab}, ΔH^*_{ab}) and the total color difference (ΔE^*_{ab}) were also calculated. ΔL^* and ΔC^*_{ab} represent the difference between both considered values of L^* and C^*_{ab}, respectively, whereas H^*_{ab} is given by $\Delta H^*_{ab} = [(\Delta E^*_{ab})^2 - (\Delta L^*)^2 - (\Delta C^*_{ab})^2]^{1/2}$ (CIE 2004). Following the recommendations for textured samples reported by Huertas et al. 2006, the classical CIELAB (CIE 1976) color equation, $\Delta E^*_{ab} = [(\Delta L^*)^2 + (\Delta a^*)^2 + (\Delta b^*)^2]^{1/2}$, was applied rather than the newer improved formulas.

Gloss Measurements

Specular gloss was measured at an angle on incidence of 60° according to ASTM D 523-95 (ASTM 1995) with a GretagMacbeth (now XRite) portable spectrophotometer (CE-XTH). To obtain an overall description of each surface finish in each studied rock, 40 readings were taken with substitution in random zones of the surface area, considering one specimen of each type of rock and surface finish, and expressing the results as mean values. A previous study (Huang et al. 2002) was used as reference in which 20 measurements were made on more homogeneous granite with respect to color and texture.

Statistical Analysis

Statistical analyses were performed with SPSS version 17.0 for Windows (http://www-01.ibm.com/software/analytics/spss/). Average roughness values (*Ra*) and specular gloss (G^{60}) data were subjected to analysis of variance (ANOVA) at $p < 0.05$. CIELAB color data were subjected to a multivariate analysis of variance (MANOVA) at $p < 0.05$. A student's *t*-test ($p < 0.05$) was used to compare the CIELAB color coordinates obtained in specular component included (SCI) and excluded (SCE) modes.

Results and Discussion

The average roughness values [*Ra* (μm)] induced by each surface finish in each ornamental granite are shown in Table 2. The same trend was observed in each granite studied, i.e., the *Ra* values increased significantly from the polished or polished without glow finish to the flamed or bush hammered finish. Comparison of *Ra* values with those obtained in other studies is difficult because the aim of most studies on the roughness of ornamental granite is to compare roughness before and after the salt crystallization test to analyze decay patterns in monumental granite (Alonso et al. 2008; López-Arce et al. 2010). Moreover, the latter studies did not provide any information about the surface finish of the samples. Grissal and Rosa Porriño are two of the granites studied by Alonso et al. (2008), who reported larger *Ra* values for Rosa Porriño than for Grissal, which is consistent with the results obtained in this study. Considering only the polished surfaces, Labrador Claro is the granite with the lowest *Ra* value followed by Blanco Cristal and Grissal, then by Rosa Porriño, and finally Silvestre.

The values of each color coordinate measured in the specular component included (SCI) and excluded (SCE) modes for each type of ornamental granite and surface finish are shown in Table 3. Considering the set of samples to be representative of the ornamental granites, a range of values can be established for this type of rock. Thus, parameter L^*, lightness, varied most widely from 34.2 ± 0.5 in the darker rocks to 74.9 ± 1.0 in the lighter rocks in SCI mode and between 30.7 ± 4.8 and 75.5 ± 3.5 in SCE mode. The chromatic parameter a^* varied between 2.7 ± 0.5 and -0.9 ± 0.1 in SCI mode and between 3.3 ± 2.6 and -0.8 ± 0.3 in SCE

Table 2. Roughness Average and Specular Gloss of Each Ornamental Granite and Surface Finish

Type of granite[a]	Roughness average *Ra* (μm)[b]	Specular gloss, G^{60} (gu)[b]
Gp	0.4 ± 0.2^a	67.4 ± 10.8^a
Gh	4.4 ± 1.8^b	17.0 ± 9.9^b
Gs	21.8 ± 2.2^c	19.0 ± 4.5^b
Gf	above limit	15.6 ± 1.2^b
BCp	0.4 ± 0.2^a	69.9 ± 5.8^a
BCh	3.5 ± 0.8^a	22.0 ± 6.0^b
BCs	25.4 ± 4.8^b	24.6 ± 0.3^b
BCf	above limit	35.0 ± 12.0^c
RPp	0.6 ± 0.3^a	77.2 ± 6.6^a
RPh	5.3 ± 1.7^b	21.5 ± 6.6^b
RPs	24.0 ± 4.0^c	24.8 ± 2.9^b
RPf	above limit	23.9 ± 2.7^b
LCp	0.3 ± 0.2^a	89.3 ± 3.4^a
LCh	3.5 ± 2.1^a	8.5 ± 0.6^b
LCs	21.8 ± 5.0^b	12.5 ± 5.4^b
Spwg	2.6 ± 1.6^a	19.9 ± 7.8^a
Sh	4.1 ± 0.7^a	18.2 ± 5.3^a
Ss	23.1 ± 4.0^b	18.2 ± 1.1^a
Sb	above limit	22.5 ± 7.2^a

[a]G = Grissal; BC = Blanco Cristal; RP = Rosa Porriño; LC = Labrador Claro; S = Silvestre; p = polished; pwg = polished without gloss; h = honed; s = sawn; b = bush hammered; and f = flamed.

[b]*Ra* data are the mean of six measurements ± SD. G^{60} data are the mean of 40 measurements ± SD. Different superscript letters indicate significant differences ($p < 0.05$) between the mean values of six measurements for the roughness and forty measurements for the specular gloss in the same type of granite in relation to surface finish.

Table 3. CIELAB Color Coordinates of Each Ornamental Granite and Surface Finish, Measured With the Spectrophotometer in SCI and SCE Modes

	SCI (specular component included) mode					SCE (specular component excluded) mode				
Type of granite[a]	L^*	a^*	b^*	C^*_{ab}	h_{ab} (°)	L^*	a^*	b^*	C^*_{ab}	h_{ab} (°)
Gp	$62.5 \pm 1.4^{a,A}$	$-0.9 \pm 0.1^{a,A}$	$1.0 \pm 0.4^{a,A}$	$1.5 \pm 0.3^{a,A}$	$143.5 \pm 12.8^{a,A}$	$59.4 \pm 7.0^{a,B}$	$-0.8 \pm 0.3^{a,B}$	$0.9 \pm 0.8^{a,A}$	$1.3 \pm 0.7^{a,A}$	$142.0 \pm 29.0^{a,A}$
Gh	$67.1 \pm 1.4^{b,A}$	$-0.8 \pm 0.1^{b,A}$	$0.4 \pm 0.5^{b,A}$	$1.2 \pm 0.2^{b,A}$	$164.6 \pm 17.5^{b,A}$	$68.1 \pm 5.4^{b,A}$	$-0.7 \pm 0.3^{a,B}$	$0.5 \pm 1.2^{a,A}$	$1.2 \pm 1.0^{a,A}$	$163.7 \pm 42.1^{b,A}$
Gs	$66.5 \pm 1.0^{b,A}$	$-0.9 \pm 0.1^{ab,A}$	$2.4 \pm 0.8^{c,A}$	$2.6 \pm 0.7^{c,A}$	$112.0 \pm 6.5^{c,A}$	$65.5 \pm 4.2^{c,A}$	$-0.8 \pm 0.3^{a,A}$	$2.4 \pm 0.7^{b,A}$	$2.6 \pm 0.7^{b,A}$	$110.7 \pm 6.8^{c,A}$
Gf	$71.3 \pm 1.9^{c,A}$	$-0.3 \pm 0.2^{c,A}$	$3.2 \pm 0.5^{d,A}$	$3.2 \pm 0.5^{d,A}$	$97.6 \pm 2.7^{d,A}$	$70.8 \pm 4.6^{d,A}$	$-0.4 \pm 0.3^{b,A}$	$2.8 \pm 1.1^{c,A}$	$2.9 \pm 1.1^{b,A}$	$99.6 \pm 7.9^{d,A}$
BCp	$73.3 \pm 1.5^{a,A}$	$-0.6 \pm 0.1^{a,A}$	$3.6 \pm 0.2^{a,A}$	$3.7 \pm 0.2^{a,A}$	$100.6 \pm 1.5^{a,A}$	$71.0 \pm 4.8^{a,B}$	$-0.5 \pm 0.3^{a,B}$	$3.7 \pm 0.9^{a,A}$	$3.7 \pm 0.9^{a,A}$	$99.2 \pm 6.9^{a,A}$
BCh	$74.5 \pm 1.1^{ab,A}$	$-0.4 \pm 0.1^{b,A}$	$2.2 \pm 0.7^{b,A}$	$2.2 \pm 0.7^{b,A}$	$105.2 \pm 4.5^{b,A}$	$75.5 \pm 3.5^{b,A}$	$-0.5 \pm 0.3^{a,A}$	$2.8 \pm 0.9^{b,B}$	$2.9 \pm 0.9^{b,B}$	$101.0 \pm 6.5^{b,B}$
BCs	$72.7 \pm 1.0^{c,A}$	$-0.3 \pm 0.3^{b,A}$	$7.4 \pm 1.5^{c,A}$	$7.4 \pm 1.5^{c,A}$	$93.3 \pm 2.4^{c,A}$	$74.6 \pm 1.9^{b,B}$	$-0.6 \pm 0.2^{a,B}$	$5.2 \pm 1.0^{c,B}$	$5.2 \pm 1.0^{c,B}$	$96.7 \pm 2.7^{c,B}$
BCf	$74.9 \pm 1.0^{b,A}$	$-0.2 \pm 0.1^{c,A}$	$3.1 \pm 0.5^{d,A}$	$3.2 \pm 0.5^{d,A}$	$93.8 \pm 3.4^{c,A}$	$75.0 \pm 6.5^{b,A}$	$-0.2 \pm 0.3^{b,A}$	$2.5 \pm 0.9^{b,B}$	$2.5 \pm 0.8^{d,B}$	$95.5 \pm 8.5^{c,A}$
RPp	$60.4 \pm 2.9^{a,A}$	$2.7 \pm 0.5^{a,A}$	$7.1 \pm 1.0^{a,A}$	$7.6 \pm 1.1^{a,A}$	$71.8 \pm 1.7^{a,A}$	$61.0 \pm 8.1^{a,A}$	$3.3 \pm 2.6^{a,A}$	$8.6 \pm 3.6^{a,B}$	$9.3 \pm 4.2^{a,B}$	$71.9 \pm 8.6^{a,A}$
RPh	$66.4 \pm 1.6^{b,A}$	$1.6 \pm 0.4^{b,A}$	$4.5 \pm 0.7^{b,A}$	$4.8 \pm 0.8^{b,A}$	$73.9 \pm 4.0^{a,A}$	$67.4 \pm 5.8^{b,A}$	$2.0 \pm 1.5^{b,A}$	$5.8 \pm 2.4^{b,B}$	$6.2 \pm 2.7^{b,B}$	$72.3 \pm 10.1^{a,A}$
RPs	$67.9 \pm 0.8^{c,A}$	$0.6 \pm 0.1^{c,A}$	$4.3 \pm 0.4^{b,A}$	$4.4 \pm 0.4^{b,A}$	$83.9 \pm 1.4^{b,A}$	$67.6 \pm 3.8^{b,A}$	$1.1 \pm 1.0^{c,B}$	$5.1 \pm 1.6^{b,B}$	$5.3 \pm 1.8^{b,B}$	$80.0 \pm 7.8^{b,B}$
RPf	$63.9 \pm 1.6^{d,A}$	$2.3 \pm 0.2^{a,A}$	$6.8 \pm 0.6^{a,A}$	$7.2 \pm 0.6^{a,A}$	$72.6 \pm 1.1^{a,A}$	$66.2 \pm 5.7^{b,B}$	$2.6 \pm 1.4^{ab,A}$	$7.5 \pm 2.4^{c,A}$	$7.9 \pm 2.7^{c,A}$	$71.5 \pm 4.9^{a,A}$
LCp	$34.2 \pm 0.5^{a,A}$	$-0.4 \pm 0.1^{a,A}$	$-1.2 \pm 0.1^{a,A}$	$1.3 \pm 0.1^{a,A}$	$244.5 \pm 5.8^{a,A}$	$30.7 \pm 4.8^{a,B}$	$-0.4 \pm 0.4^{ab,A}$	$-1.1 \pm 1.0^{a,A}$	$1.4 \pm 0.8^{a,A}$	$237.2 \pm 46.0^{a,A}$
LCh	$50.0 \pm 1.4^{b,A}$	$-0.7 \pm 0.1^{b,A}$	$-2.8 \pm 0.3^{b,A}$	$3.0 \pm 0.3^{b,A}$	$253.7 \pm 6.1^{b,A}$	$48.0 \pm 3.4^{b,B}$	$-0.6 \pm 0.3^{a,B}$	$-1.4 \pm 1.6^{a,B}$	$1.9 \pm 1.0^{b,B}$	$219.4 \pm 58.8^{a,B}$
LCs	$61.0 \pm 0.9^{c,A}$	$-0.4 \pm 0.1^{a,A}$	$1.0 \pm 0.5^{c,A}$	$1.1 \pm 0.5^{c,A}$	$119.3 \pm 11.8^{c,A}$	$58.8 \pm 2.5^{c,B}$	$-0.4 \pm 0.2^{b,A}$	$0.6 \pm 0.9^{b,B}$	$1.0 \pm 0.6^{c,A}$	$148.6 \pm 48.7^{b,B}$
Spwg	$70.5 \pm 1.2^{a,A}$	$-0.2 \pm 0.1^{a,A}$	$5.8 \pm 0.4^{a,A}$	$5.8 \pm 0.4^{a,A}$	$92.2 \pm 1.4^{a,A}$	$69.6 \pm 4.3^{a,A}$	$0.0 \pm 0.4^{a,B}$	$5.8 \pm 1.1^{a,A}$	$5.8 \pm 1.1^{a,A}$	$90.1 \pm 4.1^{a,B}$
Sh	$74.9 \pm 0.2^{b,A}$	$-0.2 \pm 0.1^{a,A}$	$3.5 \pm 0.5^{b,A}$	$3.5 \pm 0.5^{b,A}$	$94.0 \pm 1.4^{b,A}$	$73.7 \pm 2.5^{c,B}$	$-0.3 \pm 0.2^{b,A}$	$2.5 \pm 0.8^{b,B}$	$2.6 \pm 0.8^{b,B}$	$96.9 \pm 4.8^{b,B}$
Ss	$70.8 \pm 2.0^{a,A}$	$-0.1 \pm 0.2^{b,A}$	$3.8 \pm 0.5^{b,A}$	$3.8 \pm 0.5^{b,A}$	$91.4 \pm 2.2^{a,A}$	$71.6 \pm 2.2^{b,A}$	$-0.1 \pm 0.3^{a,A}$	$4.2 \pm 1.1^{c,B}$	$4.2 \pm 1.1^{c,B}$	$91.6 \pm 3.2^{c,A}$
Sb	$74.0 \pm 0.4^{b,A}$	$0.1 \pm 0.1^{c,A}$	$4.4 \pm 0.2^{c,A}$	$4.4 \pm 0.2^{c,A}$	$89.4 \pm 0.8^{c,A}$	$74.1 \pm 2.7^{c,A}$	$0.2 \pm 0.2^{c,B}$	$4.7 \pm 0.9^{d,B}$	$4.7 \pm 0.9^{d,B}$	$88.0 \pm 2.6^{d,B}$

Note: Data are the mean of 70 measurements ± S.D. Different superscript letters (lowercase) indicate significant differences ($p < 0.05$) between the means of five independent granite specimens (the reported color parameters for each specimen are the mean values of fourteen measurements) for the values of CIELAB parameters L^*, a^*, b^*, C^*_{ab}, and h_{ab} in the same type of granite in relation to surface finish; and different superscript letters (capitals) indicate significant differences ($p < 0.05$) for each type of granite and surface finish between SCI and SCE modes.

[a]G = Grissal; BC = Blanco Cristal; RP = Rosa Porriño; LC = Labrador Claro; S = Silvestre; p = polished; pwg = polished without gloss; h = honed; s = sawn; b = bush hammered; and f = flamed.

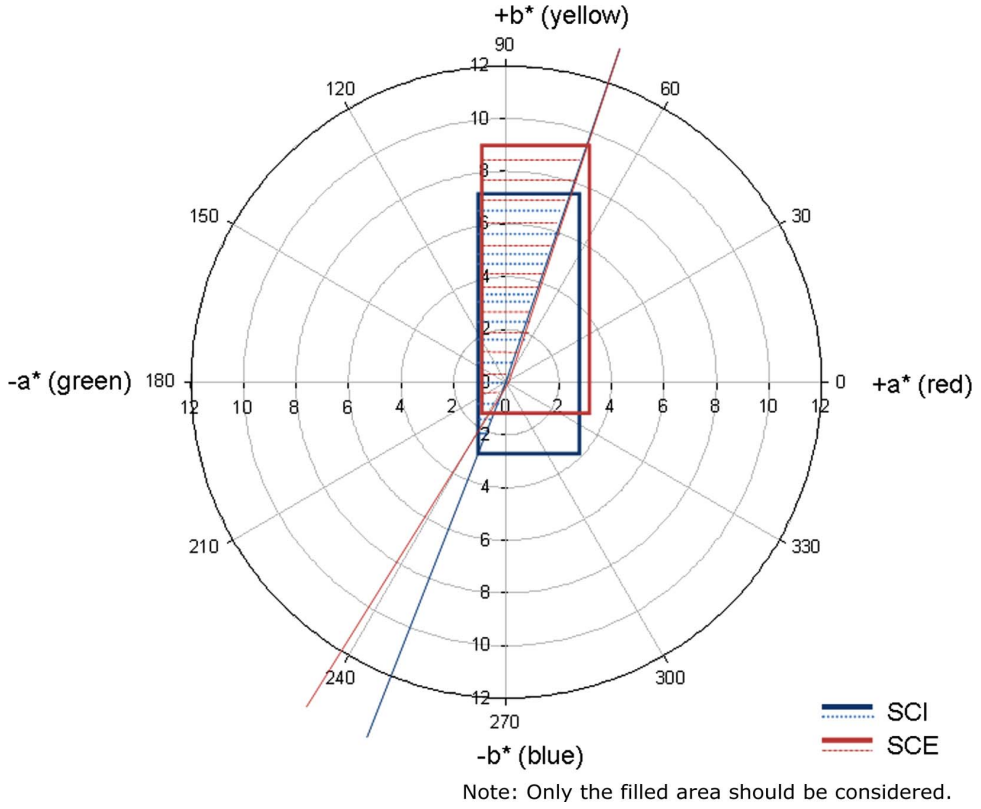

Fig. 2. $a^* - b^*$ diagram; representation of the area in which the parameters a^*, b^*, and h_{ab} of the studied ornamental granites by using the SCI and SCE modes are included

mode, whereas the chromatic parameter b^* varied between 7.4 ± 1.5 and -2.8 ± 0.3 in SCI mode and between 8.6 ± 3.6 and -1.4 ± 1.6 in SCE mode. The red component predominated over green in this type of rock, and the yellow predominated over blue (Fig. 2). On the other hand, and as expected, the lowest chroma values (C^*_{ab} were 1.1 ± 0.5 in SCI and 1.0 ± 0.6 in SCE) were obtained in Labrador Claro and the highest (7.6 ± 1.1 in SCI and 9.3 ± 4.2 in SCE) in Rosa Porriño. The range of values of h_{ab} was $71.8° \pm 1.7°$ to $253.7° \pm 6.1°$ in SCI and $71.5° \pm 4.9°$ to $237.2° \pm 46.0°$ in SCE mode, which enabled identification of possible tones for the studied ornamental granites in the $a^* - b^*$ diagram, and tones resulting from the combination of blue and red were excluded (Fig. 2). However, this wide variation in h_{ab} is scarcely noticeable because of the low chroma C^*_{ab}. In the present study, only sound stones were analyzed and higher chroma values may have been observed in the weathered granites as a result of the segregation of iron oxyhydroxides, a process that occurs as a consequence of weathering processes (Taboada and Garcia 1999).

When the surface of a smooth-colored object becomes rough, the apparent color of the object changes (Simonot and Elias 2003), and therefore to determine whether the color of the ornamental granites varied with the surface finish or roughness, the present data were subjected to a MANOVA test for each type of ornamental granite and surface finish (Table 3). The surface finish had a significant effect on the color of granites measured in both SCI and SCE modes, unlike in other materials such as dental porcelain (Kim et al. 2003) and injection-molded plastics (Ariño et al. 2007), in which color variations owing to differences in surface roughness were only observed by using the specular component excluded (SCE) mode. Inclusion or exclusion of the specular component was important for measurement of the color of ornamental granite specimens because significant differences (student t-test at $p < 0.05$) were seen between the CIELAB color coordinates measured in both modes (Table 3). Thus, in SCE mode, the b^* values, and to a lesser extent the a^* values, were significantly higher in most cases. A yellower and redder color was obtained in SCE mode compared to SCI mode (Fig. 2). Moreover, standard deviations (SD) of the color parameters in SCE mode were higher than in SCI mode (Table 3).

To analyze color variations caused by the different surface finishes (roughness), the partial color differences (ΔL^*, Δa^*, Δb^*, ΔC^*_{ab}, and ΔH^*_{ab}) and total color difference (ΔE^*_{ab}) between each surface finish and the smoother finish (polished or polished without gloss for Silvestre) were calculated (Table 4). Changes in total color (ΔE^*_{ab}), lightness (ΔL^*), chroma (ΔC^*_{ab}), and hue (ΔH^*_{ab}) were plotted against changes in roughness expressed as logarithmic roughness difference [$\log(\Delta \mathrm{Ra})$] (Fig. 3). As the surface roughness of the granite increased, the apparent color of the rocks changed because of variations in total color, lightness, chroma, and hue. The total color difference (ΔE^*_{ab}) between most of the surface finishes for the ornamental granites studied was perceptible (CIELAB units > 3; Prieto et al. 2010; Benavente et al. 2003). An upper limit of 6 CIELAB units was considered an acceptable color change (Hardeberg 1999), and this upper limit was not surpassed in the lightest granites (Blanco Cristal and Silvestre). By contrast, the limit was greatly surpassed in Labrador Claro, the darkest rock, indicating that this type of ornamental granite is the most variable in color with the surface finish or roughness (Table 4; Fig. 3).

Table 4. Partial Color Differences (ΔL^*, Δa^*, Δb^*, ΔC^*_{ab}, ΔH^*_{ab}) and Total Color Difference (ΔE^*_{ab}) between the Polished Finish (Polished without Gloss for Silvestre) and Each of the Other Surface Finishes for Each Ornamental Granite, Measured with the Spectrophotometer in SCI and SCE Modes

	SCI (specular component included) mode						SCE (specular component excluded) mode					
Type of granite[a]	ΔL^*	Δa^*	Δb^*	ΔC^*_{ab}	ΔH^*_{ab}	ΔE^*_{ab}	ΔL^*	Δa^*	Δb^*	ΔC^*_{ab}	ΔH^*_{ab}	ΔE^*_{ab}
Gf-p	8.8	0.6	2.2	1.7	1.5	9.1	11.4	0.4	1.9	1.6	1.1	11.6
Gs-p	4.0	0.1	1.4	1.1	1.0	4.2	6.1	0.0	1.5	1.3	0.7	6.3
Gh-p	4.6	0.1	−0.6	−0.4	0.5	4.6	8.7	0.1	−0.4	−0.1	0.4	8.7
BCf-p	1.6	0.4	−0.5	−0.5	0.4	1.7	4.0	0.3	−1.2	−1.2	0.3	4.2
BCs-p	−0.6	0.3	3.8	3.7	0.7	3.8	3.6	−0.1	1.5	1.5	0.1	3.9
BCh-p	1.2	0.2	−1.4	−1.4	0.2	1.8	4.5	0.0	−0.9	−0.8	0.4	4.6
RPf-p	3.5	−0.4	−0.3	−0.4	0.2	3.5	5.2	−0.7	−1.1	−1.4	0.0	5.4
RPs-p	7.5	−2.1	−2.8	−3.3	1.2	8.3	6.6	−2.2	−3.5	−4.0	1.0	7.8
RPh-p	6.0	−1.1	−2.6	−2.8	0.3	6.6	6.4	−1.3	−2.8	−3.1	0.0	7.1
LCs-p	26.8	0.0	2.2	−0.3	2.1	26.9	28.1	0.0	1.7	−0.4	1.7	28.2
LCh-p	15.9	−0.2	−1.6	1.6	0.2	16.0	17.3	−0.2	−0.3	0.5	0.0	17.3
Sb-pwg	3.5	0.3	−1.4	−1.4	0.2	3.8	4.5	0.2	−1.1	−1.1	0.2	4.6
Ss-pwg	0.3	0.2	−1.9	−1.9	0.0	2.0	2.0	−0.1	−1.6	−1.6	0.1	2.6
Sh-pwg	4.4	0.0	−2.3	−2.3	0.0	4.9	4.1	−0.3	−3.3	−3.2	0.9	5.3

[a]G = Grissal; BC = Blanco Cristal; RP = Rosa Porriño; LC = Labrador Claro; S = Silvestre; p = polished; pwg = polished without gloss; h = honed; s = sawn; b = bush hammered; and f = flamed.

A similar result was found by Benavente et al. (2003) in different types of marble and limestones. In dark specimens with high chroma values the changes in total color (ΔE_{94}) were more affected by surface finish than in light-colored specimens with low chroma values, which scarcely showed any change in color in relation to finish.

In this regard, Prieto et al. (2006) defined the limits of the perceptual change in the human vision for two of the granites used for

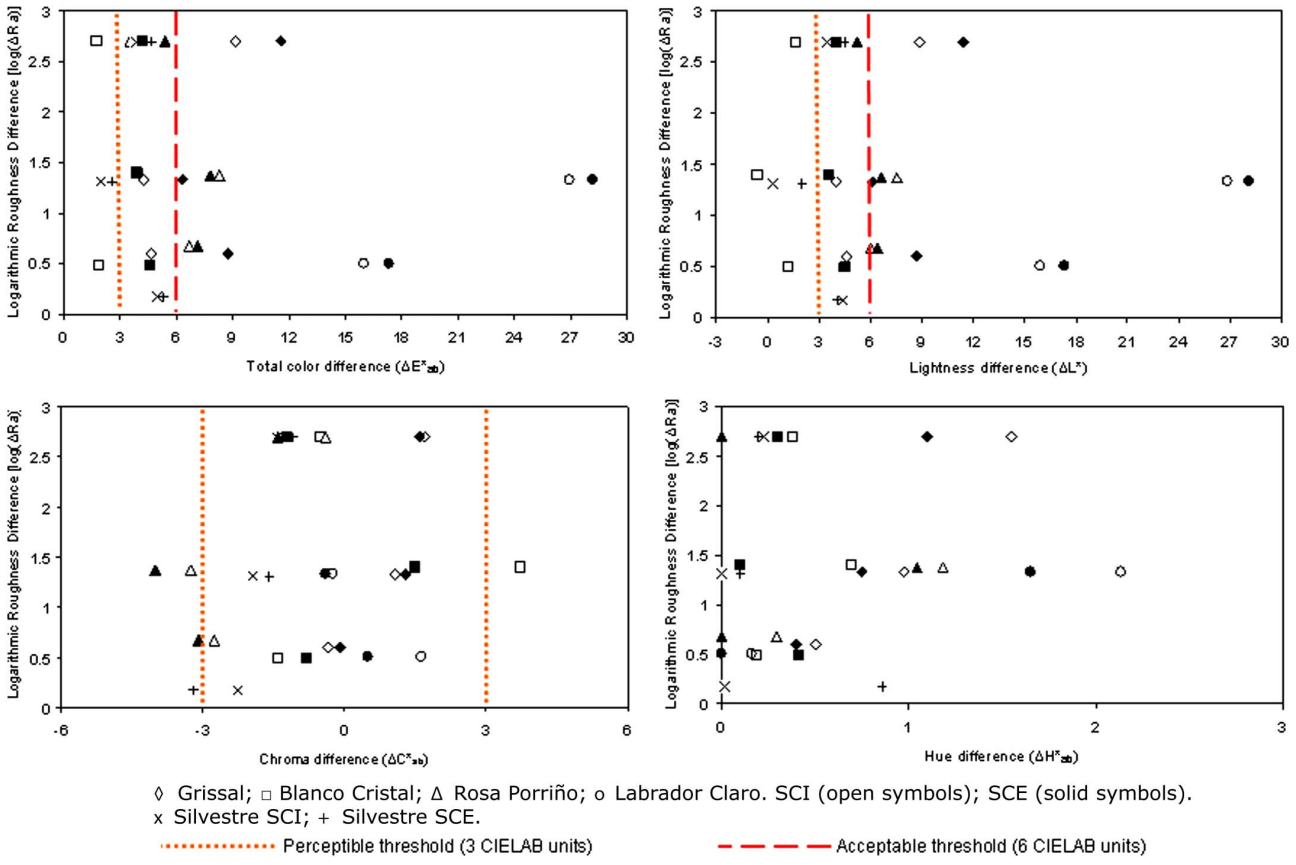

Fig. 3. Relationships between the roughness expressed as logarithmic roughness difference [log(ΔRa)] and changes in total color (ΔE^*_{ab}), lightness (ΔL^*), chroma (ΔC^*_{ab}), and hue (ΔH^*_{ab}); calculated between the polished finish (polished without gloss for Silvestre) and each of the other surface finishes for each ornamental granite measured with the spectrophotometer in SCI and SCE modes

this study: Blanco Cristal and Rosa Porriño. Following their results, qualitative terms can be assigned to the total color changes, ΔE^*_{ab}, between different surface finishes. Thus, in Blanco Cristal, the total color differences between polished and honed and polished and flamed were inappreciable (< 2.63 units), whereas a slight difference was seen in color between polished and sawn finishes (between 2.63 and 4.66 units). In Rosa Porriño, the differences in color between polished and honed and between polished and sawn were evident (between 6 and 10.78 units), but the differences between flamed and polished were only slight (between 2.96 and 4.74 units).

Regardless of the type of granite and surface finish, the ΔE^*_{ab} values measured in SCE mode were slightly higher than those measured in SCI mode except for sawn Rosa Porriño. The SCE mode therefore magnifies the differences owing to surface finish or roughness on ornamental granite.

With regard to the partial differences in lightness, ΔL^*, more than half of the cases surpassed the visual threshold of 3 CIELAB units, and again the greatest difference in this color parameter was observed in Labrador Claro (Table 4; Fig. 3). By contrast, although significant differences existed between C^*_{ab} and h_{ab} values measured in both SCI and SCE modes in relation to the different surface finishes for each ornamental granite (Table 3), scarcely any perceived differences were noted (> 3 CIELAB units) in either chroma (ΔC^*_{ab}) or hue (ΔH^*_{ab}) partial differences (Table 4; Fig. 3). This is consistent with the fact that the value of C^*_{ab} is low in the rocks under study, and thus differences are not appreciable and the hue angle may vary greatly without being of any real significance.

Analysis of these data revealed that lightness, L^*, is the color parameter most affected by changes in roughness. Ignell et al. (2009) reported similar findings for polymeric surfaces in which the darker the material, the larger the increase in lightness L^* as the surface became rougher.

However, the variation in color parameters, and therefore in the total color, with different finishes does not depend on roughness because none of the parameters changed in relation to differences in the roughness of the surface, and therefore no general conclusions could be drawn regarding the influence of the roughness on the ornamental granite color (Fig. 3).

As expected, the most important changes in parameter a^*, which represents the redness-greenness changes, were obtained with the flamed finish. The action of fire on the granite causes dehydration of the oxyhydroxides from the biotite and gives rise to the formation of dehydrated oxides, e.g., hematies (Fe_2O_3) of a reddish color. However, this effect was not observed in the only stone that was already reddish in color, Rosa Porriño.

Mean specular gloss values at 60° [G^{60} (gu)] of each surface finish in each type of ornamental granite are shown in Table 2. Many authors have reported an inverse relationship between roughness and gloss on homogeneous surfaces from the point of view of color and composition (Briones et al. 2006; Ariño et al. 2005; Wang et al. 2000; Thomas 1999; Hunter and Harold 1987). However, in the case of the ornamental granites under study, although the gloss of smooth surfaces (polished) is more than 30 gloss units higher than gloss of the rough surfaces, gloss is not a function of roughness (Fig. 4) because it did not differ significantly within a wide range of roughness values (from 2.59 to more than 500 μm), except in the case of Blanco Cristal (Table 2). Moreover, analysis of the gloss values within that range of roughness, i.e., without considering polished finish, revealed a slight increase in gloss with increased roughness (Table 2). This lack of agreement with the findings of other studies may be explained by the following: (1) neither of these studies was accomplished with arbitrary heterogeneous samples, such as granite rocks, in which the relationship

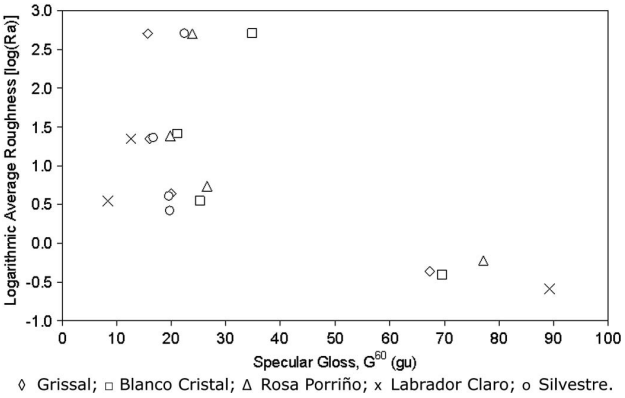

Fig. 4. Relationship between roughness expressed as logarithmic roughness difference [log(ΔRa)] and specular gloss measured at 60° (G^{60})

between roughness and gloss may be more complex because of competition between surface and volume scattering; (2) high values of roughness were considered in the present study, and this relationship probably only exists in the range of the lower roughness values (from *Ra* 0.26 to 5.53 μm in this case); (3) although the *Ra* values are consistent with the surface finish, i.e., *Ra* increases from the polished or polished without glow finish to the flamed or bush hammered finish, optical methods for measuring roughness can be very problematic when the measured object is transparent (Rodriguez et al. 2009) and quartz crystals in polished granites can be highly transparent; and (4) the studied material is a polymineral rock in which the gloss of each mineral is different and the overall surface gloss depends on the exposed area of each mineral. Most of the minerals in ornamental granites tend to split along definite crystallographic structural planes (cleavage planes) (López-Arce et al. 2010) giving rise to smooth surfaces, and therefore the treatments used to achieve the different finishes may increase the total surface roughness but also create small flat surfaces that may cause a slight increase in gloss. Thus, for instance, the increases in roughness and gloss between sawn and flamed finishes probably occur because of the increase in the coherent component of the reflected light owing to an increase in the number of flat surfaces (as large as the size of the mineral grains).

Moreover, gloss values are affected by the color of the rock because as lightness (L^*) decreased, the gloss increased in smooth specimens (polished; Fig. 5). Because the material under study is a polymineral rock, the refraction index of the different minerals must be taken into account because this property is directly related to gloss. The refractive index (Díaz Mauriño 1976) of the most abundant minerals (quartz, feldspar, and plagioclases) in the lightest of the rocks under study (Blanco Cristal, Rosa Porriño, Silvestre, and Grissal) is near 1.5, whereas the refractive indexes of two of the most abundant minerals in Labrador Claro are higher (Pyroxene: 1.6–1.7; Olivine: 1.6–1.8). The lower gloss of polished Grissal relative to polished Blanco Cristal, Rosa Porriño, and Silvestre may be related to the lower amount of biotite, which is among the minor minerals that having the higher refractive index (1.5–1.7).

However, in rough specimens there was a direct relationship between gloss and L^* as gloss increased with lightness. Ignell et al. (2009) obtained similar results with rough surfaces of polymineral materials, although they did not find any relationship between gloss and lightness in smooth surfaces. These authors argued that because gloss is governed by diffusely reflected light on rough surfaces and surface texture is independent of color, the increase

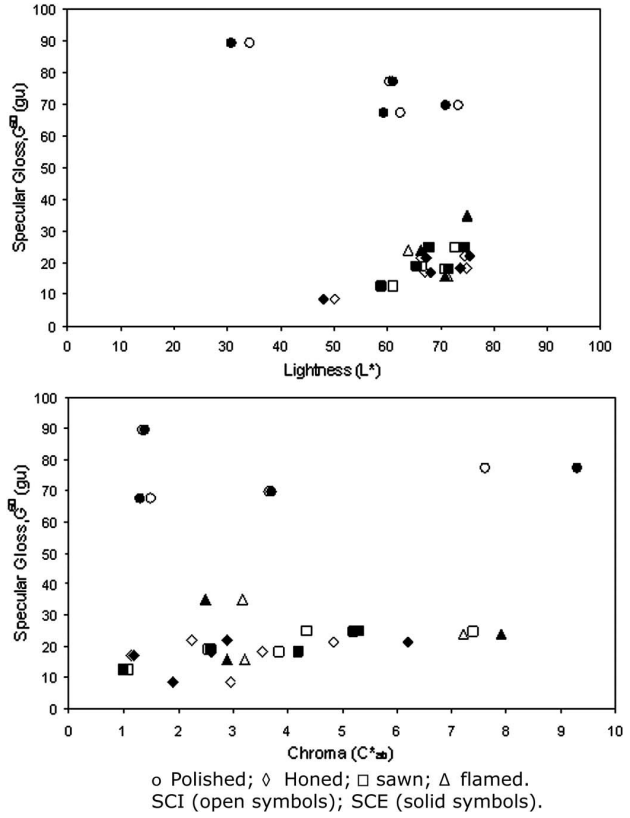

Fig. 5. Relationship between the specular gloss measured at 60° (G^{60}) with the lightness (L^*) and the chroma (C^*_{ab})

in gloss is probably associated with bulk scattering. Because lighter specimens are less absorbent, this contribution is expected to be more pronounced as the lightness increases.

By contrast, chroma (C^*_{ab}) did not affect the gloss of either polished or rough finishes (Fig. 5).

Conclusions

The study of the effects of different types of surface finish on the aesthetic properties of ornamental granites revealed that:

- Roughness induced by different types of surface finish on the granite surface causes a change in the color (in most cases perceptible) primarily because of changes in L^* values. Moreover, the magnitude of the change in color with roughness is governed by the color of the material and is higher in rocks with the lowest L^* values. However, the variation in color parameters, and therefore in the total color (ΔE^*_{ab}), with different finishes does not depend on roughness because the values of these parameters do not change with changes in the roughness of the surface. No general conclusions could therefore be drawn regarding the influence of the roughness on the ornamental granite color.
- In ornamental granites, an inverse relationship exists between gloss and roughness only for low values of roughness. Moreover, gloss values are affected by the color of the rock but in different ways in smooth and rough surfaces. Gloss and L^* are inversely related in smooth surfaces and directly related in rough surfaces. The mineral composition of polymineral rocks must be taken into account as it determines the topography of the rough surface and also the refractive index.
- The specular component excluded (SCE) mode magnifies the differences in color owing to surface finish or roughness on ornamental granite.

Moreover, the results obtained in this study enable identification of the area of the CIELAB color space in which the color of the studied ornamental granites is defined: in the range of the maximum values L^*: 74.9 ± 1.0; a^*: 2.7 ± 0.5; b^*: 7.4 ± 1.5; C^*_{ab}: 7.6 ± 1.1; and h_{ab}: $253.7° \pm 6.1°$ in SCI mode; and L^*: 75.5 ± 3.5; a^*: 3.3 ± 2.6; b^*: 8.6 ± 3.6; C^*_{ab}: 9.3 ± 4.2; and h_{ab}: $237.2° \pm 46.0°$ in SCE mode. The minimum L^*: 34.2 ± 0.5; a^*: -0.9 ± 0.1; b^*: -2.8 ± 0.3; C^*_{ab}: 1.1 ± 0.5; and h_{ab}: $71.8° \pm 1.7°$ in SCI mode; and L^*: 30.7 ± 4.8; a^*: -0.8 ± 0.3; b^*: -1.4 ± 1.6; C^*_{ab}: 1.0 ± 0.6; and h_{ab}: $71.5° \pm 4.9°$ in SCE mode. Although h_{ab} (hue) varied most widely, the variation does not have any real significance because of the low chroma of all the studied rocks.

The information obtained in this study should be taken into account when aesthetic criteria are used in selecting ornamental granites for building and construction materials.

However, it should be highlighted that the polymineral nature of the material under study is a handicap because no specific methodology exists to determine properties such as gloss and roughness that are affected by this polymineral nature. Future research should focus on this subject.

Acknowledgments

The present study was financed by the Xunta de Galicia (09TMT014203PR) and the Science and Innovation Ministry of Spain (BIA2006-02233/BES-2007-16996). The authors thank Professor Antonio Martínez-Cortizas for his helpful suggestions and Dr. Francesca Cappitelli for assistance with the roughness measurements.

References

Alonso, F. J., Vázquez, P., Esbert, R. M., and Ordaz, J. (2008). "Ornamental granite durability: Evaluation of damage caused by salt crystallization test." *Mater. Construcc.*, 58(289-290), 191–201.

Ariño, I., Johansson, S., Kleist, U., Liljenström-Leander, E., and Rigdahl, M. (2007). "The effect of texture on the pass/fail color tolerances of injection-molded plastics." *Color Res. Appl.*, 32(1), 47–54.

Ariño, I., Kleist, U., Mattsson, L., and Rigdahl, M. (2005). "On the relation between surface texture and gloss of injection-molded pigmented plastics." *Polym. Eng. Sci.*, 45(10), 1343–1356.

ASTM. (1995). "Standard test method for specular gloss ." *D523-1995*, Philadelphia.

ASTM. (1997). "Standard test method for measurement of gloss of high-gloss surfaces by goniophotometry." *E430-1997*, Philadelphia.

Barnett, S. (1973). "Freezing of coffee extract to produce a dark colored freeze-dried product." *Engineering of food preservation and biochemical processes*, C. J. King, ed., AIChE Symp. Series, Vol. 69(132), 26–32.

Benavente, D., et al. (2003). "Influence of surface roughness on color changes in building stones." *Color Res. Appl.*, 28(5), 343–351.

Briones, V., Aguilera, V. J., and Brown, C. (2006). "Effect of surface topography on color and gloss of chocolate samples." *J. Food Eng.*, 77(4), 776–783.

Catalina, F., and Bruna, J. M. (1997). "Principios de colorimetría práctica. Sistema CIE de medida diferencial de color." *Rev. Plast. Mod.*, 73(488), 164–171 (in Spanish).

Commission International de l'Eclairage (CIE). (1932). "Colorimétrie, Resolutions 1–4. Recueil des travaux et compte rendu des séances." Bureau Central de la Commission, The National Physical Laboratory Teddington, Cambridge University Press, 19–29 (in French).

Commission International de l'Eclairage (CIE). (1986) "Colorimetry." *Pub. 15-2*, CIE Central Bureau, Vienna, Austria.
Commission International de l'Eclairage (CIE). (1976). "Recommendations on uniform colour spaces, colour-difference equations, psychometric colour terms." *Proc., 18th Session CIE*, Bureau Central de la CIE, Paris.
Dalal, E. N., and Natale-Hoffman, K. M. (1999). "The effect of gloss on color." *Color Res. Appl.*, 24(5), 369–376.
Díaz Mauriño, C. (1976). *Iniciación práctica a la mineralogía*, S. A. Alhambra, Madrid, Spain (in Spanish).
Durán-Suárez, J., García-Beltrán, A., and Rodríguez-Gordillo, J. (1995). "Colorimetric cataloguing of stone materials (biocalcarenite) and evaluation of the chromatic effects of different restoring agents." *Sci. Total Environ.*, 167(1-3), 171–180.
Eliades, T., Gioka, E., Heim, M., Eliades, G., and Makou, M. (2004). "Color stability of orthodontic adhesive resins." *Angle Orthod.*, 74(3), 391–393.
García-Talegón, J., Vicente, M. A., Vicente-Tavera, S., and Molina-Ballesteros, E. (1998). "Assessment of chromatic changes due to artificial ageing and/or conservation treatments of sandstones." *Color Res. Appl.*, 23(1), 46–51.
Grossi, C. M., Alonso, F. J., Esbert, R. M., and Rojo, A. (2007a). "Effect of laser cleaning on granite color." *Color Res. Appl.*, 32(2), 152–159.
Grossi, C. M., Brimblecombe, P., Esbert, R. M., and Alonso, F. J. (2007b). "Color changes in architectural limestones from pollution and cleaning." *Color Res.Appl.*, 32(4), 320–331.
Hardeberg, J. Y. (1999). "Acquisition and reproduction of color images: Colorimetric and multispectral approaches." Ph.D. dissertation, Ecole Nationale Superieure des Telecommunications, Paris.
Huang, H., Li, Y., Shen, J. Y., Zhu, H. M., and Xu, X. P. (2002). "Microstructure detection of a glossy granite surface machined by the grinding process." *J. Mater. Process. Technol.*, 129(1–3), 403–407.
Huertas, R., Melgosa, M., and Hita, E. (2006). "Influence of random-dot textures on perception of suprathreshold color differences." *J. Opt. Soc. Am. A*, 23(9), 2067–2076.
Hunter, R. S. (1937). "Methods of determining gloss." *J. Res. Natl. Bur. Stand.*, 18(77), 281.
Hunter, R. S., and Harold, R. W. (1987). *The measurement of appearance*, Wiley, New York.
Ignell, S., Kleist, U., and Rigdahl, M. (2009). "On the relations between color, gloss, and surface texture in injection-molded plastics." *Color Res.Appl.*, 34(4), 291–298.
Iñigo, A. C., Vicente-Tavera, S., and Rives, V. (2004). "MANOVA-Biplot statistical analysis of the effect of artificial ageing (freezing/thawing) on the colour of treated granite stones." *Color Res. Appl.*, 29(2), 115–120.
Iñigo, A. C., Vicente-Tavera, S., Rives, V., and Vicente, M. A. (1997). "Color changes in the surface of granitic materials by consolidated and/or water repellent treatments." *Color Res.Appl.*, 22(2), 133–141.
International Commission on Illumination (CIE). (2004). Colorimetry, *015:2004*, 3rd Ed., Vienna.
ISO. (1984). "Surface roughness—terminology: Part 1. Surface and its parameters." *ISO 4287-1:1984*, Geneva.
Keyf, F., and Etikan, I. (2004). "Evaluation of gloss changes of two denture acrylic resin materials in four different beverages." *Dent. Mater.*, 20(3), 244–251.
Kim, I. J., Lee, Y. K., Lim, B. S., and Kim, C. W. (2003). "Effect of surface topography on the color of dental porcelain." *J. Mater. Sci. Mater. Med.*, 14(5), 405–409.
López-Arce, P., Varas-Muriel, M. J., Fernández-Revuelta, B., Álvarez de Buergo, M., Fort, R., and Pérez-Soba, C. (2010). "Artificial weathering of Spanish granites subjected to salt crystallization tests: Surface roughness quantification." *Catena*, 83(2-3), 170–185.
López Jiménez, C., ed. (1996). *Manual de rocas ornamentales*, S. L. Entorno Gráfico, Madrid (in Spanish).
Prieto, B., Sanmartín, P., Silva, B., and Martínez-Verdú, F. (2010). "Measuring the color of granite rocks: A proposed procedure." *Color Res. Appl.*, 35(5), 368–375.
Prieto, B., Silva, B., Aira, N., and Álvarez, L. (2006). "Toward a definition of a bioreceptivity index for granitic rocks: Perception of the change in appearance of the rock." *Int. Biodeterior. Biodegrad.*, 58(3-4), 150–154.
Rodriguez, J. M., Curtis, R. V., and Bartlett, D. W. (2009). "Surface roughness of impression materials and dental stones scanned by non-contacting laser profilometry." *Dent. Mater.*, 25(4), 500–505.
Rojo, A., Alonso, F. J., and Esbert, R. M. (2003). "Hydric properties of some Iberian ornamental granites with different superficial finishes: A petrophysical interpretation." *Mater. Construcc.*, 53(269), 61–72.
Shih, T.-S., Wei, P.-S., and Wu, C.-L. (2008). "Effect of abrasives on the glossiness and reflectance of anodized aluminum alloys." *J. Mater. Sci.*, 43(6), 1851–1858.
Simonot, L., and Elias, M. (2003). "Color change due to surface state modification." *Color Res. Appl.*, 28(1), 45–49.
Taboada, T., and Garcia, C. (1999). "Smectite formation produced by weathering in a coarse granite saprolite in Galicia (NW Spain)". *Catena*, 35(2-4), 281–290.
Thomas, T. R. (1999). *Rough surfaces*, 2nd Ed., Imperial College Press, London.
Wang, L., Huang, T., Kamal, M. R., and Rey, A. D. (2000). "The surface topography and gloss of polyolefin blown films." *Polym. Eng. Sci.*, 40(3), 747–760.
Wyszecki, G., and Stiles, W. S. (1982). *Color science: Concepts and methods, quantitative data and formulae*, Wiley, New York.

2ª línea de trabajo

Desarrollo de la metodología de medida y caracterización del color de las cianobacterias

2nd line of research

Fine-tuning of the methodology for measuring and characterizing the color of cyanobacteria

Chapter 3[*]. Color of cyanobacteria: some methodological aspects

Prieto, B.; Sanmartín, P.; Aira, N.; Silva, B.

Applied Optics 49 (11): 2022-2029 (2010)

JCR index (IF) 2010 = 1.703 (23/78, 29 percentile in Optics)

Total number of times cited: 4

[*] Selected for publication in Virtual Journal for Biomedical Optics. Sec. Microbiology, Vol. 5(8).
This article was ranked one of the top 20 articles published on the same topic (domain of article 20390000) since its publication (2010). BioMedLib, "Who Is Publishing in My Domain?". April 14, 2012

Color of cyanobacteria: some methodological aspects

Beatriz Prieto,* Patricia Sanmartín, Noelia Aira, and Benita Silva

Dpto. Edafología y Química agrícola, Fac. Farmacia, University Santiago de Compostela, 15782-Santiago de Compostela, Spain

*Corresponding author: beatriz.prieto@usc.es

Received 8 December 2009; revised 5 March 2010; accepted 9 March 2010; posted 10 March 2010 (Doc. ID 120994); published 1 April 2010

Although the color of cyanobacteria is a very informative characteristic, no standardized protocol has, so far, been established for defining the color in an objective way, and, therefore, direct comparison of experimental results obtained by different research groups is not possible. In the present study, we used colorimetric measurements and conventional statistical tools to determine the effects on the measurement of the color of cyanobacteria, of the concentration of the microorganisms and their moisture content, as well as of the size of the target area and the minimum number of measurements. It was concluded that the color measurement is affected by every factor studied, but that this can be controlled for by making at least 10 consecutive measurements/9.62 cm^2 at different randomly selected points on the surface of filters completely covered by films of cyanobacteria in which the moisture contents are higher than 50%.

OCIS codes: 120.3940, 120.4290, 330.1710.

1. Introduction

Although color is one of the defining characteristics of cyanobacteria and provides the name of blue-green algae, it has, so far, not been defined in an objective way. Many studies have explored the color changes that cyanobacteria undergo in response to alterations in the energy distribution in the light spectrum, but none of these studies provide colorimetric data expressed in any of the standard International Commission on Illumination (CIE) color spaces: CIEXYZ, CIELUV, and CIELAB [1,2]. Likewise, in the scientific literature on cyanobacteria, objective terms are not used to refer to the color of the microorganisms. Thus, for instance, bleaching or chlorosis is defined as color change of the cells from "blue-green" to "yellow-green" by phycobilisome degradation, and nitrogen chlorosis is defined as the "yellowing" of cyanobacterial cells following the onset of nitrogen starvation. In some cases the language used is more precise and more specific names of colors, such as red, green, blue, and yellow, are given. However, as communication of the color has an important cultural component, sometimes it is difficult to know the real meaning of the words.

The characteristic blue-green color of cyanobacteria is due to their photosynthetic pigment composition of chlorophyll a, which is a greenish pigment that makes photosynthesis possible by passing on charged electrons to other molecules to manufacture energy, and phycobiliproteins, which capture light energy and are exclusive of cyanobacteria and red algae. Between phycobiliproteins, phycocyanin is responsible for the blue color. Other colored photosynthetic pigments in cyanobacteria are phycoerythrin, pink, phycoerythrocyanin, purple, and allophycocyanin, greenish-blue, which are phycobiliproteins, and the yellow-orange pigments called carotenoids.

As pigment content is closely associated with environmental conditions, such as nitrogen source, light intensity, light quality, and nutrient availability, among others parameters [3–6], variation in environmental conditions gives rise to an appreciable change in the color of cyanobacteria cultures. Thus, for example, in some cyanobacteria, the light quality,

0003-6935/10/112022-08$15.00/0

i.e., the relative number of photons of blue, green, red, far red, and other portions of the light spectrum emitted from a light source, influences the composition of phycobilisomes. In green light, the cells accumulate more phycoerythrin, whereas in red light, they produce more phycocyanin, and, hence, the bacteria appear green in red light and red in green light. This process is known as complementary chromatic adaptation and is a way for the cells to maximize the use of available light for photosynthesis.

Taking into account relationships between pigment content and color, and pigment content and environmental conditions, the health of the cultures or the influence of environmental changes could be assessed by their color. To date, no objective color data have been reported in relation to cultures because there is no standardized protocol for the measurement of cyanobacterial color, even though it is a common practice in microbiological laboratories to make a first assessment of the health of the cultures by visual inspection.

Thus, the objective measurement of color is of great importance, not only for a common understanding among researchers, but also for carrying out scientific studies on the ecology and physiology of cyanobacteria. In this sense, it is important to bear in mind that the objective measurement of color is affected by the color measuring devices used and the protocol applied, and comparable results should be obtained by different operators and instruments. Regarding the devices, it must be taken into account that the discrepancies in the color obtained by several contact-type color measuring devices are due to integration of the field of view, which is circular and of a size determined by the diameter of the measuring head (3 – 60 mm), and only highly homogeneous colors will be unaffected by this fact.

Regarding the protocol, objective colorimetric characterization of cyanobacteria has been carried out in only two studies [7,8]. In the first study [7], organisms were previously deposited on a 47 mm diameter acetate filter by means of vacuum filtration of 5 ml of culture, five times (i.e., 1 ml each time) to obtain a homogeneous distribution of the cells in a circular area (35 mm diameter); the color of the deposits was then measured with a contact-type color measuring device. To obtain a representative color of the cyanobacteria culture, 10 sequential circular measurements of 8 mm diameter were made and color was expressed as the average of the 10 measurements, in the CIELAB color space. The procedure yielded good results and was used in a subsequent study [8]. However, the 10 measurements used in the former studies cannot be considered as standard since the diameter of the circular measurement head differs from one device to another, and as demonstrated with other types of surface [9], the minimum number of measurements required to characterize the color of a surface depends on the diameter of the measuring head, among other factors. Thus, to standardize the measurement of the color of cyanobacteria in order to obtain reproducible and comparable results, independently of the dimensions of the measuring head of the device, the number of measurements required in relation to the surface area must first be determined.

Furthermore, taking into account that, in the first study [7], the moisture content of the cyanobacteria was found to affect the colorimetric characterization, relationships between moisture content and colorimetric parameters must be studied to obtain sufficient information to enable selection of the most appropriate conditions for standardization of the measurement of cyanobacterial color.

In view of the above, and with the aims of encouraging communication between researchers and of obtaining a standardized protocol for the measurement of cyanobacterial color, the number of measurements, in relation to the surface area, required to characterize their color independently of the dimensions of the measuring head of the device, the amount of cyanobacteria, and the proper moisture content of the microorganisms to obtain reproducible and comparable results were established by a combination of colorimetric and statistical methodology.

2. Materials and Methods

Experiments were carried out on a mixed culture ($713\,\mu g\,ml^{-1}$) of three filamentous N_2- fixing heterocyst-forming cyanobacteria: *Nostoc* sp. strain PCC 9104, *Nostoc* sp. strain PCC 9025 and *Scytonema* sp. CCC 9801. All strains were grown in $BG-11_0$ medium [10], a diazotrophic culture medium commonly used for nitrogen-fixing strains, composed of $K_2PO_4.3H_2O(0.04\,g\,l^{-1})+MgSO_4.7H_2O(0.075\,g\,l^{-1})+CaCl_2.2H_2O(0.036\,g\,l^{-1})$ + Citric acid$(0.006\,g\,l^{-1})$ + Ferric ammonium citrate $(0.006\,g\,l^{-1})$ + EDTA $(0.001\,g\,l^{-1})$ + $Na_2CO3(0.02\,g\,l^{-1})$ + Trace metal mix $A5(1\,ml\,l^{-1}) : H_3BO_3(2.86\,g\,l^{-1})$ + $MnCl_2\cdot 4H_2O$ $(1.81\,g\,l^{-1})$ + $ZnSO_4\cdot 7H_2O$ $(0.222\,g\,l^{-1})$ + $Na_2MoO_4\cdot 2H_2O$ $(0.39\,g\,l^{-1})$ + $CuSO_4\cdot 5H_2O$ $(0.079\,g\,l^{-1})$ + $Co(NO_3)_2\cdot 6H_2O$ $(0.0494\,g\,l^{-1})$ + distilled water.

Depending on the experiment, five replicates of different aliquots of the culture were filtered under vacuum through nitrocellulose filter discs ($0.45\,\mu m$ and 47 mm diameter) to achieve $9.62\,cm^2$ of coated area (35 mm diameter). The color of the coated areas of the filters in Fig. 1 was then measured with one or two contact-type color measuring devices.

To determine the appropriate range of humidity of the cyanobacteria for characterization of their color, a larger volume (20 ml) of the culture was filtered to achieve complete coating of the filter. In this case, the filters were first dried in an oven (105 °C) to constant weight. The filters with the cyanobacterial deposits were then immersed in water until saturated, then air dried, and color and weight were measured at different times (10, 20, 30, 45, 60, 90, 120, and 150 min) until the filters appeared completely dry. Finally, the filters were dried in an oven (at 105 °C) to

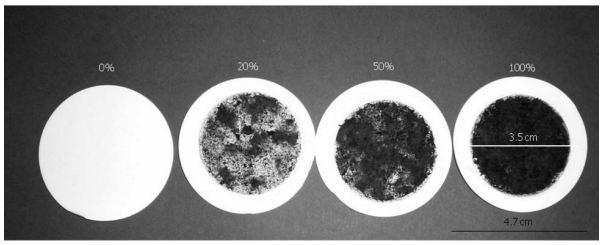

Fig. 1. Appearance of the filters after depositing the aliquots of cultures containing 0%, 20%, 50%, and 100% cyanobacteria.

constant weight to enable determination of the moisture content of the cyanobacteria.

The color was measured with a Gretag Macbeth portable spectrophotometer (CE-XTH) with two diameter viewing apertures of 5 and 10 mm. The following measuring conditions were selected: 5 mm viewing aperture, illuminant D65, which represents a typical phase of daylight with a correlated color temperature of approximately 6500 K, and a 2° observer (CIE 1931). The measurements were made by spectral reflectance, by use of diffuse illumination geometry, with an integration sphere covered with a white material so that the light was uniformly diffuse in all directions illuminating the sample and was observed with the specular component included. A total of 20 measurements were made consecutively at different randomly selected points on the surface of the filters, in order to obtain sufficient data to characterize the color. The results were expressed as the average of only 10 measurements since this was established as the minimum number of measurements required for each 9.62 cm^2 of surface (see Subsection 3.B).

Color measurements were pointed in the CIELAB color space, the most perceptually uniform of the color spaces [11–13]. The CIELAB system has been widely used (since 1976) for calculating color differences for most practical applications. Use of the CIELAB system enables estimation of three color parameters: L^*, a^*, and b^*, where L^* represents lightness (a value of 100 indicates white, and a value of 0, black), a^* is associated with changes in redness-greenness (positive a^* is red, and negative a^* is green), and b^* is associated with changes in yellowness-blueness (positive b^* is yellow, and negative b^* is blue). The three parameters are plotted on three orthogonal axes in a Cartesian coordinate system. In addition, the classic CIELAB formula (ΔE^*ab) [2] and three CIELAB-based color-difference formulas {$\Delta E94$(1:1:1) [14], CMC(2:1) [15], and $\Delta E00$(1:1:1) [11]} were applied.

In order to determine the minimum number of measurements required to characterize the color of cyanobacteria, independently of the dimensions of the measuring head of the device and the concentration of the microorganisms, three dilutions (1/5; 1/2, and 1/1) of the culture were prepared (to provide relative concentrations of 20%, 50%, and 100%), and 5 ml aliquots were filtered. As a control, a 5 ml aliquot of the culture medium was also filtered (0% concentration). In this case, the color was measured with a Gretag Macbeth portable spectrophotometer (CE-XTH) with two diameter viewing apertures of 5 and 10 mm, and a Minolta colorimeter, with one measuring head (CR-300) with an 8 mm diameter viewing area. Thus, the areas measured with the two devices were circular areas of 5, 8, and 10 mm diameters. The same measuring conditions as above were fixed in both devices so that the measurements were comparable.

A total of 20 measurements were made consecutively, with each of the three measuring heads, of 5, 8, and 10 mm diameters, at different randomly selected points on the surface of the filters within the appropriate range of moisture contents (see Subsection 3.A).

All the data were subjected to multivariate analysis of variance (MANOVA) and the Tukey-B multiple comparison test, by use of SPSS (version 15.0).

3. Results and Discussion

A. Range of Moisture Contents

The variations in the L^*, a^*, and b^* values for the cyanobacteria deposits with moisture content (expressed as a percentage) are shown in Fig. 2. The values of the L^* parameter were relatively low in 28.07–20.00 CIELAB units. The values of the a^* chromatic parameter were negative, ranging from −1.21 to −2.51 CIELAB units, whereas the values of the b^* chromatic parameter were positive, ranging from 10.46 to 4.25 CIELAB units, so that the color of the cyanobacteria was within the zone of the yellow-

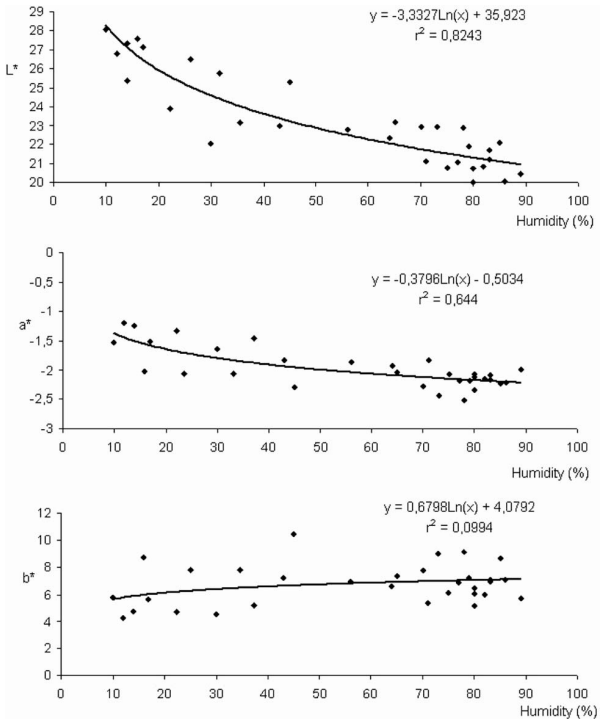

Fig. 2. Variation in L^*, a^*, and b^* values of the filters containing cyanobacteria deposits with moisture content (%).

greenish colors, regardless of the moisture content (see Fig. 3).

On the other hand, L^* initially decreased rapidly with increasing moisture content in Fig. 2. However, it remained practically constant for moisture contents higher than 50%, since the variation in that part of the curve is only 2 L^* units, which is below the perceptibility threshold [16,17]. This was not observed with the a^* and b^* parameters, for which differences between ranges of moisture content were not noticeable, since there was no variation in these parameters with moisture content. Moreover, the results of the MANOVA, with the CIELAB color parameters L^*, a^*, and b^* as dependent variables, and the moisture content as the independent variable confirmed statistically significant differences only among the L^* values obtained at the different moisture contents (Wilks lambda, 0.024; F-value, 26.294; degrees of freedom, 69; significance, 0.000). Therefore, L^* is the only CIELAB parameter related to moisture content, and decreased exponentially with increasing humidity, so that moisture content clearly affected the lightness values, as it caused a darkening of the color. A similar result was obtained in a previous study [7], in which variation in the L^* parameter with moisture content was observed during the 15 days during which samples were left to dry, but not thereafter.

The above results clearly suggest that, in order to obtain comparable results, color measurements must be made on test samples with a moisture content of more than 50%, as in that range, the L^*, a^*, and b^* values remain fairly constant. To determine the color of liquid cultures deposited on filters, the measurements must be made immediately after deposition of cyanobacteria, while the microorganisms are still moist; when determining the color of cyanobacteria colonizing surfaces, such as building facades, the measurement protocol should ensure that the moisture content of the surface is above 50%.

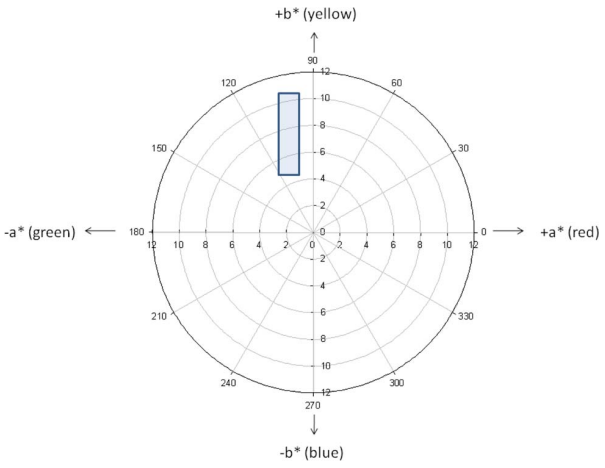

Fig. 3. (Color online) $a^* - b^*$ diagram representing the yellow-greenish area corresponding to the filters containing cyanobacteria in relation to range of moisture contents.

B. Minimum Number of Measurements

In order to determine the minimum number of measurements required to characterize the color of cyanobacteria, the cumulative averages of the CIELAB color parameters (L^*, a^*, and b^*) were plotted for each of the filters. The general shape of the graphs obtained was an inverted exponential decay model with a horizontal asymptote, with the stable section corresponding to the number of measurements after which the mean become constant; consequently, the first point of this section of the curve represents the minimum number of measurements required to characterize the L^*, a^*, and b^* coordinates for each case. By way of example, the plots obtained for one of the filters are shown in Fig. 4. In each of the three graphs, the number of measurements after which the horizontal asymptote is reached and the mean

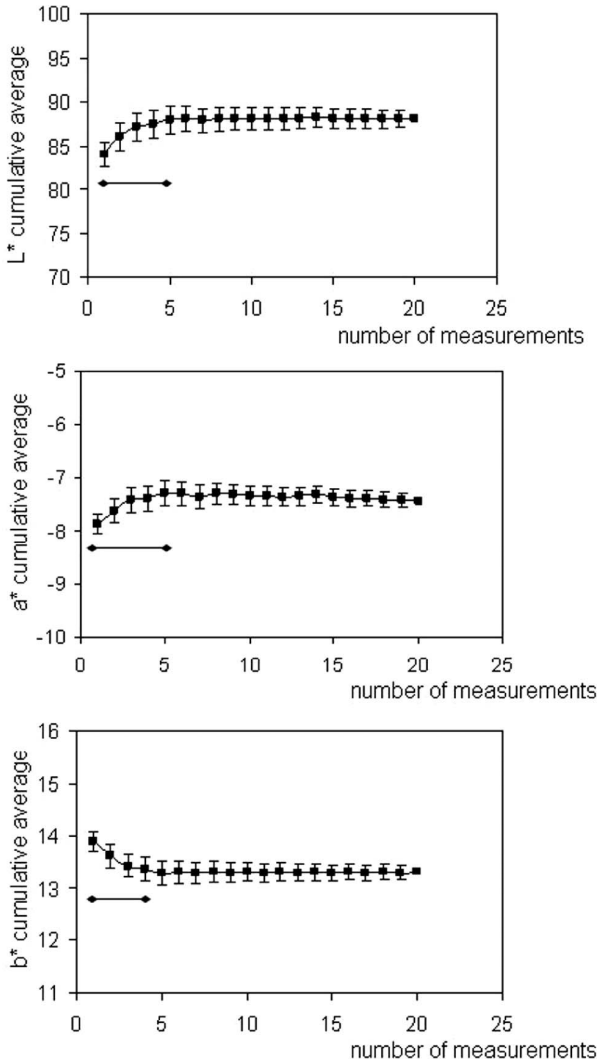

Fig. 4. Example of the graphs used to determine the minimum number of measurements required. Cumulative averages of the CIELAB color parameters: L^*, a^*, and b^* in relation to the number of measurements, corresponding to filters containing 20% cyanobacteria, filter *b*, and 10 mm measurement head.

becomes constant, is indicated by the marked segment. The minimum number of measurements required for characterization of each color coordinates, for the coated area of each filter and for each measuring head, is shown in Table 1. The number of measurements required was different for each of the coordinates (L^*, a^*, and b^*).

The data were subjected to MANOVA, with the minimum number of measurements determined for L^*, a^*, and b^* as dependent variables and concentration of the microorganisms and diameter of the measuring head as independent variables. The results of the analysis revealed that both the concentration of microorganisms and the diameter of the measuring head produced significantly different results in terms of the minimum number of measurements required to characterize L^*, a^*, and b^*. The results, including the Wilks lambda, the F-factor, the level of significance, and the number of degrees of freedom are shown in Table 2, and the significant differences between the average value of number of measurements required to define L^*, a^*, and b^* for each organisms concentration and measurement head are indicated in Table 3. There were significant differences in the minimum number of measurements required for color characterization of the filters with concentrations of 0% or 100% microorganisms and those with 20% or 50% microorganisms, for all three CIELAB color parameters (L^*, a^*, and b^*), with fewer measurements required for the former than the latter. This may be attributed to the greater heterogeneity of the color of the measured area corresponding to the filters with intermediate concentrations of microorganisms (20% and 50%): as the deposits did not cover the whole area [see Fig. 1], this gave rise to an irregular layer of microorganisms in which two very different colors—the yellow-greenish, fairly dark color of the cyanobacteria, and the pure, bright white color of the filters—appeared together. Thus, depending on the concentration of filtered organisms, these chromatic patches on an achromatic support provided different scales of heterogeneity, which did not exist in the filters without cyanobacteria (0%) and was almost absent in the filters with 100% microorganisms, as a rather homogeneous layer of microorganisms was obtained. The minimum number of measurements required also increased with the heterogeneity of the color of the filters (see Table 1).

Regarding the measuring head, the minimum number of measurements required to characterize b^* was independent of this factor, while the significant differences for L^* and a^* were determined by the 5 mm measuring head, for which the number of measurements required was greater than for the 8 and 10 mm measuring heads (see Table 3).

Since the color value of each of the five filters with the same concentration of microorganisms must be approximately equal, irrespective of the number of measurements, the greatest differences in partial and total color between filters with the same concen-

Table 2. Three-Way MANOVA of the Number of Measurements[a]

Source	Wilks Lambda	F-Value	Degrees of Freedom	Significance
Organism concentration	0.327	6.315	9	0.000
Diameter of the measuring head	0.676	2.882	6	0.014

[a]Dependent: L^*, a^*, and b^*.

Table 1. Minimum Number of Measurements Determined for Characterization of Each CIELAB Color Parameter, for Each Filter with Different Concentrations of Cyanobacteria, and for Different Measuring Heads

		Diameter of the Measuring Head (mm)								
		10			8			5		
Dilution (%)	Filter	L^*	a^*	b^*	L^*	a^*	b^*	L^*	a^*	b^*
0	a	2	3	4	2	2	2	2	3	3
	b	2	2	2	2	2	2	2	2	2
	c	2	2	2	2	2	2	2	2	2
	d	2	2	2	2	2	2	3	3	2
	e	2	2	2	2	2	2	2	2	2
20	a	3	5	3	3	3	3	6	5	3
	b	5	5	4	8	3	3	8	7	4
	c	6	6	5	4	4	4	3	3	3
	d	5	6	3	8	8	8	8	8	7
	e	4	6	5	2	7	6	3	5	5
50	a	4	4	4	3	2	3	7	7	5
	b	6	5	4	2	2	10	10	9	9
	c	8	8	5	5	9	5	8	8	3
	d	8	8	8	5	4	5	10	10	3
	e	4	4	3	3	3	3	9	10	10
100	a	2	2	2	4	4	3	3	5	2
	b	2	2	2	3	3	4	5	5	3
	c	4	2	2	4	3	3	4	4	3
	d	3	2	2	4	3	3	4	4	3
	e	4	3	3	3	3	3	5	5	3

Table 3. Tukey-B Test for the Number of Measurements in Relation to Different Concentrations of Cyanobacteria and Diameter of the Measuring Head[a]

Dilution (%)	L^*	a^*	b^*
0	2.07^a	2.20^a	2.20^a
20	4.86^b	5.28^b	4.23^b
50	$6b$	6.07^b	5.36^b
100	3.36^a	3.18^a	2.73^a
Diameter of the measuring head (mm)	L^*	a^*	b^*
10	3.67^a	3.83^a	3.33^a
8	3.53^a	3.53^a	3.84^a
5	5.12^b	5.35^b	3.94^a

[a]Different superscript letters indicate significant differences ($\alpha : 0.05$).

Table 4. Minimum Number of Measurements Required to Characterize Each Filter for Each Measuring Head

		Diameter of the Measuring Head (mm)		
Dilution (%)	Filter	10	8	5
0	a	4	2	3
	b	2	2	2
	c	2	2	2
	d	2	2	3
	e	2	2	2
20	a	5	3	6
	b	5	8	6
	c	6	4	5
	d	6	8	8
	e	6	7	5
50	a	4	3	7
	b	6	10	10
	c	8	9	8
	d	8	5	10
	e	4	3	10
100	a	2	4	5
	b	2	4	5
	c	4	4	4
	d	3	4	4
	e	4	3	5

tration of microorganisms were calculated. The number of measurements required to characterize the color of each filter (see Table 4) was the highest number of measurements from among those for L^*, a^*, and b^* (see Table 1) for each filter and each measuring head. Assuming a large tolerance of five CIELAB units [16–18], partial (ΔL^*, Δa^*, and Δb^*) and total [ΔE^*ab, $\Delta E94(1{:}1{:}1)$, CMC(2:1), and $\Delta E00(1{:}1{:}1)$] color differences between filters with the same concentration of microorganisms were not perceptible (see Table 5), and were far from the six CIELAB units considered as a perceptible but acceptable difference in color [19]. In addition, taking into account previous studies in which three CIELAB units are considered as the upper limit of perceptibility of the color [8,20,21], all values of the total color differences obtained, except those obtained with the 8 and 5 mm measuring heads for filters with a covering of 20% microorganisms, were below this threshold.

The total color differences were minimized by use of the newer and improved color formulas, i.e., $\Delta E94(1{:}1{:}1)$, CMC(2:1) and $\Delta E00(1{:}1{:}1)$. It was also found that there was no equivalence of the scale factor among the results obtained with the three formulas considered. Moreover, the changes in total color were mainly produced by the partial differences of the lightness ΔL^*, except for filters with 0% microorganisms, in which the changes were mainly due to Δb^*, owing to the tendency to yellowing of nitrocellulose filters when they are exposed to ultraviolet light. The greatest effect of ΔL^* on the filters with concentrations of microorganisms that gave rise to an irregular layer (20%, 50%, and 100%) was due to the textured nature of the samples, where L^* is the color parameter that varied most between the white and the green patches. A reduction in the total color differences would be unfeasible, even if more measurements were made, as the values of L^*, a^*, and b^* would not change [see Fig. 1].

Since the minimum number of measurements required varied with the color parameter, the concentration of microorganisms and the diameter of the measuring head, the minimum number required to characterize the color of cyanobacteria, irrespective of the concentration of microorganisms, would be the largest number obtained for all the

Table 5. Maximum Partial (ΔL^*, Δa^*, and Δb^*) and Total [ΔE^*ab, $\Delta E94(1{:}1{:}1)$, $\Delta E00(1{:}1{:}1)$, and CMC(2:1)] Color Differences for Each Concentration of Cyanobacteria Deposited on the Filters

Diameter of the Measuring Head (mm)	Dilution (%)	ΔL^*	Δa^*	Δb^*	ΔE^*ab	$\Delta E94(1{:}1{:}1)$	CMC(2:1)	$\Delta E00(1{:}1{:}1)$
10	0	0.15	0.04	0.23	0.28	0.28	0.25	0.25
	20	2.31	0.47	0.66	2.45	2.37	1.28	1.56
	50	1.63	0.80	0.24	1.83	1.71	0.96	1.25
	100	2.84	0.57	0.77	2.99	2.88	1.50	2.47
8	0	0.06	0.12	0.29	0.32	0.29	0.29	0.29
	20	3.49	1.39	1.82	4.17	3.78	2.26	2.62
	50	2.37	0.86	–0.85	2.66	2.45	1.34	1.74
	100	1.92	0.64	0.47	2.08	1.97	1.05	1.55
5	0	0.16	0.06	0.34	0.38	0.37	0.35	0.35
	20	2.76	1.30	1.93	3.61	3.12	2.02	2.27
	50	2.62	0.94	0.91	2.93	2.70	1.46	1.91
	100	2.33	0.69	0.11	2.43	2.36	1.23	1.87

concentrations tested for each measuring head. Thus, 10 measurements/9.62 cm^2 are required for measuring heads of 8 and 5 mm diameter and 8 measurements/9.62 cm^2 for a measuring head of 10 mm diameter.

C. Influence of Target Area Diameter

Once the minimum number of measurements was established in relation to the dimensions of the measuring head, the color values obtained with each measuring head were compared in order to establish whether the results were equivalent. The result of a MANOVA with values of L^*, a^*, and b^* as dependent variables and the diameter of the measurement head as the independent variable revealed no statistically significant differences ($p > 0.05$), among the values obtained with the different measuring heads. Therefore, the color characteristics obtained with the different measuring heads are comparable when the established minimum number of measurements is applied (see Subsection 3.B).

From a practical point of view, and taking into account that in heterogeneous surfaces an increase in the field of view of the device reduces the effect of the different colors in the target area, with the consequent similarity in sequential measurements, the use of a 10 mm measuring head is more convenient, as fewer measurements are required (8/9.62 cm^2) and the error derived from heterogeneity in the filter color is also reduced.

4. Conclusions

The results of the study demonstrate the influence of both the microorganisms and the measuring instrument on the characterization of the color of cyanobacterial biofilms. Instrument properties, such as the diameter of the measuring head, affect the minimum number of measurements required to characterize the color, and properties of the microorganisms, such as concentration and moisture content, affect both the minimum number of measurements required and the color obtained.

The minimum number of measurements required increased with increasing heterogeneity of the color of the area measured, which depended on the concentration of the microorganisms, and decreased with the diameter of the measuring head. To control for the influence of the heterogeneity of the color of the area measured, the color of cyanobacteria should be measured on filters that are completely covered by the microorganisms, so that the white color of the filter is hidden. The influence of the size of the measuring head is more difficult to control for, as researchers usually only have one color measuring device available. However, if the number of measurements corresponds to those established in this study in relation to the measuring head diameter, results thus obtained will be comparable. It was established that a total of 10 measurements/9.62 cm^2 are required for measuring heads of 8 and 5 mm diameter and 8 measurements/9.62 cm^2 for a measuring head of 10 mm diameter. We therefore suggest that in order to standardize measurement of the color of cyanobacteria, 10 measurements/9.62 cm^2 are sufficient for characterization of the color, regardless of the dimensions of the measuring head of the device.

However, we also recommend that, when possible, a 10 mm measuring head should be used, as fewer measurements are required (8/9.62 cm^2) and the error derived from heterogeneity in the color of the filter is reduced.

The L^* values were greatly affected by the moisture content of the samples, whereas the chromatic parameters a^* and b^* were unaffected. Since the values of L^* decreased exponentially with moisture contents up to 50%, which can be considered as the point from which a stable asypmtote is reached on the corresponding graph, characterization of the cyanobacterial color should be made with samples with moisture contents of more than 50%. Otherwise, the results will not be comparable.

The methodology proposed here allows objective measure of the color of cyanobacteria, which would be very useful in those studies where knowledge of pigment content variations leads to conclusions. Moreover, it provides some advantages on traditional methodology as it is nondestructive and saves time and materials.

The present study was financed by the Science and Education Ministry of Spain (MEC, BIA2006-02233/BES-2007-16996).

References

1. http://www.cie.co.at
2. G. Wyszecki and W. S. Stiles, *Color Science: Concepts and Methods, Quantitative Data and Formulae* (Wiley, 1982).
3. L. G. Erokhina, "Spectral effects of the chromatic adaptation of nitrogen-fixing cyanobacteria grown on different nitrogen sources," Mikrobiologiya **61**, 960–967 (1992).
4. S. Liotenberg, D. Campbell, R. Rippka, J. Houmard, and N. Tandeau de Marsac, "Effect of the nitrogen source on phycobiliprotein synthesis and cell reserves in a chromatically adapting filamentous cyanobacterium," Microbiology **142**, 611–622 (1996).
5. S. R. Miller, M. Martin, J. Touchton, and R. W. Castenholz, "Effects of nitrogen availability on pigmentation and carbon assimilation in the cyanobacterium Synechococcus sp. strain SH-94-5," Arch. Microbiol. **177**, 392–400 (2002).
6. E. Miśkiewicz, A. G. Ivanov, J. P. Williams, M. U. Khan, S. Falk, and N. P. A. Huner, "Photosynthetic acclimation of the filamentous cyanobacterium, *Plectonema boryanum* UTEX 485, to temperature and light," Plant Cell Physiol. **41**, 767–775 (2000).
7. B. Prieto, T. Rivas, and B. Silva, "Rapid quantification of phototrophic microorganisms and their physiological state through their colour," GBIF **18**, 237–245 (2002).
8. B. Prieto, B. Silva, N. Aira, and L. Laiz, "Induction of biofilms on quartz surfaces as a means of reducing the visual impact of quartz quarries," GBIF **21**, 237–246 (2005).
9. B. Prieto, P. Sanmartín, B. Silva, and F. Martínez-Verdú, "Measuring the color of granite rocks. a proposed procedure," Color Res. Appl., article in press, doi:10.1002/col.20579 (2010).
10. R. Rippka, J. Deruelles, J. B. Waterbury, M. Herdman, and R. Y. Stanier, "Generic assignments, strain histories and

properties of pure cultures of cyanobacteria," J. Gen. Microbiol. **111**, 1–61 (1979).
11. CIE"Improvement to industrial color-difference evaluation," 142-2001 (CIE Central Bureau, 2001).
12. CIE, "Colorimetry," 3rd ed., 15:2004 (CIE Central Bureau, 2004).
13. J. Schanda, *Colorimetry: Understanding the CIE System* (Wiley, 2007).
14. CIE, "Industrial colour-difference evaluation, 116-1995 (CIE Central Bureau, 1995).
15. F. J. J. Clarke, R. McDonald, and B. Rigg, "Modification to the JPC79 color-difference formula," J. Soc. Dyers Col. **100**, 128–132 (1984).
16. R. S. Berns, *Billmeyer and Saltzman's Principles of Color Technology*, 3rd ed. (Wiley, 2000).
17. H. G. Völz, *Industrial Color Testing* (Wiley—VCH, 2001).
18. L. Gómez-Robledo, M. Melgosa, R. Huertas, R. Roa, M. J. Moyano, and F. J. Heredia, "Virgin-olive-oil color in relation to sample thickness and the measurement method," J. Am. Oil Chem. Soc. **85**, 1063–1071 (2008).
19. A Y. Hardeberg, "Acquisition and reproduction of color images: colorimetric and multispectral approaches," Ph.D. thesis (Ecole Nationale Superieure des Telecommunications, 1999).
20. D. Benavente, F. Martínez-Verdú, A. Bernabeu, V. Viqueira, R. Fort, M. García del Cura, C. Illueca, and S. Ordóñez, "Influence of surface roughness on color changes in building stones," Color Res. Appl. **28**, 343–351 (2003).
21. C. Grossi, P. Brimblecombe, R. M. Esbert, and F. J. Alonso, "Color changes in architectural limestones from pollution and cleaning," Color Res. Appl. **32**, 320–331 (2007).

Chapter 4*. Relationship between color and pigment production in two stone biofilm-forming cyanobacteria (*Nostoc* sp. PCC 9104 and *Nostoc* sp. PCC 9025)

Sanmartín, P.; Aira, N.; Devesa-Rey, R.; Silva, B.; Prieto, B.

Biofouling: The Journal of Bioadhesion and Biofilm Research 26 (5): 499-509 (2010)

JCR index (IF) 2010 = 3.333 (5/92, 5 percentile in Marine and Freshwater Biology; 38/160, 23 percentile in Biotechnology and Applied Microbiology)

Total number of times cited: 7

* This article was ranked one of the top 10 articles published on the same topic (domains of article 20425659 and 20390000) since its publication (2010). BioMedLib, "Who Is Publishing in My Domain?". April 15-14, 2012.

Biofouling
Vol. 26, No. 5, July 2010, 499–509

Taylor & Francis
Taylor & Francis Group

Relationship between color and pigment production in two stone biofilm-forming cyanobacteria (*Nostoc* sp. PCC 9104 and *Nostoc* sp. PCC 9025)

P. Sanmartín*, N. Aira, R. Devesa-Rey, B. Silva and B. Prieto

Departamento Edafología y Química Agrícola, Fac Farmacia, Universidad de Santiago de Compostela, 15782-Santiago de Compostela, Spain

(*Received 18 December 2009; final version received 11 March 2010*)

Previous studies have provided evidence that color measurements enable *on site* quantification of superficial biofilms, thereby avoiding the need for sampling. In the present study, the efficiency of color measurements to evaluate to what extent pigment production is affected by environmental parameters such as light intensity, combined nitrogen and nutrient availability, was tested with two cyanobacteria, *Nostoc* sp. strains PCC 9104 and PCC 9025, which form biofilms on stone. Both strains were acclimated, in aerated batch cultures for 2 weeks, to three different culture media: BG-11, BG-11$_0$, and BG-11$_0$/10 at either high or low light intensity. The content of chlorophyll *a*, carotenoids, and phycocyanins was measured throughout the experiment, together with variations in the color of the cyanobacteria, which were represented in the CIELAB color space. The results confirmed that the CIELAB color parameters are correlated with pigment content in such a way that variations in the latter are reflected as variations in color.

Keywords: color measurements; pigments; CIELAB color space; environmental parameters; cyanobacteria

Introduction

The adhesion and growth of biofilms on stone surfaces is a serious problem in relation to conservation of stone monuments, as the films produce a vast range of undesirable effects associated with increased colonization and mineral weathering (Silva et al. 1999; Warscheid and Braams 2000; Silva and Prieto 2004; McNamara and Mitchell 2005; Crispim et al. 2006; Gorbushina 2007), although in some cases the presence of biofilms prevents further weathering of the stone (Grondona et al. 1997, Ramírez et al. 2010). Since colonization of stone surfaces is almost inevitable (Warscheid and Braams 2000), research in this field must focus on the development of new technologies that enable early detection of colonization so that proliferation of the microorganisms can be treated at incipient stages, before biofilm formation. Previous studies have provided evidence that color measurements enable accurate *on site* quantification of the progress of epilithic colonization in natural conditions, even when the level of colonization is not detectable by the human eye (Prieto et al. 2002, 2005; Thornbush 2008).

The systematic use of color measurements to quantify the colonization of stone surfaces by organisms must be applied with caution, as many environmental parameters, such as light intensity, light quality, nitrate availability, and the presence of other nutrients may significantly alter the composition and/or abundance of the photosynthetic pigments, and therefore a particular strain may display different colors. In relation to this, Tandeu de Marsac (1977) observed that certain photosynthetic organisms can acclimate to different conditions of light in their surroundings by varying cellular pigmentation. Thus, although each strain has a range of optimal growth in terms of light intensity, low and intermediate light intensities generally stimulate synthesis of chlorophyll *a* (chl *a*) (Raven 1984; Fernández-Valiente and Leganés 1989; Martín-Trillo 1995; Jonte et al. 2003; Loreto et al. 2003) and phycobilisomes (PBS), thereby increasing the phycocyanin (PC) content (Lonneborg et al. 1985; Loreto et al. 2003), although this may lead to a reduction of carotenoids (Raps et al. 1983).

In contrast, limitation of major nutrients may result in a decrease in pigment content and hence the photosynthetic rate (Stebvens et al. 1981; Bartual et al. 2002) and in extensive PBS breakdown, especially when there is nitrogen limitation (Collier and Grossman 1992). Thus in nitrogen-deprived cultures, the PC content may decrease to undetectable levels; whereas the content of chlorophyll is often less affected whilst carotenoid content remains relatively stable (Duke and Allen 1990).

*Corresponding author. Email: patricia.sanmartin@usc.es
Published online 26 April 2010

ISSN 0892-7014 print/ISSN 1029-2454 online

DOI: 10.1080/08927011003774221
http://www.informaworld.com

Since most changes in the content of photosynthetic pigments give rise to an appreciable change in the color of cyanobacterial cultures, their health is often assessed by their color. However, although the application of spectroscopic methods to the evaluation of growth in cultures of cyanobacteria should exist, there are few references describing the evaluation of objective color data for phototrophic organism such by the CIELAB system (Thornsbush 2008). Furthermore, there have been relatively few attempts to quantitatively evaluate changes in color by different culture conditions. The aim of the present study was to develop a novel, non-destructive technology that enables early detection of biofilms on stone monuments. Thus, variation in color and pigment content of two cyanobacteria (*Nostoc* sp. PCC 9104 and *Nostoc* sp. PCC 9025), which form biofilms on stone (Saiz-Jimenez et al. 1991; Satapathy and Adhikary 1993), was explored in relation to different environmental parameters.

The specific objectives of the study were: (i) to characterize the variation in color of *Nostoc* sp. PCC 9104 and *Nostoc* sp. PCC 9025 through the standardized CIELAB color system, in order to obtain an objective assessment, not affected by subjectivity of the human eye; (ii) to evaluate color variations in response to: (a) different light intensities, (b) diazotrophic conditions (nitrogen-fixing conditions in the absence of available nitrates) and non-diazotrophic conditions (nitrate-grown conditions), (c) macronutrient limitation, (d) age of the culture; and (iii) to evaluate the relationship between color variation and pigment production, estimated by measurement of the content of chl *a*, carotenoids and PCs.

Materials and methods

Growth conditions and Nostoc *sp. strains*

Experimental work was carried out with *Nostoc* sp. PCC 9104 and *Nostoc* sp. PCC 9025 strains, two filamentous N_2-fixing heterocyst-forming cyanobacteria (Figure 1). Cells in exponential growth were incubated at room temperature for 2 weeks in 80 ml aerated photobioreactors, containing 60 ml of liquid medium, with precultures of 20 ml of BG-11_0 medium (Rippka et al. 1979) as inoculum. Three culture media, containing different amounts of nitrate, were chosen: BG-11, a non-diazotrophic culture medium; BG-11_0, which is a modification of the previous medium (with nitrate omitted), often used for selection of nitrogen-fixing strains; and BG-11_0/10, a tenfold dilution of BG-11_0. The latter was chosen as a representative of a 'low nutrient' culture medium, and the latter two media generate diazotrophic conditions.

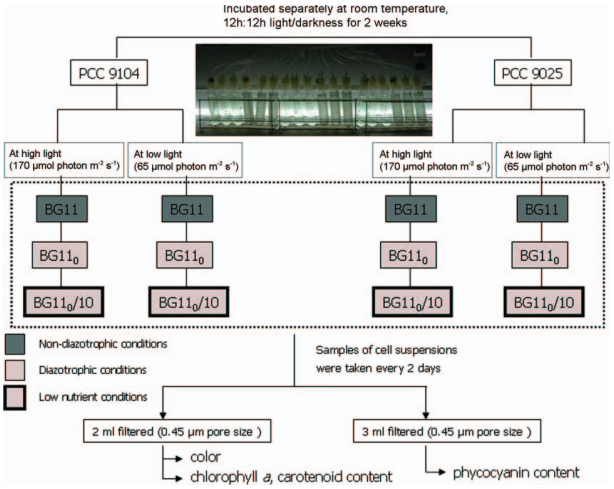

Figure 1. Scheme of the experimental set-up, including a photograph of the aerated photobioreactors.

Photobioreactors were maintained with aeration under two different light intensities, 170 and 65 μmol photon m^{-2} s^{-1}, with a 12h:12h light:dark photoperiod. Lighting was provided by fluorescent lamps (Mazda Fluor Lumiere du Jour C9 TF 65, 85 W), and the light intensity was measured with a radiometer (DHD 2302.0, HERTER). All analyses were run in triplicate, and water loss by evaporation was corrected daily by the addition of sterilized distilled water.

Extraction and determination of photosynthetic pigments

Samples of cell suspension (7 ml) were taken every 2 days over a period of 14 days and the chl *a*, carotenoid and PC contents were measured. For quantification of chl *a* and carotenoids, an accurate volume of each sample, 2 ml of homogeneous suspension, was filtered under vacuum, through nitrocellulose filter discs (0.45 μm and 25 mm diameter), which were added to 4 ml of dimethylsulfoxide and heated to 65°C for 1 h. The samples were filtered and the extracts were measured in a UV Visible Spectrophotometer (Varian Cary 100) by the method of Bell and Sommerfeld (1987), using the equations of Wollenweider (1969) for chl *a*, and Wellburn (1994) for carotenoids. PCs were determined by a modified osmotic shock method (Wyman and Fay 1986): 3 ml aliquots of the sample were filtered under vacuum through nitrocellulose filter discs (0.45 μm and 47 mm diameter). The cells deposited on the filter were recovered by addition of 600 μl of glycerol (10% total volume) and incubated in the dark at 4.5°C for 24 h. Distilled water (5.4 ml) was then added to lyse the cells. After 30 min, the samples were filtered and the extracts were measured in a UV

Visible Spectrophotometer (Varian Cary 100), according to the method of Bennet and Bogorad (1973).

Color measurements

Color was measured directly on the same filters used for extraction of chl *a* and carotenoids, before carrying out the extraction, and while the filters were still humid (humidity content > 50% w/w. Prieto et al. 2010). A solid reflection spectrophotometer (CE-XTH) equipped with OptiviewSilver/i QC Basic software, illuminant D65, observer 2° and a 5 mm diameter target area was used. A total of five readings were taken at different randomly selected zones in each filter. Color measurements were analyzed by considering the CIE 1976 (L^*, a^*, b^*) or CIELAB color system, which is widely accepted by both the scientific community and industry, since is the most 'perceptually uniform' of the color spaces (Berns 2000; Völz 2001). Perceptually uniform means that a change of the same amount in a color value should produce a change of about the same visual importance. The CIELAB color system is organized with three axes in a spherical form: L^*, a^*, and b^*. The L^* axis is associated with the lightness of the color and moves from top (value: 100, white) to bottom (value: 0, black), whereas the a^* and b^* axes are associated with changes in redness-greenness (positive a^* is red and negative a^* is green) and in yellowness-blueness (positive b^* is yellow and negative b^* is blue); both move in the two axes that form a plane orthogonal to L^*, and do not have specific numerical limits. In this regard, ΔL^*, Δa^*, and Δb^* represent the degree of difference between two samples or the same sample at different times. Furthermore, the color parameters most closely related to the psychophysical characteristics of color, ie more related to color perception, and which correspond to the angular coordinates of chroma or saturation [$C^* = (a^{*2} + b^{*2})^{1/2}$] and hue or hue angle [$h = \arctan(b^*/a^*)$], were also calculated. Likewise, the total color difference was expressed as $\Delta E_{ab} = [(\Delta L^*)^2 + (\Delta a^*)^2 + (\Delta b^*)^2]^{1/2}$ or $\Delta E_{ab} = [(\Delta L^*)^2 + (\Delta C^*)^2 + (\Delta H^*)^2]^{1/2}$, where ΔL^*, Δa^*, Δb^* and ΔC^* represent respectively the differences in the values of L^*, a^*, b^*, and C^* considered, and ΔH^* is given by $\Delta H_{ab} = [2(C_1^* C_2^*)^{1/2}.\sin(\Delta h_{ab}/2)]$, where Δh_{ab} is the difference in hue angle $\Delta h_{ab} = \tan^{-1}(b_2^*/a_2^*) - \tan^{-1}(b_1^*/a_1^*)$.

Statistical analyses

Data were subjected to MANOVA and the Student's *t*-test (for paired comparison) or the Mann–Whitney *U*-test (for non-parametric data) at the 5% significant level (p-value < 0.05) and two-tailed-Bivariate Spearman's correlations. Statistical analyses were performed with SPSS (SPSS v15.0 for Windows).

Results

Growth and pigment contents

The changes in the pigment contents of the two strains studied (*Nostoc* sp. PCC 9104 and PCC 9025) are shown in Figure 2. Growth, measured as pigment concentration, was higher in *Nostoc* sp. PCC 9104 than in strain PCC 9025 and the maximum final pigment content in both strains was obtained in non-diazotrophic conditions, followed by diazotrophic and modified diazotrophic conditions. The growth response to light intensity, combined nitrogen and nutrient availability differed depending on the strain considered. Growth of *Nostoc* sp. PCC 9104 was more strongly affected by nutrient limitation than by availability of nitrate and light intensity, whereas in *Nostoc* sp. PCC 9025, the presence of nitrate and high light intensity were the parameters that determined further growth. In both strains these results were common for the three pigments studied: chl *a*, PCs and carotenoids, and were not noted until 8 days of culturing. In both strains, the concentrations of chl *a*

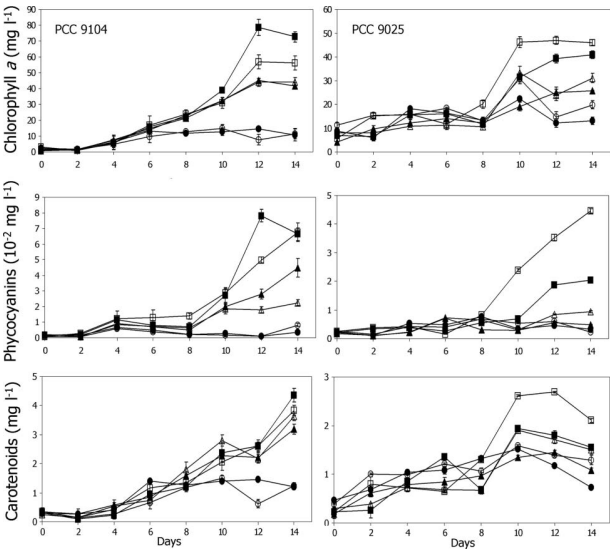

Figure 2. Pigment content. Top: chl *a* concentration (mg l^{-1}), middle: PC concentration (10^{-2} mg l^{-1}) and bottom: carotenoid concentration (mg l^{-1}), in aerated batch cultures of *Nostoc* sp. strain PCC 9104 (left) and *Nostoc* sp. strain PCC 9025 (right). -■- = non-diazotrophic medium BG-11, -▲- = diazotrophic medium BG-11_0, -●- = modified diazotrophic medium BG-11_0/10 under low light (solid symbols) and high light (open symbols). Data points represent the average of three replicates; vertical bars represent the SD.

and PCs were higher in cultures grown on nitrate containing media than in the cultures grown on media without nitrate, from the 12th day of culture onward. However, from the 10th day of culture, the concentration of carotenoids was affected by different factors, depending on the strain: the availability of nutrients was the main factor affecting carotenoid concentration for *Nostoc* sp. strain PCC 9104, whereas the presence of nitrates together with the high light intensity affected *Nostoc* sp. strain PCC 9025 to a greater extent.

Statistical comparison of chl *a*, PC, and carotenoid concentrations relative to culture age was performed for both *Nostoc* strains (Table 1). For all six experimental cultures, ie with two different light intensities and three different culture media, the mean concentration of each pigment increased significantly during the culture period in both strains. At the end of the experiment, the concentration of chl *a* in strain PCC 9104 was higher in non-diazotrophic medium under low light conditions (72.63 mg l^{-1}) and lower in

Table 1. Mean concentrations of the pigments of *Nostoc* sp. strains PCC 9104 and PCC 9025 for the six experimental cultures over a 14-day growth period.

	Day	0	2	4	6	8	10	12	14
Nostoc sp. PCC 9104									
Chl a (mg l^{-1})									
BG11	HL	2.99^{a}	1.07^{a}	5.93^{ab}	16.83^{abc}	23.92^{bc}	30.96^{c}	56.96^{d}	56.17^{d}
	LL	1.52^{a}	0.89^{a}	5.44^{ab}	15.76^{ab}	22.12^{ab}	39.04^{b}	78.62^{c}	72.63^{c}
$BG11_0$	HL	1.87^{a}	1.70^{a}	7.39^{a}	13.87^{ab}	23.17^{bc}	32.35^{cd}	44.00^{d}	44.24^{d}
	LL	0.59^{a}	1.48^{a}	7.49^{ab}	14.92^{bc}	21.50^{c}	32.58^{d}	45.00^{e}	41.58^{de}
$BG11_0/10$	HL	0.98^{a}	1.58^{a}	4.70^{ab}	9.78^{bc}	12.72^{c}	14.67^{c}	7.68^{abc}	11.30^{bc}
	LL	2.51^{a}	1.80^{a}	6.31^{ab}	13.26^{c}	11.71^{bc}	12.83^{bc}	14.38^{c}	10.76^{bc}
PCs (10^{-2} mg l^{-1})									
BG11	HL	0.1^{a}	0.3^{a}	1.2^{ab}	1.3^{ab}	1.4^{ab}	2.9^{b}	5.0^{c}	6.7^{c}
	LL	0.2^{a}	0.2^{a}	1.1^{ab}	1.0^{ab}	0.7^{a}	2.7^{b}	7.8^{c}	6.6^{c}
$BG11_0$	HL	0.2^{ab}	0.1^{a}	0.8^{b}	0.7^{b}	0.6^{ab}	1.8^{cd}	1.5^{c}	2.2^{d}
	LL	0.2^{a}	0.1^{a}	0.9^{ab}	0.7^{ab}	0.5^{a}	2.0^{b}	1.8^{b}	4.5^{c}
$BG11_0/10$	HL	0.1^{a}	0.1^{a}	0.6^{a}	0.5^{a}	0.2^{a}	0.2^{a}	0.1^{a}	0.8^{a}
	LL	0.1^{a}	0.2^{a}	0.7^{b}	0.9^{a}	0.2^{a}	0.3^{a}	0.1^{a}	0.3^{a}
Carotenoids (mg l^{-1})									
BG11	HL	0.35^{ab}	0.15^{a}	0.42^{ab}	1.18^{bc}	1.34^{bc}	2.05^{cd}	2.60^{d}	3.83^{e}
	LL	0.31^{a}	0.10^{a}	0.23^{a}	0.96^{a}	1.21^{a}	2.38^{b}	2.60^{b}	4.36^{c}
$BG11_0$	HL	0.26^{a}	0.15^{a}	0.54^{a}	0.73^{a}	1.80^{b}	2.80^{cd}	2.17^{bc}	3.63^{d}
	LL	0.36^{a}	0.27^{a}	0.59^{a}	0.86^{ab}	1.60^{bc}	2.28^{c}	2.22^{c}	3.19^{d}
$BG11_0/10$	HL	0.35^{a}	0.14^{a}	0.28^{a}	0.65^{ab}	1.18^{bc}	1.51^{c}	0.63^{ab}	1.24^{bc}
	LL	0.30^{a}	0.16^{a}	0.41^{a}	1.39^{b}	1.26^{b}	1.39^{b}	1.47^{b}	1.20^{b}
Nostoc sp. PCC 9025									
Chl a (mg l^{-1})									
BG11	HL	5.77^{a}	15.24^{b}	15.77^{b}	11.79^{ab}	20.20^{b}	46.27^{c}	46.99^{c}	46.02^{c}
	LL	6.84^{a}	6.54^{a}	15.52^{ab}	16.15^{ab}	11.78^{ab}	31.39^{bc}	39.33^{c}	40.96^{c}
$BG11_0$	HL	7.99^{a}	8.14^{a}	10.76^{a}	11.24^{a}	10.64^{a}	33.36^{b}	24.00^{c}	31.14^{b}
	LL	4.08^{a}	9.73^{b}	12.25^{b}	14.11^{bc}	12.14^{b}	19.12^{c}	25.00^{d}	25.74^{d}
$BG11_0/10$	HL	11.17^{a}	15.38^{ab}	15.75^{ab}	18.35^{ab}	13.07^{ab}	30.73^{c}	14.70^{ab}	19.85^{b}
	LL	8.74^{ab}	5.91^{a}	18.08^{cd}	16.22^{bcd}	13.31^{abc}	22.20^{d}	12.16^{abc}	13.17^{abc}
PCs (10^{-2} mg l^{-1})									
BG11	HL	0.3^{a}	0.4^{a}	0.4^{a}	0.2^{a}	0.8^{a}	2.4^{b}	3.5^{bc}	4.5^{c}
	LL	0.2^{a}	0.4^{a}	0.4^{a}	0.3^{a}	0.6^{a}	0.7^{a}	1.9^{b}	2.0^{b}
$BG11_0$	HL	0.2^{ab}	0.1^{a}	0.2^{ab}	0.7^{c}	0.7^{c}	0.3^{ab}	0.8^{c}	0.9^{c}
	LL	0.2^{ab}	0.1^{a}	0.2^{ab}	0.7^{c}	0.3^{b}	0.3^{b}	0.6^{cd}	0.5^{d}
$BG11_0/10$	HL	0.2^{ab}	0.1^{a}	0.4^{abc}	0.4^{abc}	0.7^{c}	0.5^{bc}	0.6^{c}	0.2^{ab}
	LL	0.2^{ab}	0.1^{a}	0.6^{cd}	0.5^{bc}	0.8^{d}	0.3^{abc}	0.5^{bc}	0.3^{abc}
Carotenoids (mg l^{-1})									
BG11	HL	0.23^{a}	0.80^{ab}	0.71^{ab}	0.65^{ab}	1.30^{b}	2.61^{c}	2.69^{c}	2.11^{c}
	LL	0.23^{a}	0.26^{a}	0.86^{abc}	1.35^{bcd}	0.68^{ab}	1.94^{d}	1.80^{d}	1.55^{cd}
$BG11_0$	HL	0.30^{a}	0.39^{a}	0.73^{a}	0.68^{a}	0.68^{a}	1.91^{b}	1.71^{b}	1.51^{b}
	LL	0.18^{a}	0.61^{ab}	0.78^{bc}	0.84^{bcd}	0.98^{bcd}	1.35^{cd}	1.45^{d}	1.08^{bcd}
$BG11_0/10$	HL	0.39^{a}	1.01^{b}	0.99^{b}	1.21^{bc}	1.06^{b}	1.59^{d}	1.40^{cd}	1.43^{cd}
	LL	0.47^{a}	0.68^{ab}	1.04^{bc}	1.09^{bc}	1.32^{c}	1.52^{c}	1.17^{bc}	0.73^{ab}

Different superscript letters in each row indicate significant differences ($p < 0.05$) between the means of three independent replicates for the pigment content of a given culture. Chl *a* = chlorophyll *a*; PCs = phycocyanins; BG-11 = non-diazotrophic medium; $BG\text{-}11_0$ = diazotrophic medium; $BG\text{-}11_0/10$ = modified diazotrophic medium; HL = grown under high light intensity; LL = grown under low light intensity.

modified diazotrophic conditions at both light intensities (11.30 and 10.76 mg l^{-1}). In strain PCC 9025, the lowest chl *a* content was also found in nutrient-deficient cultures, but the greatest amount of chl *a* corresponded to growth medium containing nitrate and a high light intensity. Similar results were observed for the concentrations of PCs, which, in non-diazotrophic media, reached values of 6.6 and 6.7 $\times$ 10^{-2} mg l^{-1} for strain PCC 9104 and 2.0 and 4.5 $\times$ 10^{-2} mg l^{-1} for strain PCC 9025 by the end of the experiment. The concentrations of carotenoids were similar in the six cultures, and ranged from 4.36 (BG11 at LL) to 1.20 mg l^{-1} ($BG11_0$/10 at LL) in strain PCC 9104 and from 2.11 (BG11 at HL) to 0.73 mg l^{-1} ($BG11_0$/10 at LL) in strain PCC 9025.

Significant differences in the mean values of each pigment in relation to the six experimental conditions referred to above are shown in Table 2. The different light intensities (high: 170 μmol photon m^{-2} s^{-1} and low: 65 μmol photon m^{-2} s^{-1}) did not have significant effects on the concentration of any of the pigments in *Nostoc* sp. PCC 9104, irrespective of the culture medium (Table 2). However, for *Nostoc* sp. PCC 9025 it caused significant changes for all pigments, on BG11 and $BG11_0$, ie on both non nutrient-limited cultures.

On the other hand, under high light intensity, the concentrations of chl *a* and carotenoids were significantly different in *Nostoc* sp. PCC 9104 grown in nutrient-deficient culture medium; in the case of PCs under high light, significant differences were observed between BG11 and both diazotrophic media. In the case of *Nostoc* sp. PCC 9025, although there was no difference in the concentration of carotenoids in the different media, the concentrations of chl *a* and PC were significantly different in this strain growing in BG11 medium (Table 2).

CIELAB color parameters: L*, a*, b*, C*, h

Both strains of *Nostoc* underwent perceptible and objectively measured variations in color throughout the entire experiment (Figure 3). Statistical tests applied to the color data revealed significant differences for each CIELAB color parameter (L^*, a^*, b^*, C^* and h) in relation to age of the culture (Table 3), culture medium (Table 4) and light intensity (Table 4).

In the case of *Nostoc* sp. strain PCC 9104, the L^* parameter decreased (the culture darkened) from day 0 to day 10, regardless of the culture medium and light intensity, with values ranging from 86.34 to 47.26 CIELAB units. However, from the 10th day of culture, nutrient-deficient cultures recovered lightness (the L^* value increased up to 78.17 CIELAB units), whereas the lightness of the other cultures stabilized at the

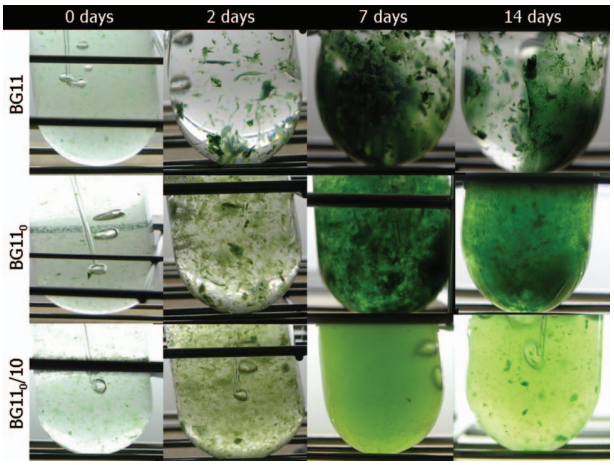

Figure 3. Cultures of *Nostoc* sp. PCC 9104 over a 14-day growth period, showing difference in appearance consequent on the culture medium. Only cultures grown under low light intensity are shown.

Table 2. Mean concentrations of the pigments of *Nostoc* sp. strains PCC 9104 and PCC 9025 grown in three different culture media and exposed to either high or low light intensity.

Light intensity	*Chl a* (mg l^{-1})		PCs (10^{-2} mg l^{-1})		Carotenoids (mg l^{-1})	
	HL	LL	HL	LL	HL	LL
Nostoc sp. PCC 9104						
BG11	24.36^{a}_{a}	29.50^{a}_{a}	2.5^{a}_{a}	2.8^{a}_{a}	1.49^{a}_{a}	1.52^{a}_{a}
$BG11_0$	21.08^{a}_{a}	20.64^{a}_{ab}	1.1^{a}_{b}	1.4^{a}_{ab}	1.51^{a}_{a}	1.42^{a}_{a}
$BG11_0$/10	7.93^{a}_{b}	9.19^{a}_{b}	0.3^{a}_{b}	0.3^{a}_{b}	0.75^{a}_{b}	0.96^{a}_{a}
Nostoc sp. PCC 9025						
BG11	26.01^{a}_{a}	21.06^{b}_{a}	1.6^{a}_{a}	0.8^{b}_{a}	1.39^{a}_{a}	1.08^{b}_{a}
$BG11_0$	17.16^{a}_{b}	15.27^{b}_{ab}	0.5^{a}_{b}	0.3^{b}_{b}	0.99^{a}_{a}	0.91^{b}_{a}
$BG11_0$/10	17.37^{a}_{b}	13.72^{a}_{b}	0.4^{a}_{b}	0.4^{a}_{b}	1.13^{a}_{a}	1.00^{a}_{a}

Different superscript letters indicate significant differences ($p < 0.05$) between means pigment contents in the same culture medium in relation to light intensity. Different subscript letters indicate significant differences ($p < 0.05$) between means pigment contents in the same light intensity in relation to culture medium. Chl *a* = chlorophyll *a*; PCs = phycocyanins; BG-11 = non-diazotrophic medium; BG-11_0 = diazotrophic medium; BG-11_0/10 = modified diazotrophic medium; HL = grown under high light intensity; LL = grown under low light intensity.

Table 3. Values of CIELAB parameters for *Nostoc* sp. strains PCC 9104 and PCC 9025 for the six experimental cultures over a 14-day growth period.

		Nostoc sp. PCC 9104								*Nostoc* sp. PCC 9025							
	Day	0	2	4	6	8	10	12	14	0	2	4	6	8	10	12	14
*L**																	
BG11	HL	84.68^{a}	82.96^{ab}	85.72^{a}	75.43^{bc}	72.77^{c}	68.19^{d}	51.12^{de}	47.37^{e}	91.82^{a}	86.31^{a}	66.22^{b}	57.84^{b}	58.57^{b}	44.22^{c}	36.85^{c}	43.59^{c}
	LL	82.33^{ab}	86.34^{a}	76.50^{b}	78.82^{b}	69.14^{c}	60.02^{d}	49.38^{e}	50.43^{e}	92.39^{a}	87.48^{a}	70.28^{bc}	64.96^{cd}	77.27^{b}	55.76^{e}	57.35^{de}	61.58^{de}
$BG11_0$	HL	80.56^{a}	77.89^{ab}	71.28^{cd}	73.15^{bc}	66.25^{d}	47.26^{e}	48.75^{e}	41.47^{f}	91.06^{a}	90.66^{a}	71.78^{c}	71.63^{c}	80.02^{b}	56.25^{d}	56.39^{d}	60.58^{d}
	LL	83.98^{a}	80.58^{a}	66.27^{b}	75.96^{c}	67.03^{b}	49.12^{d}	52.69^{d}	44.33^{e}	90.20^{a}	89.33^{a}	74.77^{b}	75.67^{b}	78.95^{b}	61.59^{c}	59.66^{c}	65.55^{c}
$BG11_0/10$	HL	81.77^{a}	78.50^{ab}	70.89^{c}	74.75^{bc}	70.54^{c}	62.71^{d}	78.17^{ab}	75.38^{bc}	83.85^{a}	83.99^{a}	71.17^{b}	67.08^{bc}	70.69^{b}	58.39^{d}	52.89^{d}	64.77^{c}
	LL	80.17^{a}	77.86^{ab}	65.88^{d}	76.20^{abc}	72.86^{c}	61.11^{e}	67.32^{d}	75.12^{bc}	88.08^{a}	90.66^{a}	66.92^{b}	71.89^{c}	73.30^{c}	60.23^{d}	53.70^{e}	61.78^{d}
*a**																	
BG11	HL	-7.80^{a}	-4.54^{b}	-4.07^{b}	-9.28^{a}	-15.33^{c}	-14.92^{c}	-19.67^{d}	-19.44^{d}	-2.30^{a}	-4.59^{b}	-9.57^{c}	-11.19^{c}	-13.83^{d}	-15.01^{d}	-13.48^{d}	-14.74^{d}
	LL	-6.95^{a}	-2.50^{b}	-9.41^{cd}	-8.13^{ac}	-11.02^{d}	-17.23^{e}	-16.71^{e}	-18.01^{e}	-2.28^{a}	-3.99^{a}	-7.78^{b}	-10.21^{c}	-8.20^{bc}	-12.85^{d}	-14.65^{e}	-13.39^{de}
$BG11_0$	HL	-7.49^{a}	-6.08^{b}	-14.20^{c}	-11.10^{d}	-17.07^{e}	-21.31^{f}	-23.28^{g}	-20.45^{f}	-2.42^{a}	-2.87^{a}	-6.02^{b}	-9.73^{c}	-8.69^{c}	-13.57^{d}	-16.83^{e}	-14.27^{d}
	LL	-7.72^{a}	-5.78^{b}	-18.42^{c}	-13.44^{d}	-19.69^{c}	-23.21^{e}	-23.49^{e}	-23.92^{e}	-2.57^{a}	-3.51^{a}	-4.92^{b}	-9.47^{c}	-9.10^{c}	-12.31^{d}	-17.24^{e}	-15.67^{e}
$BG11_0/10$	HL	-7.01^{a}	-5.44^{a}	-14.04^{b}	-12.25^{b}	-14.44^{b}	-16.91^{c}	-12.51^{b}	-13.73^{b}	-4.85^{a}	-5.82^{a}	-8.12^{b}	-12.09^{c}	-12.34^{c}	-15.11^{d}	-17.39^{e}	-15.76^{d}
	LL	-7.33^{a}	-5.76^{a}	-15.72^{cd}	-12.68^{b}	-14.49^{bc}	-17.09^{de}	-19.10^{e}	-14.77^{bc}	-3.42^{a}	-3.21^{a}	-9.87^{b}	-10.80^{b}	-12.73^{c}	-14.95^{d}	-18.18^{e}	-16.16^{de}
*b**																	
BG11	HL	9.00^{a}	4.03^{b}	4.31^{b}	9.45^{a}	17.91^{c}	14.93^{d}	21.88^{e}	21.81^{e}	2.88^{a}	5.76^{b}	7.21^{bc}	8.73^{cd}	10.68^{de}	10.05^{de}	9.61^{de}	10.87^{e}
	LL	7.06^{a}	1.30^{b}	9.82^{cd}	8.18^{ac}	11.12^{d}	15.75^{e}	17.44^{ef}	19.62^{f}	3.21^{a}	5.32^{b}	5.72^{b}	7.68^{c}	7.22^{c}	7.93^{c}	10.59^{d}	9.78^{d}
$BG11_0$	HL	7.22^{a}	11.80^{b}	26.17^{c}	20.25^{d}	34.22^{e}	31.59^{e}	33.74^{e}	32.21^{e}	3.13^{a}	4.18^{a}	4.99^{a}	10.54^{bc}	9.68^{b}	11.74^{c}	15.55^{d}	15.53^{d}
	LL	8.53^{a}	10.92^{a}	28.79^{bd}	19.35^{c}	31.60^{d}	27.76^{b}	30.21^{bd}	30.89^{d}	3.04^{a}	5.37^{b}	3.14^{a}	9.65^{c}	10.15^{c}	9.26^{c}	14.47^{d}	9.66^{c}
$BG11_0/10$	HL	7.22^{a}	10.18^{a}	24.51^{b}	24.60^{b}	30.28^{c}	30.40^{c}	24.10^{b}	27.00^{bc}	5.20^{a}	8.33^{b}	8.09^{b}	15.49^{c}	17.56^{d}	18.35^{d}	23.57^{e}	22.69^{e}
	LL	7.76^{a}	9.55^{a}	27.57^{b}	25.67^{b}	33.09^{cd}	29.73^{bc}	35.22^{d}	28.02^{b}	4.15^{a}	4.44^{a}	10.45^{b}	13.79^{c}	17.29^{d}	17.87^{d}	22.47^{e}	18.38^{d}
*C**																	
BG11	HL	11.93^{a}	6.16^{b}	5.96^{b}	13.27^{a}	23.60^{c}	21.13^{c}	29.46^{d}	29.23^{d}	3.71^{a}	7.37^{b}	12.01^{c}	14.23^{cd}	17.54^{e}	18.09^{e}	16.58^{de}	18.36^{e}
	LL	9.93^{a}	2.94^{b}	13.60^{cd}	11.57^{ac}	15.67^{d}	23.36^{e}	24.18^{e}	26.64^{e}	3.95^{a}	6.66^{b}	9.74^{c}	12.82^{de}	10.96^{cd}	15.12^{ef}	18.10^{g}	15.85^{fg}
$BG11_0$	HL	10.42^{a}	13.29^{b}	29.78^{c}	23.12^{d}	38.25^{e}	38.11^{e}	41.00^{e}	38.16^{e}	3.97^{a}	5.08^{a}	7.88^{b}	14.37^{c}	13.03^{c}	17.95^{d}	22.93^{e}	21.09^{e}
	LL	11.52^{a}	12.37^{a}	34.19^{bd}	23.61^{c}	37.25^{d}	36.19^{b}	38.30^{bd}	39.16^{d}	4.01^{a}	6.42^{b}	5.88^{b}	13.53^{c}	13.64^{c}	15.41^{d}	22.51^{e}	13.58^{c}
$BG11_0/10$	HL	10.08^{a}	11.55^{a}	28.28^{bc}	27.51^{bc}	33.58^{cd}	34.79^{d}	27.17^{b}	30.29^{bcd}	7.15^{a}	10.17^{b}	11.49^{b}	19.67^{c}	21.48^{c}	23.78^{d}	29.30^{e}	27.64^{e}
	LL	10.79^{a}	11.17^{a}	31.74^{bc}	28.66^{b}	36.13^{cd}	34.31^{c}	40.07^{d}	31.68^{bc}	5.41^{a}	5.48^{a}	14.38^{b}	17.53^{c}	21.47^{d}	23.32^{d}	28.90^{e}	22.58^{d}
h																	
BG11	HL	131.54^{a}	141.61^{b}	131.93^{a}	134.16^{a}	130.66^{a}	135.20^{a}	132.23^{a}	131.92^{a}	128.33^{a}	128.24^{a}	143.39^{b}	141.73^{b}	141.71^{b}	146.23^{b}	144.72^{b}	143.87^{b}
	LL	135.73^{a}	158.80^{b}	133.51^{a}	134.29^{a}	134.57^{a}	137.63^{a}	134.37^{a}	132.63^{a}	124.89^{a}	127.24^{a}	143.99^{cd}	142.47^{bc}	138.36^{b}	148.49^{d}	143.87^{cd}	141.12^{bc}
$BG11_0$	HL	136.36^{a}	118.63^{b}	118.51^{b}	118.35^{b}	116.51^{b}	124.02^{c}	124.65^{c}	122.56^{c}	127.76^{a}	124.35^{ab}	142.18^{e}	133.12^{c}	131.51^{bc}	139.21^{de}	137.35^{d}	132.51^{c}
	LL	132.52^{a}	118.66^{b}	122.64^{c}	124.07^{c}	121.96^{c}	129.95^{ad}	127.89^{d}	128.07^{d}	130.06^{a}	123.14^{b}	149.43^{c}	134.31^{c}	131.88^{ac}	143.25^{d}	139.95^{d}	134.60^{c}
$BG11_0/10$	HL	134.36^{a}	118.48^{bc}	120.31^{b}	117.13^{cd}	115.48^{d}	119.13^{bc}	117.37^{cd}	117.11^{cd}	132.13^{a}	124.65^{c}	135.25^{b}	128.20^{cd}	124.88^{c}	129.57^{ad}	126.42^{cd}	124.65^{c}
	LL	137.70^{a}	121.40^{b}	119.60^{b}	116.20^{bc}	113.60^{c}	119.90^{b}	118.43^{c}	117.78^{c}	129.15^{ab}	125.97^{ad}	133.44^{c}	128.52^{abd}	126.37^{ad}	129.90^{b}	128.98^{ab}	125.40^{d}

Different superscript letters indicate significant differences ($p < 0.05$) between the means of three independent replicates (the reported color parameters for each replicate are the mean values of five measurements) for the values of CIELAB parameters for a given culture (same row). L^* = lightness; a^* = redness-greenness changes; b^* = yellowness-blueness changes; C^* = chroma or saturation; h = hue or tone; BG-11 = non-diazotrophic medium; BG-11_0 = diazotrophic medium; BG-11_0/10 = modified diazotrophic medium; HL = grown under high light intensity; LL = grown under low light intensity.

Table 4. Values of CIELAB parameters of *Nostoc* sp. strains PCC 9104 and PCC 9025 in three different culture media and exposed to either high or low intensity.

	L^*		a^*		b^*		C^*		h	
Light intensity	HL	LL	HL	LL	HL	LL	HL	LL	HL	LL
Nostoc sp. PCC 9104										
BG11	69.59^{a}_{a}	69.12^{a}_{a}	-11.88^{a}_{a}	-11.25^{a}_{a}	12.92^{a}_{a}	11.29^{b}_{a}	17.59^{a}_{a}	15.99^{b}_{a}	133.66^{a}_{a}	137.69^{b}_{a}
$BG11_0$	63.33^{a}_{b}	64.99^{a}_{b}	-15.12^{a}_{b}	-16.96^{a}_{b}	24.65^{a}_{b}	23.51^{a}_{b}	29.02^{a}_{b}	29.08^{a}_{b}	122.45^{a}_{b}	125.72^{a}_{b}
$BG11_0/10$	74.09^{a}_{c}	72.06^{a}_{a}	-12.04^{a}_{a}	-13.37^{a}_{c}	22.29^{a}_{b}	24.58^{a}_{b}	25.41^{a}_{b}	28.07^{b}_{b}	119.92^{a}_{b}	120.60^{a}_{c}
Nostoc sp. PCC 9025										
BG11	60.68^{a}_{a}	70.88^{b}_{a}	-10.59^{a}_{ab}	-9.04^{a}_{a}	8.22^{a}_{a}	7.18^{a}_{a}	13.48^{a}_{a}	11.65^{a}_{a}	139.77^{a}_{a}	138.80^{b}_{a}
$BG11_0$	71.05^{a}_{b}	74.46^{b}_{a}	-9.30^{a}_{a}	-8.58^{b}_{a}	9.42^{a}_{a}	8.09^{b}_{a}	13.29^{a}_{a}	11.87^{b}_{a}	133.50^{a}_{b}	135.83^{b}_{b}
$BG11_0/10$	67.85^{a}_{b}	70.82^{a}_{a}	-11.43^{a}_{b}	-10.78^{a}_{b}	14.91^{a}_{b}	13.60^{a}_{b}	18.84^{a}_{b}	17.39^{a}_{b}	128.24^{a}_{c}	128.47^{a}_{c}

Different superscript letters indicate significant differences ($p < 0.05$) between the means of three independent replicates (the reported color parameters for each replicate are the mean values of five measurements) for the values of CIELAB parameters in the same culture medium in relation to light intensity. Different subscript letters indicate significant differences ($p < 0.05$) between the means of three independent replicates (the reported color parameters for each replicate are the mean values of five measurements) for the values of CIELAB parameters in the same light intensity in relation to culture medium. L^* = lightness; a^* = redness-greenness changes; b^* = yellowness-blueness changes; C^* = chroma or saturation; h = hue or tone; BG-11 = non-diazotrophic medium; $BG\text{-}11_0$ = diazotrophic medium; $BG\text{-}11_0/10$ = modified diazotrophic medium; HL = grown under high light intensity; LL = grown under low light intensity.

lowest values (Figure 4 and Table 3). In the same way, the L^* values decreased throughout the experiment for *Nostoc* sp. strain PCC 9025, although in this case, from 8 days, the L^* values of cultures growing in nitrate containing medium under high light intensity were lower than in the other cultures, and only reached 36.85 CIELAB units (Figure 4 and Table 3).

Color parameters (a^* and b^*) associated to redness-greenness and yellowness-blueness changes respectively, ranged between −2.50 and −23.92 for a^* in *Nostoc* sp. PCC 9104, and between −2.28 and −18.18 for *Nostoc* sp. PCC 9025, while b^* values ranged between 35.22 and 1.30 for *Nostoc* sp. PCC 9104, and between 23.57 and 2.88 for *Nostoc* sp. PCC 9025. Thus, both strains of *Nostoc* showed a yellow-greenish color, irrespective of the growth conditions, although *Nostoc* sp. PCC 9104 turned a stronger bluish-greener color. In both strains, the response of a^* to the age of the culture was similar to that reported for L^*, with a significant decrease up to the 10th day of culture for *Nostoc* sp. PCC 9104, and up to the 12th day for *Nostoc* sp. PCC 9025, followed by stabilization of values (Figure 4). With respect to b^*, a significant and notable difference in values corresponding to non-diazotrophic cultures from the diazotrophic cultures was observed for *Nostoc* sp. PCC 9104 from the second day onwards, while in the case of *Nostoc* sp. PCC 9025, the difference was between the nutrient-deficient culture and non nutrient-deficient cultures. The b^* values of the samples growing on the nitrate-containing medium ranged from 1.30 to 21.88 for *Nostoc* sp. PCC 9104, and between 2.88 and 10.87 for *Nostoc* sp. PCC 9025, indicating that such samples were bluer than those growing on nitrate-free media, which

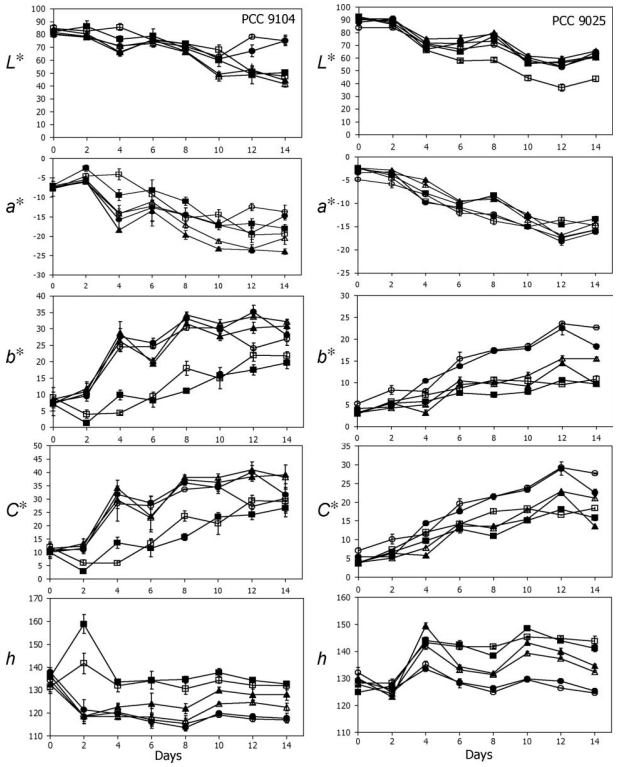

Figure 4. CIELAB color data. Values of L^* (lightness), a^* (redness-greenness changes), b^* (yellowness-blueness changes), C^* (chroma or saturation) and h (hue or tone) in aerated batch cultures of *Nostoc* sp. PCC 9104 (left) and *Nostoc* sp. PCC 9025 (right). -■- = non-diazotrophic medium BG-11, -▲- = diazotrophic medium $BG\text{-}11_0$, -●- = modified diazotrophic medium $BG\text{-}11_0/10$ under high light intensity (open symbols) and low light (solid symbols). Data points represent the average of three replicates; vertical bars represent the SD.

exhibited the highest *b** values (between 7.22 and 35.22 for *Nostoc* sp. PCC 9104, and between 4.15 and 23.57 for *Nostoc* sp. PCC 9025) (Table 3). Regarding the chroma or saturation of the samples, in both strains, the results for *C** showed a similar pattern to those observed for *b**, with values ranging between 2.94 and 41.00 CIELAB units for *Nostoc* sp. PCC 9104 and between 3.71 and 29.30 CIELAB units for *Nostoc* sp. PCC 9025.

Hue angle (h) varied significantly in *Nostoc* sp. PCC 9104 at the second day of culture in all growth conditions, with increasing values in non-diazotrophic medium and decreasing values in diazotrophic and modified diazotrophic media; from the second day in the case of non-diazotrophic medium, the *h* values returned to the initial values and remained stable until the end of the experiment (Figure 4). The initial increase, which was greater in non-diazotrophic medium under low light intensity (Figure 4), appeared to reflect the sharp change in appearance (color and density) that the culture underwent on the second day (Figure 3). In *Nostoc* sp. PCC 9025, significant changes in non-diazotrophic cultures began from the fourth day, whereas they began on the second day in the diazotrophic cultures (Table 3). However, there was no acute change during the experiment (Figure 4).

The effects of light intensity on the value of CIELAB color parameters are shown in Table 4. In the case of *Nostoc* sp. PCC 9104, differences in light intensity only gave rise to differences in *b**, *C**, and *h* when this strain was grown in non-diazotrophic medium and in *C** when it was grown in modified diazotrophic medium. In the case of *Nostoc* sp. PCC 9025, differences in light intensity gave rise to significant differences in all CIELAB parameters, on diazotrophic medium, and only in *L** and *h* on non-diazotrophic medium.

Differences in the composition of the culture medium had significant effects on the CIELAB color parameters (Table 4). The changes in color of the strains in response to nutritional status differed: in *Nostoc* sp. strain PCC 9025, growth on modified diazotrophic medium gave rise to significant differences in most of the CIELAB color parameters, while in *Nostoc* sp. strain PCC 9104, the non-diazotrophic medium resulted in highly significant differences.

Correlations between pigment content and CIELAB color parameters

Spearman correlation coefficients were calculated to evaluate relationships between pigment contents and CIELAB color parameters (Table 5). All CIELAB parameters, except h, were correlated [(**), $p < 0.01$] with all pigment concentrations (chl *a*, carotenoids, PCs) in both strains, and were more closely correlated in *Nostoc* sp. strain PCC 9104 than in strain PCC 9025. Moreover, there was a closer correlation between carotenoid concentration and CIELAB color parameters than between either chl *a* or PCs, and CIELAB color parameters. The Spearman correlation coefficients revealed that the increase in pigment content led

Table 5. Bivariate Spearman's correlation matrix among pigment contents and CIELAB color parameters for *Nostoc* sp. strains PCC 9104 and PCC 9025.

	PCs	Chl *a*	Carotenoids	*L**	*a**	*b**	*C**	*h*
Nostoc sp. PCC 9104								
PCs	1.000							
Chl *a*	0.686**	1.000						
Carotenoids	0.631**	0.941**	1.000					
*L**	−0.689**	−0.836**	−0.833**	1.000				
*a**	−0.608**	−0.798**	−0.816**	0.891**	1.000			
*b**	0.262**	0.538**	0.597**	−0.668**	−0.819**	1.000		
*C**	0.360**	0.621**	0.671**	−0.745**	−0.897**	0.983**	1.000	
h	0.305**	0.079	−0.006	0.022	0.146	−0.626**	−0.508**	1.000
Nostoc sp. PCC 9025								
PCs	1.000							
Chl *a*	0.586**	1.000						
Carotenoids	0.610**	0.876**	1.000					
*L**	−0.603**	−0.800**	−0.844**	1.000				
*a**	−0.598**	−0.735**	−0.825**	0.913**	1.000			
*b**	0.452**	0.545**	0.670**	−0.687**	−0.883**	1.000		
*C**	0.529**	0.643**	0.762**	−0.811**	−0.962**	0.970**	1.000	
h	0.383**	0.518**	0.401**	−0.551**	−0.315**	−0.069	0.102	1.000

$n = 144$; significance level $^{**}p < 0.01$. PCs = phycocyanin concentration; Chl *a* = chlorophyll *a* concentration; Carotenoids = carotenoid concentration; *L**, *a**, *b**, *C**, *h* = CIELAB color parameters.

to a significant decrease in L^* and a^* values and a significant increase in b^* and C^* values.

Discussion

Previous studies have shown that the color of epilithic cyanobacterial biofilms growing on rocky substrata changes as the biofilm develops and that the directions in which the color parameters move in the CIELAB space indicate whether the population is developing or aging (Prieto et al. 2002, 2005). This was considered in further detail in the present study, and the relationship between color and pigments such as chlorophyll (green), phycocyanins (blue), and carotenoids (orange) was investigated. Moreover, since growth and pigment production are affected by environmental conditions, different culture conditions were employed in order to cover a wider range of color so that differences in color could be analyzed and relationships established.

The experimental design enabled significant differences in the appearance of the cultures to be observed, and their color characterized objectively. The results confirmed the original hypotheses: (a) color, as pigment content, is a changing characteristic related to environmental parameters, and (b) there is a close relationship between pigment production and color of the microorganisms.

The same optimal range of growth was observed for both strains of cyanobacteria tested, in terms of the presence of nitrates and availability of nutrients. In contrast, the effect of light intensity differed: low intensity favored growth of strain PCC 9104, and high intensity favored growth of strain PCC 9025. Assessment of the optimal conditions for growth was made by assessing the concentrations of pigments. However, the results obtained showed that values of CIELAB color parameters could have been employed for the same purpose, as the concentration of each pigment was correlated with each CIELAB color parameter, except for h; thus when the pigment content increased, b^* and C^* increased, and L^* and a^* decreased (Table 5). However, not all CIELAB color parameters are equally sensitive to changes in pigment concentrations. Thus, a^* moved to negative values (the culture became greener) as the culture aged (Figure 4) and pigment content increased (Figure 2), but did not respond to the differences in concentrations of chl *a*, PCs, and carotenoids that occurred from the 10th day among cultures (Figure 2). L^* appears to be most informative parameter since, besides being the CIELAB color parameter most closely related to each pigment studied (Table 5), it reflects the changes in pigment concentrations due to the different environmental conditions considered (Figures 3 and 4).

The increase in the concentration of chl *a*, PCs, and carotenoids throughout the experiment was reflected in the increase in parameters b^* and C^*. Moreover, as expected, both parameters provided important information about the amount of PCs in relation to the amount of the other pigments studied (carotenoids + chl *a*). Proof of this is that the evolution of b^* and C^* was different on the second and fourth days for both strains growing on nitrate cultures. On these days, the b^* and C^* values for *Nostoc* sp. PCC 9025 hardly changed relative to the culture growing on the other media (Δb^* and ΔC^* under 10 CIELAB units); however, in *Nostoc* sp. PCC 9104 there was an acute difference between nitrate-containing cultures and culture without nitrate. Thus although the values of b^* and C^* increased sharply (cultures became more yellow) in cultures without nitrate, they decreased (cultures became more blue) on the second and fourth days in nitrate-containing cultures under high light intensity and only on the second day in nitrate-containing cultures under low light intensity (Figure 4). These variations are reflected in the variations in the ratio between PCs and carotenoids + chl *a* for both strains (data not shown). It can be deduced that the increase in the concentrations of PCs, with the concomitant increase in the blue color of the organisms is revealed by the b^* and C^* values.

Although h is correlated with each pigment in *Nostoc* sp. PCC 9025 and with chl *a* concentration in *Nostoc* sp. PCC 9104 (Table 5), the correlation coefficients are too low to establish any relationship between pigments and the CIELAB color parameter. However, the constant surveillance to which cultures were subjected, together with analysis of the h values enabled this parameter to be related to changes in the appearance of the cultures (color and density) since the most important change in appearance occurred between day 2 and day 4 in PCC 9025 and day 0 and day 2 in PCC 9104, for all conditions analyzed, and on the second day the appearance of the PCC 9104 cultures growing in media with nitrate was quite different from the cultures growing in media without nitrate (Figure 3). These changes are clearly reflected in the h values (Figure 4). This is consistent with the findings of other authors, considering h angle as the color parameter most closely related to human color perception (Wyszecky and Stiles 1982; Martínez-Verdú 2002).

It is important to note that while differences in pigment contents were most notable from the eighth day, differences in CIELAB color parameters occurred earlier, which indicates that color quantification provides information not only on pigment production but also on changes in appearance. The color data recorded in this work indicate the area of CIELAB space in which both strains define their color, with

maximum values as follows: L^*: 86.34, a^*: −2.50, b^*: 35.22, C^*: 41.00, and h: 158.80° for *Nostoc* sp. PCC 9104 and L^*: 92.39, a^*: −2.28, b^*: 23.57, C^*: 29.30, and h: 149.43° for *Nostoc* sp. PCC 9025, and minimum values as follows: L^*: 41.47, a^*: −23.92, b^*: 1.30, C^*: 2.94, and h: 113.60° for *Nostoc* sp. PCC 9104 and L^*: 36.85, a^*: −18.18, b^*: 2.88, C^*: 3.71, and h: 123.14° for *Nostoc* sp. PCC 9025. This is the first time that objective color values of different species of cyanobacteria growing in different environmental conditions have been obtained, and is a first approximation to the definition of the color gamut of cyanobacteria, which is essential information for the development of any color-based methodology for monitoring cyanobacterial growth.

Conclusions

The results of the present study demonstrate that *Nostoc* sp. strain PCC 9104 and *Nostoc* sp. strain PCC 9025 respond in different ways in terms of color and pigment production to environmental conditions such as light intensity, macronutrient limitation, and availability of nitrates. While PCC 9104 is more strongly affected by nutrient limitations, the presences of nitrate together with high light intensity are the factors that determine growth of strain PCC 9025. Moreover, the effect of these factors was only observed from the eighth day of culture. The color of the strains differed throughout the experiment; PCC 9104 was lighter and more chromatic than PCC 9025.

CIELAB color parameters were correlated with the chl *a*, carotenoid and PC contents so that variations in pigment contents were reflected by variations in color. Each CIELAB color parameter adequately described a specific aspect of the development of the two *Nostoc* strains. L^*, and to a lesser extent a^*, was related to the chl *a*, PC, and carotenoid concentrations; b^* and C^* were related to the concentration of PCs, and h, which refers to the dominant wavelength, reflected the changes in appearance of the cultures, ie changes in color and density, and this parameter represents the major color perception attribute.

Analysis of cyanobacterial color in relation to a set of environmental conditions is a useful method to study growth thereby enabling the relationships between color and other physiological properties to be established. It should also provide useful information needed to develop the method of quantification for early detection of epilithic biofilms on rocky substrata. However, it must be stressed that the conclusions are based on data for two samples cultured for only a short period of time. Future research in this field will focus on the study of communities forming biofilms subjected to different environmental conditions in the field.

Acknowledgments

The present study was financed by the Spanish Ministry of Science and Education (MEC, BIA2006-02233/BES-2007-16996). The authors thank Prof. Dr A. Otero for her discussion and constructive suggestions for this work.

References

Bartual A, Lubian LM, Galvez JA, Niell FX. 2002. Effect of irradiance on growth, photosynthesis, pigment content and nutrient consumption in dense cultures of *Rhodomonas salina* (Wislouch) (Cryptophyceae). Cienc Mar 28:381–392.

Bell RA, Sommerfeld MR. 1987. Algal biomass and primary production within a temperature zone sandstone. Am J Bot 74:294–297.

Bennet A, Bogoard L. 1973. Complementary chromatic adaptation in a filamentous blue-green alga. J Cell Biol 58:419–435.

Berns RS. 2000. Billmeyer and Saltzman's principles of color technology. 3rd ed. New York: John Wiley & Sons.

Collier JL, Grossman AR. 1992. Chlorosis induced by nutrient deprivation in *Synechococcus* sp. strain PCC 7942: not all bleaching is the same. J Bacteriol 174:4718–4726.

Crispim CA, Gaylarde PM, Gaylarde CC, Neilan BA. 2006. Deteriogenic cyanobacteria on historic buildings in Brazil detected by culture and molecular techniques. Int Biodeterior Biodegr 57:239–243.

Duke CS, Allen MM. 1990. Effects of nitrogen starvation on polypeptide composition, ribulose-1,5-bisphosphate carboxylase/oxygenase, and thylakoid carotenoprotein content of *Synechocystis* sp. strain PCC6308. Plant Physiol 94:752–759.

Fernandez-Valiente E, Leganés F. 1989. Regulatory effect of pH and incident irradiance on the levels of nitrogenase activity in the cyanobacterium *Nostoc* UAM205. J Plant Physiol 135:623–627.

Gorbushina AA. 2007. Life on the rocks. Environ Microbiol 9:1613–1631.

Grondona I, Monte E, Rives V, Vicente MA. 1997. Lichenized association between *Septonema tormes* sp. nov., a coccoid cyanobacterium, and a green alga with an unforeseen biopreservation effect of Villamayor sandstone at Casa Lis of Salamanca, Spain. Mycol Res 101:1489–1495.

Jonte L, Rosales N, Briceño B, Morales E. 2003. La irradiancia y la salinidad modulan el crecimiento de la cianobacteria *Synechocystis minuscula* en cultivos discontinuos. Multiciencias 3:7–14.

Lonneborg A, Lind LK, Kalla SR, Gustafsson P, Oquist G. 1985. Acclimation processes in the light-harvesting system of the cyanobacterium *Anacystis nidulans* following a light shift from white to red light. Plant Physiol 78:110–114.

Loreto C, Rosales N, Bermúdez J, Morales E. 2003. Producción de pigmentos y proteínas de la cianobacteria *Anabaena* PCC 7120 en relación a la concentración de nitrógeno e irradiancia. Gayana Bot 60:83–90.

Martín-Trillo M. 1995. Afloramientos masivos (blooms) de cianobacterias en los arrozales valencianos: seguimiento de su desarrollo y caracterización de dos estirpes formadoras [PhD Dissertation]. Universidad Autónoma de Madrid, Spain: Ciencias Biológicas.

Martínez-Verdú F. 2002. Revisión de los aspectos cromáticos sobre la captura de imágenes (II). Óptica Pura Aplic 35:61–75.

McNamara CJ, Mitchell R. 2005. Microbial deterioration of historic stone. Front Ecol Environ 3:445–451.

Prieto B, Rivas T, Silva B. 2002. Rapid quantification of phototrophic microorganisms and their physiological state through their colour. Biofouling 18:229–236.

Prieto B, Silva B, Aira N, Laiz L. 2005. Induction of biofilms on quartz surfaces as a means of reducing the visual impact of quartz quarries. Biofouling 21:237–246.

Prieto B, Sanmartín P, Aira N, Silva B. 2010. Color of cyanobacteria: some methodological aspects. Appl Optics 49:2022–2029.

Ramírez M, Hernández-Mariné M, Novelo E, Roldán M. 2010. Cyanobacteria-containing biofilms from a Mayan monument in Palenque, Mexico. Biofouling 26:399–409.

Raps S, Wyman K, Siegelman HW, Falkowski PG. 1983. Adaption of the cyanobacterium *Microcystis aeruginosa* to light intensity. Plant Physiol 72:829–832.

Raven J. 1984. A cost-benefit analysis of photon absorption by photosynthetic unicells. New Phytol 98:593–625.

Rippka R, Deruelles J, Waterbury JB, Herdman M, Stanier RY. 1979. Genetic assignments, strain histories and properties of pure cultures of cyanobacteria. J Gen Microbiol 111:1–61.

Saiz-Jimenez C, Hermosin B, Ortega-Calvo JJ, Gómez-Alarcón G. 1991. Aplication of analytical pyrolysis to the study of stony cultural properties. J Anal Appl Pyrol 20:239–251.

Satapathy DP, Adhikary SP. 1993. Epilithic algae from temple walls and caves at Brubaneswar, Puri and Konark. Phykos 32:17–20.

Silva B, Prieto B. 2004. Deteriorative effects of lichens on granite monuments. In: Clair LL, Mark RD, editors. Biodeterioration of stone surfaces: lichens and biofilms as weathering agents of rocks and cultural heritage. Dordrecht, The Netherlands: Kluwer Academic Publishers. p. 69–77.

Silva B, Rivas T, Prieto B. 1999. Effects of lichens on the geochemical weathering of granitic rocks. Chemosphere 39:379–388.

Stebvens WA, Spurdon C, Onyon LJ, Stirpe F. 1981. Effect of inhibitors of protein synthesis from plants on tabacco mosaic virus infection. Experientia 37:257–259.

Tandeau de Marsac N. 1977. Ocurrence and nature of chromatic adaptation in cyanobacteria. J Bacteriol 130:82–91.

Thornbush MJ. 2008. Grayscale calibration of outdoor photographic surveys of historical stone walls in Oxford, England. Col Res Appl 33:61–67.

Völz HG. 2001. Industrial color testing. Weinheim: Wiley–VCH.

Warscheid T, Braams J. 2000. Biodeterioration of stone: a review. Int Biodeterior Biodegr 46:343–368.

Wellburn AR. 1994. The spectral determination of chlorophylls *a* and *b*, as well as total carotenoids, using various solvents with spectrophotometers of different resolution. J Plant Physiol 144:307–313.

Wollenweider RA. 1969. A manual on methods for measuring primary production in aquatic environments. IBP Handbook. No. 12. Oxford, England: Blackwell Scientific Publishers.

Wyman M, Fay P. 1986. Underwater light climate and the growth and pigmentation of planktonic blue-green algae (Cyanobacteria). I. Influence of light quantity. Proc R Soc Lond 227:367–380.

Wyszecki G, Stiles WS. 1982. Color science. Concepts and methods, quantitative data and formulae. New York: John Wiley and Sons.

Chapter 5*. Color measurements as a reliable method for estimating chlorophyll degradation to phaeopigments

Sanmartín, P.; Villa, F.; Silva, B.; Cappitelli, F.; Prieto, B.

Biodegradation 22 (4): 763-771 (2011)

JCR index (IF) 2010 = 2.012 (77/160, 48 percentile in Biotechnology and Applied Microbiology)

Total number of times cited: 5

* This article was ranked one of the top 20 articles published on the same topic (domain of article 20425659) since its publication (2011). BioMedLib, "Who Is Publishing in My Domain?". April 15, 2012.

Biodegradation (2011) 22:763–771
DOI 10.1007/s10532-010-9402-8

ORIGINAL PAPER

Color measurements as a reliable method for estimating chlorophyll degradation to phaeopigments

P. Sanmartín · F. Villa · B. Silva · F. Cappitelli · B. Prieto

Received: 20 April 2010 / Accepted: 3 August 2010 / Published online: 17 August 2010

Abstract The application of biocides is a traditional method of controlling biodecay of outdoor cultural heritage. Chlorophyll degradation to phaeopigments is used to test the biocidal efficacy of the antimicrobial agents. In the present study, the usefulness of color measurements in estimating chlorophyll degradation was investigated. An aeroterrestrial stone biofilm-forming cyanobacterium of the genus *Nostoc* was chosen as test organism, comparing its different behaviour in both planktonic and biofilm mode of growth against the isothiazoline biocide Biotin T®. Changes in $A_{435\ nm}/A_{415\ nm}$ and $A_{665\ nm}/A_{665a\ nm}$ and in the chlorophyll *a* and adenosine triphosphate (ATP) cell content were compared with the variations in the CIELAB color parameters (L*, a*, b*, C^*_{ab} and h_{ab}). Our findings showed that both the phaeophytination indexes are useful in describing degradation of chlorophyl *a* to phaeopigments. Moreover, the CIELAB color parameters represented an effective tool in describing chlorophyll degradation. L* CIELAB parameter appeared to be the most informative parameter in describing the biocidal activity of Biotin T® against *Nostoc* sp. in both planktonic and biofilm mode of growth.

Keywords Chlorophyll · Phaeophytination · Non-destructive methods · CIELAB color measurements · Biocide

P. Sanmartín (✉) · B. Silva · B. Prieto
Departamento de Edafología y Química Agrícola. Fac. Farmacia, Universidad de Santiago de Compostela, 15782 Santiago de Compostela, Spain
e-mail: patricia.sanmartin@usc.es

F. Villa · F. Cappitelli
Dipartimento di Scienze e Tecnologie Alimentari e Microbiologiche, DISTAM, Università degli Studi di Milano, Via Celoria 2, 20133 Milano, Italy

Introduction

It is widely recognised that all the cultural heritage, defined as the totality of tradition-based creations of a cultural community (UNESCO 2000), exposed to open air is susceptible to biodeterioration, the undesirable change in the properties of a material caused by the activities of organisms (Hueck 1965). Phototrophs, like algae and cyanobacteria, are pioneer microorganisms able to readily colonize outdoor surfaces and develop biofilms, which, in turn, causes aesthetic, chemical and physical decay. Microbial abatement is commonly achieved using biocides (Cappitelli et al. 2009; De Saravia et al. 2008; Fonseca 2009; Gladis et al. 2010; Young et al. 2008).

The effectiveness of biocides towards phototrophic organisms can be tested as the degree of chlorophyll degradation (Silkina et al. 2009; Underwood and Paterson 1993). When chlorophyll degrades, it forms a series of degradation products, the nature of which depends on the part of the molecular structure of chlorophyll affected. Chlorophyll molecule consists

of a flat hydrophilic ring-like structure called "porphyrin", which has in the center a magnesium molecule, and a lipid-soluble hydrocarbon phytol, "tail". If the degradation causes the loss of the magnesium from the center of the molecule, the resulting molecule is termed *phaeophytin*, while if the degradation causes the loss of the phytol tail, the former molecule is *chlorophyllide*. Further degradation of either *phaeophytin* or *chlorophyllide* produces *phaeophorbide*: phaeophytin is degraded by the loss of the phytol tail and a chlorophyllide loses its magnesium ion (Fig. 1). The three degradation products of chlorophyll: *phaeophytin*, *chlorophyllide* and *phaeophorbide* are called phaeopigments.

Although the measurement of chlorophyll degradation to phaeopigments has been well investigated in lichens (Barnes et al. 1992; Manrique et al. 1989; Pisani et al. 2007; Ronen and Galun 1984) and aquatic bryophytes (Lopez et al. 1997; Martínez-Abaigar and Núñez-Olivera 1998; Martínez-Abaigar et al. 2008), knowledge about this process is currently very limited in algae and cyanobacteria (Agrawal 1992; Louda et al. 1998). In all these studies, the ratio of absorbances at 435 and 415 nm (A_{435}/A_{415}) was interpreted as the phaeophytinization quotient, which reflects the ratio of chlorophyll to phaeopigments. Similarly, the ratio between A_{665} and A_{665a}, obtained after acidification with hydrochloric acid, was used to indicate phaeophytinization of chlorophyll. In both cases a decrease in that ratio indicates the degradation of chlorophyll to phaeopigments.

However, the spectrophotometric methods are often time- and labor-intensive and require invasive manipulation of the attached microbial community and destructive sample preparation. Furthermore, due to the need of sampling, they can only be applied when the amount of sample is enough to take sample which never occurs before the biofilm is visible to the naked eye. By contrast, on site color measurements do not present these disadvantageous features as they can be applied even before the naked eye detects the presence of biofilm. In fact, they have successfully been applied for quantifying the growth and the physiological state of phototrophic organisms on solid substrata (De Muynck et al. 2009; Dubosc 2000; Escadeillas et al. 2009; Prieto et al. 2002, 2005) and to study the effect of environmental parameters, such as light and nutrients on the pigment content of cyanobacteria (Sanmartín et al. 2010). Since there are relationships between some color parameters and the amount of chlorophyll (Prieto et al. 2002; Sanmartín et al. 2010), relationships between color and chlorophyll degradation should exist. Thus, the main aim of the present work was to investigate whether color measurements could be used as an indicator of chlorophyll degradation in order to develop non-invasive and non-destructive study methodologies which can be applied to the cultural heritage. Furthermore, the validity of both phaeophytinization ratios ($A_{435\ nm}/A_{415\ nm}$ and $A_{665\ nm}/A_{665a\ nm}$) for evaluating the chlorophyll degradation in *Nostoc* sp. PCC 9104 both in planktonic and biofilm lifestyles will be assessed.

Materials and methods

Cyanobacterial strain, medium and antimicrobial agent

Nostoc sp. PCC 9104, a filamentous N_2-fixing heterocyst-forming cyanobacterium was chosen as

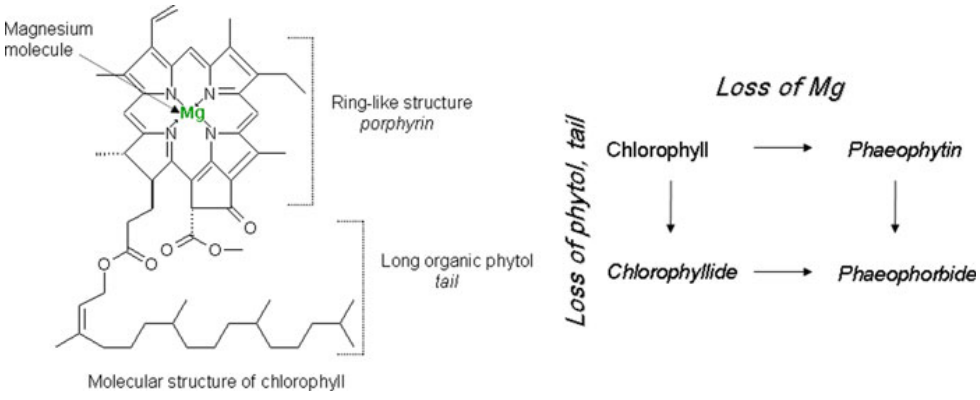

Fig. 1 Molecular structure and degradations pathways of chlorophyll (from Carlson and Simpson 1996, with permission of North American Lake Management Society)

test organism. This strain is an aeroterrestrial specie isolated in Galicia (NW Spain). It has previously been characterised with respect to its growth, pigment content and color (Acea et al. 2001, 2003; Prieto et al. 2002; Sanmartín et al. 2010). PCC 9104 was routinely grown in liquid and solid N-free $BG11_0$ medium (Rippka et al. 1979), at room temperature under sunlight illumination.

A biocide based on *N*-octyl Isothiazolinone (OIT) and quaternary ammonium salt (cationic surfactant), Biotin T® supplied by CTS (Italy), was employed as active antimicrobial agent. A volume of Biotin T® stock solution was added to culture broth for the planktonic experiments or was added to molten culture medium supplemented with Bacto Agar to create a biocide-amended agar for biofilm experiments. The final Biotin T® concentration in both planktonic and biofilm assays was 2% v/v following the recommendations of the commercial supplier. The isothiazoline-based biocide Biotin T® exhibits a broad-spectrum activity against phototrophs and it is often used in buildings (Fonseca 2009; Gladis et al. 2010) and water systems (Batista et al. 2000). It interacts with thiol-groups of amino acids, degrading proteins that play an important role in protecting the organism cells (Collier et al. 1990).

Planktonic culture and biocide susceptibility assay

Logarithmic-phase planktonic culture (1.55 mg L^{-1}) was divided into two equal volumes and Biotin T® was added to one aliquot and an equal volume of water was added to the second aliquot. Both cultures were placed in an orbital shaker at room temperature and sampled at 0, 3, 9, and 24 h. Cells were harvested by centrifugation at 4000*g* for 15 min, rinsed with phosphate-buffered saline (PBS, Sigma-Aldrich, Italy) and resuspended in the buffers. The resulting cell suspension was analysed for color measurements, pigments and ATP contents as reported in detail below. Experiments were performed in triplicate.

Biofilm culture and biocide susceptibility assay

Sub-aerial biofilms of this strain were prepared following the procedure described by Anderl et al. (2000). Fifty microliters of cell suspension (0.32 mg L^{-1}) were used to inoculate sterile black polycarbonate filter membranes (0.22 μm pore size and 25 mm diameter, Millipore, Italy) resting on agar $BG\text{-}11_0$ culture medium (Rippka et al. 1979). Using a sterile forcep, membranes were transferred to fresh agar plates every 3 days. Biomass of 40 days-old mature biofilms was assessed gravimetrically. Mature biofilms were transferred to Biotin T®-containing agar and incubated at room temperature for 24 h. Biofilms were sampled at 0, 3, 9 and 24 h and each membrane-supported biofilm was placed in 2 mL of PBS. Biofilm was dispersed by vortexing at 2,000 rpm for 2 min. The resulting cell suspension was analysed for color measurements, pigments and ATP contents as reported in detail below. Additional control samples were performed using biofilm-free polycarbonate filter membranes. Experiments were performed in triplicate.

Staining, cryosectioning and microscopy

Forty days-old membrane-supported biofilm was stained with the Alexa fluor® 488-labelled Concanavalin A (ConA, Invitrogen, Italy) as per the manufacturer's instructions to study the extracellular polymer substances (EPS). Stained biofilms on polycarbonate membrane filters were covered carefully with a layer of Killik (Bio Optica, Italy) and placed on dry ice until completely frozen. Frozen samples were sectioned at −19°C using a Leitz 1720 digital cryostat (Leica, Italy). The 10-μm thick cryosections were mounted on a poly-L-lysine coated slides (VWR International srl, Italy), examined by fluorescence microscopy using Leica DM 4000 B microscope at a magnification of 400×. Digital images were acquired using the CoolSNAP CF digital camera (Photometrics Roper Scientific, Germany) and elaborated using the Imagej ver. 1.34s software (Rasband 1997–2007, downloaded from http://rsbweb.nih.gov/ij/).

Color measurements

Two millilitres and 0.6 mL of homogeneous cell suspensions from planktonic and biofilm assays, respectively, were filtered under vacuum, through nitrocellulose filter discs (0.22 μm and 25 mm diameter, Millipore, Italy), and reflectance color measurements were taken directly on the still humid filters (Prieto et al. 2010). A Konica Minolta colorimeter with a measuring head CR-300 (8-mm-diameter viewing area) was used. The measuring conditions

were: (a) diffuse illumination geometry with an integration sphere, covered with a white material, so that the light is uniformly diffuse in all directions illuminating the sample, and is observed with the specular component included in 0° (d/0°) in relation to normal, (b) illuminant D65, (c) observer 2°.

A total of five readings were taken at different randomly selected zones on each filter (Prieto et al. 2010). Color measurements were analyzed by considering the CIELAB color system (CIE Publication 15-2 1986), which is organized with three axes in a spherical form: L*, a* and b*. The L* axis is associated with the lightness of the color and moves from top (value: 100, white) to bottom (value: 0, black), whereas the a* and b* axes are associated with changes in redness-greenness (positive a* is red and negative a* is green) and in yellowness-blueness (positive b* is yellow and negative b* is blue); both move in the two axes that form a plane orthogonal to L*, and do not have specific numerical limits. Furthermore, the color parameters most closely related to the psychophysical characteristics of color, i.e., more related to color perception, and which correspond to the angular coordinates of chroma [$C^*_{ab} = (a^{*2} + b^{*2})^{1/2}$] and hue angle [$h_{ab} = \arctan (b^*/a^*)$] were also calculated. C^*_{ab} is the relative strength of a color, chroma or saturation of color, and h_{ab} refers to the dominant wavelength, starts with 0° and increases counterclockwise (Wyszecki and Stiles 1982).

ATP cell content

ATP contents were measured by a luminescence assay employing the luciferine–luciferase-based biomass test kit (Promicol, The Netherlands) with a luminometer Berthold Detection System (R-Biopharm, Italy). ATP was extracted and measured on 200 µL of cell suspension following the instructions of the manufacturer and relative luminescence units were converted to ATP concentrations with the use of a standard ATP curve as previously described by Principi et al. (2006). The values obtained were normalised for dry biomass.

Chlorophyll *a* quantification and phaeophytinization indexes

After color measurements, the cellular lawns deposited on membrane filters were resuspended into 2 mL of dimethylsulfoxide (DMSO, Sigma-Aldrich, Italy) and heated to 65°C for 1 h according to Bell and Sommerfeld 1986. The samples were centrifuged 10 min at 7,000*g* and the supernatant was measured using the 6705 UV/VIS Spectrophotometer (JENWAY, Italy) at 665, 435 and 415 nm. Chlorophyll *a* content was calculated using the equation of Wollenweider (1969). The ratio of absorbances at 435 and 415 nm ($A_{435\ nm}/A_{415\ nm}$), and the ratio of absorbances at 665 and 665a nm obtained after acidification with 100 µl HCl 1 M ($A_{665\ nm}/A_{665a\ nm}$) were used to indicate phaeophytinization of chlorophyll *a* (Martínez-Abaigar and Núñez-Olivera 1998). The values obtained were normalised for dry biomass.

Statistical analyses

Statistical analyses were performed with SPSS (SPSS v17.0 for Windows). Data were subjected to MANOVA at the 5% significant level (p value <0.05) and two-tailed-Bivariate Spearman's correlations.

Results and discussion

The effectiveness of Biotin T® was tested against *Nostoc* sp. PCC 9104 in both planktonic and biofilm mode of growth. The biocide activity of 2% Biotin T® in planktonic biocide susceptibility assays led to the majority of the population being killed within 24 h as demonstrated by the ATP cell content (82% reduction). Chlorophyll *a* content significantly decreased over biocide time exposure (99.8% reduction) following the same trend of ATP (Table 1).

After 40 days of growth as a colony biofilm, *Nostoc* sp. 9104 organisms accumulated to level of 3.70 ± 0.57 mg of dry weight per membrane. Alexa Fluor-labelled Concanavalin A staining was used to investigate the extracellular polymer substances (EPS) (Fig. 2). The fluorescently-labelled ConA mainly accumulated inside the cell-free void of mature microcolonies, demonstrating the presence of the EPS fraction and the growth of a biofilm defined as a complex community embedded in a self-produced polymeric matrix attached to a surface (Costerton 2007). Membrane-supported biofilms method might be an attractive and simple model system for recreating cyanobacterial sub-aerial biofilms. As expected, biofilm retained its relative

Table 1 Values of chlorophyll *a* content, phaeophytination indexes: ($A_{435\ nm}/A_{415\ nm}$ and $A_{665\ nm}/A_{665a\ nm}$), and ATP cell content of *Nostoc* sp. PCC 9104 strain in planktonic state and forming biofilm

	Planktonic assay				Biofilm assay			
Exposure time (h)	0	3	9	24	0	3	9	24
µg chlorophyll *a*/µg biomass	2.84 ± 0.28^{a}	0.62 ± 0.22^{b}	0.12 ± 0.22^{c}	0.01 ± 0.01^{d}	5.78 ± 0.29^{a}	9.07 ± 0.07^{b}	9.64 ± 1.81^{b}	3.91 ± 1.25^{a}
pmol ATP/µg biomass	4.76 ± 1.84^{a}	2.34 ± 0.45^{b}	0.91 ± 0.31^{c}	0.86 ± 0.47^{c}	62.85 ± 16.81^{a}	0.05 ± 0.01^{b}	0.06 ± 0.02^{b}	0.04 ± 0.00^{b}
$(A_{435\ nm}/A_{415\ nm})$/µg biomass	0.39 ± 0.02^{a}	0.31 ± 0.01^{b}	0.33 ± 0.02^{b}	0.31 ± 0.05^{b}	2.73 ± 0.03^{a}	3.02 ± 0.01^{b}	2.87 ± 0.01^{c}	1.93 ± 0.00^{d}
$(A_{665\ nm}/A_{665a\ nm})$/µg biomass	0.65 ± 0.02^{a}	0.32 ± 0.10^{b}	0.20 ± 0.04^{b}	$0.43 \pm 0.18^{a,b}$	1.60 ± 0.10^{a}	1.62 ± 0.04^{a}	1.55 ± 0.05^{a}	1.27 ± 0.02^{b}

Different superscript letters indicate significant differences ($p < 0.05$) between the means of three independent replicates for the values of chlorophyll *a*, both phaeophytination indexes and ATP in planktonic and biofilm assays, in relation to the exposure time to biocide

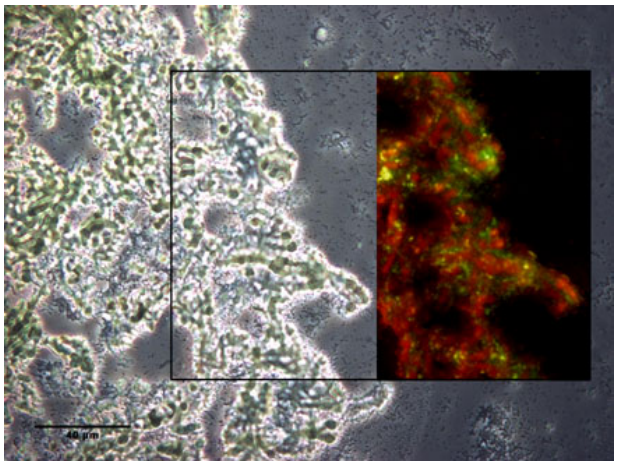

Fig. 2 Bright-field and fluorescence cryosectioning image from *Nostoc* sp. PCC 9104 sub-aerial biofilm. Biofilm matrix was stained in *green* (*bright*) with Alexa fluor® 488-labelled Concanavalin A. The *red* (*dull*) autofluorescence of individual cells showed the total biomass. *Scale bar* represents 40 µm (Color figure online)

resistance to Biotin T® compared to that of its planktonic counterpart after 24 h of treatment. Degradation of chlorophyll *a* occurred by 32% (Table 1). It is well known that biofilms are less susceptible to biocidal agents due to: (a) the barrier properties of the EPS matrix; (b) the physiological state of biofilm organisms and (c) the presence of subpopulations of resistance phenotypes called persisters (Xu et al. 2000; Hall-Stoodley et al. 2004; Costerton 2007). Interestingly, in the biofilm assays, the chlorophyll *a* content increased within 9 h of biocide treatment. Phototrophs may adjust their intracellular concentration of pigments in response to external stress in spite of the energy cost (Ricart et al. 2009). It is worth noting that this behaviour occurred only in the biofilm lifestyle, suggesting a better response to external stress. The ATP cell contents were not correlated with the chlorophyll *a* degradation and probably underestimated because the ATP extraction and detection were strongly hindered by the presence of the EPS matrix. In contrast, DMSO treatment used in the pigment extraction protocol disrupting polymer chain aggregation in EPS polysaccharides (Herasimenka et al. 2008) might improve cell release from biofilm and lysis leading to an efficient recovery of chlorophyll *a*. The colorimetric measurements showed that the biocidal activity of Biotin T® against both *Nostoc* sp. planktonic and biofilm lifestyles

Table 2 Values of CIELAB color parameters (L*, a*, b*, C^*_{ab}, h_{ab}) of *Nostoc* sp. PCC 9104 strain in planktonic state and forming biofilm

	Planktonic assay				Biofilm assay			
Exposure time (h)	0	3	9	24	0	3	9	24
L*	58.21 ± 2.92^{a}	71.37 ± 5.77^{b}	79.86 ± 3.38^{c}	85.17 ± 2.77^{d}	60.51 ± 6.32^{a}	60.68 ± 7.33^{a}	62.04 ± 0.42^{a}	74.06 ± 4.78^{b}
a*	-20.23 ± 1.29^{a}	-8.14 ± 1.44^{b}	-2.73 ± 0.41^{c}	-0.88 ± 0.17^{d}	-15.09 ± 1.82^{a}	-9.45 ± 0.65^{b}	-5.80 ± 0.60^{c}	-2.39 ± 0.39^{d}
b*	27.03 ± 2.03^{a}	8.72 ± 0.96^{b}	8.49 ± 0.87^{b}	9.96 ± 0.29^{c}	11.78 ± 1.44^{a}	6.70 ± 0.91^{b}	11.76 ± 0.15^{a}	4.35 ± 1.41^{c}
C^*_{ab}	33.77 ± 2.39^{a}	12.04 ± 0.29^{b}	8.94 ± 0.74^{c}	10.00 ± 0.29^{c}	19.15 ± 2.23^{a}	11.63 ± 0.37^{b}	13.12 ± 0.35^{c}	4.98 ± 1.40^{d}
h_{ab}	126.82 ± 0.38^{a}	132.85 ± 8.15^{b}	108.05 ± 4.08^{c}	95.04 ± 0.93^{d}	142.01 ± 1.95^{a}	144.66 ± 5.14^{a}	116.19 ± 2.20^{b}	120.16 ± 5.57^{c}

Different superscript letters indicate significant differences ($p < 0.05$) between the means of three independent replicates (the reported color parameters for each replicate are the mean values of five measurements) for the values of CIELAB color parameters in planktonic and biofilm assays, in relation to the exposure time to biocide

resulted in a significant color change (Table 2). The L* parameter, associated to lightness, increased significantly with the exposure time of biocide. The increase of L* was higher in planktonic assay, with values ranging from 58.21 to 85.17 CIELAB units, whereas biofilm assay had a slighter range of variation between 60.51 and 74.06 CIELAB units. Previous studies evidenced the suitability of L* parameter to estimate the cell population growth (Prieto et al. 2002; Sanmartín et al. 2010), being the decrease in L* close related with the population growth, and its increase with the end of growth. Thus, in both planktonic and biofilm biocide susceptibility assays, cell activity and growth were affected, which could have been followed by a degradation of pigments. This process was more severe in planktonic cells where the reduction of L* parameter was two times higher with respect to biofilm assay (Table 2).

Regarding a*, associated to greenness (−)–redness (+) changes, ranged between −20.23 and −0.88 for planktonic assay, and between −15.09 and −2.39 for biofilm assay. b* values, associated to blueness (−)–yellowness (+) changes, ranged between 27.03 and 8.49 for planktonic assay, and between 11.78 and 4.35 for biofilm assay (Table 2). Thus, application of the biocide gave rise to a decrease in the green and yellow components of the color, being higher in the planktonic culture. The latter indicates a better physiological state (Prieto et al. 2002; Sanmartín et al. 2010) of *Nostoc* sp PCC 9104 forming biofilm at the end of the experiment.

Results for chroma C^*_{ab}, showed a similar pattern to that observed for b*, with values ranging between 33.77 and 8.94 CIELAB units for planktonic assay and between 19.15 and 4.98 CIELAB units for biofilm assay. In both cases *Nostoc* sp. PCC 9104 cells lost chroma in their color.

Hue angle (h_{ab}) of *Nostoc* sp. PCC 9104 cells decreased significantly with the exposure time of biocide, varied in planktonic assay between a yellow–greenish hue (126.82°) and a yellow hue (95.04°); and in biofilm assay between a very slightly bluish green hue (142.01°) and a yellow–greenish hue (120.16°). h_{ab} offered a clear and comprehensive vision of color changes occurred in *Nostoc* sp. PCC 9104 in both planktonic and biofilm biocide susceptibility assays. It described the lower chlorophyll *a* degradation occurred in the biofilm tests.

Table 3 Correlation matrices showing the Pearson coefficients (r) found among the phaeophytination indexes, the chlorophyll *a* content, ATP values and CIELAB color parameters

	Planktonic assay							Biofilm assay						
	Chl *a*	ATP	L*	a*	b*	C^*_{ab}	h_{ab}	Chl *a*	ATP	L*	a*	b*	C^*_{ab}	h_{ab}
$A_{435\ nm}/A_{415\ nm}$	0.615**	0.690**	−0.603**	−0.735**	0.088	0.467	0.541*	0.916**	0.081	−0.676*	−0.408	0.292	0.204	0.317
$A_{665\ nm}/A_{665a\ nm}$	0.727**	0.564*	−0.547*	−0.536*	0.269	0.620**	0.387	0.578*	0.534	−0.613*	−0.697*	0.574	0.613*	0.368

Significance level $*p < 0.05$; $**p < 0.01$

Spearman correlation coefficients were calculated to evaluate relationships among phaeophytination indexes and CIELAB color parameters, chlorophyll *a* and ATP cell contents (Table 3). The statistical analysis revealed that the phaeophytination indexes $A_{435\ nm}/A_{415\ nm}$ and $A_{665\ nm}/A_{665a\ nm}$ were related to chlorophyll *a* content in both planktonic ($r_{435/415}$: 0.615**; $r_{665/665a}$: 0.727** Pearson correlation test) and biofilms tests ($r_{435/415}$: 0.916**; $r_{665/665a}$: 0.578* Pearson correlation test). These findings demonstrated the validity of the phaeophytinization ratios in evaluating the chlorophyll *a* degradation for both *Nostoc* sp. planktonic and biofilm lifestyle. Pearson correlation tests also showed that the L* CIELAB color parameter represents an effective tool in describing chlorophyll degradation as is correlated to both phaeophytinization ratios in both lifestyles. Moreover, a* and C^*_{ab} are correlated to the $A_{665\ nm}/A_{665a\ nm}$ index in both lifestyles.

Conclusions

The suitability of color measurements as a reliable method for estimating chlorophyll degradation to phaeopigments has been stated in this work. The determination of the phaeophytination indexes $A_{435\ nm}/A_{415\ nm}$ and $A_{665\ nm}/A_{665a\ nm}$, which have been proved as useful in describing degradation of chlorophyl *a* to phaeopigments in both *Nostoc* sp. PCC 9104 planktonic and biofilm biocide susceptibility assays, could be substituted by color measurements as there is a closed relation between them and the color parameters. Among the CIELAB parameters L* appeared to be the most informative parameter in describing the biocidal activity of Biotin T® against *Nostoc* sp. in both planktonic and biofilm mode of growth.

The methodology tested in this study will be very useful in those fields where sampling is a critical aspect, as in the field of conservation of works of art, since it will allows to monitorizate the effectiveness of biocides as the degree of chlorophyll degradation to phaeopigment avoiding sampling.

Acknowledgments The present study was financed by Xunta de Galicia (REF: 09TMT014203PR) and Science and Education Ministry of Spain (MEC) (BES-2007-16996). The authors would like to thank Dr Pamela Principi for critically reading this manuscript.

References

Acea MJ, Diz-Cid N, Prieto-Fernandez A (2001) Microbial populations in heated soils inoculated with cyanobacteria. Biol Fertil Soils 33(2):118–125

Acea MJ, Prieto-Fernandez A, Diz-Cid N (2003) Cyanobacterial inoculation of heated soils: effect on microorganisms of C and N cycles and on chemical composition in soil surface. Soil Biol Biochem 35(4):513–524

Agrawal SB (1992) Effect of supplemental UV-B radiation on photosynthetic pigment, protein and glutathione contents in green algae. Environ Exp Bot 32:137–143

Anderl JN, Franklin MJ, Stewart PS (2000) Role of Antibiotic penetration limitation in *Klebsiella pneumoniae* biofilm resistance to ampicillin and ciprofloxacin. Antimicrob Agents Chemother 44:1818–1824

Barnes JD, Balaguer L, Manrique E, Davison AW (1992) A reappraisal of the use of DMSO for the extraction and determination of chlorophyll *a* and *b* in lichens and higher plants. Environ Exp Bot 32:85–90

Batista JF, Pereira RFC, Lopes JM, Carvalho MFM, Feio MJ, Reis MAM (2000) In situ corrosion control in industrial water systems. Biodegradation 11(6):441–448

Bell RA, Sommerfeld MR (1986) Algal biomass and primary production within a temperature zone sandstone. Am J Bot 74:294–297

Cappitelli F, Abbruscato P, Foladori P, Zanardini E, Ranalli G, Principi P, Villa F, Polo A, Sorlini C (2009) Detection and elimination of Cyanobacteria from Frescoes: The case of the St. Brizio Chapel (Orvieto Cathedral, Italy). Microb Ecol 57:633–639

Carlson RE, Simpson J (1996) A coordinator's guide to volunteer lake monitoring methods. North American Lake Management Society, Madison

Collier PJ, Ramsey AJ, Waigh RD, Douglas KT, Austin P, Gilbert P (1990) Chemical reactivity of some isothiazolone biocides. J Appl Bacteriol 69:578–584

CIE Publication 15-2. Colorimetry (1986) CIE Central Bureau, Vienna

Costerton JW (2007) The biofilm primer Springer. Springer, Berlin

De Muynck W, Maury Ramirez A, De Belie N, Verstraete W (2009) Evaluation of strategies to prevent algal fouling on white architectural and cellular concrete. Int Biodeterior Biodegrad 63(6):679–689

De Saravia SGG, Naranjo JDLP, Guiamet P, Arenas P, Borrego SF (2008) Biocide activity of natural extracts against microorganisms affecting archives. Boletin latinoamericano y del caribe de plantas medicinales y aromaticas 7(1):25–29

Dubosc A (2000) Etude du développement de salissures biologiques sur les parements en béton: mise au point d'essais accélérés de viellissement. Laboratoire Matériaux et Durabilité des Constructions. Toulouse (France), INSA

Escadeillas G, Bertron A, Ringot E, Blanc P, Dubosc A (2009) Accelerated testing of biological stain growth on external concrete walls. Part 2: quantification of growths. Mater Struct 42(7):937–945

Fonseca AMD (2009) Avaliação da eficácia de tratamentos convencionais e aplicações alternativas para prevenir a biodeterioração em património cultural. Dissertação de Mestrado em Conservação e Restauro. Departamento de Conservação e Restauro Faculdade de Ciências e Tecnologia, Universidade Nova de Lisboa

Gladis F, Eggert A, Karsten U, Schumann R (2010) Prevention of biofilm growth on man-made surfaces: evaluation of antialgal activity of two biocides and photocatalytic nanoparticles. Biofouling 26(1):89–101

Hall-Stoodley L, Costerton JW, Stoodley P (2004) Bacterial biofilms: from the natural environment to infectious diseases. Nat Rev Microbiol 2(2):95–108

Herasimenka Y, Cescutti P, Sampaio Noguera CE, Ruggiero JR, Urbani R, Impallomeni G, Zanetti F, Campidelli S, Prato M, Rizzo R (2008) Macromolecular properties of cepacian in water and in dimethylsulfoxide. Carbohydr Res 343(1):81–89

Hueck HJ (1965) The biodeterioration of materials as part of hylobiology. Material und Organismen 1(1):5–34

Lopez J, Retuerto R, Carballeira A (1997) D665/D665a index vs. frequencies as indicators of bryophyte response to physicochemical gradients. Ecology 78(1):261–271. Ecological Society of America, USA

Louda JW, Li J, Liu L, Winfree MN, Baker EW (1998) Chlorophyll-*a* degradation during cellular senescence and death. Org Geochem 29(5–7):1233–1251

Manrique E, Redondo EL, Seriña E, Izco J (1989) Estimation of chlorophyll degradation into phaeophytin in *Anaptychia ciliaris* as a method to detect air pollution. Lazaroa 11:141–148

Martínez-Abaigar J, Núñez-Olivera E (1998) Ecophysiology of photosynthetic pigments in aquatic bryophytes. In: Bates JW, Ashton NW, Duckett JG (eds) Bryology for the Twenty-first Century. Maney Publishing and the British Bryological Society, Leeds, pp 277–292

Martínez-Abaigar J, Otero S, Tomás R, Núñez-Olivera E (2008) High-level phosphate addition does not modify UV effects in two aquatic bryophytes. Bryologist 111(3): 444–454

Pisani T, Paoli L, Gaggi C, Pirintsos SA, Loppi S (2007) Effects of high temperature on epiphytic lichens: Issues for consideration in a changing climate scenario. Plant Biosyst 141(2):164–169

Prieto B, Rivas T, Silva B (2002) Rapid quantification of phototrophic microorganisms and their physiological state through their colour. Biofouling 18:229–236

Prieto B, Silva B, Aira N, Laiz L (2005) Induction of biofilms on quartz surfaces as a means of reducing the visual impact of quartz quarries. Biofouling 21(5–6):237–246

Prieto B, Sanmartín P, Aira N, Silva B (2010) Color of cyanobacteria: some methodological aspects. Appl Opt 49: 2022–2029

Principi P, Villa F, Bernasconi M, Zanardini E (2006) Metal toxicity in municipal wastewater activated sludge investigated by multivariate analysis and in situ hybridization. Water Res 40(1):99–106

Ricart M, Barceló D, Geiszinger A, Guasch H, de Alda ML, Romaní AM, Vidal G, Villagrasa M, Sabater S (2009) Effects of low concentrations of the phenylurea herbicide diuron on biofilm algae and bacteria. Chemosphere 76(10):1392–1401

Rippka R, Deruelles J, Waterbury JB, Herdman M, Stanier RY (1979) Generic assignments, strain histories and properties of pure cultures of cyanobacteria. J Gen Microbiol 111:1–61

Ronen R, Galun M (1984) Pigment extraction from lichens with dimethyl sulfoxide (DMSO) and estimation of chlorophyll degradation. Environ Exp Bot 24:239–245

Sanmartín P, Aira N, Devesa-Rey R, Silva B, Prieto B (2010) Relationship between color and pigment production in two stone biofilm-forming cyanobacteria (*Nostoc* sp. PCC 9104 and *Nostoc* sp. PCC 9025). Biofouling 26(5):499–509

Silkina A, Bazes A, Vouve F, Le Tilly V, Douzenel P, Mouget JL, Bourgougnon N (2009) Antifouling activity of macroalgal extracts on *Fragilaria pinnata* (Bacillariophyceae): A comparison with Diuron. Aquat Toxicol 94(4):245–254

Underwood GJC, Paterson DM (1993) Recovery of intertidal benthic diatoms after biocide treatment and associated sediment dynamics. J Mar Biol Assoc UK 73(1):25–45

UNESCO (2000) Unesco to protect masterpieces of the oral and intangible heritage of humanity. http://www.unesco.org/bpi/eng/unescopress/2000/00-48e.shtml

Wollenweider RA (1969) A manual on methods for measuring primary production in aquatic environments. IBP Handbook 12 Davis Co. 213

Wyszecki G, Stiles WS (1982) Color science, concepts and methods, quantitative data and formulae, 2nd edn. Wiley, New York

Xu KD, McFeters GA, Stewart PS (2000) Biofilm resistance to antimicrobial agents. Microbiology 146:547–549

Young ME, Alakomi HL, Fortune I, Gorbushina AA, Krumbein WE, Maxwell I, McCullagh C, Robertson P, Saarela M, Valero J, Vendrell M (2008) Development of a biocidal treatment regime to inhibit biological growths on cultural heritage: BIODAM. Env Geol 56(3–4):631–664

3ª línea de trabajo

Detección y cuantificación de los organismos sobre las construcciones

3rd line of research

Detection and quantification of microorganisms colonizing the surface of buildings and monuments

Chapter 6 .Quantification of phototrophic biomass on rocks: optimization of chlorophyll-a extraction by response surface methodology

Fernández-Silva, I.; Sanmartín, P.; Silva, B.; Moldes, A.; Prieto, B.

Journal of Industrial Microbiology and Biotechnology 38: 179-188 (2011)

JCR index (IF) 2010 = 2.416 (63/160, 39 percentile in Biotechnology and Applied Microbiology)

Total number of times cited: 2

J Ind Microbiol Biotechnol (2011) 38:179–188
DOI 10.1007/s10295-010-0843-1

ORIGINAL PAPER

Quantification of phototrophic biomass on rocks: optimization of chlorophyll-*a* extraction by response surface methodology

I. Fernández-Silva · P. Sanmartín · B. Silva · A. Moldes · B. Prieto

Received: 18 March 2010 / Accepted: 26 July 2010 / Published online: 6 September 2010

Abstract Biological colonization of rock surfaces constitutes an important problem for maintenance of buildings and monuments. In this work, we aim to establish an efficient extraction protocol for chlorophyll-*a* specific for rock materials, as this is one of the most commonly used biomarkers for quantifying phototrophic biomass. For this purpose, rock samples were cut into blocks, and three different mechanical treatments were tested, prior to extraction in dimethyl sulfoxide (DMSO). To evaluate the influence of the experimental factors (1) extractant-to-sample ratio, (2) temperature, and (3) time of incubation, on chlorophyll-*a* recovery (response variable), incomplete factorial designs of experiments were followed. Temperature of incubation was the most relevant variable for chlorophyll-*a* extraction. The experimental data obtained were analyzed following a response surface methodology, which allowed the development of empirical models describing the interrelationship between the considered response and experimental variables. The optimal extraction conditions for chlorophyll-*a* were estimated, and the expected yields were calculated. Based on these results, we propose a method involving application of ultrasound directly to intact sample, followed by incubation in 0.43 ml DMSO/cm^2 sample at 63°C for 40 min. Confirmation experiments were performed at the predicted optimal conditions, allowing chlorophyll-*a* recovery of 84.4 ± 11.6% (90% was expected), which implies a substantial improvement with respect to the expected recovery using previous methods (68%). This method will enable detection of small amounts of photosynthetic microorganisms and quantification of the extent of biocolonization of stone surfaces.

Keywords Chlorophyll-*a* · Incomplete factorial design · Response surface methodology · Stone biofilms · Ultrasonic methods

This article is part of the BioMicroWorld 2009 Special Issue.

I. Fernández-Silva · P. Sanmartín · B. Silva · B. Prieto (✉)
Dpto. Edafoloxía e Química Agrícola, Fac. Farmacia,
Universidade de Santiago de Compostela,
15782 Santiago de Compostela, Spain
e-mail: beatriz.prieto@usc.es

A. Moldes
Dpto. Ingeniería Química. E.T.S. Ingenieros Industriales,
Vigo, Spain

Introduction

Stone surfaces exposed to the open air are inevitably colonized by a variety of organisms, some of which are responsible for biofilm formation. Among them, algae and cyanobacteria have great importance, since they feature an extracellular matrix composed primarily of exopolymers (EPS) which are involved in the formation of the biofilm and in the resistance of biofilms to adverse abiotic conditions [1–4]. Once established, algal-cyanobacterial biofilms are added to by heterotrophic bacteria and fungi, forming a microbial biocenosis [5]. Biofilms are responsible for apparent staining of rocks due to the biogenic pigments of phototrophic organisms [1, 6] and the formation of black patinas [7, 8], and may also affect the physicochemical properties of mineral materials [5]. This process is particularly important when the stone under consideration is the building material of monuments of historic and cultural interest [9–12].

Thus, determining the extent of algal and cyanobacterial colonization is crucial for the study of the deterioration of rocky works of art and for the development of methods to

control their deterioration, as well as for the development of bioreceptivity assays of building materials. Therefore, as a starting point, it is necessary to establish a reliable method for quantifying biocolonization on stone surfaces.

One of the most commonly used biomarkers for quantifying microalgal and cyanobacterial biomass is chlorophyll-*a*, which has been extensively used to estimate photosynthetic growth in water, liquid media, and soil, and to a minor extent for estimating algal biomass in rocky substrata [13–16]. Prieto et al. [17] compared several methods for biomass quantification on stone surfaces, and found that chlorophyll-*a* was a good estimator of biofilm biomass. However, they observed problems in the total extraction of chlorophyll-*a* from stone and obtained a relatively high value as a lower limit of detection, which would prevent early detection of stone biocolonization below this lower limit. These authors suggested that the stone itself impedes total chlorophyll-*a* extraction, and concluded that optimization experiments carried out on stone samples were necessary.

Traditional optimization methods examine a single factor at a time, while fixing all other variables at one level. Their major disadvantage is that these methods do not include the interactive effects among the variables studied. As a consequence, these techniques do not depict the complete effects of the parameters on the response. To avoid this problem, response surface methodology (RSM) was developed by Box and collaborators in the 1950s [18]. RSM is a collection of mathematical and statistical techniques based on the fit of a polynomial equation to the experimental data, which must describe the behavior of a data set with the objective of making statistical predictions. It can be applied when a response is influenced by several variables with the objective of simultaneously optimizing the levels of these variables to attain the best system performance [19]. Response surface designs are useful for modeling a curved quadratic surface to continuous factors. A response surface model can pinpoint a minimum or maximum response inside the factor region. Three distinct values for each factor are necessary to fit a quadratic function, so standard two-level designs cannot fit curved surfaces. Three-level full factorial designs are used, in which factors can take on three values: low, medium or center, and high. Generally, if midpoints or center points are added to a 2^k full factorial design then it will become a 3^k full factorial design, where k is the number of factors. However, the main disadvantage of this design (3^k) is the need for a large number of experimental runs, which produces unwanted high-order interactions, and in addition can be expensive and time consuming. Therefore, designs that present a smaller number of experimental points, such as the Box–Behnken method where the number of experiments required (N) is given by $N = 2k(k - 1) + C_0$, where k is the number of variables and C_0 is the number of center points, are more often used.

In this work, we tried various combinations of mechanical and ultrasonic methods as pretreatments to improve the extraction efficiency of chlorophyll-*a* from stone samples, as this is the primary photosynthetic pigment present in organisms responsible for biofilm formation on building materials. To find the optimal conditions of the three independent variables (sample-to-extractant ratio, temperature, and extraction time) potentially influencing the efficiency of phytopigment extraction with dimethyl sulfoxide (DMSO), we performed a response surface analysis following a Box–Behnken design. Finally, we compare the results achieved by the different pretreatments and discuss the adequacy of these methods for quantification of the extent of biocolonization on rock surfaces.

Materials and methods

Preparation of samples

Experiments were carried out with a mixed culture of the filamentous N_2-fixing heterocyst-forming cyanobacteria strains *Nostoc* PCC 9025, *Nostoc* PCC 9104, and *Scytonema* CCC 9801, grown in $BG11_0$ medium. The mixed inoculum consisted of 0.42 g (dry weight) of each strain per liter of medium. Ten milliliters of mixed culture (equivalent to 12.7 g total dry weight and 90.5 μg chlorophyll-*a*) was sprayed onto the surface of 6 × 6 × 1 cm^3 blocks cut from a granite rock. The blocks were placed in a climatic chamber for 2 days under stationary conditions at 25°C, 95% humidity, and 12 h of light (1,600 lx) to induce biofilm formation before pigment extraction was carried out.

To determine the chlorophyll-*a* content from the culture mixture, five replicate aliquots of 5 ml culture were filtered, and the filters were added to 5 ml DMSO and heated to 65°C for 1 h as described in [17]. After filtration of the samples to remove filter fragments, absorbance of the extracts was measured at 649.1 and 665.1 nm wavelength ($A_{665.1}$ and $A_{649.1}$). The concentration of chlorophyll-*a* (C_a) was calculated using the equation proposed by Wellburn [20]:

$$C_a = 12.47A_{665.1} - 3.62A_{649.1}.$$

Mechanical pretreatment of samples

Three different block pretreatments were assayed to determine the best procedure for complete chlorophyll-*a* extraction (Table 1). For the first method (pretreatment A), 15 inoculated blocks were crushed to obtain fragments no larger than 0.25 cm^3, which were added to DMSO following the protocol described by Prieto et al. [17]. For pretreatment B, 15 inoculated blocks were

Table 1 Independent and dependent variables employed in this study

Sample pretreatment		Nomenclature	
Experiment			
Block crushing		A	
Block crushing and sonication in DMSO (ultrasonic bathing 30 min)		B	
Whole blocks sonication in DMSO (tip ultrasonic generator 2 min 30 s)		C	
Variable	Nomenclature	Units	Variation range
Independent variables			
Extractant/sample (v/v) ratio[a,b] or extractant volume/sample surface[c]	*ES*	ml/cm^{3}[a,b] or ml/cm^{2}[c]	1.39–1.94[a]; 1.67–2.22[b]; 0.28–0.56[c]
Temperature	*T*	°C	30–80
Time	*t*	min	30–90
Variable	Nomenclature	Definition	Variation range
Dimensionless, coded independent variables			
Dimensionless extractant/sample ratio	x_1	(*ES*-1.67)/1.39[a]; (*ES*-1.94)/1.67[b]; (*ES*-0.42)/0.28[c]	(−1, 1)
Dimensionless temperature	x_2	(*T*-55)/40	(−1, 1)
Dimensionless time	x_3	(*t*-60)/30	(−1, 1)
Variable	Nomenclature	Units	
Dependent variables			
Chlorophyll-*a*	y_1	μg	

[a] Pretreatment A

[b] Pretreatment B

[c] Pretreatment C

crushed and introduced into 250-ml glass flaks, DMSO was added, and the flasks were introduced into an ultrasonic bath (Transonic T780, Elma™) filled with enough water to apply ultrasound to the whole of each sample, during 30 min (the water temperature was measured during this process to ensure that no heating was taking place). For pretreatment C, 15 intact inoculated blocks (without crushing) were placed onto Petri plates containing DMSO and sonicated by inserting the narrow tip of an ultrasonic generator (UP200S; Dr Hielscher GmbH) into the extractant. Sonication was for 5 × 30 s (0.5 duty cycle, 60% amplitude), with 30 s breaks to avoid overheating.

Design of experiments

For each pretreatment we performed a Box–Behnken design for three-variable optimization with 13 experimental points plus 2 additional experiments at the central point (three central replicates), to study the influence of the experimental conditions on the extraction yield. (Note that this makes a total of 15 experiments, which in comparison with a 3^3 design with 27 experiments, is more economical and efficient.) The independent variables used in this study and their variation limits are listed in Table 1. *ES* corresponds to the extractant/sample ratio, expressed as volume of DMSO/volume of the sample blocks (v/v) for the crushed samples (pretreatments A and B) and as volume of DMSO/sample surface (cm^2) for the intact blocks (pretreatment C); *T* corresponds to the temperature of extraction (°C); and *t*, to the extraction time (min). The levels of the variable were coded, namely each studied real value was transformed into coordinates inside a scale with dimensionless values proportional to its location in the experimental space. Codification enables the investigation of variables of different orders of magnitude without the greater influencing the evaluation of the lesser [19]. The standardized (coded) dimensionless independent variables employed, having variations limits (−1, 1), were defined as x_1 (coded extractant/sample ratio), x_2 (coded temperature), and x_3 (coded extraction time). The correspondence between coded and uncoded variables was established by linear equations deduced from their respective variation limits (Table 1). The dependent variable considered was chlorophyll-*a*, measured by the variable y_1. After incubation in DMSO at their corresponding conditions, samples were filtered, and the concentration of chlorophyll-*a* was determined, as described before.

Model fitting

To evaluate the importance of the independent factors studied in the extraction of chlorophyll-*a*, for each pretreatment, the experimental data were subjected to analysis of variance (ANOVA). Tests on equality of the different factor levels were performed, and main (linear and quadratic) and interaction (linear by linear) effects were estimated. The main effect of a factor is the change in the average response produced by a change in the level of that factor. The interpretation of the quadratic main effects is analogous to that of the linear main effects; this is, the estimated quadratic main effect is the difference between the medium setting and the average of the low and high settings for the respective factors. Interaction effects exist if the difference in response between the levels of one factor is not the same at all levels of another factor. Replicates at the center point allow estimation of the pure error associated with repetitions. Thus, the sum of the square of residuals (SS_{res}) can be separated into two contributions: the sum of squares due to pure error (SS_{pe}) and the sum of squares due to lack of fit (SS_{lof}). To evaluate the adequacy of the model, a lack-of-fit test was performed. The key idea of this test is that, if the mathematical model is well fitted to the experimental data, the mean of the squares of the lack of fit (MS_{lof}) should reflect only the random errors inherent to the system. Additionally, the mean of the square of the pure error (MS_{pe}) is also an estimate of these random errors, and it is assumed that these two values are not statistically different. Thus, it is possible to use the Fisher distribution (*F*-test) to evaluate whether there is some statistical difference between these two means:

$$MS_{lof} / MS_{pe} \approx F\, v_{lof}, v_{pe},$$

where v_{lof} and v_{pe} are, respectively, the degrees of freedom associated with the lack of fit and the pure error variances. If this ratio is higher than the tabulated value of *F*, it is concluded that there is evidence of lack of fit and that the model needs to be improved [19].

Optimization of experimental variables

Finally, the experimental data were analyzed by the response surface methodology [18] using Statistica software (version 8.0; Stat Soft Inc., Tulsa, OK [http://www.statsoft.com]), which allowed the development of empirical models describing the interrelationship between operational and experimental variables by equations including linear, interaction, and quadratic terms:

$$y = b_0 + b_1x_1 + b_2x_2 + b_3x_3 + b_{12}x_1x_2 + b_{13}x_1x_3 + b_{23}x_2x_3 + b_{11}x_1^2 + b_{22}x_2^2 + b_{33}x_3^2, \quad (1)$$

where *y* is the dependent variable, *b* denotes the regression coefficients (calculated from experimental data by multiple regression using the least-squares method), and *x* denotes the independent variables. This model enabled the prediction of optimal conditions (x_1, x_2, and x_3 values) corresponding to the best extraction yield (maximum y_1).

Influence of concentration on the accuracy of spectrophotometric estimation of chlorophyll-*a*

Chlorophyll-*a* was extracted with DMSO from five aliquots of a mixed culture of the three cyanobacteria (0.24 g of each strain per liter), as described above. Serial dilutions (1, 1/2, 1/4, 1/8, 1/16, 1/32, and 1/64) were made, and the concentration of chlorophyll-*a* of the 35 samples (7 dilutions × 5 replicates) was estimated using the equations proposed by Wellburn [20]. The mathematical relationship between chlorophyll-*a* concentration and dilution factor was determined by regression analysis using the JMP statistical package (version 8.0; SAS Institute, Cary, NC [http://www.jmp.com]). The same analysis was performed with a subset of samples corresponding to the four most diluted cases (1/8, 1/16, 1/32, and 1/64). In each case, the coefficient of determination (R^2) and the 99% confidence interval were calculated.

Results and discussion

Design of experiments

Tables 2, 3, 4 show the set of experimental conditions assayed for the 3^3 Box–Behnken design (expressed in terms of both coded variables and real values), as well as the experimental data obtained for chlorophyll-*a* (y_1). It should be noted that experiments 1–12 allowed the calculation of the regression coefficients, whereas experiments 13–15 were replications at the central point of the design to estimate the influence of experimental error (pure error) and to determine whether quadratic effects should be included.

The most efficient extraction was achieved by crushing the sample blocks followed by ultrasonic bathing (pretreatment B), with subsequent incubation under the following conditions: in 1.94 (v/v) DMSO at 80°C for 90 min.

Optimization of chlorophyll-*a* extraction

Experimental results were employed to construct a second-order model with linear, quadratic, and interaction effects, which can predict the total weight of chlorophyll-*a* extracted (dependent variable) as a function of the extractant/sample ratio, temperature, and extraction time

Table 2 Operational conditions for the factorial design considered in this study, and experimental results for phytopigment extraction achieved after sample crushing (pretreatment A)

Experiment	Independent variables			Dependent variable
	ES (x_1) (v/v)	*T* (x_2) (°C)	*t* (x_3) (min)	y_1 (μg)
1	1.67 (0)	80 (1)	30 (−1)	77.6
2	1.67 (0)	30 (−1)	30 (−1)	56.7
3	1.67 (0)	80 (1)	90 (1)	70.2
4	1.67 (0)	30 (−1)	90 (1)	47.0
5	1.39 (−1)	80 (1)	60 (0)	96.1
6	1.39 (−1)	30 (−1)	60 (0)	49.7
7	1.94 (1)	80 (1)	60 (0)	109.1
8	1.94 (1)	30 (−1)	60 (0)	41.2
9	1.39 (−1)	55 (0)	30 (−1)	45.3
10	1.39 (−1)	55 (0)	90 (1)	70.2
11	1.94 (1)	55 (0)	30 (−1)	57.4
12	1.94 (1)	55 (0)	90 (1)	71.1
13	1.67 (0)	55 (0)	60 (0)	49.4
14	1.67 (0)	55 (0)	60 (0)	67.9
15	1.67 (0)	55 (0)	60 (0)	60.7

Levels for coded dimensionless variables are indicated in brackets

Table 3 Operational conditions for the factorial design considered in this study, and experimental results for phytopigment extraction achieved after sample crushing and ultrasonic bathing (pretreatment B)

Experiment	Independent variables			Dependent variable
	ES (x_1) (v/v)	*T* (x_2) (°C)	*t* (x_3) (min)	y_1 (μg)
1	1.94 (0)	80 (1)	30 (−1)	102.5
2	1.94 (0)	30 (−1)	30 (−1)	61.6
3	1.94 (0)	80 (1)	90 (1)	115.4
4	1.94 (0)	30 (−1)	90 (1)	62.3
5	1.67 (−1)	80 (1)	60 (0)	97.1
6	1.67 (−1)	30 (−1)	60 (0)	53.4
7	2.22 (1)	80 (1)	60 (0)	104.4
8	2.22 (1)	30 (−1)	60 (0)	63.1
9	1.67 (−1)	55 (0)	30 (−1)	59.5
10	1.67 (−1)	55 (0)	90 (1)	79.9
11	2.22 (1)	55 (0)	30 (−1)	72.8
12	2.22 (1)	55 (0)	90 (1)	82.0
13	1.94 (0)	55 (0)	60 (0)	75.0
14	1.94 (0)	55 (0)	60 (0)	90.1
15	1.94 (0)	55 (0)	60 (0)	89.4

Levels for coded dimensionless variables are indicated in brackets

(independent variables). The sums of squares (SS) and *F*-tests associated with the combined linear and quadratic effects and their interactions are presented in Table 5. The mean of squares due to pure error (MS_{pe}) and the mean of squares due to lack of fit (MS_{lof}) were also estimated. In all cases (pretreatments A, B, and C), the ratios MS_{lof}/MS_{pe} were lower than the tabulated value of $F(v_{lof},v_{pe})$, indicating that the model fitness can be considered satisfactory.

Table 4 Operational conditions for the factorial design considered in this study, and experimental results for phytopigment extraction achieved after sonication of the intact block samples without crushing (pretreatment C)

Experiment	Independent variables			Dependent variable
	ES (x_1) (v/cm^2)	*T* (x_2) (°C)	*t* (x_3) (min)	y_1 (μg)
1	0.42 (0)	80 (1)	30 (−1)	88.8
2	0.42 (0)	30 (−1)	30 (−1)	52.7
3	0.42 (0)	80 (1)	90 (1)	67.0
4	0.42 (0)	30 (−1)	90 (1)	68.4
5	0.28 (−1)	80 (1)	60 (0)	71.3
6	0.28 (−1)	30 (−1)	60 (0)	56.4
7	0.56 (1)	80 (1)	60 (0)	69.9
8	0.56 (1)	30 (−1)	60 (0)	58.7
9	0.28 (−1)	55 (0)	30 (−1)	65.6
10	0.28 (−1)	55 (0)	90 (1)	51.2
11	0.56 (1)	55 (0)	30 (−1)	76.1
12	0.56 (1)	55 (0)	90 (1)	78.0
13	0.42 (0)	55 (0)	60 (0)	64.8
14	0.42 (0)	55 (0)	60 (0)	79.2
15	0.42 (0)	55 (0)	60 (0)	90.6

Levels for coded dimensionless variables are indicated in brackets

Table 6 presents estimates of the main (linear and quadratic) and interaction effects. These represent the difference in process performance caused by a change from low (−1) to high (+1) levels of the corresponding factor [21]. Both Student tests (*t*-tests) and their associated probabilities (*P*-values) were used to confirm the significance of the factors studied. Temperature of incubation was the most relevant variable with respect to pretreatment for recovery of chlorophyll-*a* (*T*, $P < 0.05$). Raising the temperature from 30°C to 80°C led to an increase in chlorophyll-*a* extraction, on average, of 39.61, 44.76, and 15.20 μg (after pretreatments A, B, and C, respectively). The *P*-values for the main effects of *ES* and *t* were higher than 0.05, and their corresponding coefficients had very low values in the equations proposed by the coded models. Consequently, these parameters will not have a great influence on the values of y_1. This result contrasts with the observations made in similar studies [22], where it was found that the extraction efficiency of DMSO for epilithic biofilms was greatly influenced by both the ratio of extractant volume to sample weight and extraction time. However, in our case, the volume of DMSO (*ES*) varied within a range that was probably too narrow to have a significant effect, the limits being defined by experimental

Table 5 Results of ANOVA and lack-of-fit tests for pretreatments A, B, and C

Factor	SS	*df*	MS	*F*	*P*
Pretreatment A (crushing)					
ES	38.13	1	38.13	0.44	0.58
ES × *ES*	153.09	1	153.09	1.76	0.32
T	3,137.27	1	3,137.27	36.02	0.03*
T × *T*	252.56	1	252.56	2.90	0.23
t	57.29	1	57.29	0.66	0.50
t × *t*	82.89	1	82.89	0.95	0.43
ES × *T*	116.64	1	116.64	1.34	0.37
ES × *t*	31.63	1	31.63	0.36	0.61
T × *t*	1.17	1	1.17	0.01	0.92
Lack of fit	1,011.52	3	337.17	3.87	0.21
Pure error	174.21	2	87.10		
Total SS	5,070.59	14			$R^2 = 0.77$
Pretreatment B (crushing and ultrasonic bathing)					
ES	131.12	1	131.12	1.80	0.31
ES × *ES*	273.77	1	273.77	3.75	0.19
T	4,007.05	1	4,007.05	54.96	0.02*
T × *T*	39.73	1	39.73	0.54	0.54
t	234.68	1	234.68	3.22	0.21
t × *t*	26.85	1	26.85	0.37	0.61
ES × *T*	1.46	1	1.46	0.02	0.90
ES × *t*	31.49	1	31.49	0.43	0.58
T × *t*	37.13	1	37.13	0.51	0.55
Lack of fit	42.55	3	14.18	0.19	0.89
Pure error	145.82	2	72.91		
Total SS	4,982.84	14			$R^2 = 0.96$
Pretreatment C (sonication without crushing)					
ES	182.60	1	182.60	1.09	0.41
ES × *ES*	224.05	1	224.05	1.34	0.37
T	462.22	1	462.22	2.77	0.24
T × *T*	146.23	1	146.23	0.88	0.45
t	42.91	1	42.91	0.26	0.66
t × *t*	26.07	1	26.07	0.16	0.73
ES × *T*	3.51	1	3.51	0.02	0.90
ES × *t*	65.98	1	65.98	0.40	0.59
T × *t*	350.69	1	350.69	2.10	0.28
Lack of fit	179.05	3	59.68	0.36	0.79
Pure error	333.62	2	166.81		
Total SS	1,975.24	14			$R^2 = 0.74$

* $P < 0.05$; *SS* sum of squares, *df* degrees of freedom, *MS* mean square, R^2 coefficient of determination

constraints. In experiments A and B, the receptacles had to be filled up to a level that covered the crushed blocks with DMSO completely without diluting the phytopigments too much. In experiment C, smaller volumes could be employed, as only the bottom face of the blocks had to be immersed in DMSO, but the volume had to be sufficient to allow introduction of the sonicator tip, and the upper limit was defined by the plate capacity. Anyway, the fact that *ES* did not have a significant effect enables the use of small volumes of extractant and consequently reduces experimental costs. Similarly, a 30 min extraction time was probably long enough to extract the maximum amount of chlorophyll-*a* under the test conditions; as a consequence, no improvement was observed at longer extraction times. Our results show that the problem of chlorophyll-*a* extraction from rock materials cannot be simply overcome by longer extraction periods, enabling the use of shorter incubation times than used by other authors [13, 17, 23].

The regression coefficients for equation Eq. 1 are presented in Table 7. These were used to construct the response surfaces for pretreatments A, B, and C, depicted in Fig. 1. The surfaces illustrate how higher temperatures, mainly, and longer extraction times, to a lesser extent, improved extraction of chlorophyll-*a* in these experiments. Visual inspection of the surfaces reveals the quadratic effects: variables with positive values for the regression coefficients of linear effects and negative coefficients for quadratic effects exhibit a maximum inside the experimental region.

Our model predicts the total weight of chlorophyll-*a* that will be extracted as a function of *ES*, *T*, and *t*. It thus allows determination of the optimum conditions at which maximum extraction will be achieved. Table 8 shows the optimal conditions for extraction of chlorophyll-*a* for pretreatments A, B, and C and also the predicted results, both in terms of total weight of chlorophyll-*a* and extraction yield. The model predicts that, under the optimal conditions, pretreatments A and B will yield the maximum weight of chlorophyll-*a* compared with pretreatment C. However, these values correspond to extraction yields superior to 100%, indicating a systematic error in the estimation of the chlorophyll-*a* concentration derived from the fact that the utilization of crushed blocks necessitates the use of large volumes of extractant, and therefore the total weight of chlorophyll-*a* is estimated from absorbances measured from very dilute solutions. This was corroborated by a complementary experiment in which the relationship between microorganism and chlorophyll-*a* concentration was studied with serial dilutions of a mixed culture with characteristics similar to those used in the optimization experiment. A strong linear relationship between concentrations of microorganism and chlorophyll-*a* was observed when all samples were considered ($R^2 = 0.99$, $P < 0.0001$), but this relationship was weakened when only the most diluted samples were taken into account ($R^2 = 0.85$, $P < 0.0001$) (Fig. 2). Thus, we conclude that the precision of the spectrophotometric method for calculation of chlorophyll-

Table 6 Estimates of main and interaction effects analysis for significant models of chlorophyll-*a* extraction after pretreatments A, B, and C

Factor	Effect (μg)	Pure error	*t*-value	*P*-value	Significance	Regression coeff.[#]
Pretreatment A (crushing)						
Mean/intercept	65.98	2.69	24.49	0.002	**	65.98
ES	4.37	6.60	0.66	0.576		2.18
ES × *ES*	−6.44	4.86	−1.33	0.316		−3.21
T	39.61	6.60	6.00	0.027	*	19.80
T × *T*	−8.27	4.86	−1.70	0.230		−4.14
t	5.35	6.60	0.81	0.503		2.68
t × *t*	4.73	4.86	0.98	0.432		2.37
ES × *T*	10.80	9.33	1.16	0.367		5.40
ES × *t*	−5.62	9.33	−0.60	0.608		−2.81
T × *t*	1.08	9.33	0.12	0.918		0.54
Pretreatment B (crushing and ultrasonic bathing)						
Mean/intercept	79.51	2.46	32.25	<0.001	***	79.51
ES	8.10	6.04	1.34	0.312		4.05
ES × *ES*	8.61	4.44	1.94	0.192		4.30
T	44.76	6.04	7.41	0.018	*	22.38
T × *T*	−3.28	4.44	1.94	0.192		−1.64
t	10.83	6.04	1.79	0.215		5.42
t × *t*	2.70	4.44	0.61	0.606		1.35
ES × *T*	−1.21	8.54	−0.14	0.900		−0.61
ES × *t*	−5.61	8.54	−0.66	0.579		−2.81
T × *t*	6.09	8.54	0.71	0.549		3.05
Pretreatment C (sonication without crushing)						
Mean/intercept	67.00	3.73	17.97	0.003	**	67.00
ES	9.56	9.13	1.05	0.405		4.78
ES × *ES*	7.79	6.72	1.16	0.366		3.89
T	15.20	9.13	1.66	0.238		7.60
T × *T*	6.29	6.72	0.94	0.448		3.15
t	−4.63	9.13	−0.51	0.662		−2.32
t × *t*	2.65	6.72	0.40	0.731		1.33
ES × *T*	−1.87	12.92	−0.15	0.898		−0.94
ES × *t*	8.12	12.92	0.63	0.594		4.06
T × *t*	−18.73	12.92	−1.45	0.284		−9.36

* $P < 0.05$; ** $P < 0.01$; [#] For coded variables

a concentration decreases when samples are much diluted, probably as a consequence of the spectrometer precision per se and the inadequacy of the equations of Wellburn et al. [19] in this range. An additional drawback derived from the use of large volumes of extractant is that there is a lower detection limit (sensitivity) bellow which fewer colonizing organisms cannot be detected [17]. Moreover, the experimental error (intrinsic and derived from device precision) is magnified when chlorophyll-*a* total weight values are inferred from large volumes. All these problems are overcome when chlorophyll-*a* is extracted and quantified from whole blocks, making the quantification of chlorophyll-*a* and the estimation of microbial biomass much more accurate. As a final consideration, this method is more convenient from a practical perspective, since it avoids labor-intensive and time-consuming crushing of rock materials.

Our results predict that direct extraction from whole blocks after ultrasonic treatment (treatment C) will enable extraction yields over 90% for chlorophyll-*a*. To experimentally confirm the prediction of the model, granite blocks were inoculated with 10 ml mixed culture of cyanobacteria of known chlorophyll-*a* content. After 2 days, chlorophyll-*a* was extracted by direct sonication of the intact blocks in 0.43 ml DMSO/cm^2 sample at 63°C for 40 min, which enabled 84.4 ± 11.6% chlorophyll-*a* recovery. Optimization of the sonication conditions (time, intensity, and/or frequency) might eventually improve the efficiency of extraction. To compare the efficacy of this protocol with other methods, we compare our results with

Table 7 Regression coefficients (b_n) and lack-of-fit analysis for the proposed regression models for extraction of chlorophyll-*a* (y_1) from rock biofilms following sample pretreatments A, B, and C

Coefficient	A y_1	B y_1	C y_1
Linear			
b_0	290.11	−455.59	−82.47
b_1	−292.83	473.55	327.27
b_2	−2.00	0.24	2.27
b_3	1.24	0.97	0.56
Quadratic			
b_{11}	83.45	−111.60	−403.82
b_{22}	0.01	0.01	−0.01
b_{33}	−0.01	0.00	0.00
Interaction			
b_{12}	0.78	−0.09	−0.27
b_{13}	−0.34	−0.34	0.97
b_{23}	0.00	0.00	−0.01

those reported by Prieto et al. [17], who applied a procedure similar to pretreatment A, in which they crushed the granite sample blocks and incubated in 0.83 ml DMSO/cm^3 sample (v/v) at 65°C for 1 h, obtaining a 68% extraction yield for the same amount of inoculated chlorophyll-*a*. The method we propose therefore implies a substantial improvement of extraction efficacy compared with previous studies.

Conclusions

From the obtained results it can be concluded that:

(a) The application of ultrasonic methods improved extraction of chlorophyll-*a* from biofilms developed on rocky substrata.

(b) The precision of the spectrophotometric method for calculation of chlorophyll-*a* concentration decreases when samples are highly diluted, thus methods requiring a lower volume of extractant are more convenient.

(c) The temperature of extraction (*T*) is the most important factor (compared with *t* and *ES*) in chlorophyll-*a* extraction from biofilms on rocky substrata.

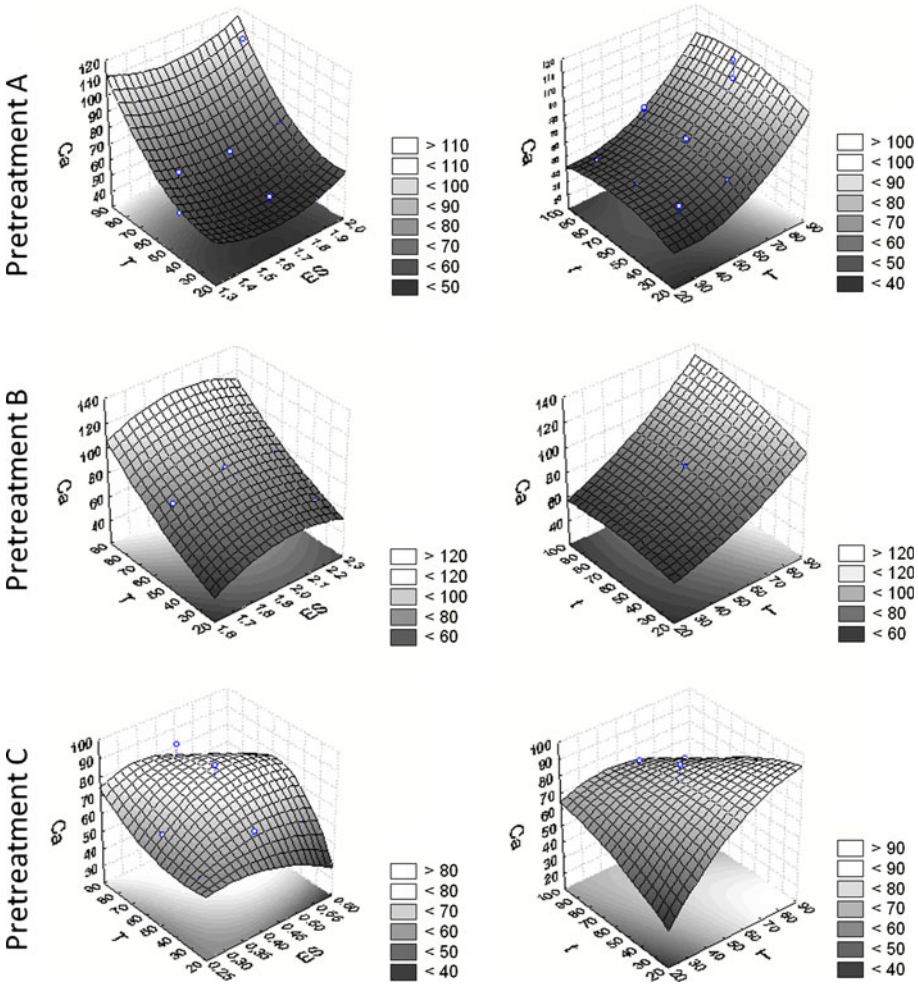

Fig. 1 Response surfaces for pretreatments A, B, and C showing dependence of chlorophyll-*a* (expressed in μg) on extractant-to-sample ratio (*ES*) and temperature (*T*) predicted for samples extracted during 60 min (*left*) and on extraction time (*t*) and temperature (*T*) for samples extracted in 1.67 DMSO:sample (v/v), 1.94 DMSO:sample (v/v) or 0.42 ml/cm^2 (pretreatments A, B, and C, respectively) (*right*)

Table 8 Chlorophyll-*a* recovery predicted by the model after extraction with DMSO under the optimal experimental conditions after pretreatments A, B, and C

	Independent variables			Dependent variables	
	ES ratio[a]	*T* (°C)	*t* (min)	Chlorophyll-*a* total dry weight (μg)	Chlorophyll-*a* extraction yield (%)
Pretreatment A	2.00	80	61	105.77	117
Pretreatment B	1.95	78	90	115.40	128
Pretreatment C	0.43	63	40	82.35	91

[a] Units are ml/cm^3 for pretreatments A and B, and ml/cm^2 for pretreatment C

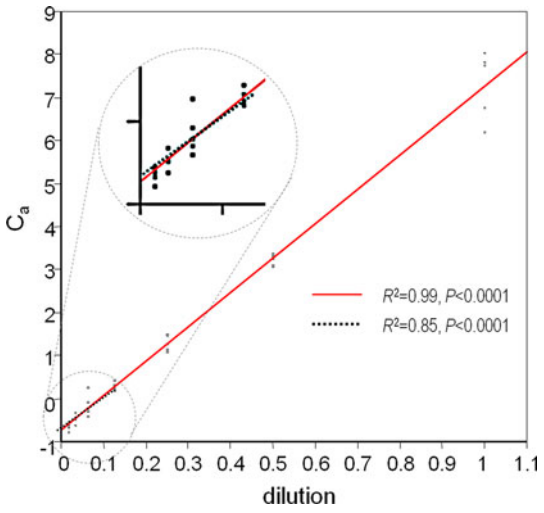

Fig. 2 Regression analysis between microorganism and phytopigment concentration. Chlorophyll-*a* concentration was estimated with the help of Wellburn's equations. Measurements correspond to serial dilutions of a mixed culture of cyanobacteria at 0.72 g dry weight/l (1, 1/2, 1/4, 1/8, 1/16, 1/32, 1/64 dilutions corresponding to 0.72, 0.36, 0.18, 0.09, 0.045, 0.0225, 0.01125 g/l)

Thus, we propose the application of ultrasound directly to uncrushed rock samples followed by incubation in 0.43 ml DMSO/cm^2 sample (vol/surface) at 63°C for 40 min, as an efficient method for chlorophyll-*a* extraction from rock materials, which will allow detection of small amounts of photosynthetic microorganisms and quantification of the extent of biocolonization.

Acknowledgments This work was funded by the Spanish Ministry of Education and Science and the Xunta de Galicia (PGIDIT09TMT014203PR/BES-2007-16996). We are grateful to Javier Rodriguez Grille for his help.

References

1. Urzi CE, Krumbein WE, Warscheid TH (1992) On the question of biogenic colour changes of mediterranean monuments (coatingcrust- microstromatolite-patina-scialbatura-skin-rock varnish), In: Decrouez D, Chamay J, Zezza F (ed) Proceedings second international symposium conservation of monuments in Mediterranean, Basins, Geneva. pp 397–420
2. Costerton JW (1999) The role of bacterial exopolysaccharides in nature and disease (Reprinted from Developments in Industrial Microbiology, vol 26, pp 249–261, 1985). J Ind Microbiol Biotechnol 22(4–5):551–563
3. Albertano P, Moscone D, Palleschi G, Hermosin B, Saiz-Jiménez C, Sánchez-Moral S, Hernández-Mariné M, Urzí C, Groth I, Schroeckh V, Gallon JR, Graziottin F, Bisconti F, Giuliani R (2003) Cyanobacteria attack rocks (CATS): control and preventive strategies to avoid damage caused by cyanobacteria and associated microorganisms in Roman hypogean monuments. In: Saiz-Jiménez C (ed) Molecular biology and cultural heritage. Swets & Zeitlinger, Lisse, The Netherlands, pp 151–162
4. Barberousse H, Tell G, Yéprémian C, Couté A (2006) Diversity of algae and cyanobacteria growing on building facades in France. Algol Stud 120:83–110
5. Gaylarde CC, Morton LHG (1999) Deteriogenic biofilms on buildings and their control: a review. Biofouling 14:59–74
6. Urzi CE, Criseo G, Krumbein WE, Wollenzien U, Gorbushina AA (1993) Are colour changes of rocks caused by climate, pollution, biological growth, or by interactions of the three? In: Thiel M-J (ed) Conservation of stone and other materials, vol 1. E & FN Spon, London, pp 279–286
7. Aira N, Jurado V, Silva B, Prieto B (2007) Gas chromatography applied to cultural heritage. Analysis of dark patinas on granite surfaces. J Chromatogr A 1147:79–84
8. Prieto B, Aira N, Silva B (2007) Comparative study of dark patinas on granitic outcrops and buildings. Sci Total Environ 381(1–3):280–289
9. Saiz-Jimenez C, Garcia-Rowe J, Garcia del Cura MA, Ortega-Calvo JJ, Roekens E, Van Grieken R (1990) Endolithic cyanobacteria in Maastricht limestones. Sci Total Environ 94:209–220
10. Danin A, Caneva G (1990) Deterioration of limestone walls in Jerusalem and marble monuments in Rome caused by cyanobacteria and cyanophilous lichens. Internat Biodet 26:397–417
11. Ortega-Morales O, Guezennec J, Hernandez-Duque G, Gaylarde CC, Gaylarde PM (2000) Phototrophic biofilms on ancient Mayan buildings in Yucatan, Mexico. Curr Microbiol 40(2):81–85
12. Crispim CA, Gaylarde CC (2005) Cyanobacteria and biodeterioration of cultural heritage: a review. Microb Ecol 49:1–9
13. Bell RA, Sommerfeld MR (1987) Algal biomass and primary production within a temperate zone sandstone. Am J Bot 74(2):294–297
14. Nagarkar S, Willians GA (1997) Comparative techniques to quantify cyanobacteria dominated epileptic biofilms on tropical rocky shores. Mar Ecol Prog Ser 154:281–291
15. Yordanov RV, Nicholson K (1997) Effect of hydrocarbons on biofilm development on sandstone. Abstr. SWAPNET'97, the stone weathering and atmospheric pollution network 1997 meeting. Aberdeen, UK
16. Yallop ML, Paterson DM, Wellsbu P (2000) Interrelationships between rates of microbial production, exopolymer production,

microbial biomass, and sediment stability in biofilms of intertidal sediments. Microb Ecol 39(2):116–127
17. Prieto B, Silva B, Lantes O (2004) Biofilm quantification on stone surfaces: comparison of various methods. Sci Total Environ 333:1–7
18. Box GEP, Wilson KB (1954) The exploration and exploitation of response surfaces: some general considerations and examples. Biometrics 10:16–60
19. Bezerra MA, Santelli RE, Oliveira EP, Villar LS, Escaleira LA (2008) Response surface methodology (RSM) as a tool for optimization in analytical chemistry. Talanta 76:965–977
20. Wellburn AR (1994) The spectral determination of chlorophylls a and b, as well as total carotenoids, using various solvents with spectrophotometers of different resolution. J Plant Physiol 144:307–313
21. Haaland PD (1989) Experimental design in biotechnology. Marcel Dekker, New York, NY
22. Devesa R, Moldes A, Díaz-Fierros F, Barral MT (2007) Extraction study of algal pigments in river bed sediments by applying factorial designs. Talanta 72:1546–1551
23. Ariño, X (1996) Estudio de la colonización, distribución e interacción de líquenes, algas y cianobacterias con materiales pétreos de los conjuntos arqueológicos de Baelo Claudia y Carmona. Ph.D. thesis. Universidad de Barcelona and IRNA de Sevilla

Chapter 7. Spectrophotometric color measurement for early detection and monitoring of greening on granite buildings

Sanmartín, P.; Vázquez-Nion, D.; Silva, B; Prieto, B.

Biofouling: The Journal of Bioadhesion and Biofilm Research 28 (3): 329-338 (2012)

JCR index (IF) 2010 = 3.333 (5/92, 5 percentile in Marine and Freshwater Biology; 38/160, 23 percentile in Biotechnology and Applied Microbiology)

Total number of times cited: 0

Biofouling
Vol. 28, No. 3, March 2012, 329–338

Taylor & Francis
Taylor & Francis Group

Spectrophotometric color measurement for early detection and monitoring of greening on granite buildings

P. Sanmartín*, D. Vázquez-Nion, B. Silva and B. Prieto

Departamento Edafología y Química Agrícola, Facultad Farmacia, Universidad de Santiago de Compostela, 15782-Santiago de Compostela, Spain

(*Received 12 January 2012; final version received 1 March 2012*)

This paper addresses the detection and monitoring of the development of epilithic phototrophic biofilms on the granite façade of an institutional building in Santiago de Compostela (NW Spain), and reports a case study of preventive conservation. The results provide a basis for establishing criteria for the early detection of phototrophic colonization (greening) and for monitoring its development on granite buildings by the use of color changes recorded with a portable spectrophotometer and represented in the CIELAB color space. The results show that parameter b* (associated with changes of yellowness-blueness) provides the earliest indication of colonization and varies most over time, so that it is most important in determining the total color change. The limit of perception of the greening on a granite surface was also established in a psycho-physical experiment, as Δb^*: +0.59 CIELAB units that correspond, in the present study, to 6.3 μg of biomass dry weight cm^{-2} and $(8.43 \pm 0.24) \times 10^{-3}$ μg of extracted chlorophyll *a* cm^{-2}.

Keywords: preventive conservation; CIELAB color system; biofouling; greening; monitoring; phototrophic colonization

Introduction

The fouling of stone surfaces by abiotic substances and organisms poses serious problems for the maintenance of all types of buildings. Fouling by microorganisms, known as biofouling, is considered to start with phototrophic organisms (algae and cyanobacteria) conditioning the inert surfaces for subsequent growth of heterotrophic organisms (eg Grant 1982; Ortega-Calvo et al. 1993; Saiz-Jimenez and Ariño 1995; Prieto et al. 2005; Miller et al. 2010). However in the absence of a primary colonizing film of phototrophs, heterotrophic bacteria and fungi can grow on building façades, using organic compounds from organic pollutants, painted surfaces or conservation treatments (eg Cappitelli et al. 2005, 2007). Unlike heterotrophic biofilms, phototrophic biofilms have received little attention until recently (Di Pippo et al. 2009, 2011).

Biofilms that grow in areas exposed to light tend to contain photosynthetic organisms (Ramírez et al. 2010). The presence of these pioneer photosynthetic-based microbial communities generally result in the appearance of thin green films, which usually adhere to the stone substratum (ICOMOS-ISCS 2008) in a phenomenon often referred to as greening. The presence of greening depends on a variety of factors, such as a suitable combination of dampness, warmth and light on the stone surface (Tiano 2002) as well as the intrinsic characteristics of stone, such as permeability, porosity and surface roughness, which influence its bioreceptivity (Guillitte 1995; Prieto and Silva 2005; Miller et al. 2006). Factors such as the exposure site (Barberousse et al. 2006), the presence or absence of adjacent vegetation (Smith et al. 2011) and the urban or rural location (Tanaca et al. 2011) also affect the development of biofouling.

The study of greening on building façades deserves considerable attention because pollution-related soiling has been widely superseded by algal growth. Since the beginning of the twentieth century, when the first data on the aspect of some important buildings were recorded, there has been an apparent decrease in the occurrence of black deposits (Newby et al. 1991; Davidson et al. 2000; Brimblecombe and Grossi 2009), partly because of the decrease in air pollution resulting from the declining use of coal and the switch to gas and electrical heating (Brimblecombe 1987; Grossi and Brimblecombe 2008). At the same time, there has been an increase in biological activity, favored by lower concentrations of sulfur dioxide and greater deposition of organic compounds and nitrogen (Grossi and Brimblecombe 2008). Higher humidity caused by climate change also favors the development of greening

*Corresponding author. Email: patricia.sanmartin@usc.es

ISSN 0892-7014 print/ISSN 1029-2454 online

http://dx.doi.org/10.1080/08927014.2012.673220
http://www.tandfonline.com

as it increases the time that stone structures remain wet and possibly the depth of penetration of moisture. This has already been observed on buildings in places such as Northern Ireland and London, as respectively, an increased incidence of algal greening (Smith et al. 2011) and a decreased incidence of blackening (Brimblecombe and Grossi 2009).

Several authors have demonstrated that the discoloration of stone caused by the growth of microorganisms can be easily determined by a non-invasive (non-destructive) technique based on measurement of the reflectance by a spectrophotometer or a tristimulus colorimeter. The data are expressed in CIE-L*a*b* color system units (Wyszecki and Stiles 1982; Sanmartín et al. 2010). Using this technique, Urzì and Realini (1998) correlated the orange or grey color of the patina on Noto's calcareous sandstone with the associated microflora, Prieto et al. (2005) quantified the development of biofilm induced on the open rock faces of quartz quarries to reduce the visual impact, De Muynck et al. (2009) evaluated strategies for preventing algal fouling on two types of concrete (man-made stone), and more recently Tanaca et al. (2011) evaluated fungal colonization on three fiber cement (man-made stone) formulations exposed to urban, rural and coastal environments. Nevertheless, to the authors' knowledge, the color measurement technique has not previously been used to study the phototrophic colonization (greening) of granite stone buildings naturally exposed to the outdoor environment.

Apart from the chemical and/or physical deterioration of buildings caused by phototrophic-based microbial communities, greening must be considered as aesthetic damage that depends not only on the general conditions of the local environment, but also on the individual perception by the people involved (Smith et al. 2011). In this respect, green is more easily perceived than other colors, since the differences detected by the human eye are not of the same magnitude in the different parts of the spectrum; wavelengths close to 400 (blues) and 700 nm (reds) are less important from the point of view of perception than those around 500 nm. Five hundred and sixty nm (corresponding to the green area) is the wavelength at which the human eye is most sensitive (Gescheider 1976; McDonald 1997). Green has been used for the quantification of biomass of the green alga *Ulva* (syn. *Enteromorpha*) on test panels coated with a range of experimental formulations (Cassé et al. 2007). Knowledge of the threshold of perception of greening by the human eye would be very useful for the effective and sustainable management of stone buildings and monuments. To date, few studies have addressed the human perception of changes in the appearance of stone due to general fouling, and most of the existing studies have investigated the changes in appearance in terms of blackening or darkening (Newby et al. 1991; Andrew 1992; Grossi and Brimblecombe 2004; Brimblecombe and Grossi 2005). As far as the authors are aware, only one laboratory-based study has examined the limits of perception of the phototrophic colonization on building stones (Prieto et al. 2006). In the latter study the qualitative terms, ranging from inappreciable to very intense, referred to the change in appearance caused by the live microorganisms on the surface of granite rocks were related to the total color change (ΔE^*_{ab}). However, variations in the three color parameters, lightness-darkness ΔL^*, redness-greenness Δa^* and yellowness-blueness Δb^*, were not analyzed. In the present study, these variations were taken into account with the aim of selecting the parameter that provides most information regarding the detection and monitoring of greening on granite façades.

Thus, the overall aim of the study was to demonstrate the suitability of a spectrophotometric measurement technique for detecting phototrophic colonization (greening) and real-time monitoring of the development of the colonization in a real case of a granite building. The specific purposes of the study were as follows: (1) to establish the threshold of human perception of greening on granite rock and its value in terms of partial color differences (ΔL^*, Δa^* and Δb^*), amount of phototrophic biomass (dry weight) and extracted chlorophyll *a* (chl *a*) content; (2) to analyze the changes in the L*, a* and b* CIELAB coordinates in a real case involving the cleaning and recolonization of a granite façade, with the aim of determining the parameter or parameters that best indicate the start of the greening process; and (3) to describe a methodology that could be used as a tool for making decisions about the required frequency of cleaning and biocide treatment in a real case.

Materials and methods

The perception of color depends on the incident light and variations in illumination, thus changes in the natural light affect the judgment of the observer about the color observed. For this reason, a visual sorting task used to estimate the threshold of perception of greening by the human eye was carried out in a laboratory test, under standard conditions of illumination. Detection and monitoring of greening were performed outside, since measurements made with a portable spectrophotometer are not affected by external light parameters. Psycho-physical and monitoring experiments were carried out with granite rocks of similar color characteristics and mineralogical nature in order to obtain comparable results.

Psycho-physical experiment

A visual sorting task (psycho-physical experiment) was conducted to investigate the threshold of perception of greening on granite surfaces. Blanco Cristal, a medium-grain, heterogranular-panallotriomorphic, biotitic adamellitic leucogranite (with dark minerals absent), and feldspar-K, plagioclases, quartz, biotite, chlorite and moscovite as major minerals was selected for the experiments. The petrographic characteristics and mineral composition of this lithotype were described in a previous study (Sanmartín et al. 2011). Twenty-one blocks (6 × 3 × 1 cm) were cut and sterilized before starting the experiments. The upper surface of each granite block (18 cm^2) was inoculated in a laminar flow cabinet with a mixed culture of three isolates of subaerial stone biofilm-forming cyanobacteria grown in $BG11_0$ medium (Rippka et al. 1979), viz. *Nostoc* sp. PCC 9025, *Nostoc* sp. PCC 9104 and *Scytonem*a sp. CCC 9801. The mixed inoculum consisted of 0.21 mg (dry weight) of each strain per ml of medium giving 0.63 mg (dry weight) per ml of mixed inoculum. Distinct volumes from 150 μl (the minimum volume required to fully cover the total area of 18 cm^2 of the surface block) to 540 μl mixed cyanobacterial suspension, were inoculated uniformly with the point of a pipette onto the surface blocks, in order to adjust phototrophic biomass between 0 (to exclude the possibility of an abiotic contribution to the green color) and 18.9 μg of biomass (dry weight) cm^{-2} of surface area. Experiments were performed in triplicate.

Each inoculated block was assessed by eight different observers (five females and three males aged from 25 to 60 years) with normal color vision, ie normal trichromat observers without color blindness (see Fletcher and Voke (1985) for details of color vision examination). The task of each observer was to decide if the greening due to the presence of organisms was perceptible. The responses reported by the observers (yes/no) were recorded and analyzed. The point at which the observers began to note the green color has been coined as the just noticeable difference (jnd). The conceptualization of the greening threshold has its roots in the study of thresholds for other sensory-related stimuli (Gescheider 1976).

The color of the upper surface of each granite block was measured before and after inoculation, following the methods proposed by Prieto et al. (2010a, 2010b). The CIELAB coordinates (L*, a* and b*) were measured before and after inoculation, with a portable spectrophotometer (Konica Minolta CM-700d/600d) equipped with CM-S100w (SpectraMagicTM NX) software; the measuring conditions were illuminant D65, observer 2° and a 8-mm diameter viewing area. A total of 14 readings were taken at different randomly selected zones on each wet surface block, and the results expressed as the mean values.

To relate the phototrophic biomass (dry weight) to color and extracted chl *a* content, the concentration of chl *a* on each block was determined after the visual evaluation and color measurements, following the protocol for the extraction of chl *a* from microorganisms colonizing rocks, recently proposed by Fernández-Silva et al. (2011). The extracts were measured in a UV–Visible spectrophotometer (UVIKON XS, Bio-Tek), and the equation proposed by Wellburn (1994) was used to calculate the concentration of chl *a*, expressed as μg chl *a* cm^{-2} of surface area.

In addition, the thresholds between imperceptible and perceptible greening, in terms of partial color differences (ΔL^*, Δa^* and Δb^*), amount of phototrophic biomass (dry weight) and extracted chl *a* content, were estimated (Prieto et al. 2006). For this purpose, a data table was built in which for each sample (1–21), including its measured parameters, the eight answers from observers were included (1–8) (Berns 2000). The whole of cases (1–1, 1–2, (...), 1–8, 2–1, 2–2, (...), 21–8; ie sample-observer) were sorted into two sets, imperceptible and perceptible, and cumulative percentages were calculted for each group using the following equations where n_p represents the number of answers that were 'yes, ie perceptible, n_i represents the number of answers that were 'no, ie imperceptible', and z represents answer 1, 2, ... , n_p or n_i:

$$\text{Cumulative}_{\text{perceptible,z}} = 100(z/n_p);$$
$$\text{Cumulative}_{\text{imperceptible,z}} = 100 - 100(z/n_i)$$

The greening thresholds on granite were derived by plotting the cumulative percentages, cumulative frequency of answers for each qualitative term (imperceptible and perceptible) *vs* ordered partial color differences, phototrophic biomass (dry weight) and extracted chl *a* content. The intersection of the two sets of data defines the jnd in greening.

Monitoring experiment

The progress of recolonization of the granite façade of the Supercomputing Centre of Galicia (CESGA, www.cesga.es), a centre par excellence in research and high-performance computing services built in 1993 in Santiago de Compostela (Galicia, NW Spain), was monitored fortnightly for a period of 10 months (289 days, March/2009–January/2010), using a spectrophotometer for instrumental color measurements. Three target areas (1, 2, 3) of the south facing wall, each of which was divided in two subareas, upper (A) and lower (B), were selected and cleaned mechanically with distilled water and a brush to remove the existing phototrophic colonization

(Figure 1). The six study areas (1A, 1B, 2A, 2B, 3A and 3B), each of 21.5 cm × 31.0 cm, did not receive direct sunlight because of the proximity of the neighboring buildings. They are also very damp due to water run-off. The weather conditions in Santiago de Compostela during the experiment (according to data from the Galician regional meteorological office: MeteoGalicia, www.meteogalicia.es) are shown in Table 1.

Following the methodology proposed by Prieto et al. (2010b), a total of 234 readings were taken fortnightly at random points in the six study areas. A portable reflection spectrophotometer (CE-XTH) equipped with OptiviewSilver/i QC Basic software, was used under the following conditions: illuminant D65; observer 2° and a 10-mm diameter viewing area. Color measurements were analyzed by considering the CIELAB color system (CIE Publication 15-2, 1986),

Figure 1. Granite façade of the Supercomputing Centre of Galicia (CESGA), showing extensive phototrophic colonization (greening) developed as streaks following the path of water run-off. (a) On site measurement of the color on the façade; (b) overview of the façade with perceptible colored stains (greening) in humid zones; (c) location of the six study areas before cleaning; (d) location of the six study areas after cleaning. Six study areas: three target areas (1, 2, 3) each of which was divided in two subareas, upper (A) and lower (B).

Table 1. Temperature, humidity, sunshine duration and daily global radiation during the exposure period (March 2009 to January 2010), recorded at the Santiago EOAS meteorological station (Santiago de Compostela) and captured by Meteogalicia.

Date	Average air temperature (°C)	Dew point temperature (°C)	Mean relative humidity (%)	Rain (l m^{-2})	Sunshine duration (h)	Daily global radiation (10 KJ m^{-2} day^{-1})
March 2009	11.1	4.5	68	30.4	246.6	1617
April 2009	10.3	6.2	79	106.2	177.6	1581
May 2009	14.5	8.9	73	55	241.6	1932
June 2009	17.2	12.9	78	106.6	218.4	1942
July 2009	17.1	13.1	80	105.2	211.4	1917
August 2009	18.8	14.4	78	24.5	236.9	1917
September 2009	18.0	13.5	78	13.5	248.6	1691
October 2009	16.2	13.4	86	189	149.0	935
November 2009	11.7	9.9	92	272.2	60.1	433
December 2009	8.1	5.9	89	424.5	96.6	434
January 2010	7.6	5.6	91	200.2	85.4	489

taking into account the mean values of CIELAB coordinates (L*, a* and b*). Variations in the three color parameters (partial color differences), lightness-darkness ΔL*, redness-greenness Δa* and yellowness-blueness Δb*, were calculated as follows:

$$\Delta L^* = L_t^* - L_0^*;$$
$$\Delta a^* = a_t^* - a_0^*;$$
$$\Delta b^* = b_t^* - b_0^*,$$

where $L_0^*,\ a_0^*,\ b_0^*$ = the mean value of CIELAB color parameter at the study area after cleaning, and $L_t^*,\ a_t^*,\ b_t^*$ = the mean value of CIELAB color parameter at the study area after a period of exposure (t).

Results and discussion

The laboratory-induced epilithic cyanobacterial biofilms on granite blocks served to emulate the presence of initial green fouling. Photographs of the granite blocks inoculated for the psycho-physical experiment, along with the data for the amount of phototrophic biomass (dry weight) and the concentration of chl *a* extracted are shown in Table 2.

On the basis of the visual evaluation, the threshold of human perception between imperceptible and perceptible greening in terms of the partial color differences (ΔL*, Δa* and Δb*), biomass (dry weight) and extracted chl *a* content, were calculated by plotting the cumulative frequency of answers given by each observer (Figure 2). The visual perception of the color difference differed with each observer, and the point at which individuals began to note the greening on the surface due to phototrophic biomass also differed among the different observers. From the results summarized in Figure 2, it was concluded that greening became perceptible when colonization resulted in a decrease of 4.37 CIELAB units in parameter L*, or when the values of parameters a* and b* decreased and increased, respectively, by only 0.41 and 0.59 CIELAB units. In terms of mg biomass (dry weight) and extracted chl *a* content, a lower abundance of phototrophic biomass was required to reach the greening threshold or jnd in greening in terms of yellowness-blueness variations, Δb* (6.3 μg biomass dry weight cm^{-2} and $(8.43 \pm 0.24) \times 10^{-3}$ μg extracted chl *a* cm^{-2}) and a larger quantity was required for the other two color parameters, lightness-darkness, ΔL*, and redness-greenness, Δa* (12.6 μg biomass dry weight cm^{-2} and $(20.33 \pm 1.60) \times 10^{-3}$ μg extracted chl *a* cm^{-2}). This indicates that of the CIELAB color parameters, parameter b* provides the earliest indication of the presence of phototrophic microorganisms.

The thresholds calculated for the partial color differences were used in the outdoor experiment, in

Table 2. Blanco Cristal granite specimens inoculated with mixed cyanobacterial culture used in the psycho-physical experiment.

Photograph of the granite block surface										
Phototrophic biomass (μg dry weight cm^{-2})	0.0	0.4	0.7	1.1	1.4	2.1	3.2	6.3	12.6	18.9
Chlorophyll a extracted (*) (10^{-3} μg cm^{-2})	0.0	1.65 ± 0.12	2.49 ± 0.21	4.04 ± 0.08	4.49 ± 0.02	5.74 ± 0.02	4.95 ± 0.91	8.43 ± 0.24	20.33 ± 1.60	31.50 ± 2.47

Note: Scale bar = 3.5 cm. *Mean value of three replicates ± SD.

which the rate of greening on building granite was monitored for 10 months after cleaning, by changes in L*, a* and b*. The results are shown in Figure 3 as a summary of the variations in L*, a* and b* values in the six study areas after the exposure period; the time at which the observers began to note the greening is indicated by a shaded circle in the figure. This corresponds to $\Delta L^* < -4.37$; $\Delta a^* < -0.41$ and $\Delta b^* > +0.59$ CIELAB units. Thus, the first bar of the histograms (BC) represents the color difference before and after cleaning the colonized surface, and was used as a reference. Subsequent bars reflect the development of the recolonization process, ie the difference between the value on the first day after cleaning and the subsequent values. In all cases, the trends were all in the same direction as the value of the difference between the colonized and the clean rock (BC) (Figure 3), thus indicating that the color change was due to recolonization. Thus, during the recolonization process a decrease in the ΔL* and Δa* values and an increase in the Δb* value were observed, indicating that the façade became darker and more yellow-greenish color.

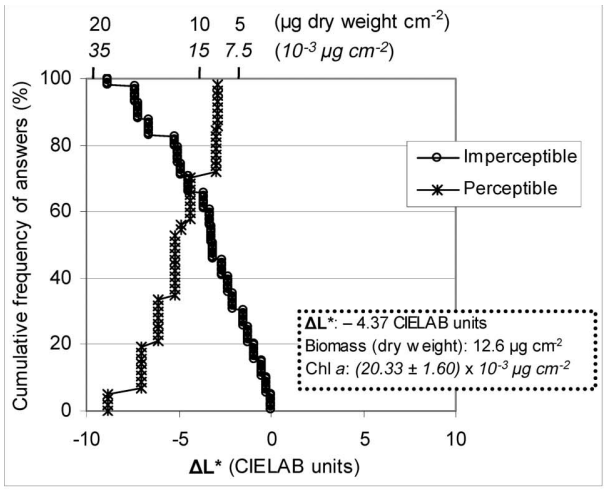

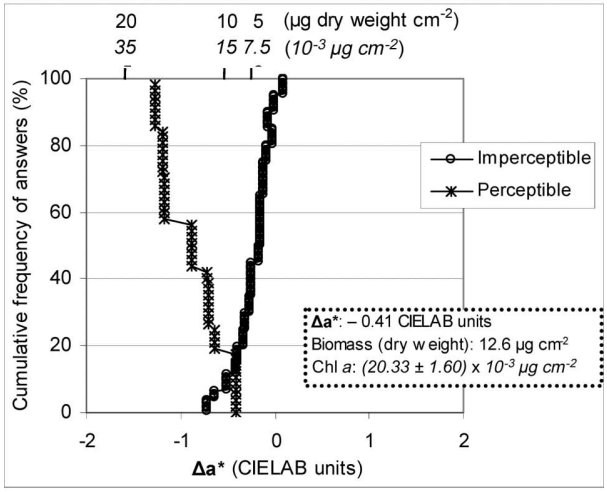

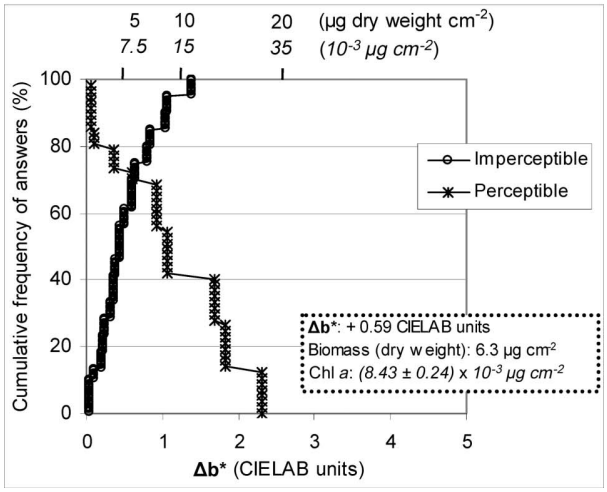

Figure 2. Results of the psycho-physical experiment. Top: lightness-darkness ΔL*, middle: redness-greenness Δa*, and bottom: yellowness-blueness Δb*. Partial color differences CIELAB units (on the bottom x-axis) and μg biomass (dry weight) cm^{-2} surface area and μg extracted chl *a* cm^{-2} surface area (in italics) (on the top x-axis) plotted against the cumulative frequency of answers for perceptible and imperceptible qualitative term (%). The values of the greening threshold in terms of these parameters are shown in a box in the figures.

One important aspect of the results obtained is that analysis of the Δa* and Δb* parameters enabled identification of the point at which recolonization began, as in both cases the difference (Δ) remained constant for a certain period of time and then increased gradually. The moment at which the difference (Δ) began to increase also coincided with the moment at which the value of the increase changed direction towards the reference value (BC), thus indicating the start of colonization. Analysis of the values in Figure 3 shows that recolonization began at between 80 and 129 days (marked with an arrow in the Figure 3). However, analysis of the ΔL* values was not as useful for identifying the moment at which recolonization began as the variations were more erratic (Figure 3).

Comparison of the day on which recolonization began, determined by analysis of the trends (direction changes towards reference value) in the Δa* and Δb* values, and the moment at which greening is considered perceptible in terms of the Δa* and Δb* values (both indicated in Figure 3), revealed that in all cases, the earliest detection of recolonization was by analysis of the trends. Thus monitoring the color of granite façades using a portable spectrophotometer enables early detection of the appearance of greening, even

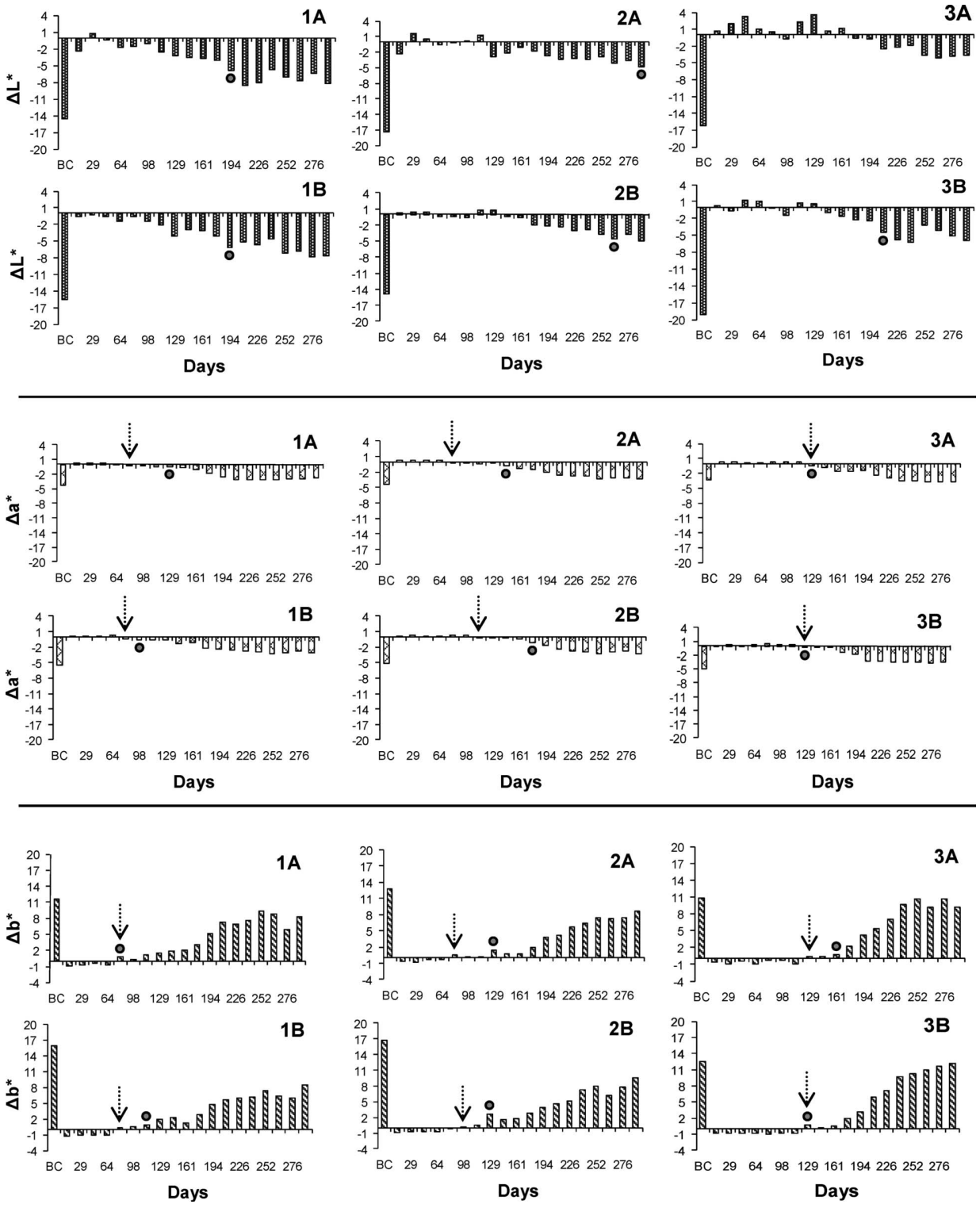

Figure 3. Results of the monitoring experiment. Color changes (top: ΔL*, middle: Δa* and bottom: Δb*) during the period of exposure (289 days) at the six study areas (1A, 1B, 2A, 2B, 3A and 3B, see Figure 1). $\Delta L^* = L^*_t - L^*_0$; $\Delta a^* = a^*_t - a^*_0$; $\Delta b^* = b^*_t - b^*_0$, where L^*_0, a^*_0, b^*_0 = mean value of CIELAB color parameter at the study area after cleaning with water and a brush, and L^*_t, a^*_t, b^*_t = mean value of CIELAB color parameter at the study area after a period of exposure (t). For comparison, the color change before and after cleaning is shown as BC (Before Cleaning). The change in the direction of the partial color difference is indicated by an arrow, and the time when colonization becomes perceptible by a shaded circle ($\Delta L^* < -4.37$; $\Delta a^* < -0.41$ and $\Delta b^* > +0.59$ CIELAB units).

before it is perceptible to the human eye. As in most cases, the greening threshold was reached several days after the value at which colonization was considered to begin, building managers therefore have a period of time in which to decide when cleaning or treatment should be applied.

Another aspect to take into account is that when biological colonization develops, the Δb* values, which tend to more positive values, underwent a faster change than the Δa* values, which tend to more negative values. This is consistent with the previous finding that Δb* provides the earliest indication of perceptible greening due to the presence of phototrophic microorganisms. In addition, if the magnitude of the change caused by colonization is taken into account, it was found that, taking into account the 6 plots, parameter L* varied on average by 6.12 ± 1.78 CIELAB units, a* by 3.40 ± 0.24 CIELAB units and b* by 9.82 ± 1.42 CIELAB units. Therefore parameter b* varied most and thus contributed most to the total variation in color ($\Delta E^*_{ab} = [(\Delta L^*)^2 + (\Delta a^*)^2 + (\Delta b^*)^2]^{1/2}$, Wyszecki and Stiles 1982). This is consistent with previous observations for other stone materials such as quartz (Prieto et al. 2005) and concrete (De Muynck et al. 2009) and shows that parameter b* is the most informative for detecting phototrophic colonization. This finding suggests that the technique proposed here can be extrapolated to buildings other than those built from granite.

For maintenance of granite buildings affected by greening, decisions about the required frequency of cleaning and biocide treatment should therefore take into account the time at which greening becomes perceptible, as well as the time at which colonization is present but not perceived; both parameters are easily determined by use of a portable spectrophotometer. If the cleaning and/or treatment processes are carried out when colonization exists but is not yet perceptible, it would be easier to establish a target level of color of the original surface (Doehne and Price 2010). Moreover, cleaning when greening is marked can lead to the use of chemicals or excessive quantities of water, which may also cause damage (Maxwell 1992).

According to Escadeillas et al. (2007), it generally takes a year for stains to appear on walls, although under favorable growth conditions, development may be extremely rapid. In practice, and under favorable growth conditions (porous support such as concrete walls), it takes 1 year before the first greening is visible and 2–5 years for intense greening to develop. Thornbush and Viles (2006) showed that biological colonization of stonework by fungi was evident after just 2 years. Smith et al. (2004) demonstrated the rapid surface colonization (<2 years) of sandstone by algae in exposure trials in Belfast. In the present case, recolonization (greening) of the granite façade was apparent within a much shorter time. Recolonization took no more than 129 days (just over 4 months), and greening due to the phototrophic microorganisms was perceptible after approximately 178 days (almost 6 months). This rapid biological colonization was undoubtedly favored by the mild wet climate of Santiago de Compostela, especially the microclimate affecting the most shaded walls of the buildings, as also occurs in other buildings in the city (Silva et al. 1997).

Conclusions

This study demonstrated that measurement of color changes with a portable spectrophotometer was a reliable method for the early detection and real-time monitoring of phototrophic growth (greening) on granite façades, even when it is not perceptible to the human eye. In this sense changes in parameter b* were demonstrated to be the most informative. Thus, Δb*: +0.59 CIELAB units, that correspond in this study to 6.3 μg biomass dry weight cm^{-2} and (8.43 ± 0.24) × 10^{-3} μg extracted chl *a* cm^{-2}, was established as the greening threshold.

Cleaning and/or treatment should be carried out taking into account both the greening threshold in terms of Δb* and the time that the trend in the value of Δb* changes and becomes positive, ie indicates the occurrence of phototrophic colonization. In this sense, monitoring changes in b* of a cleaned granite façade exposed to the natural environment in Santiago de Compostela (NW Spain) revealed that recolonization by phototrophic microorganisms (greening) took no more than 129 days (just over 4 months), and greening was perceptible after approximately 178 days (almost 6 months).

Acknowledgments

The present study was financed by the Xunta de Galicia (09TMT014203PR). The authors thank all the observers who generously agreed to collaborate in the psycho-physical experiment and CESGA building staff who allowed the authors to take the color measurements on the building façade.

References

Andrew C. 1992. Towards an aesthetic theory of building soiling. In: Webster RGM, editor. Stone cleaning and the nature, soiling and decay mechanisms of stone. London (UK): Donhead. p. 63–81.

Barberousse H, Lombardo RJ, Tell G, Couté A. 2006. Factors involved in the colonisation of building façades by algae and cyanobacteria in France. Biofouling 22:69–77.

Berns RS. 2000. Billmeyer and Saltzman's principles of color technology. 3rd ed. New York (USA): John Wiley & Sons. 272 pp.

Brimblecombe P. 1987. The big smoke. London (UK): Methuen. 185 pp.
Brimblecombe P, Grossi CM. 2005. Aesthetic thresholds and blackening of stone buildings. Sci Total Environ 349:175–189.
Brimblecombe P, Grossi CM. 2009. Millennium-long damage to building materials in London. Sci Total Environ 407:1354–1361.
Cappitelli F, Principi P, Pedrazzani R, Toniolo L, Sorlini C. 2007. Bacterial and fungal deterioration of the Milan Cathedral marble treated with protective synthetic resins. Sci Total Environ 385:172–181.
Cappitelli F, Vicini S, Piaggio P, Abbruscato P, Princi E, Casadevall A, Nosanchuk JD, Zanardini E. 2005. Investigation of fungal deterioration of synthetic paint binders using vibrational spectroscopic techniques. Macromol Biosci 5:49–57.
Cassé F, Ribeiro E, Ekin A, Webster DC, Callow JA, Callow ME. 2007. Laboratory screening of coating libraries for algal adhesion. Biofouling 23:267–276.
CIE Publication 15-2. 1986. Colorimetry CIE. Vienna (Austria): Central Bureau of the Commission Internationale l'Eclairage (CIE). 74 pp.
Davidson C, Tang W, Finger S, Etyemezian V, Striegel F, Sherwood S. 2000. Soiling patterns on a tall limestone building: changes over 60 years. Environ Sci Technol 34:560–565.
De Muynck W, Maury Ramirez A, De Belie N, Verstraete W. 2009. Evaluation of strategies to prevent algal fouling on white architectural and cellular concrete. Int Biodeterior Biodegr 63:679–689.
Di Pippo F, Bohn A, Cavalieri F, Albertano P. 2011. ^{1}H-NMR analysis of water mobility in cultured phototrophic biofilms. Biofouling 27:327–336.
Di Pippo F, Bohn A, Congestri R, De Philippis R, Albertano P. 2009. Capsular polysaccharides of cultured phototrophic biofilms. Biofouling 25:495–504.
Doehne E, Price CA. 2010. Stone conservation: an overview of current research, 2nd ed. Los Angeles (CA): Getty Publications, the Getty Conservation Institute. 175 pp.
Escadeillas G, Bertron A, Blanc P, Dubosc A. 2007. Accelerated testing of biological stain growth on external concrete walls. Part 1: development of the growth tests. Mater Struct 40:1061–1071.
Fernández-Silva I, Sanmartín P, Silva B, Moldes A, Prieto B. 2011. Quantification of phototrophic biomass on rocks: optimization of chlorophyll-a extraction by response surface methodology. J Ind Microbiol Biot 38:179–188.
Fletcher R, Voke J. 1985. Defective colour vision: fundamentals, diagnosis and management. Boston (MA): Adam Hilger Ltd. 624 pp.
Gescheider GA. 1976. Psychophysics: method and theory. Hillsdale (NJ): Lawrence Erlbaum Associates. 190 pp.
Grant C. 1982. Fouling of terrestrial substrates by algae and implications for control – a review. Int Biodeterior Bull 18:57–65.
Grossi CM, Brimblecombe P. 2004. Aesthetics and perception of soiling. In: Saiz-Jimenez, C, editor. Air pollution and cultural heritage. London (UK): Taylor & Francis. p. 199–208.
Grossi CM, Brimblecombe P. 2008. Past and future colouring patterns of historic stone buildings/distribución pasada y futura del color en edificios históricos de piedra. Mater Construcc 58:143–160.
Guillitte O. 1995. Bioreceptivity: a new concept for building ecology studies. Sci Total Environ 167:215–220.
ICOMOS-ISCS. 2008. Illustrated glossary on stone deterioration patterns. Monuments and Sites XV. Paris (France): ICOMOS. 78 pp.
Maxwell I. 1992. Stone cleaning: for better or worse? An overview. In stone cleaning and the nature, soiling and decay mechanisms of stone. In: Webster RGM, editor. Proceedings of the International Conference, Edinburgh, UK, 14–16 April 1992. London (UK): Donhead Publishing. p. 3–49.
McDonald R. 1997. Colour physics for industry, 2nd ed. Bradford (UK): Society of Dyers and Colourists. 534 pp.
Miller A, Dionisio A, Macedo MF. 2006. Primary bioreceptivity: a comparative study of different Portuguese lithotypes. Int Biodeterior Biodegr 57:136–142.
Miller A, Rogerio-Candela MA, Laiz L, Wierzchos J, Ascaso C, Sequeira Braga MA, Hernández-Mariné M, Mauricio A, Dionisio A, Macedo MF, et al. 2010. Laboratory-induced endolithic growth in calcarenites: biodeteriorating potential assessment. Microb Ecol 60:55–68.
Newby PT, Mansfield TA, Hamilton RS. 1991. Sources and economic implications of building soiling in urban areas. Sci Total Environ 100:347–365.
Ortega-Calvo JJ, Hernandez-Marine M, Saiz-Jimenez C. 1993. Cyanobacteria and algae on historic buildings and monuments. In: Garg KL, Garg N, Mukei KG, editors. Recent advances in biodeterioration and biodegradation. Calcutta (India): Naya Prokash. p. 173–203.
Prieto B, Silva B. 2005. Estimation of the potential bioreceptivity of granitic rocks from their intrinsic properties. Int Biodeterior Biodegr 56:206–215.
Prieto B, Silva B, Aira N, Álvarez L. 2006. Toward a definition of a bioreceptivity index for granitic rocks: perception of the change in appearance of the rock. Int Biodeterior Biodegr 58:150–154.
Prieto B, Silva B, Aira N, Laiz L. 2005. Induction of biofilms on quartz surfaces as a means of reducing the visual implact of quartz quarries. Biofouling 21:237–246.
Prieto B, Sanmartín P, Aira N, Silva B. 2010a. Color of cyanobacteria: some methodological aspects. Appl Optics 49:2022–2029.
Prieto B, Sanmartín P, Silva B, Martínez-Verdú F. 2010b. Measuring de the color of granite rocks. A proposed procedure. Color Res Appl 35:368–375.
Ramírez M, Hernández-Mariné M, Novelo E, Roldán M. 2010. Cyanobacteria-containing biofilms from a Mayan monument in Palenque, Mexico. Biofouling 26:399–409.
Rippka R, Deruelles J, Waterbury JB, Herdman M, Stanier RY. 1979. Genetic assignments, strain histories and properties of pure cultures of cyanobacteria. J Gen Microbiol 111:1–61.
Saiz-Jimenez C, Ariño X. 1995. Biological colonization and deterioration of mortars by phototrophic organisms/colonización biológica y deterioro de morteros por organismos fotótrofos. Mater Construct 45:5–16.
Sanmartín P, Silva B, Prieto B. 2011. Effect of surface finish on roughness, color and gloss of ornamental granites. J Mater Civil Eng 23:1239–1248.
Sanmartín P, Aira N, Devesa-Rey R, Silva B, Prieto B. 2010. Relationship between color and pigment production in two stone biofilm-forming cyanobacteria (*Nostoc* sp. PCC 9104 and *Nostoc* sp. PCC 9025). Biofouling 26:499–509.
Silva B, Prieto B, Rivas T, Sanchez-Biezma MJ, Paz G, Carballal G. 1997. Rapid biological colonization of a granitic building by lichens. Int Biodeterior Biodegr 40:263–267.

Smith BJ, Warke PA, Curran JM. 2004. Implications of climate change and increased 'time-of-wetness' for the soiling and decay of sandstone structures in Belfast, Northern Ireland. In: Prikryl R, editor. Dimension stone. London (UK): Taylor & Francis. p. 9–14.

Smith BJ, McCabe S, McAllister D, Adamson C, Viles HA, Curran JM. 2011. A commentary on climate change, stone decay dynamics and the 'greening' of natural stone buildings: new perspectives on 'deep wetting'. Environ Earth Sci 63:1691–1700.

Tanaca HK, Dias CMR, Gaylarde CC, John VM, Shirakawa MA. 2011. Discoloration and fungal growth on three fiber cement formulations exposed in urban, rural and coastal zones. Build Environ 46:324–330.

Tiano P. 2002. Biodegradation of cultural heritage: decay mechanisms and control methods. Available from: http://www.arcchip.cz/w09/w09_tiano.pdf.

Thornbush M, Viles H. 2006. Changing patterns of soiling and microbial growth on building stone in Oxford, England after implementation of a major traffic scheme. Sci Total Environ 367:203–211.

Urzì C, Realini M. 1998. Colour changes of Noto's calcareous sandstone as related to its colonisation by microorganisms. Int Biodeterior Biodegr 42:45–54.

Wellburn AR. 1994. The spectral determination of chlorophylls *a* and *b*, as well as total carotenoids, using various solvents with spectrophotometers of different resolution. J Plant Physiol 144:307–313.

Wyszecki G, Stiles WS. 1982. Color science, concepts and methods, quantitative data and formulae, 2nd ed. New York (USA): Wiley. 968 pp.

4ª línea de trabajo

Aplicación práctica de la medida del color a otros sustratos inorgánicos naturales

4th line of research

Practical application of color measurement on other naturally occurring inorganic substrates

Chapter 8. Color characterization of roofing slates from the Iberian Peninsula for restoration purposes

Prieto, B.; Ferrer, P.; Sanmartín, P.; Cárdenes, V.; Silva, B.

Journal of Cultural Heritage 12 (4): 420-430 (2011)

JCR index (IF) 2010 = 1.162 (107/222, 48 percentile in Materials Science Multidisciplinary; 92/165, 56 percentile in Geosciences Multidisciplinary)

Total number of times cited: 2

Journal of Cultural Heritage 12 (2011) 420–430

Available online at ScienceDirect
www.sciencedirect.com

Elsevier Masson France
EM|consulte
www.em-consulte.com/en

Original article

Color characterization of roofing slates from the Iberian Peninsula for restoration purposes

Beatriz Prieto*, Perla Ferrer, Patricia Sanmartín, Victor Cárdenes, Benita Silva

Departamento Edafología y Química Agrícola, Facultad Farmacia, Universidad Santiago de Compostela, 15782 Santiago de Compostela, Spain

ARTICLE INFO

Article history:
Received 10 September 2010
Accepted 7 February 2011
Available online 17 March 2011

Keywords:
CIELAB
Colorimetry
Cultural heritage
Roofing slate
Substitution criteria

ABSTRACT

Substitution of slate roofing tiles is a conventional operation during building restoration, since tiles are very difficult to restore or clean because of the high degree of alteration they suffer. Criteria for replacement of historical building stones must be based on geological, geotechnical and esthetic parameters, among which color is of great importance. In this sense, this paper constitutes a comprehensive and useful colorimetric study of roofing slates from the Iberian Peninsula, for the purposes of restoration. The color of 50 commercial varieties of roofing slate mined in quarries from the 12 mining districts in the Iberian Peninsula was analyzed with a spectrophotometer device, by considering the CIELAB color space. The results of the study were used to develop a protocol for characterizing the color of roofing slate and to define the color range of roofing slate from the Iberian Peninsula. In addition, the similarities and differences in the color and microstructure of the different commercial varieties of Iberian roofing slate were established and the limit of acceptability of replacement of one type of slate by another was determined. Parameter h_{ab} was found to be the most important CIELAB color coordinate as regards the formation of homogeneous color groups, and the specular component excluded (SCE) mode was most sensitive as regards detecting color differences between two samples.

1. Introduction

Slate has been used for centuries as a roofing material and the extraction of slate and other fissile rocks for roofing is probably as old as the art of building with stone [1]. There are some remains of slate roofs on Roman buildings in England [2] and many historical centers of European cities include Medieval and Renaissance buildings covered with slate, such as the monastery of *El Escorial* in Madrid (Spain). Before the slate industry began in the USA – slate was first quarried in the country in 1839 at Fair Haven (Vermont) – slate was exported from Europe, with France being the main producer, followed by Germany and the United Kingdom. Spanish slate deposits did not begin to be exploited industrially until the 1970s [3] in response to the exhaustion of mining resources in European quarries and the modernization of the production chain in Spain [4]. Nowadays, Spain is the principal producer of roofing slate in the world, and the main areas of exploitation are in the *Variscan* belt in the northwest of the Iberian Peninsula [1,5].

Slate can be used as roofing material because it contains a high proportion of phyllosilicates, which become aligned during metamorphism and develop a new set of planes in a process named schistosity or slaty cleavage (S_1) [6]. The material can therefore be split into thin slabs (2–8 mm thick), which maintain high mechanical strength and uniform surface [7,8]. In addition, its low water absorption index (< 0.6%) lends slate a waterproof character and makes it very resistant to frost damage and breakage due to freezing/thawing cycles [9]. However, slate tiles still undergo weathering and must be replaced by new ones, which in order to maintain the esthetic properties of the building, should be selected from the same quarry where the weathered slates were originally extracted. As the original quarry is often unknown, has been mined out or is no longer accessible, slate tiles must be obtained from other quarries in similar geological formations. In such cases, the criteria for replacement of historical building stones should be based on geological, geotechnical and esthetic parameters rather than on visual and purely qualitative-subjective methods and/or economic considerations [10,11], which too often results in inadequate replacement, giving rise to a patchwork of original and substituted slates (Fig. 1). This not only causes an unpleasant esthetic effect as regards the color of the roof, but does not comply with the basis of international criteria for restoration and the current legislation regarding national heritage monuments [12–14].

From a geological point of view, roofing slate is formed under very low metamorphic conditions (greenschists facies), with a relatively simple mineral composition of quartz, mica and chlorite, plus some accessory minerals. The mineralogy of Spanish roofing

* Corresponding author. Tel.: +34 881 814594; fax: +34 981 594912.
E-mail address: beatriz.prieto@usc.es (B. Prieto).

1296-2074/$ – see front matter © 2011 Elsevier Masson SAS. All rights reserved.
doi:10.1016/j.culher.2011.02.001

Fig. 1. Example of inadequate partial replacement of roofing slate.

slates is quite homogeneous [5,15,16], with three main components (mica, chlorite and quartz), secondary minerals (chloritoid, feldspars, iron sulphides and carbonates), and some accessory minerals. Examined with the petrological microscope, spanish roofing slate may present two different microtextures well defined, lepidoblastic, with small grain size, and porphido-lepidoblastic, with bigger blasts standing out the mica matrix. Both microtextures are characterized by the repetition of mica alignment formed during the metamorphism which coincides with S_1. The occurrence of sedimentation beds (S_0) can be easily detected by a third microstructure, granolepidoblastic, which is a mosaic of quartz crystals, present in these sedimentation beds under the form of sandy levels [17]. These mica alignments, which confer to the slates their anisotropic nature, together with the color are the two main factors involved in the appearance of the slates.

Although color is one of the main factors involved in the perceived appearance of a material, and therefore of great importance in restoration work, no studies concerning the objective characterization of this property in roofing slates have yet been published. The aims of the present study were therefore the objective characterization of the color of 50 commercial varieties of roofing slate mined from the 12 mining districts in the Iberian Peninsula [18], and the evaluation of the differences in color, in order to establish homogeneously colored groups of roofing slates. Moreover, microstructure features [6] as S_1, S_0 and the intersection between them (S_1/S_0 angle), which forms a set of lineation named intersection lineation (L_0), were analyzed. This information will help improve the replacement of roofing slates in restoration work.

2. Material and methods

2.1. Roofing slates

Slate is a fine-grained rock formed by the low-grade metamorphism of sedimentary clays [19]. The main minerals are quartz and phyllosilicates (mica and chlorites), with variable amounts of albite, chloritoid, and small amounts of tourmaline, zircon, rutile, iron sulfides and carbonates [20]. The latter two minerals are potentially highly alterable and therefore undesirable in top quality roofing slate.

Not all types of slate are useful for roofing tiles. Thus, the European Committee of Standardization defines *slate* as 'a fine-grained very low- to low-grade metamorphic rock possessing a well-developed fissility parallel to the planes of slaty cleavage' and *roofing slate* as 'rocks that are easily split into thin sheets along planes of slaty cleavage, caused by very low- to low-grade metamorphism due to tectonic compression' [21]. Commercial slate slabs are obtained by splitting, creating uneven surfaces and a natural looking finish, which contrasts with other ornamental rocks most often traded polished.

In this study, 50 commercial varieties of roofing slates from quarries in the 12 different mining districts of the Iberian Peninsula (Fig. 2) were considered. The name relative to the origin, mining district, stratigraphic level and the color description by visual assessment are given for each type of roofing slate studied in Table 1.

2.2. Colorimetric characterization: measuring protocol

With the purpose of determining the reproducible and comparable color of roofing slates, a measuring protocol, which takes into account the minimum number of measurements and the minimum area of measurement required to quantify roofing slate color in relation to the dimensions of the measuring head (circular viewing aperture), was established following the methodology proposed by Prieto et al. [22] for granite rocks. The protocol combines colorimetric measurements and the corresponding statistical analysis. Four different sizes of surface area (36, 54, 72 and 90 cm^2) of each of three specimens of the 50 commercial varieties of roofing slate ($50 \times 12 = 600$ specimens) were measured with a Minolta colorimeter, equipped with two interchangeable diameter viewing apertures, CR-300 (8 mm) and CR-310 (50 mm), and a portable spectrophotometer GretagMacbeth CE-XTH, with two diameter viewing apertures of 5 and 10 mm. The measuring conditions were: CIE standard daylight illuminant D65, 1931 (2°) CIE standard colorimetric observer, and integrating sphere geometry in which the light is uniformly diffuse in all directions illuminating the sample, and is observed at 0° in relation to normal for the colorimeter (d/0°) and at 8° for the spectrophotometer (d/8°). Twenty measurements were executed at random by reflection in speculate component included (SCI) mode, with each aperture (5, 8, 10 and 50 mm) on each surface area of the 600 specimens of roofing slates.

The CIELAB color space was used to define the measuring protocol by considering the Cartesian coordinates: L*a*b*, where L* represents the lightness of the color, which varies from 0 black to 100 white, a* the red-green coordinate on a red (+) to green (−) axis, and b* is the yellow-blue coordinate on a yellow (+) to blue (−) axis.

All of the data were subjected to multivariate analysis of variance (Manova) and the Tukey-b multiple comparison test by use of the SPSS 15.0 statistical software.

2.3. Colorimetric characterization: roofing slate color

Once the measuring protocol was defined, the color of each commercial variety of roofing slate was characterized by carrying out six measurements at random positions on three specimens (36 cm^2) by use of a GretagMacbeth CE-XTH spectrophotometer with a diameter viewing aperture of 10 mm (Section 3.1). The measurements were performed in both the specular component included (SCI) mode and specular component excluded (SCE) mode, as it has been suggested that SCE geometry is more useful for the detection of small color differences in other materials [23–25]. SCI mode, with the gloss trap of the spectrophotometer closed, includes the total reflectance (considering both specular and diffuse reflections), whereas the SCE mode, with an open gloss trap, includes the diffuse reflectance and excludes most of the specular component and is therefore more sensitive to differences in color due to differences in surface roughness [26]. In general, it is an accepted theory

Fig. 2. Location of the Iberian Peninsula roofing slate districts (from [18]) and appearance of some of the mined roofing slates. (Bar corresponds to 4 mm).

in color science that the SCE mode closely simulates the view with the naked eye, and that the SCI mode is adequate for analyzing the intrinsic color of objects.

The CIELAB color space was used to represent color measurements by use of the two different sets of coordinates, the Cartesian coordinates: $L^*a^*b^*$, preferred for achromatic colors, i.e. whites, blacks and grays [27], and the cylindrical coordinates: $L^*C^*_{ab}h_{ab}$, which represent the qualitative and quantitative psychophysical components of the color: lightness, saturation and hue [28]. In both spaces, L^* represents the lightness of the color, which varies from 0 black to 100 white, a^* represents the color on the red-green scale (red [+] to green [−]), b^* represents the color on the yellow-blue scale (yellow [+] to blue [−]), C^*_{ab} is the chroma or saturation of color ($C^*_{ab} = [a^{*2} + b^{*2}]^{1/2}$) measured as the length of the line from the neutral point to the sample point in the a^*b^* plane, and h_{ab} is the hue angle or tone ($h_{ab} = \arctan(b^*/a^*)$), refers to the dominant wavelength, as is the CIELAB color parameter that represents the major color perception attribute, indicating redness, yellowness, greenness, or blueness in a circular scale that starts at 0° and increases counterclockwise to 360°.

The total color differences were calculated by the classical CIELAB 1976 color equation, $\Delta E^*_{ab} = [(\Delta L^*)^2 + (\Delta a^*)^2 + (\Delta b^*)^2]^{1/2}$, recently recommended for the study of textured samples [29]. ΔL^*, Δa^* and Δb^* represent the difference between both considered values of L^*, a^* and b^*.

In order to analyze differences in color, the roofing slates were grouped by color, by means of a Hierarchical Cluster Analysis (HCA). The average linkage between groups was applied and the Euclidean distance was selected as a criterion of similarity. The analysis was carried out with SPSS 15.0 statistical software.

A student *t*-test ($p = 0.01$) was used to compare the CIELAB color coordinates between roofing slates depending on the color measuring mode (SCI or SCE).

2.4. Microstructure characterization: S_1/S_0 angle and Lineation L_0

Thin sections of 30 microns thickness were elaborated from the three spatial planes XY, XZ and ZY of the slate (Fig. 3). These thin sections were examined with a Polarized Light Carl-Zeiss Universal microscope. The best plane to determine the microstructures is ZY, ortogonal to S_1, S_0 and L_0, where the angle S_1/S_0 can be measured with the graduated slide of the microscope. This angle defines by itself the internal relationships of the slate, as much as this angle is close to 90°, L_0 will be more marked. Also, in regional

Table 1
Description of the 50 roofing slates collected from quarries in the 12 different mining districts of the Iberian Peninsula.

Roofing slate	Mining district	Stratigraphic level	Color by visual assessment[a]
Monte Rande (MRA)	1	Upper Ordovician	Gray-black
Lombao (LOM)	1	Upper Ordovician	Gray-black
Verde Xemil (VXE)	2	Cambrian	Green-gray
Gris Lugo (GLU)	2	Cambrian	Gray-green
Verde Lugo, Pol (VLU)	2	Cambrian	Green
Villarbacú (VIB)	3	Middle Ordovician	Dark-gray
Caurel Quiroga (CAU)	3	Middle Ordovician	Dark-gray
Pacios Quiroga alto (QIA)	3	Middle Ordovician	Black
Pacios Quiroga bajo (QIB)	3	Middle Ordovician	Black
Pebosa, Pacios de la Sierra (PEB)	3	Middle Ordovician	Dark-gray
A Lastra (LAS)	3	Middle Ordovician	Dark-gray
Vilarchao - Fonsagrada (EUP)	4	Middle Ordovician	Gray
San Víctor (SVI)	5	Upper Ordovician	Gray
Castañeiro (CTÑ)	5	Upper Ordovician	Black
Los Molinos (LMO)	5	Upper Ordovician	Gray
Rozadais (ROZ)	5	Upper Ordovician	Gray
Castrelos (CST)	5	Upper Ordovician	Dark-gray
Casaio (TRA)	5	Middle Ordovician	Black
Casaio (3C)	5	Middle Ordovician	Black
Os Vales (PIV)	5	Upper Ordovician	Dark-gray
Mormeau (CAP)	5	Upper Ordovician	Dark-gray
Riodolas (RIO)	5	Upper Ordovician	Gray
Los Campos (CAM)	5	Upper Ordovician	Gray
Domiz (DOM)	5	Upper Ordovician	Gray
Vianzola, Penedo Rayado (VIA)	5	Upper Ordovician	Gray
Gaton Mexón (GMP)	5	Upper Ordovician	Gray
Intradima, Gato Mexón (GMI)	5	Upper Ordovician	Gray
Os Follos (OFON)	5	Upper Ordovician	Dark-gray
Os Follos (OFOH)	5	Upper Ordovician	Gray
San Vicente (SVE)	5	Middle Ordovician	Gray
Alto Bierzo (ROC)	6	Middle Ordovician	Gray
Piforsa, San Pedro de Trones (UPA3)	7	Upper Ordovician	Gray
Armadilla, Benuza (CU4)	7	Upper Ordovician	Gray
Las Arcas - San Pedro (CU6)	7	Upper Ordovician	Gray
Las Arcas - Prada (UPA7)	7	Upper Ordovician	Gray
Las Arcas San Pedro (CU10)	7	Upper Ordovician	Gray
Raniella, Sotillo - Benuza (CU13)	7	Upper Ordovician	Gray
Lombilla, Piz Garramateira (CU14)	7	Upper Ordovician	Gray
Beta, Sotillo (CU25)	7	Upper Ordovician	Gray
Pizarras Carucedo (Vazfer) (VAZ)	7	Upper Ordovician	Gray
Pz Templarios (TEM)	7	Upper Ordovician	Gray
Itasi, Sigüeya-Benuza (ITA)	7	Upper Ordovician	Gray
Galir (GAL)	7	Upper Ordovician	Gray
Gonta (GON)	7	Upper Ordovician	Gray
Aliste - Pizarras Abejeda (RFR)	8	Middle Ordovician	Gray
Pizarras Riofrio, Aliste (ALI)	8	Middle Ordovician	Dark-gray
J Bernardos (BRN)	9	Precambrian	Dark-gray
Villar del Rey (VDR)	10	Devonian	Black
Valongo (VAL)	11	Middle Ordovician	Gray-blue
Canelas/Arouca (ARO)	12	Middle Ordovician	Black

[a] Color definition in García-Guinea et al. [5] and Cárdenes et al. [18].

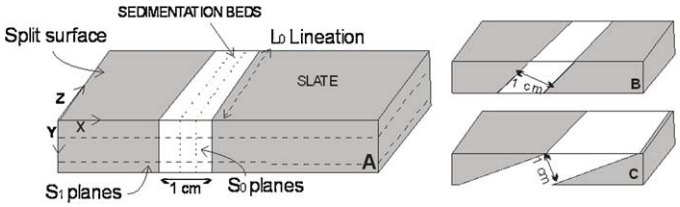

Fig. 3. A. Relationships among slaty cleavage (S_1), sedimentation beds (S_0) and lineation (L_0). B–C. Variation of the thickness of S0 on the tile surface depending on the S_1/S_0 angle.

exploration of slate outcrops, angle S_1/S_0 is very important, since it determines the orientation of the slate layers. Other important feature is the thickness of S_0 beds, since it determines the thickness of lineation over the slate tile surface (Fig. 3). S_0 laminations with thickness over a few centimetres prevent the tiles to split in flat sheets, so they are rejected during the first stages of the elaboration process. The incidence of L_0 was determined by examining the XY plane of the slate specimens with naked eye, determining the character of the L_0 trace (no trace, slightly, moderate or pronounced marked).

3. Results and discussion

3.1. Measuring protocol

The minimum number of measurements required to characterize each color coordinate (L*, a* and b*) in each sample of roofing slate was defined from the steady section of the inverted exponential decay graph, obtained by plotting the cumulative averages of Cartesian CIELAB coordinates against number of measurements [22], and taking into account the short-term repeatability of the instrument ($\Delta L^* = 0.18$, $\Delta a^* = 0.36$, $\Delta b^* = 0.42$), calculated from 20 color measurements made at the same point on black, white, orange, blue and green chips, as rapidly as the device allowed.

Table 2
Three-way multivariate analysis of variance for the number of measurements.

	λ de Wilks	F	G.L.	Sig.
Roofing Slate	0.001	4281.6	156	0.000
Diameter viewing aperture	0.276	4643.1	9	0.000
Roofing slate*Aperture	0.475	44.3	468	0.000

Dependent: L*, a*, b*.

The minimum number of measurements differed significantly (Table 2) for each CIELAB color coordinate (L*, a* and b*), each commercial variety of roofing slate and each diameter viewing aperture (50, 10, 8 and 5 mm), and varied between two and seven measurements. The largest number obtained for each diameter viewing aperture, i.e. measuring head, was taken as the minimum number required to characterize the color of the roofing slates. Thus, the minimum number of measurements required to characterize a 36 cm^2 roofing slate was seven, with a 5 mm viewing aperture diameter; for the same area with the 8 and 10 mm viewing aperture diameters six measurements were required, and for the 50 mm viewing aperture two measurements were required. In the latter case it is advisable to carry out three measurements, for statistical validity. Prieto et al. [22] obtained similar results in granite rocks, and found that the smaller the measuring head, the larger the number of measurements required.

In relation to the minimum measurement area, different sizes of specimens (surface area: 36, 54, 72 and 90 cm^2) of each of the 50 commercial varieties of roofing slate were prepared. The corresponding number of measurements was made for each area and measuring head, according to the results discussed in the previous paragraph (for example, nine measurements for 54 cm^2 with a 10 mm diameter viewing aperture). To determine whether the color varied with the measurement area, the data for each variety of roofing slate and viewing aperture were subjected to multivariate analysis of variance (Manova), with mean values of L*, a*, and b* for each specimen as dependent variables, and the roofing slate area as the independent variable. A significance more than 0.90 was obtained in each case, indicating that the color obtained with each diameter viewing aperture (50, 10, 8 and 5 mm) and the different surface areas (36, 54, 72 and 90 cm^2) was the same, and therefore a surface area of 36 cm^2 is sufficient to characterize the color of the roofing slates.

Once the number of measurements and the surface area were established in relation to the dimensions of the circular viewing aperture, the color determined by each measuring head was compared to establish whether similar results were obtained. The results of Manova, with L*, a* and b* as dependent variables and the diameter of the viewing aperture as the independent variable revealed significant differences between the values obtained with the different measuring heads (Table 3). However, if we analyze the real significance, rather than the statistical significance, of the differences in color obtained with each measuring head, the total color differences (ΔE^*_{ab}) for pairs of viewing apertures (Fig. 4) were less than one CIELAB unit, the visual color difference threshold or just noticeable difference (jnd) which constitutes the lower limit of perception in an individual with normal color vision [26]; and these are far from the three CIELAB units considered as the upper limit of rigorous color tolerance [28,30].

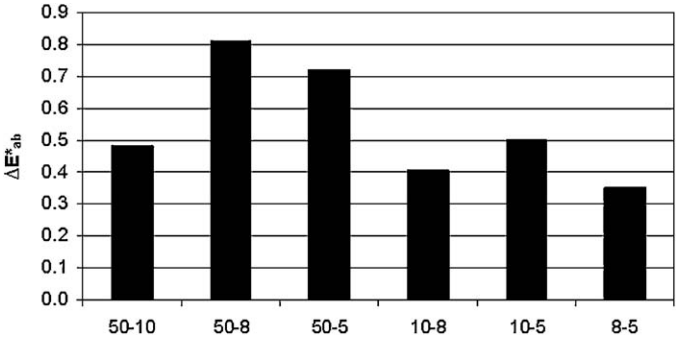

Fig. 4. Total color differences (ΔE^*_{ab}) obtained with different pairs of measuring heads (i.e. the diameter of circular viewing aperture).

Therefore, color measurements on roofing slates will be reproducible and comparable if carried out on a surface area of at least 36 cm^2, and 7, 6, 6 or 3 measurements/36 cm^2 are made with measuring heads of 5, 8, 10 or 50 mm diameter viewing aperture, respectively.

3.2. Roofing slate color

The values of the CIELAB color coordinates: L*, b*, a*, C^*_{ab} and h_{ab}, from both the Cartesian and cylindrical sets, using the SCI and SCE modes for each commercial variety of roofing slate, are shown in Table 4. Considering all 50 commercial varieties as representative of the roofing slates from the Iberian Peninsula, a range of values can be established for this type of material. Thus, L* lightness of color, varied more widely than a*, b* and C^*_{ab} coordinates, and fell within the low-central part of scale, from 33.7 ± 0.0 in the darkest roofing slate (VDR) to 53.2 ± 0.2 in the lightest roofing slate (VLU) measured in SCI mode, and between 33.5 ± 0.2 and 52.4 ± 0.7 measured in SCE mode. The chromatic parameter a* varied between −4.2 ± 0.1 and 0.0 ± 0.0 in SCI mode, and between −4.1 ± 0.1 and 0.1 ± 0.1 in SCE mode, while the chromatic parameter b* varied in both blue and yellow ranges, from −1.4 ± 0.1 to 2.0 ± 0.1 in SCI mode, and from −1.8 ± 0.2 to 1.9 ± 0.3 in SCE mode. Therefore the color of Iberian roofing slates can be described as dark-medium gray and slightly chromatic, which is consistent with the location of specimens in well-defined color areas (SCI and SCE) close to the origin of the a*-b* coordinates in the two-dimensional representation of the color (Fig. 5), with VLU exhibiting the lowest a* values (greener) and the highest b* value (yellower) in both measuring modes. On the other hand, chroma values were fairly low, indicating a low intensity of roofing slates color; the highest chroma value, C^*_{ab}: 4.6 ± 0.1 in SCI mode and 4.5 ± 0.2 in SCE mode, was obtained for VLU and the lowest, 0.5 ± 0.1 in SCI mode and 0.6 ± 0.3 in SCE mode, for BRN.

Table 3
Tukey-b tests for the four diameter viewing apertures, for an area of 36 cm^2.

Diameter viewing aperture (mm)	L*	a*	b*
50	38.28^a	-0.35^a	-1.32^a
10	38.23^a	-0.25^b	-0.85^b
8	$37.93^{b,a}$	$-0.32^{a,b}$	-0.59^c
5	37.73^b	-0.26^b	-0.88^b

Table 4
CIELAB color coordinates for each roofing slate, measured with the spectrophotometer in SCI and SCE modes.

	SCI (specular component included) mode					SCE (specular component excluded) mode				
	L^*	a^*	b^*	C^*_{ab}	h_{ab}	L^*	a^*	b^*	C^*_{ab}	h_{ab}
MRA	40.0 ± 0.1	−0.1 ± 0.0	−1.0 ± 0.1	1.0 ± 0.1	263.0 ± 2.3	39.3 ± 0.4●	−0.2 ± 0.1	−1.4 ± 0.2●	1.4 ± 0.2●	263.3 ± 3.7
LOM	37.9 ± 0.9	−0.3 ± 0.1	−1.4 ± 0.1	1.4 ± 0.1	259.5 ± 1.8	39.0 ± 0.4●	−0.1 ± 0.1●	−1.4 ± 0.1	1.4 ± 0.1	267.5 ± 3.1●
VXE	41.2 ± 0.6	−2.3 ± 0.1	−0.4 ± 0.1	2.3 ± 0.0	189.6 ± 2.6	39.8 ± 0.9	−2.1 ± 0.1	−0.8 ± 0.2●	2.3 ± 0.1	200.4 ± 4.2●
GLU	41.6 ± 0.1	−0.8 ± 0.0	−0.2 ± 0.0	0.8 ± 0.1	195.0 ± 1.4	39.5 ± 1.1●	−0.8 ± 0.1	0.2 ± 0.2●	0.9 ± 0.0	169.3 ± 16.4●
VLU	53.2 ± 0.2	−4.2 ± 0.1	2.0 ± 0.1	4.6 ± 0.1	154.6 ± 1.3	52.4 ± 0.7	−4.1 ± 0.1	1.9 ± 0.3	4.5 ± 0.2	155.3 ± 2.6
VIB	36.6 ± 0.6	0.0 ± 0.0	−0.9 ± 0.1	1.0 ± 0.1	271.9 ± 2.0	36.2 ± 0.2●	0.0 ± 0.1	−1.6 ± 0.1●	1.6 ± 0.1●	268.5 ± 2.6
CAU	40.8 ± 0.3	−0.2 ± 0.0	−1.3 ± 0.0	1.3 ± 0.0	262.3 ± 0.8	39.9 ± 0.8●	−0.1 ± 0.1	−1.6 ± 0.2●	1.6 ± 0.2●	266.8 ± 2.4
QIA	37.7 ± 0.6	−0.1 ± 0.1	−1.3 ± 0.0	1.3 ± 0.0	265.7 ± 3.2	36.8 ± 0.4●	−0.1 ± 0.1	−1.7 ± 0.2●	1.7 ± 0.2●	267.8 ± 2.3
QIB	39.6 ± 0.1	−0.2 ± 0.0	−1.3 ± 0.0	1.4 ± 0.1	263.0 ± 0.9	39.4 ± 0.4	−0.1 ± 0.0	−1.7 ± 0.1●	1.8 ± 0.1●	266.4 ± 1.6
PEB	38.8 ± 0.3	−0.2 ± 0.0	−1.2 ± 0.1	1.3 ± 0.1	262.5 ± 1.5	39.1 ± 0.4	−0.1 ± 0.1●	−1.6 ± 0.1●	1.6 ± 0.1●	267.8 ± 2.1●
LAS	37.5 ± 0.7	−0.1 ± 0.0	−0.9 ± 0.0	0.9 ± 0.0	260.4 ± 10.1	37.6 ± 0.5	−0.1 ± 0.1	−1.4 ± 0.2●	1.4 ± 0.2●	265.9 ± 5.0
EUP	43.2 ± 0.4	−0.5 ± 0.0	−1.0 ± 0.0	1.1 ± 0.0	241.1 ± 1.2	42.4 ± 0.5●	−0.4 ± 0.0	−1.3 ± 0.3●	1.4 ± 0.2●	250.3 ± 6.1●
SVI	35.1 ± 0.2	−0.1 ± 0.0	−1.2 ± 0.0	1.2 ± 0.0	263.8 ± 1.3	35.4 ± 0.9	0.0 ± 0.1●	−1.4 ± 0.3	1.4 ± 0.3	270.7 ± 2.5●
CTÑ	36.8 ± 0.3	−0.1 ± 0.1	−1.4 ± 0.0	1.4 ± 0.0	267.5 ± 2.5	35.7 ± 0.8●	0.0 ± 0.1	−1.8 ± 0.2●	1.9 ± 0.2●	270.4 ± 3.9
LMO	41.6 ± 1.1	−0.3 ± 0.0	−0.9 ± 0.1	1.0 ± 0.1	251.4 ± 2.1	36.5 ± 1.4●	−0.1 ± 0.0●	−0.8 ± 0.3	0.8 ± 0.3	264.0 ± 3.7●
ROZ	35.0 ± 0.1	−0.1 ± 0.0	−1.3 ± 0.1	1.3 ± 0.1	263.9 ± 3.3	35.3 ± 0.3●	0.0 ± 0.0●	−1.5 ± 0.1	1.5 ± 0.1	268.5 ± 1.7●
CST	37.4 ± 1.3	−0.1 ± 0.1	−0.8 ± 0.1	0.8 ± 0.1	264.2 ± 4.7	38.0 ± 0.7	−0.1 ± 0.1	−1.5 ± 0.2●	1.5 ± 0.1●	265.6 ± 2.4
TRA	38.5 ± 2.7	−0.1 ± 0.0	−1.3 ± 0.1	1.3 ± 0.1	265.8 ± 1.2	36.5 ± 0.6●	0.0 ± 0.1●	−1.6 ± 0.2●	1.6 ± 0.2●	270.4 ± 2.1●
3C	38.6 ± 0.6	−0.1 ± 0.0	−0.7 ± 0.1	0.7 ± 0.1	263.5 ± 3.0	38.1 ± 0.5●	0.0 ± 0.1	−1.4 ± 0.1●	1.4 ± 0.1●	268.6 ± 2.8
PIV	37.6 ± 0.6	0.0 ± 0.0	−0.9 ± 0.1	0.9 ± 0.1	267.3 ± 1.6	37.3 ± 1.1	0.0 ± 0.1	−1.5 ± 0.2●	1.5 ± 0.2●	270.1 ± 3.8
CAP	40.5 ± 0.5	−0.2 ± 0.0	−1.0 ± 0.0	1.1 ± 0.1	259.1 ± 1.5	40.0 ± 0.7	−0.2 ± 0.1	−1.5 ± 0.1●	1.5 ± 0.1●	261.0 ± 4.4
RIO	38.6 ± 0.2	−0.2 ± 0.0	−1.2 ± 0.0	1.2 ± 0.0	260.7 ± 1.7	38.2 ± 0.7	−0.1 ± 0.1	−1.5 ± 0.1●	1.5 ± 0.1●	264.9 ± 3.5
CAM	39.3 ± 0.2	−0.1 ± 0.1	−1.0 ± 0.1	1.0 ± 0.1	263.0 ± 3.1	38.3 ± 0.4●	−0.1 ± 0.1	−1.3 ± 0.1●	1.3 ± 0.1●	264.3 ± 3.5
DOM	39.4 ± 0.2	−0.1 ± 0.0	−1.1 ± 0.0	1.1 ± 0.0	262.1 ± 2.1	39.0 ± 0.4	−0.1 ± 0.1	−1.5 ± 0.2●	1.5 ± 0.2●	264.8 ± 3.3
VIA	36.3 ± 0.5	−0.1 ± 0.1	−0.9 ± 0.0	0.9 ± 0.0	264.6 ± 4.1	35.3 ± 0.3●	0.0 ± 0.1	−1.3 ± 0.1●	1.3 ± 0.1●	268.5 ± 4.7
GMP	35.8 ± 0.9	0.0 ± 0.1	−0.7 ± 0.2	0.7 ± 0.2	268.2 ± 12.1	35.8 ± 0.7●	0.0 ± 0.0●	−1.2 ± 0.2●	1.2 ± 0.2●	269.7 ± 1.7
GMI	39.8 ± 0.2	−0.1 ± 0.0	−1.0 ± 0.0	1.0 ± 0.0	263.0 ± 0.9	39.1 ± 0.6●	−0.1 ± 0.1	−1.4 ± 0.1●	1.4 ± 0.1●	266.4 ± 2.3
OFON	35.7 ± 0.8	−0.1 ± 0.0	−0.7 ± 0.1	0.7 ± 0.1	264.6 ± 1.0	35.1 ± 0.7	0.0 ± 0.1	−1.1 ± 0.2●	1.1 ± 0.2●	270.6 ± 6.6
OFOH	36.6 ± 0.6	0.0 ± 0.0	−0.7 ± 0.1	0.7 ± 0.1	269.0 ± 1.5	36.1 ± 2.1	0.0 ± 0.1	−0.9 ± 0.3	0.9 ± 0.3	266.9 ± 4.1
SVE	39.4 ± 0.2	0.0 ± 0.0	−1.0 ± 0.1	1.0 ± 0.0	267.5 ± 0.7	38.5 ± 0.5●	−0.2 ± 0.1	−1.6 ± 0.1●	1.6 ± 0.1●	264.4 ± 2.7
ROC	37.7 ± 0.5	−0.1 ± 0.1	−0.5 ± 0.1	0.6 ± 0.1	258.2 ± 6.9	37.4 ± 0.6●	−0.1 ± 0.1	−1.0 ± 0.1●	1.0 ± 0.1●	266.0 ± 3.6
UPA3	36.2 ± 0.2	0.0 ± 0.0	−0.9 ± 0.0	0.9 ± 0.0	266.6 ± 2.1	35.5 ± 0.2●	0.0 ± 0.1	−1.3 ± 0.1●	1.3 ± 0.1●	268.5 ± 4.1
CU4	35.8 ± 0.0	0.0 ± 0.0	−0.9 ± 0.1	0.9 ± 0.1	267.1 ± 2.8	34.9 ± 1.0	0.0 ± 0.1	−1.1 ± 0.2●	1.1 ± 0.2●	268.2 ± 6.4
CU6	36.6 ± 0.5	0.0 ± 0.0	−0.7 ± 0.1	0.7 ± 0.1	265.6 ± 2.2	35.8 ± 0.4●	−0.1 ± 0.1	−1.2 ± 0.1●	1.2 ± 0.1●	265.4 ± 5.7
UPA7	36.4 ± 0.2	−0.1 ± 0.0	−0.7 ± 0.1	0.7 ± 0.1	263.0 ± 2.0	35.9 ± 0.5	−0.1 ± 0.1	−1.1 ± 0.2●	1.1 ± 0.2●	263.3 ± 6.0
CU10	36.7 ± 0.4	0.0 ± 0.0	−0.8 ± 0.0	0.8 ± 0.0	269.0 ± 1.2	36.1 ± 0.9	−0.1 ± 0.1	−1.2 ± 0.2●	1.2 ± 0.2●	265.8 ± 5.1
CU13	37.0 ± 0.2	0.0 ± 0.1	−0.9 ± 0.1	0.9 ± 0.1	268.7 ± 4.9	37.2 ± 0.6	−0.1 ± 0.1	−1.1 ± 0.6	1.1 ± 0.5	250.2 ± 43.5●
CU14	38.1 ± 0.5	−0.2 ± 0.0	−0.9 ± 0.0	0.9 ± 0.0	259.1 ± 1.7	37.2 ± 0.3	−0.1 ± 0.1	−1.3 ± 0.1●	1.3 ± 0.1●	266.4 ± 3.1●
CU25	36.1 ± 0.3	0.0 ± 0.0	−0.7 ± 0.1	0.7 ± 0.1	266.4 ± 2.8	35.5 ± 0.5	0.0 ± 0.1	−1.3 ± 0.1●	1.3 ± 0.1●	270.9 ± 4.4
VAZ	38.7 ± 0.3	−0.1 ± 0.0	−0.9 ± 0.0	0.9 ± 0.0	261.1 ± 2.2	35.1 ± 1.3●	0.0 ± 0.1●	−0.8 ± 0.2	0.8 ± 0.2	273.3 ± 5.0●
TEM	37.3 ± 0.3	−0.1 ± 0.0	−0.9 ± 0.1	0.9 ± 0.0	263.1 ± 2.2	36.4 ± 0.7●	0.0 ± 0.0	−1.3 ± 0.2●	1.3 ± 0.2●	267.9 ± 1.7
ITA	37.9 ± 0.1	−0.1 ± 0.0	−0.9 ± 0.0	0.9 ± 0.0	264.0 ± 2.1	37.2 ± 0.3●	0.0 ± 0.1	−1.3 ± 0.1●	1.3 ± 0.1●	269.0 ± 2.6
GAL	35.3 ± 0.7	−0.1 ± 0.1	−0.8 ± 0.2	0.8 ± 0.2	266.4 ± 4.0	35.3 ± 0.4	0.0 ± 0.1	−1.5 ± 0.1●	1.5 ± 0.1●	270.1 ± 5.7
GON	37.2 ± 0.2	−0.1 ± 0.0	−0.7 ± 0.1	0.7 ± 0.1	257.8 ± 7.6	36.5 ± 0.2●	−0.1 ± 0.1	−1.2 ± 0.1●	1.3 ± 0.1●	263.8 ± 4.7
RFR	39.6 ± 0.7	−0.2 ± 0.0	−0.9 ± 0.0	0.9 ± 0.0	258.1 ± 0.3	39.5 ± 0.5●	−0.1 ± 0.1	−1.3 ± 0.1●	1.3 ± 0.2●	264.1 ± 4.1
ALI	36.8 ± 0.3	−0.1 ± 0.0	−1.1 ± 0.1	1.1 ± 0.1	262.1 ± 2.6	37.2 ± 0.3	−0.1 ± 0.1	−1.5 ± 0.1●	1.6 ± 0.1●	264.9 ± 3.6
BRN	42.5 ± 0.4	−0.3 ± 0.1	0.3 ± 0.2	0.5 ± 0.1	143.6 ± 17.9	41.2 ± 1.3●	−0.4 ± 0.1	0.0 ± 0.6	0.6 ± 0.3	189.4 ± 47.2
VDR	33.7 ± 0.0	0.0 ± 0.1	−0.9 ± 0.1	0.9 ± 0.1	270.3 ± 4.8	33.5 ± 0.2●	0.1 ± 0.1●	−1.6 ± 0.1●	1.6 ± 0.1●	272.5 ± 2.9●
VAL	35.5 ± 0.2	−0.1 ± 0.1	−0.9 ± 0.0	0.9 ± 0.0	262.2 ± 5.0	35.3 ± 0.4●	0.0 ± 0.1●	−1.3 ± 0.1●	1.3 ± 0.1●	268.0 ± 4.2●
ARO	37.8 ± 0.1	−0.1 ± 0.0	−1.1 ± 0.1	1.1 ± 0.1	263.5 ± 0.3	37.3 ± 0.2	−0.1 ± 0.1	−1.6 ± 0.1●	1.6 ± 0.1●	266.3 ± 2.0

CIELAB data for each of the 50 roofing slates are the mean values from three specimens (six measurements per specimen) ± S.D.
● indicates significant differences ($p < 0.05$) between each of the CIELAB color parameter measured in SCI and SCE mode for each type of roofing slate.

The range of values of h_{ab}: 143.6 ± 17.9 to 271.9 ± 2.0 in SCI mode and 155.3 ± 2.6 to 273.3 ± 5.0 in SCE mode enabled identification of possible tones of roofing slates in the a^*-b^* diagram; tones resulting from the combination of red and yellow were thus excluded (Fig. 5).

Inclusion or exclusion of the specular component was important for measurement of the color of specimens of roofing slate as there were significant differences in the Student *t*-test (at $p < 0.05$), between both modes in at least one of the CIELAB color coordinates in all commercial varieties, except CU13, VLU and OFOH, for which the coordinates did not differ significantly between SCI and SCE modes (Table 4). In this regard, b^* and C^*_{ab} were significantly different in most of the fifty roofing slates, L^* in more than half of them, and h_{ab} and a^* in less than fifteen commercial varieties, with the color measured in SCE mode darker and stronger (larger L^* and C^*_{ab}) and with larger hue angles and green and blue components than in SCI mode.

In order to group the Iberian roofing slates into homogeneous color groups, a hierarchical classification was made by application of Cluster Analysis to the dissimilar varieties of roofing slates according to the coordinates most closely related to the human perception factors ($L^*C^*_{ab}h_{ab}$) measured in both SCI and SCE modes. The HCA of the 50 commercial varieties yielded the dendrograms shown in Fig. 6. In both dendrograms most of the roofing slates were grouped so that only eight or six roofing slates were included in the remaining two or three groups in SCI or SCE modes, respectively. It should be noted that the last group in both dendrograms, characterized by the largest Euclidean distance from the other groups, is formed by the same commercial varieties (BRN, VXE, GLU and VLU); these are therefore the most different in color roofing slates, irrespective of the measuring mode. The EUP commercial variety was colorimetrically different from the roofing slates in the major group and from those in the last group in both measuring modes.

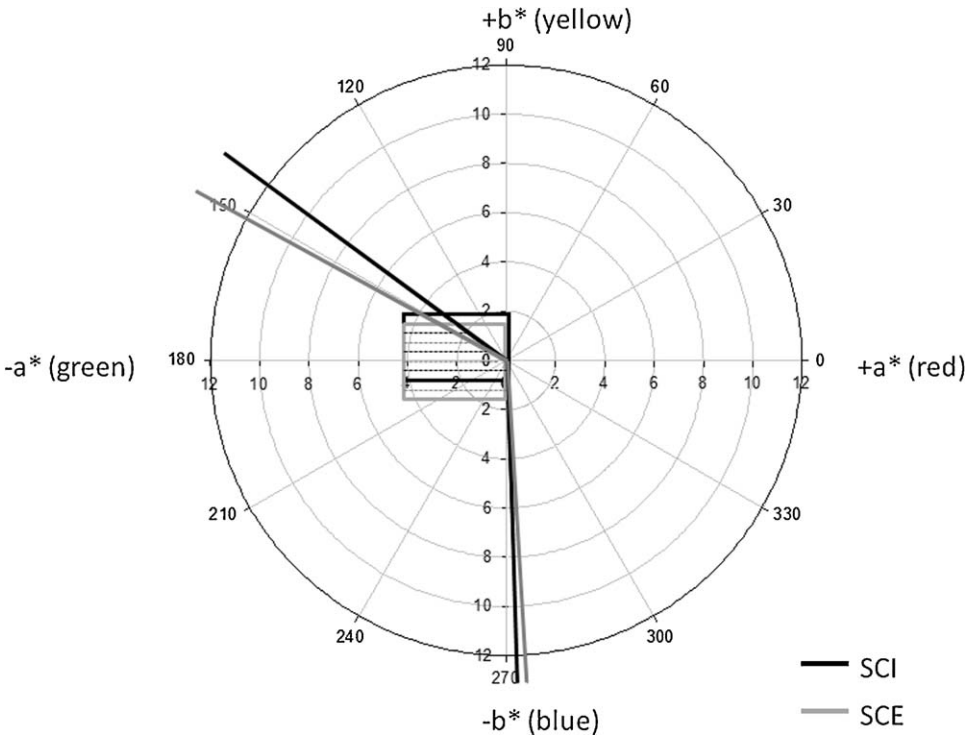

Fig. 5. a*-b* diagram: representation of the area in which the parameter a*, b* and h_{ab} of the 50 surveyed roofing slates, using the specular component included (SCI) and excluded (SCE) modes, are included.

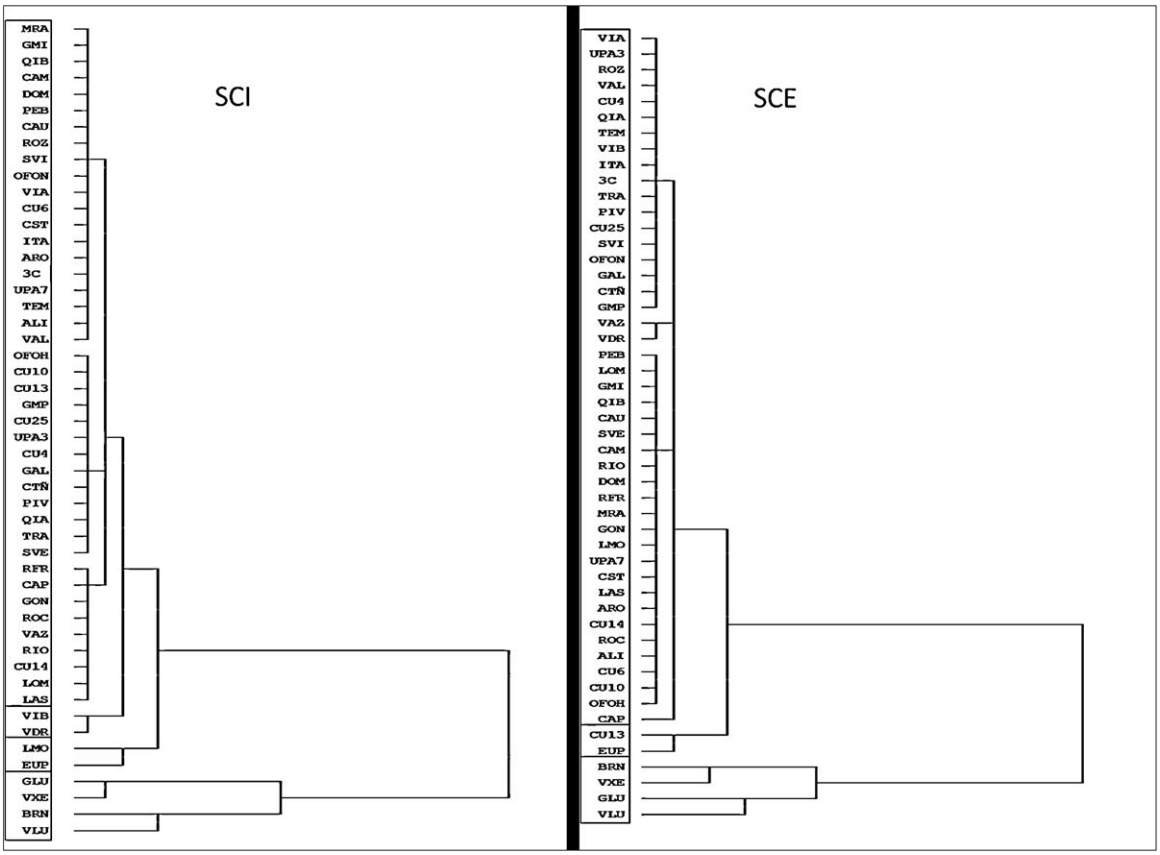

Fig. 6. Hierarchical cluster analysis (HCA) dendrogram of the Iberian roofing slates according to the coordinates most closely related to human perception factors ($L^*C^*_{ab}h_{ab}$) measured in both SCI and SCE modes. The dendrogram was calculated using the average linkage between groups based on the Euclidean distance.

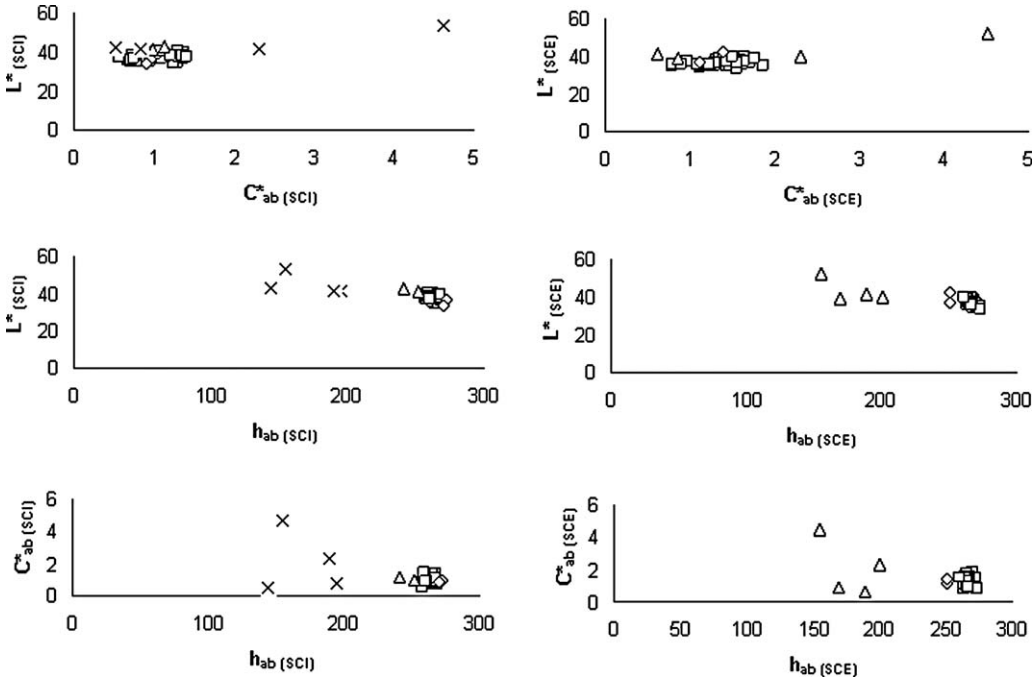

Fig. 7. Each L^*, C^*_{ab}, h_{ab} coordinate in SCI (left) and SCE (right) modes of the Iberian roofing slates into homogeneous color groups plotted against each other.

The VIB, VDR, LMO and CU13 varieties were classified in different groups depending on the measuring mode. Selection of the measuring mode is therefore important in the characterization of the color of roofing slates when the aim of the study is to classify homogeneous color groups.

To check which of the cylindrical coordinates caused the associations in the dendrogram, each $L^*_{(SCI)}$, $C^*_{ab\ (SCI)}$, $h_{ab\ (SCI)}$ and $L^*_{(SCE)}$, $C^*_{ab\ (SCE)}$, $h_{ab\ (SCE)}$ coordinate was plotted against each other (Fig. 7). The L^* and C^*_{ab} values did not discriminate among groups as, for instance, the most (VLU) and the least (BRN) chromatic roofing slates were included in the same group. However the first group was composed by the roofing slates with the highest h_{ab} values, and the last group by roofing slates with the lowest h_{ab} values. Hence, the qualitative expression of colorfulness, hue angle h_{ab}, was the most important color coordinate in the formation of homogeneous color groups. Taking into account that slate is a dark-medium gray slightly chromatic material, and that the hue angle is the attribute that allows a color to be distinguished in reference to a gray color of the same lightness [26], h_{ab} will logically have the highest discriminatory power in differentiating Iberian roofing slates.

As the final aim of this study was to provide information for adequate replacement of roofing slates in restoration work, it is important to establish the colorimetric similarity between roofing slates in the same homogeneous color group. Thus, the total color differences (ΔE^*_{ab}) between roofing slates from the same group were calculated in each measuring mode. Four ranges of colorimetric similarity were established between pairs of slate samples (Fig. 8). The limit of acceptability of replacement of one type of slate by another was established as 3 CIELAB units; below this limit, three ranges of replacement were established, considering that the difference in color between the slates was highly acceptable, of intermediate acceptability or low acceptability. Thus, pairs of slate samples with ΔE^*_{ab} values between 0 and 1 CIELAB unit, defined as the visual color difference threshold or just noticeable difference (jnd) which constitutes the lower limit of perception in an individual with normal color vision [26], are considered highly acceptable for replacement. Samples with ΔE^*_{ab} values of between 1 and 1.75 CIELAB units, considered as the suprathreshold color-difference [31], are considered of intermediate acceptability for replacement; those with ΔE^*_{ab} values comprised of between 1.75 and 3 CIELAB units, the upper limit of rigorous color tolerance [26,30], are considered of low acceptability for replacement. Pairs of slate samples for which the total color difference (ΔE^*_{ab}) is greater than 3 CIELAB units should not be used to replace each other.

For the data measured in specular component included (SCI) mode, slates LOM, ITA and ARO can replace and be replaced with greater or lesser acceptability by any of the slates in the main group. Of these ITA and ARO can be equally replaced by any of the other slates in the group, except ALI, for which replacement with ARO is preferred, as the color differences was less than 1 CIELAB unit, whereas the color differences with ITA was less than 1.75 CIELAB units. In the same way, replacement of LOM, ITA and ARO is highly acceptable ($\leq$ 1 CIELAB unit), for 16 of the 41 slates in the group (without considering ALI), of intermediate acceptability (> 1 CIELAB unit and $\leq$ 1.75 CIELAB units) for 12 of the 41 slates and of low acceptability (> 1.75 CIELAB units and $\leq$ 3 CIELAB units) for 13 of the 41 slates.

The commercial varieties QIA, LAS, PIV and ROC can be replaced, with greater or lower acceptability by all of the slates in the group except CAU, whereas the commercial varieties CST, CU13, TEM and GON can be replaced by any of the slates in the group except CAU and CAP; the slates that are most difficult to replace are therefore CAU and CAP.

In the data set measured in specular component excluded (SCE) mode, none of the slates can be replaced by all of the other slates. The slates that are easiest to replace, independently of the degree of acceptability are LAS, PIV, ROC, CU14, ITA, ALI and ARO, which are exchangeable with all of the slates in the group, except VDR, which interestingly was not included in the first group, but rather in the second group in the data measured in SCI mode. Considering the range of ΔE^*_{ab} between 0 and 1 CIELAB units: UPA3, UPA7, CU6, CU10 and CU25 are highly acceptable for replacement by 19 of the 44 slates in the group.

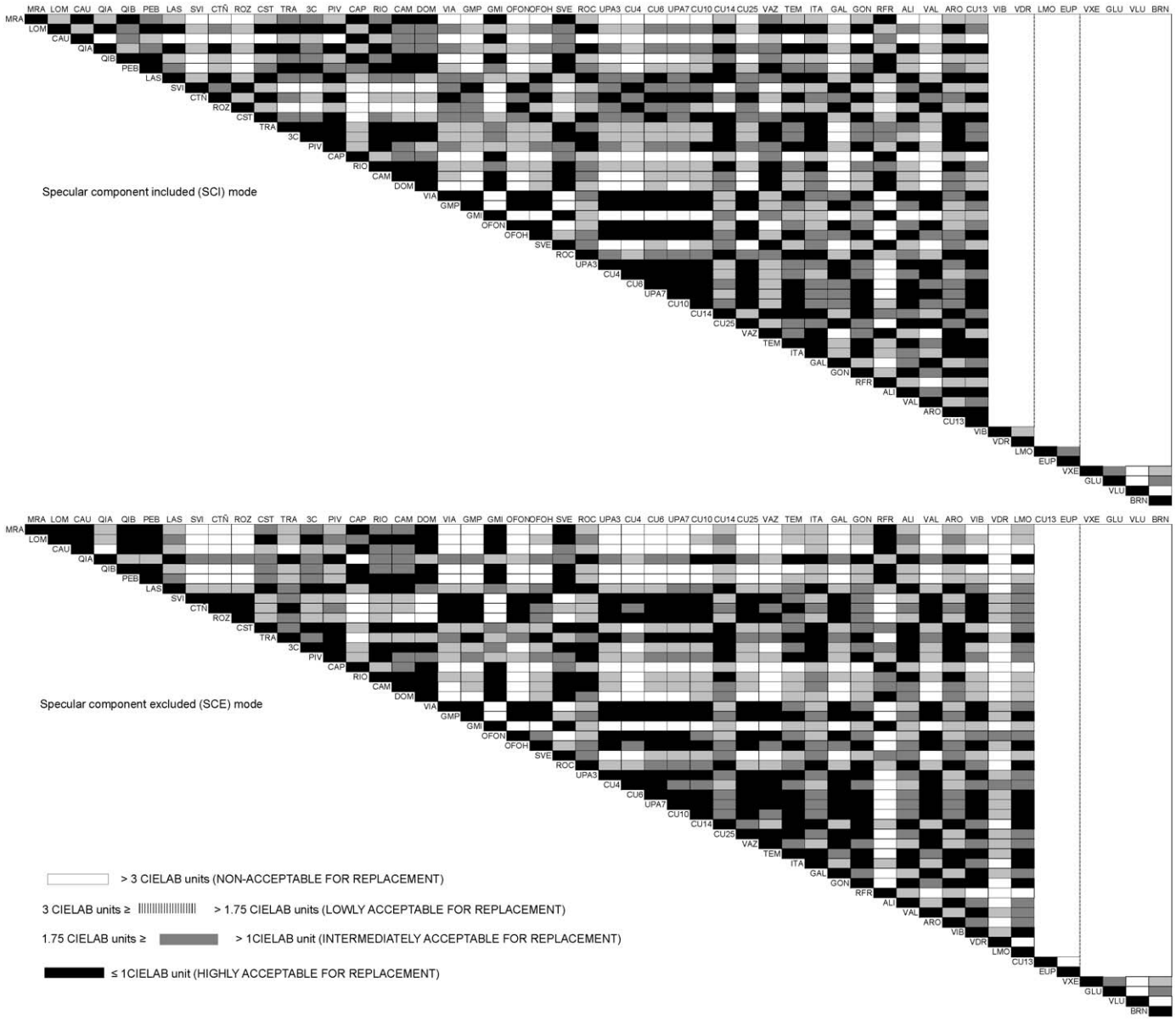

Fig. 8. Total color differences (ΔE^*_{ab}) between roofing slates.

The commercial variety VDR, followed by CAU and CAP, are the slates that are most difficult to replace. If the degree of acceptability for replacement is not taken into account, CAU is exchangeable with the same slates that CAP, which is not true for the set of data measured in specular component included (SCI) mode.

In the second and third group of data measured in specular component included (SCI) mode, slates are difficult to replace since exchange is only possible with low acceptability in the second group and with intermediate acceptability in the third group. In the second group of data measured in specular component excluded (SCE) mode, the slates are not replaceable. In the fourth group of data measured in specular component included (SCI) mode, which matches the third group of data measured in specular component excluded (SCE) mode, three of the four slates in the group (BRN, VXE and GLU) can be used to replace each other, but VLU cannot be used to replace any of the others in the group.

Taking into account both sets of data, measured in specular component included (SCI) and excluded (SCE) modes, it can be concluded that the slates that are easiest to replace by all 50 Iberian roofing slates are ITA and ARO, and to a lesser extent LAS, PIV and ROC, whereas the slate that is most difficult to replace is VLU.

Analysis of the data in Fig. 8 reveals that samples from the same area are not more similar in terms of colorimetry than samples from different areas, and therefore the region of origin should not be used as a criterion for substitution of Iberian Roofing slates. In addition, on comparing the results obtained in both measuring modes, it can be seen that the specular component excluded (SCE) mode accentuates the differences in color between the Iberian roofing slates, with more cases in which the value of ΔE^*_{ab} is greater than 3. In this regard, the difference between the value of ΔE^*_{ab} in SCI mode and in SCE mode may be as high as 3.6 CIELAB units, as for example, occurs on comparing the color of the samples of RFR and VAZ (ΔE^*_{ab} (SCI): 0.9; ΔE^*_{ab} (SCE): 4.5). Thus, the SCE geometry should be considered as more appropriate in restoration work with roofing slates, since this mode magnifies the color differences.

Table 5
Values of Lineation L_0 and S_1/S_0 Angle measured in the section parallel to lineation.

Roofing slate	Mining district	S_1/S_0 Angle	Lineation L_0
GLU	2	0	No trace
VLU	2	0	No trace
VXE	2	0	No trace
CAU	3	0	Slight
LAS	3	0	Slight
PEB	3	0	Slight
QIA	3	0	Slight
VIB	3	0	Slight
3C	5	0	Slight
CAM	5	0	Slight
CAP	5	0	Slight
CST	5	0	Slight
LMO	5	0	Slight
RIO	5	0	Slight
SVE	5	0	Slight
SVI	5	0	Slight
ROC	6	0	Slight
CU25	7	0	Slight
GAL	7	0	Slight
TEM	7	0	Slight
VAZ	7	0	Slight
ALI	8	0	Slight
VDR	10	0	Slight
VAL	11	0	Slight
ARO	12	0	Slight
RFR	8	5	Slight
EUP	4	15	Slight
ITA	7	10	Slight
QIB	3	0	Moderate
BRN	9	0	Moderate
LOM	1	5	Moderate
CU6	7	10	Moderate
PIV	5	15	Moderate
CU10	7	15	Moderate
MRA	1	25	Moderate
CU4	7	30	Moderate
UPA/	7	30	Moderate
TRA	5	40	Moderate
DOM	5	45	Moderate
VIA	5	45	Moderate
GMI	5	50	Moderate
CU13	7	70	Moderate
GON	7	0	Pronounced
UPA3	7	20	Pronounced
OFON	5	35	Pronounced
CTÑ	5	40	Pronounced
OFOH	5	45	Pronounced
ROZ	5	50	Pronounced
CU14	7	50	Pronounced
GMP	5	55	Pronounced

It is important to note that the colorimetric study has been carried out on freshly exposed rocks and it is well known that colors of the roofing slates can change as a result of the weathering of minerals components such as carbonates and iron sulfides. Slates with high carbonate contents, as some Spanich slates or the Ligurian slate undergo gypsification processes, which whiten the slate surface [1,32], while high contents in iron sulfides lead to oxidation processes, which stain or redden the slate [1]. However, nowadays no studies concerning the objective characterization of color in roofing slates have yet been published and therefore there are no objective data on color variation, which would be helpful in discussing the limits of acceptability for the replacement of one type of slate by another. Thus, future research should be focus on variation of color slates with time.

3.3. Microstructure characterization: S_1/S_0 angle and Lineation L_0

The values of the S_1/S_0 angle and Lineation L_0 are shown in Table 5. As higher the S_1/S_0 angle is, the trace of L_0 is more marked in the slate surface and therefore more visible with naked eye. Thickness of S_0 on the slate surface is determined by the original thickness of S_0 and by the S_1/S_0 angle, and, when present, it should be below a few centimetres thickness to consider the outcrop for mining [33]. Besides the S_1/S_0 angle, structural situation of the quarry determines the intensity of the lineation, since slates quarried in the hinge area of regional folds present a marker lineation, due to the structural deformation suffered in these areas.

Most of the Iberian roofing slates have a slight lineation (Table 5) and only eight of them have a pronounced lineation. However, this pronounced lineation is not perceptible with naked eye in the studied roofing slates as it can be seen in Fig. 2 were the appearance of the slate with the highest S_1/S_0 angle (CU13) could be compared to the appearance of some of the slates which were considered in Section 3.2 as replaceable by CU13. Thus, we can consider that in the whole of the samples analyzed the microstructures features should be considered as a secondary substitution criterion after color criterion.

Taking into account the intensity of the lineation of the samples ITA, ARO, LAS, PIV and ROC, which were considered in Section 3.2 as the slates that can replace all the 50 Iberian roofing slates, all of them except PIV would be appropriate for replacing slates with no trace or slight lineation, and PIV would be appropriate for replacing slates with moderate or pronounce lineation.

4. Conclusions

The results of the colorimetric study of 50 commercial varieties of slate extracted from the 12 different slate mining districts in the Iberian Peninsula showed that:

- a protocol is required for the colorimetric characterization by contact color-measurement devices of this type of material, as the number of measurements per unit of area will depend on the commercial variety and the size the measuring head of the measuring device. Analysis of the data obtained in this study shows that color measurements on roofing slates are reproducible and comparable if they are carried out on an area of at least 36 cm^2, and 7, 6, 6 or 3 measurements/36 cm^2 are made with measuring heads of 5, 8, 10 or 50 mm diameter viewing aperture, respectively;
- the inclusion or exclusion of the specular component is important for measurement of the color of roofing slate specimens as significantly different results were obtained in the two measuring modes. This must be taken into account when the total color difference (ΔE^*_{ab}) is the subject of the study since the specular component excluded (SCE) mode magnifies this difference;
- the color of the roofing slates from the Iberian Peninsula ranged from maximum values of L^*: 53.19 ± 0.2; a^*: 0.0 ± 0.0; b^*: 2.0 ± 0.1; C^*_{ab}: 4.6 ± 0.1; h_{ab}: 271.9 ± 2.0, and minimum values of L^*: 33.7 ± 0.0; a^*: -4.2 ± 0.1; b^*: -1.4 ± 0.1; C^*_{ab}: 0.5 ± 0.1; h_{ab}: 143.6 ± 17.9 in the specular component included (SCI) mode, and from maximum values of L^*: 52.4 ± 0.7; a^*: 0.1 ± 0.1; b^*: 1.9 ± 0.3; C^*_{ab}: 4.5 ± 0.2; h_{ab}: 273.3 ± 5.0 and minimum values of L^*: 33.5 ± 0.2; a^*: -4.1 ± 0.1; b^*:-1.8 ± 0.2, C^*_{ab}: 0.6 ± 0.3; h_{ab}: 155.3 ± 2.6, in the specular component excluded (SCE) mode;
- the hue angle (h_{ab}) was the most important CIELAB color coordinate in the formation of homogeneous color groups;
- considering the limits of colorimetric perception, the commercial varieties ITA, ARO, LAS, PIV and ROC can be used to replace and can be replaced by most of the 50 commercial varieties of Iberian roofing slate, whereas VLU cannot be replaced by any of the other types of slate. Considering the lineation, ITA, ARO, LAS and ROC

would be appropriate for replacing slates with no trace or slight lineation, and PIV would be appropriate for replacing slates with moderate or pronounce lineation.

Thus, in this work the general guidelines related to color that should be followed when repairing or replacing slate tiles in a roof, in order to achieve the directives recommended by the international organisms [12] are exposed. Taking into account that an adequate protocol to replace slate slabs must tackle in addition to the aesthetic aspects described in the article, the aspects related to the temporal evolution of the slab in the roof in relation to the unreplaced slabs, future considerations would be focused on the natural weathering of slate in the roof.

Acknowledgements

The present study was financed by the Xunta de Galicia (09TMT014203PR) and the Science and Innovation Ministry of Spain (BES-2007-16996).

References

[1] M. Lombardero, J. García-Guinea, V. Cárdenes, The geology of roofing slate, in: P.W. Scott, C.M. Bristow (Eds.), Industrial minerals and extractive industry geology, Geological Society, London, 2002, pp. 59–65.
[2] M.S. Briggs, Building-construction, in: C. Singer, E.J. Holmyard, A.R. Hall (Eds.), A history of technology, Oxford University Press, 1954, pp. 398–447.
[3] M. Lombardero, M. Regueiro, Spanish natural stone: cladding the world, Industrial Minerals 300 (1992) 81–97.
[4] I. García Tato, A Explotación Louxeira no Concello de Carballeda, Cuadernos Monográficos, Instituto de Estudios Valdeorreses 16, 1994.
[5] J. García-Guinea, M. Lombardero, B. Roberts, J. Taboada, Spanish roofing slate deposits, Transactions of the Institute of Mineral Metallurgy, Section B 106 (1997) 205–214.
[6] C.W. Passchier, Trouw RAJ. Microtectonics, Springer-Verlag, 2005.
[7] V. Cárdenes, M. Lombardero, J. García-Guinea, J.C. Barros, Factores de calidad en la elaboración de placas de pizarra para cubiertas en Galicia y León, Roc. Máquina 67 (2001) 90–98.
[8] V. Cárdenes Van den Eynde, A. Rubio Ordoñez, A. López-Munguira, R. De la Horra, C. Monterroso, R. Paradelo, et al., Mineralogy and modulus of rupture of roofing slate: applications in the prospection and quarrying of slate deposits, Engineering Geology 114 (2010) 191–197.
[9] W. Wagner, The basics of test methods of slates for roofing and cladding. Grundlagen für die Prüfung von Dach- und Wandschiefern, Zeitschrift der Deutschen Gesellschaft für Geowissenschaften 158 (4) (2007) 785–805.
[10] J. Taboada, A. Vaamonde, A. Saavedra, A. Arguelles, Quality index for ornamental slate deposits, Engineering Geology 50 (1998) 203–210.
[11] R. Dreesen, M. Dusar, Historical building stones in the province of Limburg (NE Belgium): role of petrography in provenance and durability assessment, Materials Characterization 53 (2004) 273–287.
[12] ICOMOS. Council of Europe 1975: European Charter of the Architectural Heritage, Amsterdam. Declaration: Congress on the European Architectural Heritage, 21–25 October (1975).
[13] C. Brandi, Teoría de la Restauración. Alianza Forma, Alianza Editorial, Madrid, 2002.
[14] AAVV, Repairing Scottish slate roofs, Historic Scotland. Published by Technical Conservation, Research and Education Group, 2006.
[15] W. Wagner, R. Le Bail, M. Hacar, S. Stanek, European Roofing Slates Part 1: remarks to the geology of mineral deposits, Zeitschrift der Deutschen Gesellschaft für Geowissenschaften 40 (1994) 68–74.
[16] C.R. Ward, F. Gómez-Fernández, Quantitative mineralogical analysis of Spanish roofing slates using the Rietveld method and X-ray powder diffraction data, European Journal of Mineralogy 15 (2003) 1051–1062.
[17] F. Gómez-Fernández, M.A. Castaño, B. Bauluz, C. Ward, Optical microscope and SEM evaluation of roofing slate fissility and durability, Materiales de Construcción 59 (296) (2009) 91–104.
[18] V. Cárdenes, R. de la Horra, C. Monterroso, J. García-Guinea, V. Pais, Depósitos de pizarras para cubiertas en la Península Ibérica, Sociedad Geológica de España, Las Palmas de Gran Canaria, 2008.
[19] D. Fettes, J. Desmons, Metamorphic rocks: a classification and glossary of terms, CU Press, 2007.
[20] F. Gómez-Fernández, C. Ward, B. Bauluz, XRD, electron microscopy (EMPA, SEM, TEM) and XRF characterization of roofing slates from NW Spain, Cuadernos do Laboratorio Xeolóxico de Laxe 34 (2009) 127–142.
[21] CEN/TC_128. EN 12326. Slate and stone products for discontinuous roofing and cladding - Parts 1 (Product Specification) and 2 (Methods of test), 2005.
[22] B. Prieto, P. Sanmartín, B. Silva, F.M. Martínez-Verdú, Measuring the color of granite rocks: a proposed procedure, Color Research and Application 35 (5) (2010) 368–375.
[23] Y.K. Lee, B.S. Lim, C.W. Kim, J.M. Powers, Color characteristics of low-chroma and high-translucence dental resin composites by different measuring modes, J. Biomed Mater Res (Appl Biomater) 58 (2001) 613–621.
[24] I.J. Kim, Y.K. Lee, B.S. Lim, C.W. Kim, Effect of surface topography on the color of dental porcelain, Journal of Materials science: Materials in Medicine 14 (2003) 405–409.
[25] I. Ariño, S. Johansson, U. Kleist, E. Liljenström-Leander, M. Rigdahl, The effect of texture on the pass/fail color tolerances of injection-molded plastics, Color Research and Application 32 (2007) 47–54.
[26] G. Wyszecki, W.S. Stiles, Color Science. Concepts and Methods. Quantitative Data and Formulae, Wiley, New York, 1982.
[27] F. Catalina, J.M. Bruna, Principios de colorimetría práctica. Sistema CIE de medida diferencial de color, Rev Plásticos Modernos 488 (1997) 164–171.
[28] R.S. Berns, Billmeyer and Saltzmanïs Principles of Color Technology, 3rd Ed., New John Wiley and Sons, New York, 2000.
[29] R. Huertas, M. Melgosa, E. Hita, Influence of random-dot textures on perception of suprathreshold color differences, Journal of the Optical Society of America A 23 (2006) 2067–2076.
[30] H.G. Völz, Industrial color testing, Wiley–VCH, Weinheim, 2001.
[31] M. Melgosa, E. Hita, A.J. Poza, D.H. Alman, R.S. Berns, Suprathreshold color-difference ellipsoids for surface colors, Color Research and Application 22 (1997) 148–155.
[32] F. Cimmino, F. Faccini, A. Robbiano, Stones and coloured marbles of Liguria in historical monuments, Periodico di Mineralogia 73 (2003) 71–84.
[33] J.C. Barros, M. Castaño, M. Hacar, M. Lombardero, A. Olmo, Metodología de investigación de los yacimientos de pizarras para cubiertas, Cuadernos do Laboratorio Xeolóxico de Laxe 10 (1985) 429–444.

Chapter 9. El color como indicador de la intensidad de los incendios en suelos de Galicia: Resultados preliminares / Color as an indicator of fire intensity on soils of Galicia, NW Spain: Preliminary results

Sanmartín, P.; Cancelo-González, J.; Rial, M.E.; Silva, B.; Díaz-Fierros, F.; Prieto, B.

Óptica Pura y Aplicada 43 (3): 167-172 (2010)

SJR index 2010 = 0.033 (55/68, 81 percentile in Atomic and Molecular Physics and Optics)

Total number of times cited: 0

Sección Especial: IX Congreso Nacional del Color

El color como indicador de la intensidad de los incendios en suelos de Galicia: Resultados preliminares

Color as an indicator of fire intensity on soils of Galicia, NW Spain: Preliminary results

Patricia Sanmartín(*,S), Javier Cancelo-González, María E. Rial, Benita Silva, Francisco Díaz-Fierros, Beatriz Prieto

Departamento de Edafología y Química Agrícola, Facultad de Farmacia, Universidad de Santiago de Compostela. Campus Vida, 15782 -A Coruña, España.

(*) Email: patricia.sanmartin@usc.es S: miembro de SEDOPTICA / SEDOPTICA member

Recibido / Received: 13/07/2010. Versión revisada / revised versión: 16/09/2010. Aceptado / Accepted: 17/09/2010

RESUMEN:

Este trabajo pretende ser una primera aproximación al estudio de la relación existente entre las variaciones de color que se producen en los suelos gallegos y la temperatura que éstos alcanzan durante un incendio, con el fin de valorar el uso del color del suelo como indicador de la intensidad de un incendio. Con este fin se realizó una quema controlada de muestras inalteradas del horizonte superficial de un Regosol úmbrico en el laboratorio empleando lámparas de infrarrojos hasta alcanzar una temperatura de 200ºC y 400ºC a 1 cm de profundidad desde la superficie, utilizando muestras sin quemar como control. Sobre la superficie de cada una de las muestras quemadas y sin quemar se determinó el color en 220 puntos con un colorímetro portátil, trabajando posteriormente con las notaciones de color Munsell y CIELAB. Los resultados obtenidos mostraron cambios significativos en el tono (*Hue* Munsell y h_{ab} CIELAB), entre las muestras que alcanzaron distintas temperaturas, no así en los valores de intensidad (*Croma* Munsell y C^*_{ab} CIELAB) y claridad (*Value* Munsell y L^* CIELAB), que sólo variaron de forma significativa entre las muestras sin quemar y las muestras quemadas. Esto parece indicar que será el tono el parámetro a tener en cuenta en el uso del color como indicador de la intensidad de incendios en suelos de Galicia.

Palabras clave: Color del Suelo, Intensidad del Incendio, Quema Controlada, CIELAB, Notación Munsell.

ABSTRACT:

This work is a preliminary approach to the study of the relationship between soil color changes and the temperature reached as a consequence of fires, in order to assess the applicability of soil color as an indicator of the fire intensity. For this purpose a controlled burn of undisturbed soil samples of the surface horizon of an Umbric Regosol was conducted in the laboratory with infrared lamps until the soil at 1 cm deep reaches a temperature of 200ºC or 400ºC. Unburned samples were used as control. Soil color of the surface of the burned and unburned samples was determined on 220 points with a portable colorimeter and represented in the CIELAB color space and Munsell notation. The results showed significant changes in the hue of soil (*Hue* Munsell and h_{ab} CIELAB) between samples reaching different temperatures (200ºC or 400ºC) however significantly change in color intensity (*Croma* Munsell and C^*_{ab} CIELAB) and brightness (*Value* Munsell and L^* CIELAB) only was noticed between the burned and unburned samples. This suggests that the hue of soil is the parameter to take into account in the use of color as an indicator of fire intensity on soils of Galicia.

Key words: Soil Color, Fire Intensity, Controlled Burn, CIELAB Color Space, Munsell Notation.

REFERENCIAS Y ENLACES

[1] http://www.greenpeace.es

[2] X. L. Pereiras, *Os Incendios Forestais en Galicia*. Baía Edicións, A Coruña. pp. 3-70. (2001).

[3] C. G. Wells, R. E. Campbell, L. F. DeBano, C. E. Lewis, R. L. Fredriksen, E. C. Franklin, R. C. Froelich, P. H. Dunn, "Effects of fire on soil". *Gen. Tech. Rep*. WO-7, U.S. For. Serv., Washington, DC. (1979).

[4] C. Chandler, P. Cheney, P. Thomas, L. Trabaud, D. Willianms, *Fire in Forestry: Forest Fire Behavior and Effects*, Vol. I. Wiley-Interscience, New York (1983).

[5] B. Soto, F. Díaz-Fierros, "Interactions between plants ash leachates and soil", *Int. J. Wildland Fire* **3**, 207-216 (1993).

[6] B. Soto, R. Basanta, F. Díaz-Fierros, "Effects of burning on nutrient balance in an area of gorse (Ulex europaeus L.)", *Sci. Total Environ.* **204**, 271-281 (1997).

[7] Munsell Color Company, *Munsell Soil Color Charts*, Munsell Color, GretagMacbeth, New Windsor, NY (2000).

[8] IUSS Grupo de Trabajo WRB, "Base referencial mundial del recurso suelo. Primera actualización 2007". Informes sobre Recursos Mundiales de Suelos No. 103. FAO, Roma. (2007).

[9] A. M. Mouazen, R. Karoui, J. Deckers, J. De Baerdemaeker, H. Ramon, "Potential of visible and near-infrared spectroscopy to derive colour groups utilising the Munsell soil colour charts", *Biosyst. Eng.* **97**, 131-143 (2007).

[10] G. Wyszecki, W.S. Stiles, *Color Science. Concepts and Methods, Quantitative Data and Formulae*, John Wiley and Sons, New York (1982).

[11] CIE Publication 15:2004, 3rd Edition, *Colorimetry (Technical Report)*, CIE Central Bureau, Vienna (2004).

[12] CIE Publication 116-1995, *Industrial Color-Difference Evaluation*, CIE Central Bureau, Vienna (1995).

[13] Publication 142-2001, *Improvement to Industrial Color-Difference Evaluation*, CIE Central Bureau, Vienna (2001).

[14] R.S. Berns, *Billmeyer and Saltzman's Principles of Color Technology*, 3rd Ed., John Wiley and Sons, New York (2000).

[15] H.G. Völz, *Industrial Color Testing*, Wiley –VCH, Weinheim (2001).

1. Introducción

Más de la mitad de los incendios forestales que tuvieron lugar en España en la última década ocurrieron en Galicia, una de las regiones europeas con mayor densidad de masa forestal, siendo el verano más crítico el de 2006 cuando casi 2000 incendios arrasaron más de 85000 hectáreas de suelo [1].

Los incendios dan lugar a un importante impacto ambiental que afecta a todos los componentes del ecosistema, tanto a las comunidades de seres vivos (fauna, vegetación, microorganismos) como al medio físico (suelo, recursos hídricos, atmósfera, microclima). La magnitud de este impacto depende muy directamente de la intensidad del incendio, la frecuencia y amplitud del mismo, así como de la estación del año en la que se produce.

La intensidad de un incendio se define como la energía liberada por unidad de tiempo y por unidad de longitud del frente del incendio [2] y depende de la temperatura máxima alcanzada y del tiempo de exposición al fuego [3]. Así se pueden clasificar en función de la temperatura a la cual se ve sometido el suelo, siendo suaves cuando la superficie del suelo alcanza temperaturas comprendidas entre 100 y 250ºC y la temperatura a 1-2 cm de profundidad no excede los 100ºC; en estos casos el horizonte superficial del suelo presenta cenizas negras formadas por restos vegetales chamuscados. Cuando la temperatura oscila entre 300 y 400ºC en superficie, con desaparición de la hojarasca y los restos vegetales al producirse la combustión parcial de la materia orgánica, y alcanza entre 200-300ºC a 1cm de profundidad, los incendios son moderados. En el caso de fuegos intensos el suelo presenta cenizas blancas, lo que indica una combustión total de la materia orgánica, alcanzándose en la zona más superficial temperaturas comprendidas entre 500 y 700ºC, y a 2 ó 3 cm de profundidad temperaturas de 150-400ºC [4].

A pesar de que el impacto de los incendios sobre los suelos forestales gallegos es bien conocido [5,6] y han sido muchos los casos en los que se han descrito variaciones apreciables en el color del

suelo (como el ennegrecimiento debido a carbonización parcial o total de la materia orgánica y el enrojecimiento debido a la deshidratación de los óxidos de Fe), la variación de los parámetros de color y su relación con la intensidad del fuego no han sido hasta ahora determinados en el contexto de los suelos gallegos. Así, el objetivo de este trabajo es analizar qué parámetros colorimétricos pueden ser empleados como indicadores de la intensidad de los incendios a partir de experimentos de laboratorio con muestras de suelo. Se presentan aquí los primeros resultados.

2. Materiales y métodos

Se utilizaron para este estudio un total de 6 muestras de suelo recogidas en campo en cajas de acero inoxidable de 12×20×45 cm, evitando que su estructura fuese alterada. El suelo estudiado presentaba un perfil AC con un epipedon úmbrico y un porcentaje de materia orgánica muy elevado, de aproximadamente 10%. Las muestras se tomaron en un pastizal con gramíneas, en zona abierta arbolada con pinos.

Las muestras, con un contenido de humedad de aproximadamente el 4%, fueron sometidas a choques térmicos en el laboratorio empleando ocho lámparas infrarrojas Philips IR375CH ubicadas a 10cm de la superficie del suelo (Fig. 1). La temperatura fue monitorizada a 1cm de profundidad desde la superficie, hasta alcanzar temperaturas de 200ºC y 400ºC. Los experimentos se realizaron por duplicado y se utilizaron muestras sin quemar como control.

La monitorización del calentamiento en cada una de las muestras durante los choques térmicos mostró diferencias entre los periodos de calentamiento necesarios para alcanzar la misma temperatura entre las replicas (Fig. 2), lo que puede ser debido a una distinta difusividad térmica de las muestras.

Tras los choques térmicos, cada muestra se dividió en 44 zonas de medida (Fig. 3), en cada una de las cuales se realizaron 5 medidas de color por contacto empleando un colorímetro portátil *Minolta* con cabezal CR-310, de 50 mm de diámetro. Las condiciones de medida fueron: iluminante D65, observador 2º, geometría de medida d/0º con componente especular incluida.

Fig. 1. Quema controlada de las muestras de suelo en el laboratorio.

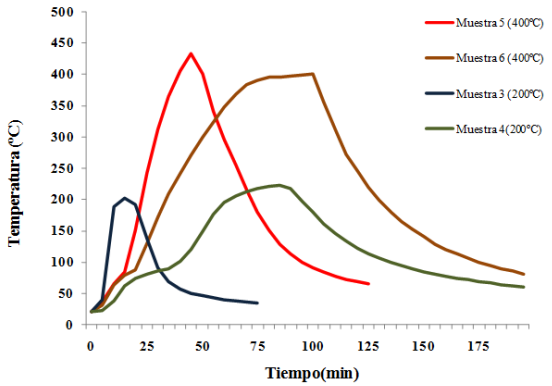

Fig. 2. Curvas de calentamiento de las muestras de suelo sometidas a choques térmicos.

Las medidas de color se analizaron considerando el espacio de color CIELAB, que está basado en el modelo de los colores opuestos. La variable L* es una medida de la claridad, luminosidad o luminancia que varía de 100 (blanco absoluto) a 0 (negro absoluto), mientras que las componentes a^* y b^* definen las componentes de color rojo-verde y amarillo-azul, respectivamente. Así, un valor negativo de a^* define un color más verde que rojo, mientras que un valor positivo de b^* define un color más amarillo que azul. Además de este grupo de coordenadas escalares ($L^*a^*b^*$) el espacio CIELAB puede ser representado mediante otro sistema de coordenadas cilíndricas o polares que sustituye a^* y b^* por *croma*

$$C^*_{ab} = \sqrt{a^{*2} + b^{*2}}\ , \qquad (1)$$

y ángulo tono

$$h_{ab} = \arctan\left(\frac{b^*}{a^*}\right). \qquad (2)$$

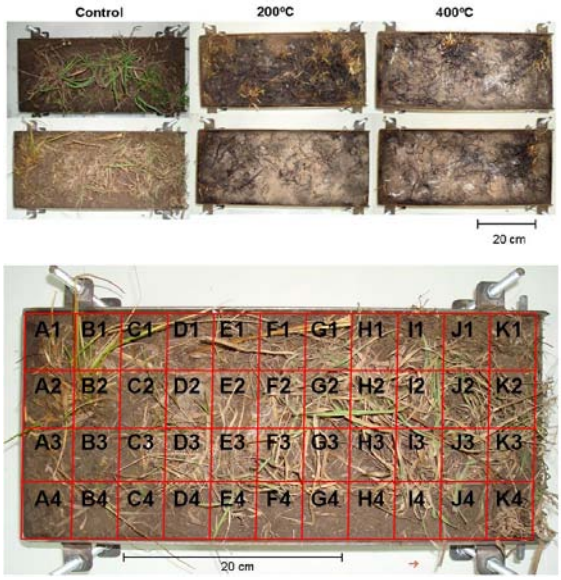

Fig. 3. Aspecto de las seis muestras de suelo al medir su color (arriba). Esquema que muestra las 44 parcelas en las que se dividió la superficie de cada una de las muestras para las medidas de color (abajo).

Considerar las coordenadas cilíndricas ($L^*C^*_{ab}h_{ab}$) en lugar de las escalares ($L^*a^*b^*$) permite cuantificar el color del mismo modo que es percibido, es decir considerando los tres atributos de apreciación visual: claridad o luminosidad (su análogo en CIELAB es L^*), croma o intensidad (su análogo en CIELAB es C^*_{ab}) y tono o matiz, (su análogo en CIELAB es h_{ab}). De la misma forma que $L^*C^*_{ab}h_{ab}$, la notación Munsell tiene en cuenta la percepción humana del color al definir sus parámetros: *Hue*, que representa el tono, *Value*, que representa la claridad, y *Croma* que representa la intensidad. Utilizando el programa de conversión de Munsell (CMC 2, versión 6.5.5) se determinaron los valores del sistema Munsell (*Value*, *Hue* y *Croma*) a partir de los valores de los parámetros CIELAB obtenidos con el colorímetro portátil *Minolta.*

Está internacionalmente aceptado y extendido el uso de las claves de color Munsell en el estudio del color del suelo [7-9] empleando un número limitado de fichas (en los Atlas Munsell para suelos el número de fichas caracterizadas cada una por un *Hue*, *Value* y *Croma* es 175). Sin embargo este criterio de medida depende de una serie de variables como son la luz incidente, el entorno de la muestra y la percepción de la persona que hace la medida. Por estos motivos hemos considerado en este estudio el empleo de un instrumento (colorímetro) que permite una caracterización objetiva del color del suelo.

Por otra parte, el espacio de color CIELAB permite cuantificar la diferencia de color entre dos muestras mediante la combinación de las diferencias de sus tres coordenadas, tanto escalares como cilíndricas, en un espacio euclidiano. Este es el fundamento de la fórmula clásica de 1976 de diferencia de color CIELAB [10] definida en la Ec. (3), que asume la uniformidad del espacio de color

$$\Delta E^*_{ab} = \sqrt{\left(\Delta L^*\right)^2 + \left(\Delta a^*\right)^2 + \left(\Delta b^*\right)^2} = \\ = \sqrt{\left(\Delta L^*\right)^2 + \left(\Delta C^*_{ab}\right)^2 + \left(\Delta H^*_{ab}\right)^2}\,. \tag{3}$$

Posteriormente, reconocida la falta de uniformidad de este espacio, la fórmula de distancia euclídea para medir la diferencia de color, ha sido progresivamente revisada y mejorada. La mayoría de las fórmulas de diferencia de color modernas parten de las coordenadas en el sistema CIELAB, introduciendo factores de ponderación apropiados sobre las diferencias CIELAB de claridad, croma y tono [11]. Estos factores de ponderación se introducen para corregir la falta de uniformidad perceptual del sistema, y así surgen, las fórmulas de diferencia de color CIE94 [12] y CIEDE2000 [13], definidas en las Ecs. (4) y (5) respectivamente:

$$\Delta E^*_{94}\left(k_L : k_C : k_H\right) = \\ = \sqrt{\left(\frac{\Delta L^*}{k_L S_L}\right)^2 + \left(\frac{\Delta C^*_{ab}}{k_C S_C}\right)^2 + \left(\frac{\Delta H^*_{ab}}{k_H S_H}\right)^2}\,, \tag{4}$$

$$\Delta E_{00}\left(k_L : k_C : k_H\right) = \\ = \left\{\left(\frac{\Delta L'}{k_L S_L}\right)^2 + \left(\frac{\Delta C'}{k_C S_C}\right)^2 + \left(\frac{\Delta H'}{k_H S_H}\right)^2 + \right. \\ \left. + R_T\left(\frac{\Delta C'\cdot\Delta H'}{k_C S_C k_H S_H}\right)\right\}^{1/2}, \tag{5}$$

donde los valores k_L, k_C, k_H sirven para ajustar las contribuciones relativas de claridad, croma y tono, y así adoptando los valores k_L=1, k_C=1, k_H=1 las fórmulas que se obtienen son CIE94 (1:1:1) y CIEDE2000 (1:1:1); y aumentando la contribución relativa a la diferencia de claridad, k_L=2, k_C=1, k_H=1, las fórmula son CIE94 (2:1:1) y CIEDE2000 (2:1:1). En cuanto a la importancia relativa de estas correcciones (CIE94 y CIEDE2000), los autores destacan que la mejora de CIE94 sobre CIELAB es notablemente superior a la mejora de CIEDE2000 sobre CIE94.

Todos los datos fueron tratados estadísticamente mediante análisis de varianza multivariable (MANOVA) empleando el paquete estadístico SPSS 17.0.

3. Resultados y discusión

En la Tabla I se muestran los valores medios de cada parámetro de color para cada una de las seis muestras del estudio, indicando con superíndices (a-c) los resultados del análisis de varianza multivariable (MANOVA). El análisis estadístico MANOVA realizado entre los tres conjuntos de muestras que habían alcanzado diferente temperatura, i.e. control, 200ºC y 400ºC, mostró diferencias significativas en todos los parámetros de color estudiados entre las muestras sin quemar (Muestras 1 y 2) y quemadas (Muestras 4 – 6); produciéndose un descenso de la claridad, reflejado en los valores de *Value* y L^*, y un descenso de la intensidad del color, marcado por *Croma* y C_{ab}^*, que probablemente estén debidos a la carbonización de la materia orgánica. Además, se produjo un empardecimiento-enrojecimiento del suelo reflejado en los valores de *Hue*, el descenso de h_{ab}, el aumento de a^* y el descenso de b^*, que debe atribuirse simplemente a la desaparición de los componentes orgánicos del suelo que enmascaraban el color de los componentes inorgánicos, principalmente óxidos de Fe. Sin embargo ninguno de estos cambios, al ocurrir entre muestras quemadas y sin quemar, informa acerca de la intensidad del incendio.

La comparación entre los valores de los suelos quemados a 200ºC y a 400ºC muestra que los únicos parámetros que establecen diferencias significativas son aquellos que se refieren a *Hue* Munsell y h_{ab} CIELAB. En este caso, las diferencias pueden ser asignadas principalmente a variaciones en el estado de deshidratación, de los compuestos de hierro como el cambio de goethita de un color anaranjado a hematite de color rojo sangre, ambos eficaces agentes pigmentantes.

Por otra parte, aunque entre los valores de *Value* Munsell y L^* CIELAB a 200ºC y 400ºC no ocurre una variación que pueda considerarse significativa desde un punto de vista estadístico, debe notarse que el valor de ambos parámetros aumenta, lo cual, sin duda es debido a la aparición en el suelo quemado a 400ºC de residuos de ceniza blanca.

Tabla I

Valores medios Munsell de tono (*Hue*), intensidad (*Croma*) y claridad (*Value*) y CIELAB de claridad (L^*), coordenada rojo-verde (a^*), coordenada amarillo-azul (b^*), croma (C^*_{ab}) y ángulo tono (h_{ab}) para las 6 muestras del estudio.

Temperatura alcanzada		*Hue*	*Croma*	*Value*	L^*	a^*	b^*	C^*_{ab}	h_{ab}
Control	Muestra 1	3,50Y^a	1,30^a	3,40^a	34,72^a	-0,04^a	12,80^a	13,17^a	86,73^a
	Muestra 2	0,05Y^a	1,90^a	3,10^a	31,77^a	2,89^a	11,15^a	11,59^a	75,21^a
200ºC	Muestra 3	9,00YR^b	0,99^b	2,20^b	22,60^b	1,79^b	5,70^b	6,03^b	68,92^b
	Muestra 4	8,88YR^b	1,01^b	2,69^b	27,73^b	2,31^b	5,80^b	6,25^b	67,61^b
400ºC	Muestra 5	7,93YR^c	0,88^b	2,44^b	24,32^b	2,20^b	4,79^b	5,30^b	63,05^c
	Muestra 6	8,20YR^c	0,99^b	2,77^b	28,36^b	2,59^b	5,41^b	6,02^b	63,41^c

Valores medios con distinto superíndice (a-c) para cada parámetro de color en relación a la temperatura alcanzada difieren significativamente (α :0,05)

Tabla II

Diferencia total de color, empleando la fórmula clásica CIELAB [10] y las fórmulas más recientes y mejoradas basadas en CIELAB: CIE94 (1:1:1) y CIE94 (2:1:1) [12], así como CIEDE2000 (1:1:1) y CIEDE2000 (2:1:1) [13].

	CIELAB	CIE94 (1:1:1)	CIE94 (2:1:1)	CIEDE2000 (1:1:1)	CIEDE2000 (2:1:1)
Control - 200ºC	10,22	9,31	6,14	7,71	5,53
Control - 400ºC	9,79	8,67	6,28	7,44	5,86
200ºC - 400ºC	1,39	1,34	0,87	1,23	0,95

Finalmente, teniendo en cuenta las diferencias totales de color (Tabla II) cabe destacar que éstas son perceptibles, i.e. son superiores a 3 unidades CIELAB [14,15] entre las muestras sin quemar y las quemadas; en cambio no son perceptibles entre los suelos quemados a dos intensidades diferentes (200ºC y 400ºC).

4. Conclusiones

En este trabajo se muestran los primeros resultados del empleo del color como indicador de la intensidad de los incendios en suelos de Galicia, concluyéndose que de entre los parámetros de color analizados son *Hue* Munsell y h_{ab} CIELAB los que marcan la diferencia entre incendios de intensidad ligera (200ºC) y moderada (400ºC). A este respecto los resultados son muy prometedores y los futuros estudios irán dirigidos al establecimiento de intervalos más estrechos de temperatura que permitan obtener información acerca de los cambios de los compuestos de hierro, que serán completados con datos físicos, químicos y mineralógicos.

Agradecimientos

Al Ministerio de Educación y Ciencia por la concesión de las becas BES-2007-16996 y AP2006-03856.

Chapter 10. Nondestructive assessment of phytopigments in riverbed sediments by the use of instrumental color measurements

Sanmartín, P.; Devesa-Rey, R.; Prieto, B.; Barral, M.T.

Journal of Soils and Sediments 11 (5): 841-851 (2011)

JCR index (IF) 2010 = 2.574 (3/32, 9 percentile in Soil Science)

Total number of times cited: 1

J Soils Sediments (2011) 11:841–851
DOI 10.1007/s11368-011-0358-z

SEDIMENTS, SEC 1 • SEDIMENT QUALITY AND IMPACT ASSESSMENT • RESEARCH ARTICLE

Nondestructive assessment of phytopigments in riverbed sediments by the use of instrumental color measurements

Patricia Sanmartín · Rosa Devesa-Rey · Beatriz Prieto · María Teresa Barral

Received: 10 November 2010 / Accepted: 13 March 2011 / Published online: 19 April 2011

Abstract
Purpose The quantification of phytopigments in riverbed sediments deserves further attention because it provides information about eutrophic levels, and therefore about sediment and water quality. Due to the current interest in the study of eutrophication processes, there is a need for the development of a rapid, simple, cost-effective, and nondestructive method of quantifying phytopigment content. We describe one method based on color measurements and without the need for extraction and chemical assay.
Materials and methods Sediment cores were collected along the watercourse of the Anllóns River (northwest Spain). The reflectance color measurements were analyzed with the CIELAB color parameters, using Cartesian (L*a*b*) and cylindrical ($L^*C^*_{ab}h_{ab}$) coordinates. Phytopigments (chlorophyll *a*, chlorophyll *b*, phaeopigments and total carotenoids) were extracted with dimethylsulphoxide and were determined spectrophotometrically.
Results and discussion The CIELAB color parameters were significantly correlated with phytopigment content (involving logarithmic, inverse, and simple data). The linear regression equations were used to predict chlorophyll *a*, chlorophyll *b*, and carotenoid contents, as well as the total pigment contents from parameter a* (redness–greenness of the color) and parameter C^*_{ab} (chroma of the color), and values of adjusted R^2 were close to 0.9. The closest relation between phytopigments and color parameters corresponded to chlorophyll *a*, which may be estimated by means of Chl*a*=46.4–70.6 $\log_{10}$ (a*) and Chl*a*=−15.7+238.1 ($1/C^*_{ab}$) as predictive equations. The phaeophytinization quotient is somewhat questionable due to the low adjusted R^2 values obtained.
Conclusions This work demonstrates that it is possible to determine phytopigment contents in riverbed sediments by means of a nondestructive colorimetric method employing the CIELAB color parameters. In addition, the abundance of phytopigments in the sediment core showed no clear trend either along the longitudinal axis of the river or in relation to sediment depth.

Keywords Benthic algae · Chlorophyll · CIELAB color measurements · River sediments · Settled phytoplankton

1 Introduction

Eutrophication, the addition of excess nutrients to an aquatic system that leads to algal blooms, can occur in response to several anthropogenic impacts, such as increased population growth, urbanization, agriculture, and inputs of sewage and food processing wastes. It causes an increase in primary production and, if this surpasses certain threshold levels, leads to detrimental impacts on the ecosystem (Pinckney et al. 2001). Eutrophication is, therefore, considered as one of the most pressing environmental problems in both developed and developing countries (Harper 1992).

Most eutrophication studies have focused on nitrogen (N) and phosphorus (P) because these are essential macronutrients for all phytoplankton and benthic groups and because their concentrations are strongly affected by human activities (Muylaert et al. 2009). In rivers, the effects of eutrophication may be moderate because phytoplankton and benthic algal growth are limited by the short water

Responsible editor: Henner Hollert

P. Sanmartín (✉) · R. Devesa-Rey · B. Prieto · M. T. Barral
Departamento Edafología y Química Agrícola, Facultad Farmacia, Universidad Santiago de Compostela,
15782 Santiago de Compostela, Spain
e-mail: patricia.sanmartin@usc.es

retention times rather than by the concentrations of inorganic nutrients (Muylaert et al. 2009). Nevertheless, studies carried out in different river basins have demonstrated a positive relationship between N and P enrichment and algal biomass (Biggs and Close 1989; Dodds et al. 1997,2002; Chételat et al. 1999, 2006; Biggs 2000; Devesa-Rey et al. 2010).

Riverbed sediments may contain phytopigments that originate from the benthic algae and settled phytoplankton. There is a considerable interest in quantifying phytopigments in order to assess the quality of freshwater bodies because this method takes into account the synergistic effect of nutrients, such as P and N, on the algal growth that causes eutrophication, resulting in a useful descriptor of the trophic state and environmental quality (Dell'Anno et al. 2002; Kowalewska et al. 2004, Kowalewska 2005; Gerbersdorf et al. 2009). For example, Devesa-Rey et al. (2009a) have demonstrated the link between phytopigments and P content in riverbed sediments and found positive significant correlations between P and chlorophyll *a*, chlorophyll *b*, and total carotenoids. Furthermore, a phytopigment analysis may be useful for assessing how biofilms develop on the surface of riverbed sediments, which adds a new and very important element to the dynamic nature of superficial riverbed sediments (Devesa-Rey et al. 2009a).

An increased focus on the eutrophication process and its effects on sediment and water quality have led to the interest in the development of a rapid, simple, cost-effective, nondestructive, and reliable method of phytopigment quantification. The existing techniques for the analysis of pigments involve extraction, with some loss of the material under study, and are relatively expensive and time-consuming. These include chemical techniques such as spectrophotometry (UV–Vis or fluorescence), high-performance liquid chromatography and thin-layer chromatography, used alone or in combination with nuclear magnetic resonance, mass spectrometry, and infrared techniques. The application of reflectance color measurements may provide an accurate method of quantifying phytopigments. The main advantages offered by this technique are the nondestructive nature of the procedure (allowing further analyses of the same sample) and the immediacy of the results (which are available at the moment of sampling, thus avoiding the need for further sample processing). In comparison with fluorescence-based portable devices, colorimetric devices are capable of sensitivities of at least an order of magnitude greater because the fluorescence is a signal caused in a short span of time, and because they take into account both alive and dead cells, while fluorescence devices only take account of live cells. In contrast to optical remote sensing devices (satellite or airborne sensors), colorimetric devices do not suffer the shadow effect caused by topography terrain and/or clouds (Schott 1997), the main disadvantage of these approaches.

Previous studies have successfully used reflectance color measurements expressed by means of the CIELAB color coordinates (CIE Publication 15–2; CIE 1986) to study the phytopigment content of several food types (e.g., Mínguez-Mosquera et al. 1991, 2005; Han et al. 2008; Moyano et al. 2008) and building stone biofilms, mainly consisting of filamentous cyanobacteria (e.g., Prieto et al. 2002, 2004; Sanmartín et al. 2010a, b). Nevertheless, to our knowledge, such measurements have not been used to study phytopigments in sediments as a proxy for the measurement of algae content. Recently, CIELAB color measurements have been applied to suspended and riverbed sediments for forensic applications (e.g., Guedes et al. 2009) and fingerprinting sediment sources (e.g., Martínez-Carreras et al. 2010a, b).

The main hypothesis of the present study is, therefore, that the phytopigment content of the riverbed sediments may be accurately estimated by the use of some CIELAB color coordinates, combined in several predictive equations. In addition, the abundance and vertical distribution of phytopigments in a series of superficial sediment core profiles were also examined, with the aim of determining trends in phytopigment content along the longitudinal axis of the river and with sediment depth.

2 Materials and methods

2.1 Research area and sampling

Superficial riverbed sediments were sampled in the River Anllóns, (northwest Spain, Fig. 1). The river basin drains a rural catchment area of 516 km^2 with a history of agricultural, forestry, and cattle farming activities. The climate is wet (the average annual precipitation is 1,200 mm), with a mean temperature of 9°C in winter and 20°C in summer. The land use in the area includes a mixed forest of *Eucalyptus globulus*, *Eucalyptus alba*, and *Pinus pinaster* (60% of the total cover), cultivated land (18%), pasture (12%), bushes (9%), and urban use (1%). The riparian vegetation is characterized by *Alnus glutinosa* and *Fraxinus excelsior* (*Alnon-padion*, *Alnion incanae*, and *Salicion albae* associations).

The upper reaches of the river flow over schists, which are replaced by a smooth profile in the middle area of the river, characterized by basic rocks (gabbros and amphibolites). Finally, the lower reaches of the river flow over a two-mica granite, followed by a biotitic gneiss at the river mouth. A gold extraction in the Corcoesto area has led to the remobilization of the associated arsenopyrites and subsequent accumulation of arsenic (As) in the riverbed sediments downstream of the mining area (Rubinos et al. 2003, 2010; Devesa-Rey et al. 2008).

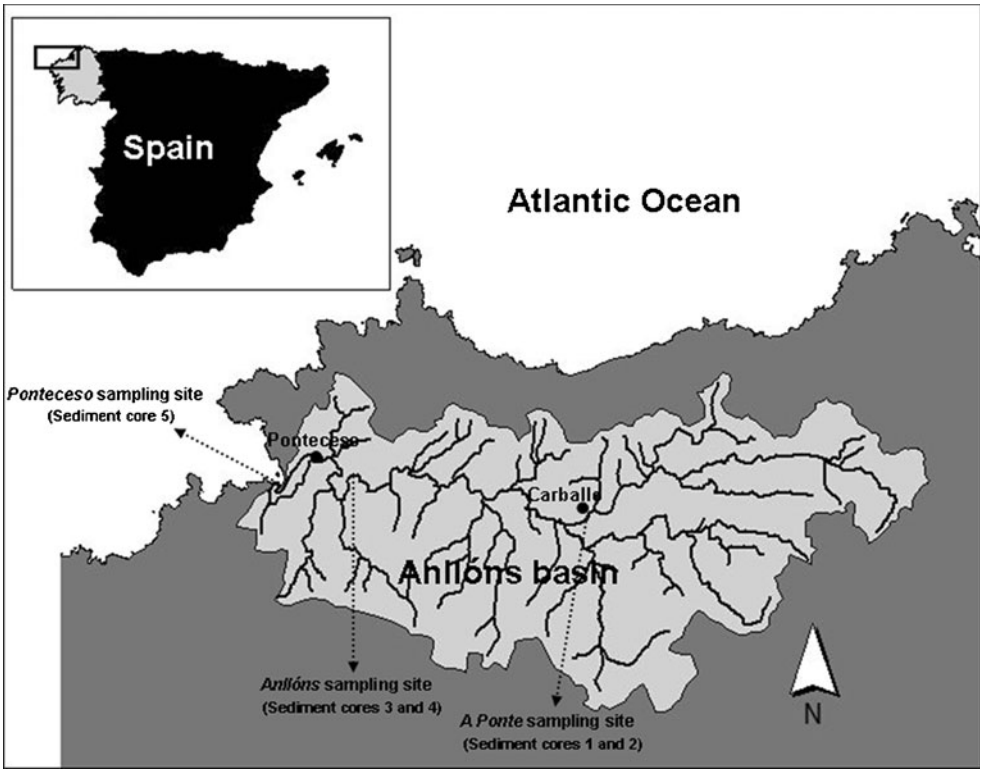

Fig. 1 Map of the Anllóns River basin showing the location of the three sampling sites where the five sediment cores were collected

The lengthwise profile of the river includes three low-slope areas (2%, 4.4%, and 1.4%) which are favorable for sediment deposition. Three sampling sites were established in these areas (see Fig. 1), between the locality of Carballo and the river mouth, covering a distance of approximately 17 km: (1) the A Ponte sampling site (sediment cores 1 and 2), located at the town of Carballo with a population of over 25,000; (2) the Anllóns sampling site (sediment cores 3 and 4), at the village of Anllóns with a population of 276; and (3) the Ponteceso sampling site (sediment core 5), at the village of Ponteceso with a population of about 7,000, located at the river mouth and therefore under the tidal influence.

Sediment cores of 5.5 cm in diameter and 4.0-cm long were taken from the surface sediment, preserved in hermetically insulated plastic containers, and transported undisturbed to the laboratory, where they were stored in an ultracold freezer. The frozen sediment cores were later minimally thawed to allow them to be extruded and sectioned into five 0.8-cm increments in order to measure the color and to study the abundance and depth-related distribution of phytopigments in the sediment profiles.

The superficial sediment was sampled to a depth of 4 cm as this is considered the active layer under the water–sediment interface and involves physical and biogeochemical exchanges between sediments and water, and can be easily resuspended. Wang et al. (2003) defined this layer as the depth of the sediment affected by bioturbation and with the potential to be resuspended.

2.2 Extraction and analysis of phytopigments: chlorophyll *a*, chlorophyll *b*, phaeopigments, and total carotenoids

Sediment core slices (n=25) were lyophilized before phytopigment extraction and were submitted to consecutive extractions (max, three) until no phytopigments were quantified in the extracts. Phytopigments (chlorophyll *a*, chlorophyll *b*, phaeopigments, and total carotenoids) were extracted with dimethylsulphoxide for 46 min at an extractant volume to sediment weight ratio of 3.6 mL g^{-1} at 57°C, following the method optimized by Devesa et al. (2007). The phytopigment content of the extracts was determined spectrophotometrically (Cary 100 Concentration Varian), and the equations proposed by Wellburn (1994) were used to determine the concentrations of chlorophyll *a* (Chl*a*) (Eq. 1) and *b* (Chl*b*) (Eq. 2), and of total carotenoids (Cx+*c*) (Eq. 3), in micrograms per liter.

$$\mathrm{Chl}a = 12.47\mathrm{A}_{665.1} - 3.62\mathrm{A}_{649.1} \quad (1)$$

$$\mathrm{Chl}b = 25.06\mathrm{A}_{649.1} - 6.5\mathrm{A}_{665.1} \quad (2)$$

$$\mathrm{Cx} + c = (1000\mathrm{A}_{480} - 1.29\mathrm{Chl}a - 53.78\mathrm{Chl}b) / 220 \quad (3)$$

where Chl*a* and Chl*b* represent the concentrations of chlorophyll *a* and chlorophyll *b*, respectively, and Cx+*c* represents the concentration of total carotenoids, comprising the oxidized forms (the xanthophylls) and the reduced

forms (the carotenes). $A_{665.1}$, $A_{649.1}$, and A_{480} represent the absorbance of the extracts at 665.1, 649.1, and 480 nm, respectively. Note that as Chl*a* and Chl*b* can be degraded to phaeopigments, which absorb at the same specific wavelengths as Chl*a* and Chl*b*, thus interfering in the measurements, the phaeopigments were estimated by adding 0.5% of 1 M HCl to the extracts and the absorbances measured after 10 min; the values were subtracted from those of the chlorophylls. The ratio of absorbances of the extracts at 435 and 415 nm (A_{435}/A_{415}) was interpreted as the phaeophytinization quotient (PQ), which reflects the ratio of chlorophyll to phaeopigments (Ronen and Galun 1984). A decrease in that ratio indicates an increased degradation of chlorophyll to phaeopigments.

2.3 Color measurements

The color was measured directly on the top face of each sediment core slice (circular target area 23.76 cm^2 approximately) before extracting the phytopigments. A total of 20 readings (with substitution) were taken with a portable reflection spectrophotometer (CE-XTH) equipped with OptiviewSilver/i QC Basic software. The measuring conditions were: (a) CIE standard daylight illuminant D65; (b) 1,931 (2°) CIE standard colorimetric observer; (c) specular component included in 8° in relation to normal (d/8°), and (d) measuring head with 10-mm diameter viewing area.

The color measurements were analyzed by considering the CIELAB color system (CIE Publication 15–2, 1986), which represents each color by means of three scalar parameters or the Cartesian coordinates: L*, lightness or luminosity of color, which varies from 0 (absolute black) to 100 (absolute white); a*, associated with changes in redness–greenness (positive a* is red and negative a* is green); and b*, associated with changes in yellowness–blueness (positive b* is yellow and negative b* is blue). Alternatively, each color is represented by means of three angular parameters or cylindrical coordinates, most closely related to the psychophysical perception of the color: L*, lightness or luminosity of color, also defined in both scalar and angular color sets; chroma ($C^*_{ab} = \left(a^{*2} + b^{*2}\right)^{1/2}$) related to the intensity of color or saturation and hue angle ($h_{ab} = \arctan\left(b^*/a^*\right)$) or tone of color which refers to the dominant wavelength and indicates redness, yellowness, greenness, or blueness on a circular scale, starting at 0° and increasing counterclockwise (Wyszecki and Stiles 1982).

2.4 Statistical analyses

The data were subjected to a multivariate analysis of variance (MANOVA) and the Tukey *B* multiple comparison tests, and differences were considered significant at $p < 0.05$. The relationships between the CIELAB color parameters and the phytopigment content were assessed by two-tailed Bivariate Pearson's correlations and stepwise linear multiple regression models. In the latter case, logarithmic and inverse data transformations were used for improving the normality of the variables. Statistical analyses were performed with SPSS (SPSS v15.0 for Windows).

3 Results and discussion

3.1 Phytopigment abundance and depth-related distribution in the riverbed sediment cores

The mean abundances of phytopigments (chlorophyll *a*, chlorophyll *b*, total carotenoids, and total phytopigments) and the PQ in the five sediment cores are shown in Table 1. The highest phytopigment content was observed in sediment core 5, which is located at the river mouth (the Ponteceso sampling site). A combination of several factors may contribute to the significantly higher content of pigments at this site. On the one hand, it is the least well shaded by trees so that more light reaches the bottom sediments, thus favoring algal development. On the other hand, adaptation to the osmotic stress may be considered as a differential element that promotes growth of the saline-resistant species, as what occurs in the estuary. This was suggested by Mishra et al. (2009) and Yeh et al. (2010), who considered that light is a minor factor in controlling algal growth. In fact, taxa typical of brackish environments, such as *Achnanthes brevipeps*, *Entomoneis* sp., *Diploneis* sp., *Melosira nummuloides*, *Pleurosigma* sp., *Surirella striatula*, and *Triblionella* sp. have been observed by Devesa-Rey et al. (2009b) at the same site. Likewise, the proximity of this site to the town of Ponteceso, which is affected by urban and industrial pollution, should also be considered, as this will affect the concentrations of macronutrients and micronutrients (Mishra et al. 2009). In fact, Devesa-Rey et al. (2009a) found a positive effect exerted by Cu (extracted in oxalate, at concentrations up to 13.3 mg kg^{-1}) on algal development in the Anllóns riverbed sediments.

The lowest phytopigment content was found in sediment cores 3 and 4, whereas the phytopigment contents in sediment cores 1 and 2 were significantly higher than in the latter core (see Table 1). This may be due to the fact that the A Ponte sampling site, where sediment cores 1 and 2 were obtained, is affected by urban activities, which may lead to inputs of N and P as at the Ponteceso sampling site (sediment core 5). Nevertheless, sediment cores 3 and 4 were obtained at the Anllóns sampling site, where the degree of pollution is expected to be low because of the small population in the area and the high water flow supplied by the two main tributaries.

Table 1 Mean phytopigment content (mean±SD, micrograms per gram of sediment) in the five sediment cores (measured in each of the five slices from each sediment core)

Core	Chlorophyll *a*	Chlorophyll *b*	Total carotenoids	Total phytopigments	Phaeophytinization quotient
1	11.9±4.3a	14.3±4.1a	7.9±2.3a	34.1	1.6±0.0a
2	12.1±1.6a	12.6±1.3a	7.4±0.6a	32.1	1.6±0.0a
3	8.2±2.2b	5.1±0.9b	4.2±1.1b	17.5	1.6±0.2a
4	2.2±1.6c	2.7±1.9b	1.0±0.6c	5.9	1.8±0.1b
5	60.1±15.3d	55.6±19.4c	24.2±2.7d	139.9	1.9±0.0b

Different letters in each column indicate significant differences ($p<0.05$) among the five cores

The chlorophyll degradation to phaeopigments, reported by the PQ values, was higher in sediment cores 1, 2, and 3, as the PQ values were significantly lower in these cores (see Table 1). This difference between the sediment cores cannot be attributed to any studied environmental parameter.

In all the sediment cores, the chlorophyll *a* content was similar to the chlorophyll *b* content (see Table 1), which suggests that cyanobacterial biomass is scarce in the algal communities, since these organisms contain only chlorophyll *a*, and therefore their presence would affect the ratio of chlorophyll *a*/*b*. The relatively low total carotenoid content relative to the chlorophyll content (see Table 1) also supports the hypothesis of a limited presence of cyanobacteria, as total carotenoids are associated with cyanobacterial blooms (Poutanen and Nikkilä 2001) and the ratio of chlorophylls/total carotenoids has been used to evaluate relative changes in cyanobacterial abundance in the algal community (Wetzel 1970). This supposition is consistent with the results of Devesa-Rey et al. (2009b), who studied the relative abundance (individuals per square centimeter) in surface samples obtained at the same time as the sediment cores, showing the dominance of *Bacillariophycea* (diatoms) at the three sites, with *Navicula* being the

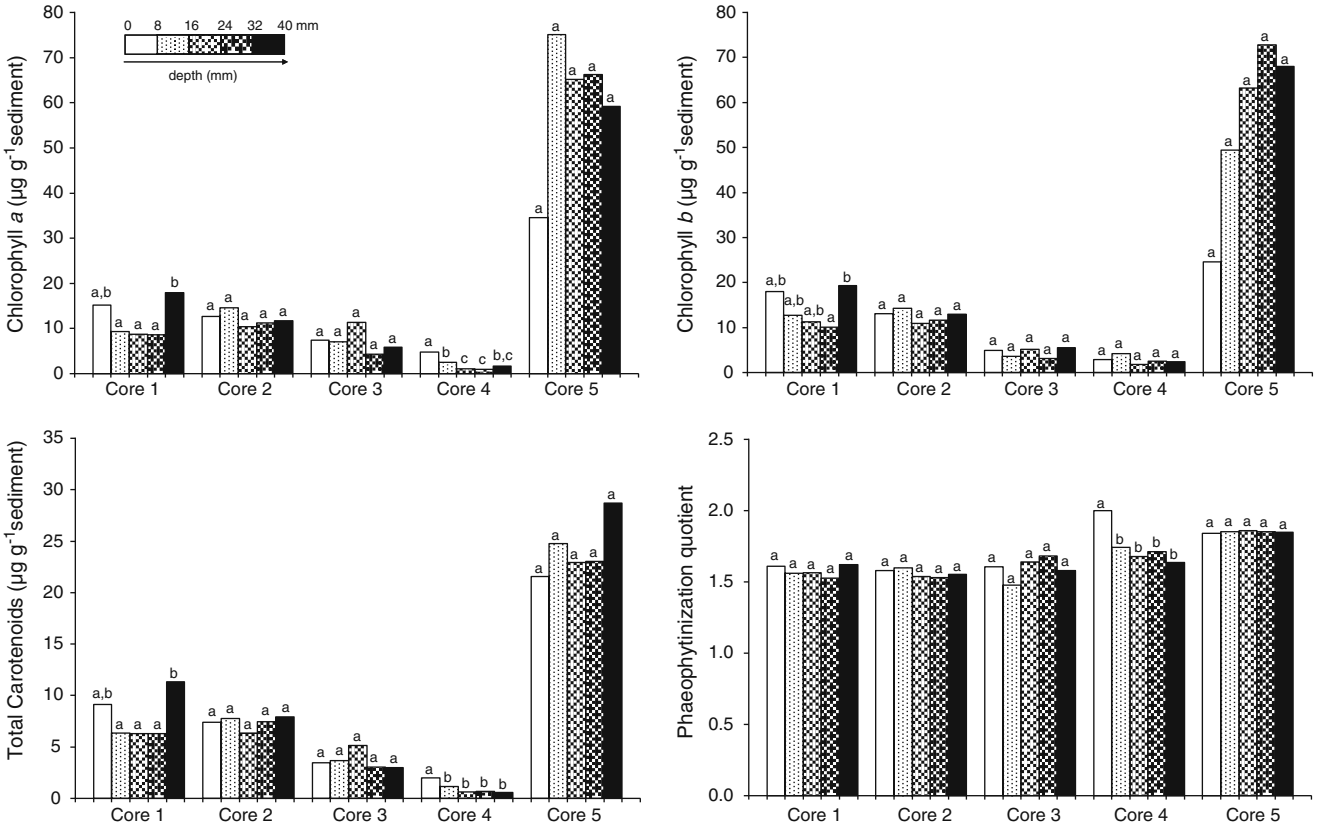

Fig. 2 Depth-related distribution of phytopigment content (chlorophyll *a*, chlorophyll *b*, and total carotenoids) and the phaeophytinization quotient in the five sediment cores. The histograms represent mean values for sediment core slices. Different *letters* indicate significant differences ($p<0.05$) among the five slices from each sediment core

Table 2 Mean (±SD) CIELAB color coordinates (CIELAB units) in the five sediment cores (measured in each of the five slices from each sediment core)

Different letters in each column indicate significant differences (p <0.05) among the five cores

Core	CIELAB-Cartesian coordinates L*a*b*			CIELAB-cylindrical coordinates L*C*$_{ab}$h$_{ab}$		
	L*	a*	b*	L*	C*$_{ab}$	h$_{ab}$ (º)
1	24.3±3.9a	2.5±0.3a	7.2±1.2a	24.3±3.9a	7.6±1.2a	70.6±1.4a
2	23.4±4.4a,b	3.0±0.4b	7.9±0.9a,b	23.4±4.4a,b	8.4±1.0b	69.5±0.8b,c
3	24.6±2.5a	3.5±0.6c	9.8±1.3c	24.6 ±2.5a	10.4±1.4c	70.2±1.3a,c
4	23.5±3.8a,b	4.6±0.7d	12.0±2.3d	23.5±3.8a,b	12.8±2.4d	69.0±1.2b
5	22.5±1.4b	0.8±0.4e	3.5±1.1e	22.5±1.4b	3.6±1.1e	77.7±3.0d

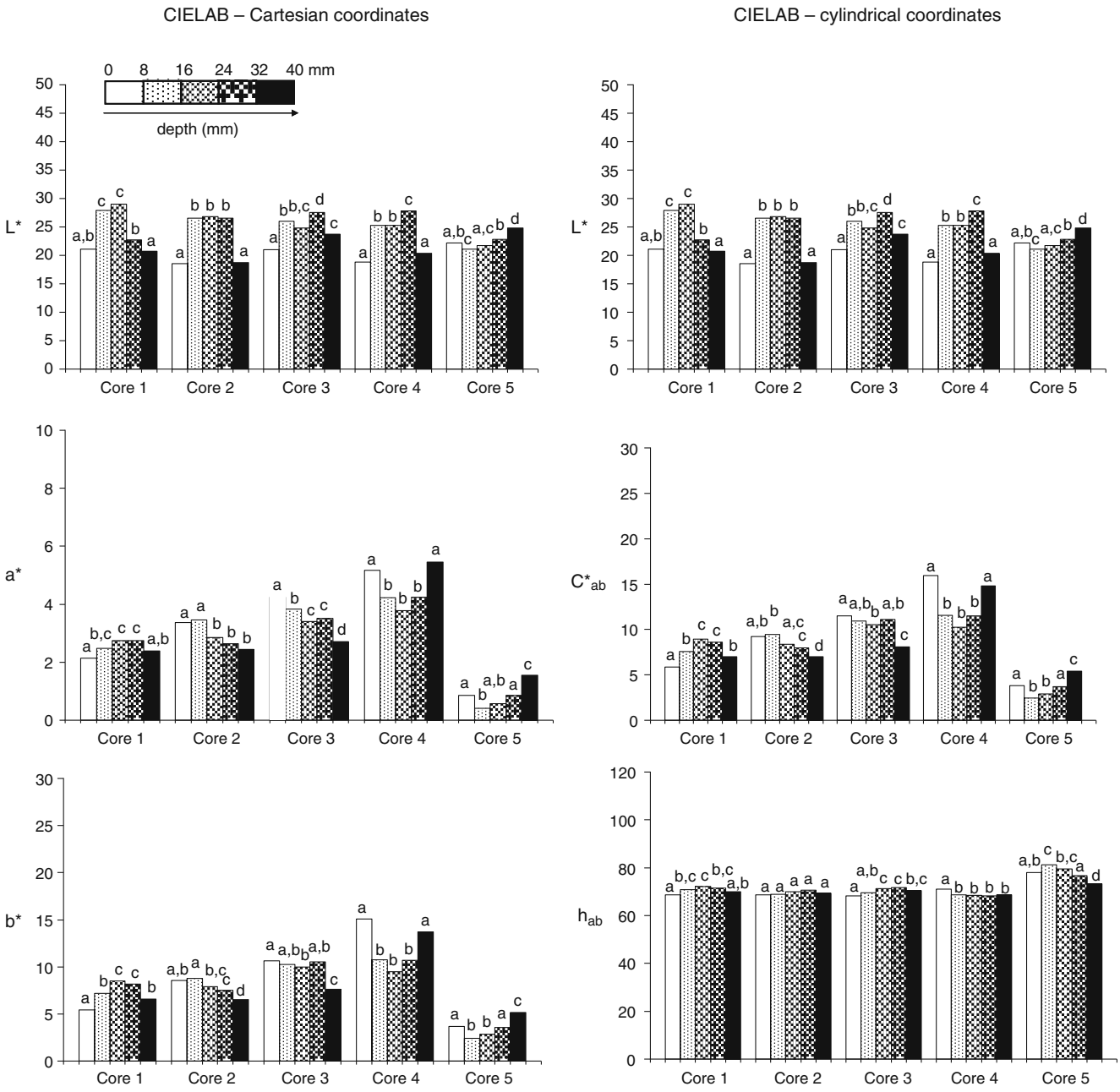

Fig. 3 Depth-related distribution of color, using the Cartesian coordinates (L*a*b) and the cylindrical coordinates (L*C*$_{ab}$h$_{ab}$), in the five sediment cores. The histograms represent mean values for sediment core slices. Different *letters* indicate significant differences (p<0.05) among the five slices from each sediment core

most common taxon. At the Anllóns and Ponteceso sampling sites, diatoms accounted for >96% of the total genera, whereas at the A Ponte sampling site, 15% of other groups, including Cyanophyta (Cyanobacteria) and Chlorophyta, were observed.

The depth-related distribution of phytopigment content (chlorophyll *a*, chlorophyll *b*, and total carotenoids) and the PQ in the five sediment cores is plotted in Fig. 2. In general, the phytopigment content did not change significantly with depth, which appears to indicate the presence of benthic phototrophic organisms and/or settled phytoplankton to a depth of 4.0 cm. The most probable reason for the almost uniform vertical pigment profile is erosion/resuspension processes (Anderson 1983). Bioturbation should cause a heterogeneous depth-related trend in phytopigment content (Cadée 1976; Grant and Daborn 1994), and migration happens only after the settled phytoplankton and benthic microalgae have been buried (Cadée and Hegeman 1974), therefore suggesting frequent resuspension and subsequent deposition. Also, although the presence of organism remains deposited in the past cannot be excluded, since phytopigments may be preserved for decades within sediment (Rabalais et al. 2004), it is unlikely at these low depths (4.0 cm). The rates of degradation differ for the various phytopigments and are affected by environmental conditions, mainly by oxidation–reduction conditions (Sun and Dai 2005). A higher pigment content would be expected in the sediment surfaces as a consequence of penetration of light to a maximum depth of 2–3 mm in the sediment (Coljin 1982; McIntyre et al. 1996). In this sense, a higher chlorophyll pigment content was observed in the upper 0–4-cm sediment layers relative to the deeper (6–10 cm) layers in the Palomares River Estuary (Moreno and Niell 2004). A slight surface maximum in the contents of chlorophyll *a* and total carotenoids was only observed in sediment core 4, in accordance with the significantly higher value of PQ in this superficial slice. The topmost slice (0–0.8-cm depth) and the deepest slice (3.2–4.0 cm) from sediment core 1 contained significantly higher contents of chlorophyll *a* and carotenoids than the other slices from this core.

3.2 CIELAB color measurements in the riverbed sediment cores

The mean values of the CIELAB color coordinates, using the Cartesian (L*a*b*) and cylindrical ($L^*C^*_{ab}h_{ab}$) coordinates, in the five sediment cores are shown in Table 2. The L* value (lightness of color) scarcely changed along the longitudinal axis of the river basin, and the L* values for all five sediment cores were low, between 22.5±1.4 and 24.6±2.5 CIELAB units. The value of a* (associated with greenness (−)–redness (+) changes) was also restricted to between 0.8±0.4 and 4.6±

Table 3 Correlation matrix showing the Pearson's coefficients for the phytopigment content and the CIELAB color coordinates

	CIELAB-Cartesian coordinates L*a*b*								CIELAB-cylindrical coordinates $L^*C^*_{ab}h_{ab}$						
	L*	$\log_{10}$ (L*)	1/L*	a*	$\log_{10}$ (a*)	1/a*	b*	$\log_{10}$ (b*)	1/b*	L*	$\log_{10}$ (L*)	1/L*	C^*_{ab}	$\log_{10}$ (C^*_{ab})	$1/C^*_{ab}$	h_{ab}	$\log_{10}(h_{ab})$
Chl*a*	−0.22	−0.19	0.22	−0.82**	−0.92**	0.89**	−0.79**	−0.89**	0.91**	−0.22	−0.19	0.22	−0.79**	−0.89**	0.92**	0.88**	0.87**
$\log_{10}$(Chl*a*)	−0.23	−0.21	0.22	−0.86**	−0.83**	0.72**	−0.81**	−0.83**	0.78**	−0.23	−0.21	0.22	−0.81**	−0.83**	0.78**	0.75**	0.75**
Chl*b*	−0.17	−0.14	0.13	−0.79**	−0.84**	0.75**	−0.77**	−0.83**	0.81**	−0.17	−0.14	0.13	−0.77**	−0.83**	0.82**	0.76**	0.76**
$\log_{10}$(Chl*b*)	−0.17	−0.15	0.16	−0.90**	−0.86**	0.72**	−0.88**	−0.88**	0.80**	−0.17	−0.15	0.16	−0.89**	−0.88**	0.81**	0.72**	0.72**
Cx+*c*	−0.20	−0.17	0.22	−0.87**	−0.90**	0.81**	−0.84**	−0.89**	0.86**	−0.20	−0.17	0.22	−0.84**	−0.89**	0.87**	0.83**	0.83**
$\log_{10}$(Cx+*c*)	−0.16	−0.14	0.15	−0.87**	−0.79**	0.64**	−0.82**	−0.80**	0.72**	−0.16	−0.14	0.15	−0.83**	−0.80**	0.71**	0.69**	0.69**
T. pig	−0.20	−0.17	0.18	−0.83**	−0.89**	0.83**	−0.80**	−0.88**	0.88**	−0.20	−0.17	0.18	−0.80**	−0.88**	0.88**	0.83**	0.83**
$\log_{10}$(T. pig)	−0.19	−0.17	0.19	−0.89**	−0.85**	0.72**	−0.85**	−0.86**	0.79**	−0.19	−0.17	0.19	−0.86**	−0.86**	0.79**	0.74**	0.74**
PQ	−0.06	−0.06	0.11	0.68**	0.53**	−0.39	0.66**	0.57**	-0.46*	−0.06	−0.06	0.11	0.66**	0.57**	−0.45*	−0.40*	−0.44*
$\log_{10}$(PQ)	−0.06	−0.06	0.11	0.68**	0.53**	−0.39	0.66**	0.57**	-0.46*	−0.06	−0.06	0.11	0.67**	0.57**	−0.46*	−0.40*	−0.44*

n=25

Chla chlorophyll *a*, *Chlb* chlorophyll *b*, *Cx+c* total carotenoids, *T. pig*, total phytopigments, *PQ* phaeophytinization quotient

*p<0.05, **p<0.01, significance level

0.7 CIELAB units, although in this case the color coordinate changed significantly between the three sampling sites and the five sediment cores. The significantly lowest value of a* (i.e., the greenest relative to the remaining four sediment cores) corresponded to sediment core 5, in which the phytopigment content was significantly higher (see Table 1). In the same way, the highest values of a* (the furthest from the green color), corresponded to sediment cores 3 and 4 from the Anllóns sampling site (see Table 2), in which the phytopigment content was significantly lower (see Table 1). Likewise, intermediate values of a* in sediment cores 1 and 2 from the A Ponte sampling site (see Table 2) corresponded to the intermediate phytopigment contents (see Table 1). The same pattern was observed for b* (associated with blueness (−) –yellowness (+) changes) and C^*_{ab} (chroma of color), as the value of b* and C^*_{ab} increased as the pigment content of the riverbed sediments decreased (see Tables 1 and 2). Regarding the hue angles, h_{ab} fell within the interval 69.0º±1.2–77.7º± 3.0, so that all the samples were located in the yellow/red–yellow hue area. In contrast to the chromatic parameters (a*, b*, and C^*_{ab}), no clear trend with the phytopigment content was found (see Tables 1 and 2).

The highest phytopigment content, therefore, was associated with the greening of the riverbed sediments (as a* decreases), together with the decrease in the yellow component (as b* decreases) and the loss of the intensity of the color (as C^*_{ab} decreases). Moreover, h_{ab} increased with the phytopigment content, shifting to green tones.

The depth-related distribution of color in the five sediment cores, using the Cartesian (L*a*b*) and cylindrical ($L^*C^*_{ab}h_{ab}$) coordinates, is plotted in Fig. 3. It is important to note that although some differences in phytopigment content were significantly related to depth (see Fig. 2), the CIELAB color coordinates changed significantly with depth in all sediment cores, except for h_{ab} (hue angle) in sediment core 2. Nonetheless, and as with phytopigment content, there was no clear trend with depth, and the vertical distribution of color was highly heterogeneous.

3.3 Relationship between phytopigment content and CIELAB color coordinates

The correlation matrix showing the Pearson coefficients for the phytopigment content and the CIELAB color coordinates is summarized in Table 3. All CIELAB coordinates, except L* (lightness of the color), were closely correlated ((**), $p<0.01$) with each of the phytopigments studied and with the sum of the pigments. Moreover, the a*, b*, and C^*_{ab} parameters, which refer to the chromaticity of the samples, were more closely correlated with the phytopigment content of the samples than the color attribute hue or tone, represented by h_{ab}. The highest correlation coefficients obtained were between the chlorophyll *a* content (Chl*a*) and the value of log-transformed a*, $\log_{10}$ (a*), (Pearson's coefficient, −0.92**); the inverse of b*, 1/b*, (Pearson's coefficient, 0.91**), and the inverse of C^*_{ab}, $1/C^*_{ab}$, (Pearson's coefficient, 0.92**). Very high correlation coefficients between chlorophyll *b*, total carotenoids, and total pigments and the parameters a*, b*, and C^*_{ab} were also obtained. PQ was closely correlated with the a*, b*, and C^*_{ab} parameters. No correlation between the PQ and L* parameter was found, which was demonstrated to be the most informative CIELAB color parameter for chlorophyll degradation in the specific case of the filamentous cyanobacterium *Nostoc* sp. PCC 9104 (Sanmartín et al. 2010b).

A stepwise multiple linear regression analysis was performed to obtain simple expressions to estimate the phytopigment content in the riverbed sediments from the

Table 4 Stepwise multiple linear regression equations for the prediction of phytopigment content (micrograms per gram of sediment) by the use of some CIELAB color coordinates

Phytopigment estimated	Predictive equation	R^2	Adjusted R^2
CIELAB-Cartesian coordinates L*a*b*			
Chlorophyll *a* (Chl*a*)	$\text{Chl}a = 46.4 - 70.6\log_{10}(\text{a}^*)$	0.92	0.84
Chlorophyll *b* (Chl*b*)	$\log_{10}(\text{Chl}b) = 1.9 - 0.3\text{a}^*$	0.90	0.81
Total carotenoids (Cx+*c*)	$Cx + c = 19.0 - 25.9\log_{10}(\text{a}^*)$	0.90	0.80
Total phytopigments	$\text{Total phytopigments} = 107.3 - 157.7\log_{10}(\text{a}^*)$	0.90	0.79
Phaeophytinization quotient (PQ)	$\text{PQ} = 1.9 + 0.2\text{a}^* - 0.9\log_{10}(\text{b}^*)$	0.60	0.57
CIELAB-cylindrical coordinates $L^*C^*_{ab}h_{ab}$			
Chlorophyll *a* (Chl*a*)	$\text{Chl}a = -15.7 + 238.1\,(1/C^*_{ab})$	0.92	0.84
Chlorophyll *b* (Chl*b*)	$\log_{10}(\text{Chl}b) = 2.0 - 0.1C^*_{ab}$	0.89	0.78
Total carotenoids (Cx+*c*)	$Cx + c = 40.9 - 35.8\log_{10}(C^*_{ab})$	0.89	0.79
Total phytopigments	$\text{Total phytopigments} = -30.3 + 523.7\,(1/C^*_{ab})$	0.88	0.77
Phaeophytinization quotient (PQ)	$\text{PQ} = 1.4 + 0.1\,C^*_{ab}$	0.44	0.42

CIELAB color coordinates. The results are shown in Table 4. The assessment of the correlations between the phytopigment contents (chlorophyll *a*, chlorophyll *b*, total carotenoids, and total phytopigments), as well as PQ, and the CIELAB color coordinates (L*, a*, b*, C^*_{ab}, and h_{ab}) were established by considering the former as dependent variables and the Cartesian (L*a*b*) or cylindrical ($L^*C^*_{ab}h_{ab}$) coordinates as the independent variables. Except for PQ, values of adjusted R^2 close to 0.9 were obtained, which validates the CIELAB color coordinates as a useful tool for quantifying phytopigment in riverbed sediments. Thus, the phytopigments studied here may be best quantified by parameters a* and C^*_{ab}. The closest relation corresponded to the chlorophyll *a* content, with an adjusted R^2 value of 0.84, and Chl*a*=46.4–70.6 $\log_{10}$ (a*) and Chl*a*=−15.7+238.1 ($1/C^*_{ab}$) as predictive equations. In this sense, it is important to note that measurements of chlorophyll *a* are used by organizations such as the US Environmental Protection Agency (EPA 2006) as a good indicator of algal biomass, and therefore by quantifying only chlorophyll *a* the potential eutrophication of a system can be evaluated (Smith et al. 1999).

Considering the information shown in Table 4, the Cartesian coordinates (L*a*b*) provided the best description of the phytopigment content, since their adjusted R^2 values were higher for each predictive equation.

Finally, to evaluate the goodness of the computed predictive equations (see Table 4) to estimate phytopigment content using CIELAB color coordinates, three River Anllóns sediment samples (A–C) that were not part of the initial data set, were analyzed (Table 5). The index of agreement between the predicted values and the measured values, expressed as a percentage of variation, did not exceed 4.2% for chlorophyll *a* and 8.5% for the rest of the phytopigments.

4 Conclusions

The proposed colorimetric method was successfully verified by a direct comparison with the conventional spectrophotometric measurements to determine the phytopigment content in cores from the surface riverbed sediments. The CIELAB color parameters were significantly correlated with the phytopigment contents. Linear regression equations were used to predict chlorophyll *a*, chlorophyll *b*, and carotenoid contents, as well as the total pigment contents from parameter a* (redness–greenness of the color) and parameter C^*_{ab} (chroma of the color), and the values of adjusted R^2 were close to 0.9. In addition, the abundance of phytopigments in the sediment cores showed no clear trend either along the longitudinal axis of the river or in relation to the sediment depth.

Table 5 Content (micrograms per gram of sediment) of chlorophyll *a*, chlorophyll *b*, total carotenoids, and total phytopigments measured and predicted by the equations using CIELAB color coordinates

Samples	Chlorophyll *a* (Chl*a*)			Chlorophyll *b* (Chl*b*)			Total carotenoids (Cx+*c*)			Total phytopigments		
	Measured	Predicted	Variation (%)	Measured	Predicted	Variation (%)	Measured	Predicted	Variation (%)	Measured	Predicted	Variation (%)
A	27.7	26.7[a]	3.6	23.4	21.9[a]	6.4	12.9	11.8[a]	8.5	64.0	63.3[a]	1.1
		27.0[b]	2.5		24.0[b]	2.6		12.5[b]	3.1		58.8[b]	8.1
B	24.0	25.0[a]	4.2	23.6	22.4[a]	5.1	12.5	11.8[a]	5.6	60.1	63.3[a]	5.3
		23.3[b]	2.9		24.5[b]	3.8		12.8[b]	2.4		55.6[b]	7.5
C	25.3	26.1[a]	3.2	24.1	24.5[a]	1.7	14.1	13.0[a]	7.8	63.5	67.0[a]	5.5
		24.7[b]	2.4		25.7[b]	6.6		13.3[b]	5.7		58.5[b]	7.9

[a] Using CIELAB-Cartesian coordinates L*a*b*

[b] Using CIELAB-cylindrical coordinates $L^*C^*_{ab}h_{ab}$

Reflectance color measurements comprise a rapid, simple, cost-effective, and nondestructive method for quantifying phytopigment content, without the need for extraction and chemical assay. Future considerations will include the application of this technique to deeper riverbed sediment samples. The application of the technique in situ may also be of great interest for selecting appropriate sampling areas.

Acknowledgments The present study has been financed by the Spanish Ministry of Science and Innovation (MEC CGL2007-62928/MEC BES-2007-16996) and by the Xunta de Galicia (Programa Ángeles Alvariño).

References

Anderson RE (1983) The northern muddy intertidal: seasonal factors controlling erosion and deposition—a review. Can J Fish Aquat Sci 40:143–159

Biggs B, Close M (1989) Periphyton biomass dynamics in gravel bed rivers: the relative effects of flows and nutrients. Freshw Biol 22:209–231

Biggs BJF (2000) Eutrophication of streams and rivers: dissolved nutrient–chlorophyll relationships for benthic algae. J N Am Benthol Soc 19:17–31

Cadée GC, Hegeman J (1974) Primary production of the benthic microflora living on tidal flats in the Dutch Wadden Sea. Neth J Sea Res 8:260–291

Cadée GC (1976) Sediment reworking by Arenicola marina on tidal flats in the Dutch Wadden Sea. Neth J Sea Res 10:440–468

Chételat J, Pick FR, Morin A (1999) Periphyton biomass and community composition in rivers of different nutrient status. Can J Fish Aquat Sci 56:560–569

Chételat J, Pick FR, Hamilton PB (2006) Potamoplankton size structure and taxonomic composition: influence of river size and nutrient concentrations. Limnol Oceanogr 51:681–689

CIE (1986) Publication 15–2: colorimetry. CIE Central Bureau, Vienna

Coljin F (1982) Light absorption in the waters of the Ems-Dollard estuary and its consequences for the growth of phytoplankton and microphytobenthos. Neth J Sea Res 15:196–216

Dell'Anno A, Mei ML, Pusceddu A, Danovaro R (2002) Assessing the trophic state and eutrophication of coastal marine systems: a new approach based on the biochemical composition of sediment organic matter. Mar Pollut Bull 44:611–622

Devesa R, Moldes AB, Díaz-Fierros F, Barral MT (2007) Extraction study of algal pigments in river bed sediments by applying factorial designs. Talanta 72:1546–1551

Devesa-Rey R, Paradelo R, Díaz-Fierros F, Barral MT (2008) Fractionation and bioavailability of arsenic in the bed sediments of the Anllóns River (NW Spain). Water Air Soil Pollut 195:189–199

Devesa-Rey R, Moldes AB, Díaz-Fierros F, Barral MT (2009a) Study of phytopigments in river bed sediments: effects of the organic matter, nutrients and metal composition. Environ Monit Assess 153:147–159

Devesa-Rey R, Paradelo R, Penalta M, Iglesias ML, Díaz-Fierros F, Barral MT (2009b) Characterization of algal and bacterial biofilm in river bed sediments: the Anllóns River, a case study. In: Proceedings of the 2nd International Multidisciplinary Conference on Hydrology and Ecology Hydro Eco 2009, Vienna

Devesa-Rey R, Moldes AB, Sanmartín P, Prieto-Fernández A, Barral MT (2010) Application of an incomplete factorial design for the formation of an autotrophic biofilm on river bed sediments at a microcosms scale. J Soils Sediments 10:1623–1632

Dodds WK, Smith VH, Zander B (1997) Developing nutrient targets to control benthic chlorophyll levels in streams: a case study of the Clark Fork River. Wat Res 31:1738–1750

Dodds WK, Smith VH, Lohman K (2002) Nitrogen and phosphorus relationships to benthic algal biomass in temperate streams. Can J Fish Aquat Sci 59:865–874

EPA (2006) Dissolved oxygen and biochemical oxygen demand. http://www.epa.gov/volunteer/stream/vms52.html. Accessed 31 May 2009

Gerbersdorf SU, Bittner R, Lubarsky H, Manz W, Paterson DM (2009) Microbial assemblages as ecosystem engineers of sediment stability. J Soils Sediments 9:640–652

Grant J, Daborn G (1994) The effects of bioturbation on sediment transport on an intertidal mudflat. Neth J Sea Res 32:63–72

Guedes A, Ribeiro H, Valentim B, Noronha F (2009) Quantitative colour analysis of beach and dune sediments for forensic applications: a Portuguese example. Forensic Sci Int 190:42–51

Han FL, Zhang WN, Pan QH, Zheng CR, Chen HY, Duan CQ (2008) Principal component regression analysis of the relation between CIELAB color and monomeric anthocyanins in young cabernet sauvignon wines. Molecules 13:2859–2870

Harper D (1992) Eutrophication of fresh waters: principles, problems and restoration. Chapman and Hall, London

Kowalewska G, Wawrzyniak-Wydrowska B, Szymczak M (2004) Chlorophyll *a* and its derivatives in sediments of the Odra estuary as a measure of its eutrophication. Mar Pollut Bull 49:148–153

Kowalewska G (2005) Algal pigments in sediments as a measure of eutrophication in the Baltic environment. Quatern Int 130:141–151

Martínez-Carreras N, Krein A, Gallart F, Iffly JF, Pfister L, Hoffmann L, Owens PN (2010a) Assessment of different colour parameters for discriminating potential suspended sediment sources and provenance: a multi-scale study in Luxembourg. Geomorphology 118:118–129

Martínez-Carreras N, Udelhoven T, Krein A, Gallart F, Iffly JF, Ziebel J, Hoffmann L, Pfister L, Walling DE (2010b) The use of sediment colour measured by diffuse reflectance spectrometry to determine sediment sources: application to the Attert River catchment (Luxembourg). J Hydrol 382:49–63

McIntyre HL, Geider RJ, Miller DC (1996) Microphytobenthos: the ecological role of the "secret garden" of unvegetated, shallow-water marine habitats I. Distribution, abundance and primary production. Estuaries 19:186–201

Meléndez-Martínez AJ, Britton G, Vicario IM, Heredia FJ (2005) Color and carotenoid profile of Spanish Valencia late ultrafrozen orange juices. Food Res Int 38:931–936

Mínguez-Mosquera MI, Rejano-Navarro L, Gandul-Rojas B, Sánchez-Gómez AH, Garrido-Fernández J (1991) Color–pigment correlation in virgin olive oil. J Am Oil Chem Soc 68:332–336

Mishra RK, Shaw BP, Sahu BK, Mishra S, Senga Y (2009) Seasonal appearance of Chlorophyceae phytoplankton bloom by river discharge off Paradeep at Orissa Coast in the Bay of Bengal. Environ Monit Assess 149:261–273

Moreno S, Niell FX (2004) Scales of variability in the sediment chlorophyll content of the shallow Palmones River estuary, Spain. Estuar Coast Shelf Sci 60:49–57

Moyano MJ, Meléndez-Martínez AJ, Alba J, Heredia FJ (2008) Comprehensive study on the color of virgin olive oils and its relationship with their chlorophylls and carotenoids indexes (II): CIELUV and CIELAB uniform color spaces. Food Res Int 41:513–521

Muylaert K, Sánchez-Pérez JM, Teissier S, Sauvage S, Dauta A, Vervier P (2009) Eutrophication and its effect on dissolved Si

concentrations in the Garonne River (France). J Limnol 68:368–374

Pinckney JL, Paerl HW, Tester P, Richardson TL (2001) The role of nutrient loading and eutrophication in estuarine ecology. Environ Health Perspect 109:699–706

Poutanen EL, Nikkilä K (2001) Carotenoid pigments as tracers of cyanobacterial blooms in recent and post-glacial sediments of the Baltic Sea. Ambio 30:179–183

Prieto B, Rivas T, Silva B (2002) Rapid quantification of phototrophic microorganisms and their physiological state through their colour. Biofouling 18:229–236

Prieto B, Silva B, Lantes O (2004) Biofilm quantification on stone surfaces: comparison of various methods. Sci Total Environ 333:1–7

Rabalais NN, Atilla N, Normandeau C, Turner RE (2004) Ecosystem history of the Mississippi River-influenced continental shelf revealed through preserved phytoplankton pigments. Mar Pollut Bull 49:537–547

Ronen R, Galun M (1984) Pigment extraction from lichens with dimethyl sulfoxide (DMSO) and estimation of chlorophyll degradation. Environ Exp Bot 24:239–242

Rubinos D, Barral MT, Ruiz B, Ruiz M, Rial ME, Álvarez M, Díaz-Fierros F (2003) Phosphate and arsenate retention in sediments of the Anllóns River (Northwest Spain). Water Sci Technol 48:159–166

Rubinos D, Iglesias ML, Devesa-Rey R, Díaz-Fierros F, Barral MT (2010) Arsenic release from contaminated river sediments: Kinetics, effect of pH and phosphate concentration. Eur J Mineral 22:665–678

Sanmartín P, Aira N, Devesa-Rey R, Silva B, Prieto B (2010a) Relationship between color and pigment production in two stone biofilm-forming cyanobacteria (*Nostoc* sp. PCC 9104 and *Nostoc* sp. PCC 9025). Biofouling 26(5):499–509

Sanmartín P, Villa F, Silva B, Cappitelli F, Prieto B (2010b) Color measurements as a reliable method for estimating chlorophyll degradation to phaeopigments. Biodegradation. doi:10.1007/s10532-010-9402-8

Schott JR (1997) Remote sensing, the image chain approach. New York: Oxford University Press

Smith VH, Tilman GD, Nekola JC (1999) Eutrophication: impacts of excess nutrient inputs on freshwater, marine, and terrestrial ecosystems. Environ Pollut 100:179–196

Sun MY, Dai J (2005) Relative influences of bioturbation and physical mixing on degradation of bloom-derived particulate organic matter: Clue from microcosm experiments. Mar Chem 96:201–218

Wang H, Appan A, Gulliver JS (2003) Modeling of phosphorus dynamics in aquatic sediments: I—model development. Water Res 37:3928–3938

Wellburn AR (1994) The spectral determination of chlorophylls a and b, as well as total carotenoids, using various solvents with spectrophotometers of different resolutions. J Plant Physiol 144:307–313

Wetzel RG (1970) Recent and postglacial production rates of a marl lake. Limnol Oceanogr 15:491–503

Wyszecki G, Stiles WS (1982) Color science, concepts and methods, quantitative data and formulae, 2nd edn. Wiley, New York

Yeh TY, Ke TY, Lin YL (2010) Algal growth control within natural water purification systems: macrophyte light shading effects. Water Air Soil Pollut 214(1–4):575–586

Discusión General

Un punto importante en la gestión del mantenimiento y rehabilitación de edificios y otras construcciones es su limpieza. A este respecto, los organismos colonizadores contribuyen de forma substancial al ensuciamiento de los edificios produciendo un daño no sólo estético sino también físico y químico en los materiales (Seaward, 1979; Grant, 1982). Puesto que la colonización biológica de las superficies expuestas a la intemperie es inevitable, es importante detectar el momento en el que comienza dicha colonización para atajarla desde un principio y así evitar daños irreparables. En el caso de labores de mantenimiento, en las que la eliminación de la colonización biológica es prácticamente siempre necesaria, se requiere una metodología adecuada para controlar la eficacia de la limpieza. Hasta el momento este control se realiza o bien visualmente, lo que induce a errores, o bien a partir de los métodos tradicionales de análisis microbiológico, lo que implica una toma de muestra (muchas veces imposible de realizar por el valor histórico artístico del elemento de la construcción), así como, un arduo y costoso trabajo de laboratorio. Por todo ello, y para el caso de microorganismos fototróficos tales como algas, cianobacterias y líquenes, todos ellos organismos coloreados colonizadores habituales de las edificaciones, esta tesis doctoral propone un método rápido, no destructivo y de aplicación directa sobre el edificio, basado en la medida del color, útil para cuantificar la colonización presente y para estudiar su evolución.

De este modo, el objetivo principal del presente proyecto de tesis fue desarrollar una nueva metodología que permita cuantificar y estudiar la evolución de la colonización epilítica fototrófica sobre las construcciones graníticas empleando la medida instrumental de color. Para conseguir este objetivo principal, en esta tesis se plantearon un conjunto de objetivos concretos de investigación relacionados con la medida, la representación y la discusión de la información de color contenida en los dos elementos implicados en el estudio: rocas graníticas y microorganismos fototróficos (cianobacterias), así como en la interacción entre ambos. El desarrollo de una metodología de medida y caracterización del color de las rocas graníticas (Capítulos 1 y 2) y de las cianobacterias (Capítulos 3–5), así como la mejora en el método de extracción de la roca de la clorofila-a, marcador de la biomasa fototrófica (Capítulo 6), ha permitido determinar las mejores condiciones de medida del color las cuales se han aplicado con éxito en casos reales de colonización fotoautotrófica y desarrollo de biofilms sobre

fachadas de granito (Capítulo 7). Asimismo, el trabajo desarrollado en el contexto de la conservación del Patrimonio monumental construido con granito ha favorecido la posterior implementación del método colorimétrico al Patrimonio natural para su uso y aplicación en otros sustratos inorgánicos, como son el estudio del color en rocas pizarrosas como criterio para su sustitución en trabajos de restauración (Capítulo 8), la caracterización del color en suelos quemados como indicador de la intensidad de un incendio (Capítulo 9) y la medida del color en sedimentos de río para estimar su contenido en fitopigmentos (Capítulo 10).

La hipótesis de partida de la presente investigación, la existencia de una relación directa entre la cantidad de microorganismos fototróficos depositados sobre una superficie y el color que generan, había sido previamente demostrada por Prieto *et al.* (2002) a partir de experimentos de laboratorio. Asimismo, la validez del uso del color como estimador de la biomasa de dichos organismos sobre superficies pétreas, fue demostrada por Prieto *et al.* (2004) a partir de comparaciones entre los métodos más usuales de cuantificación de biomasa algal. Por otra parte, previamente al planteamiento de esta tesis, se habían publicado varios trabajos en los que se determinaban variaciones en el color de rocas ornamentales empleando aparatos de medida de color por contacto, como colorímetros triestímulo y espectrofotómetros portátiles (*e.g.* Durán-Suárez *et al.*, 1995; García-Talegón *et al.*, 1998; Iñigo *et al.*, 2004; Grossi *et al.*, 2007), pero no se había establecido ningún protocolo para la caracterización del color de las rocas ornamentales. En este sentido, cabe señalar que la configuración óptica y la geometría de medida de los espectrofotómetros y los colorímetros portátiles les permiten promediar espacialmente la luz reflejada de un área fija de lectura, circular y con un diámetro que varía entre 3 y 60 mm, correspondiente a la apertura del cabezal. De esta manera el aparato registra un color integrado, resultante de las reflectancias o transmitancias provocadas por los distintos colores que recoge en esa área de lectura. Esto supone una importante ventaja en el caso de superficies relativamente homogéneas en color pero implica la necesidad de determinar previamente el área mínima de medida y el número mínimo de medidas a realizar en dicha área cuando se trata de superficies heterogéneas en color y textura, como es el caso de las rocas graníticas. El desconocimiento de dichos parámetros conduce a una pérdida de información colorimétrica que será más o menos importante dependiendo de la heterogeneidad del color e impide la comparación de resultados.

Atendiendo a esta situación, en el Capítulo 1 de esta tesis doctoral se propuso por primera vez un protocolo para la caracterización del color de las rocas graníticas ornamentales determinando el área mínima de medida y el número de medidas mínimo necesario empleando dos instrumentos de medida de color por contacto, un colorímetro portátil triestímulo y un espectrofotómetro portátil para sólidos (Prieto *et al.*, 2010a). Las rocas graníticas pueden ser consideradas como uno de los casos más difíciles en lo que a la determinación del color de rocas ornamentales se refiere, debido a la gran heterogeneidad en su color y textura ocasionada por la compleja distribución de los minerales con diferentes colores que las

componen. Para este estudio, se realizó una cuidadosa selección de rocas ornamentales con el fin de obtener la gama más amplia en color y textura dentro de las rocas graníticas más comúnmente empleadas en las edificaciones. Se trabajó con las siguientes rocas comerciales: *Labrador Claro*, de color azulado-oscuro y textura gruesa, *Grissal*, de color grisáceo y textura media, *Rosa Porriño*, de color rosado y textura gruesa, *Blanco Cristal*, de color blanquecino-claro y textura fina y *Silvestre*, de color pardo y textura fina. Además, teniendo en cuenta que todas las rocas ornamentales puestas en obra presentan un acabado superficial y que éste puede afectar al color, para cada tipo de roca granítica se estudiaron cuatro tipos diferentes de acabado comercial: pulido (el menos rugoso), apomazado, aserrado y flameado (el más rugoso), excepto para *Labrador Claro* en el que un acabado flameado no es fácil de conseguir, y para la variedad de granito *Silvestre* en la que los acabados pulido y flameado no se pueden aplicar por lo que son sustituidos por pulido sin brillo y abujardado, respectivamente.

Tres fueron los factores de variación considerados en el estudio: el tipo de roca (color y textura), el acabado (pulido, apomazado, aserrado y flameado) y el área de lectura o tamaño del cabezal de medida (aberturas circulares de 5, 8, 10 y 50 mm de diámetro). Las medidas de color se analizaron considerando el espacio de color CIELAB teniendo en cuenta el grupo de coordenadas escalares (L*a*b*). Un aspecto relevante de este trabajo fue la metodología de estudio establecida para la determinación de la influencia de estos factores en los parámetros del color, ya que hasta el momento no se había realizado ningún trabajo de este tipo. Se puso de manifiesto la importancia de analizar los datos de color tanto desde un punto de vista colorimétrico como estadístico ya que únicamente el análisis colorimétrico o únicamente el estadístico no permitieron extraer conclusiones. La combinación de ambos análisis permitió demostrar que la variabilidad de las rocas graníticas en cuanto a su color, textura y acabado superficial ha de ser considerada a la hora de estandarizar la metodología de medición del color, puesto que todos estos parámetros afectan al número de medidas mínimo que se deben realizar. Se demostró que para las rocas graníticas el número mínimo de medidas por unidad de superficie depende del área de lectura, la cual viene determinada por el tamaño del cabezal, siendo 6 medidas[†]/36 cm^2 las recomendables para un área de lectura o cabezal de 50 mm de diámetro, 14medidas/36 cm^2 para los cabezales de 10 y 8 mm de diámetro y 17 medidas/36cm^2 para un cabezal de 5 mm de diámetro. Con respecto al área de medida, se puso de manifiesto que un área de 36 cm^2 es suficiente cuando se quiere caracterizar el color de una roca granítica empleando cabezales de diámetro inferior o igual a 10 mm. En el caso de cabezales de mayor tamaño es necesario disponer de una superficie de 72 cm^2 o superior. Si se trabaja atendiendo a tales premisas, las diferencias en los parámetros de color L*, a*, b* obtenidos con los distintos cabezales de medida serán estadísticamente significativas, pero no

[†] En todos los casos son medidas por sustitución, es decir medidas consecutivas tomadas en distintos puntos de la superficie de la muestra elegidos al azar por el operador.

a nivel de tolerancias industriales de diferencias de color, por lo que en la práctica podrán ser obviadas (Prieto *et al.*, 2010a).

Posteriormente a la publicación de los resultados de la investigación recogida en el Capítulo 1 de la presente tesis, Sousa & Gonçalves (2011) realizaron un trabajo muy similar en el que evaluaron los factores que deben ser considerados en la medida del color de los granitos ornamentales empleando un colorímetro. Dichos autores analizaron únicamente un acabado superficial, el pulido, emplearon un rango de tamaño del cabezal de medida más pequeño, usando cabezales de 4, 8 y 16 mm de diámetro, y muestras de un tamaño bastante superior, losas de 100 cm^2 y 30.000 cm^2. Estas diferencias pudieran explicar las diferencias en los resultados con respecto a los obtenidos en el Capítulo 1, ya que según Sousa & Gonçalves (2011) los parámetros de color no mostraron diferencias significativas con los distintos cabezales de medida, aunque la apertura de 16 mm permitió una disminución de la desviación estándar de los valores medios, y así, empleando cualquier cabezal de medida el número de medidas mínimo resultó de 40 medidas/100 cm^2 y 60 medidas/30.000 cm^2. Otro aspecto importante a tener en cuenta es que en este estudio sólo se empleó la métrica CIELAB para el cálculo de las diferencias totales de color y no las más recientes y mejoradas CIE94 y CIEDE2000 que resultan más adecuadas para evaluar muestras con bajos valores de croma (Johnson & Fairchild, 2003), y asimismo no se contemplaron los valores supraumbrales de aceptabilidad de diferencia de color (Melgosa *et al.*, 1997).

Una vez establecidas las condiciones mínimas en cuanto al número de medidas y al área representativa, se analizó la influencia del tipo de acabado comercial (pulido, apomazado, aserrado y flameado) en el color, brillo y rugosidad de las rocas graníticas ornamentales, así como la relación existente entre estos tres parámetros estéticos (Capítulo 2). Es oportuno desarrollar este tipo de estudios por cuanto que apenas existen trabajos hasta el momento (exceptuando el realizado por Benavente *et al.* en 2003) en los cuales se analicen las relaciones entre color, brillo y rugosidad en muestras heterogéneas, contrariamente a lo que ocurre con las muestras homogéneas donde el número de estudios en ese sentido es muy amplio (Barnett, 1973; Thomas, 1999; Dalal & Natale-Hoffman, 1999; Simonot & Elias, 2003; Keyf & Etikan, 2004; Eliades *et al.*, 2004; Ariño *et al.*, 2005; Briones *et al.*, 2006; Shih *et al.*, 2008; Ignell *et al.*, 2009).

Por lo general, cuando la superficie lisa de un objeto coloreado se vuelve rugosa su color cambia (Simonot & Elias, 2003). Para el caso de las rocas graníticas ornamentales, se demostró que los diferentes acabados superficiales producen variaciones casi siempre perceptibles en el color, en especial en la claridad del color (L*). La magnitud de estos cambios resultó ser mayor en rocas más oscuras, siendo *Labrador Claro* la roca granítica que mostró mayor variación de color debido a los distintos acabados superficiales. Esto está en concordancia con los resultados obtenidos por Ignell *et al.* (2009) para superficies de

polímeros, quienes comprobaron que cuanto más oscuro es el material, más aumenta su claridad al volverse la superficie más áspera, y con los obtenidos por Benavente *et al.* (2003) en diferentes tipos de mármoles y calizas, donde muestras con un alto valor de croma (C^*_{ab}) mostraron mayores cambios en la diferencia total de color (ΔE_{94}) debido al acabado de la superficie que muestras con un bajo valor de croma que apenas mostraron cambios de color en relación al acabado superficial.

Estos cambios significativos y perceptibles de color provocados por los distintos acabados comerciales en la superficie de las rocas graníticas, ocurrieron tanto cuando estaba incluido (SCI) como excluido (SCE) el componente especular en el modo de medida, a diferencia de lo que ocurre en otros materiales como por ejemplo la porcelana dental (Kim *et al.*, 2003) y los plásticos moldeados por inyección (Ariño *et al.*, 2007), en los que las variaciones de color debidas a diferencias en la rugosidad superficial sólo son notorias al emplear el componente especular excluido (modo SCE). No obstante, se debe tener en cuenta que al comparar ambos modos en la medida del color de las rocas graníticas, el modo SCE resultó ser el que más magnifica las diferencias de color producidas por los distintos acabados comerciales. Estos resultados son de gran interés, ya que aportan información muy valiosa sobre la metodología de lectura del color que se debe emplear según la información que se quiera obtener.

Los parámetros del color ($L^*a^*b^*C^*_{ab}h_{ab}$) no variaron de forma proporcional a la rugosidad generada por los diferentes acabados, aunque los valores de dichos parámetros fueron diferentes para cada acabado. Respecto al brillo, éste depende del índice de refracción de los diferentes minerales que componen las rocas graníticas y está afectado por el color de las rocas pero de forma diferente para acabados pulidos y rugosos. En la relación rugosidad-brillo, muchos autores han demostrado que existe una relación inversa entre la rugosidad y el brillo para el caso de superficies homogéneas desde el punto de vista de su color y composición (Hunter & Harold, 1987; Thomas, 1999; Wang *et al.*, 2000; Ariño *et al.*, 2005; Briones *et al.*, 2006). Para el caso de las rocas graníticas ornamentales, el brillo no es función de la rugosidad para todo el rango de medida, sino que el brillo y la rugosidad sólo están inversamente relacionados dentro del rango de los valores bajos de rugosidad. Son varias las razones que podrían explicar este hecho pero quizás la más relevante sea que los tratamientos utilizados para lograr los acabados más rugosos, *viz.* flameado y abujardado, rompen los minerales de la superficie los cuales en su mayor parte tienden a fracturarse a lo largo de planos cristalográficos bien definidos (López-Arce *et al.*, 2010) creando así nuevas y pequeñas superficies lisas que causan un aumento del brillo superficial (Sanmartín *et al.*, 2011a).

La metodología de estudio definida en el Capítulo 1 fue empleada con éxito para definir un protocolo de medida del color de biofilms (Capítulo 3) y de rocas pizarrosas (Capítulo 8) lo que valida su uso para otro tipo de superficies heterogéneas. En el caso de los biofilms, se seleccionaron como organismos objeto de estudio las cianobacterias, por tratarse de los

principales constituyentes de los denominados "verdines" y constituir la biomasa mayoritaria que se desarrolla sobre las superficies de piedra natural (Ortega-Morales *et al.*, 2000; Gaylarde *et al.*, 2001). Las cianobacterias empleadas pertenecen a los géneros *Nostoc* y *Scytonema*, ambos del orden de las Nostocales. La elección de los géneros de cianobacterias se realizó atendiendo a sus características metabólicas y morfológicas. En concreto, los organismos seleccionados son fijadores de nitrógeno (o diazótrofos), es decir organismos que satisfacen sus requerimientos metabólicos principalmente a través de los compuestos presentes en la atmósfera, lo que les permite ser pioneros a la hora de colonizar superficies pobres en nutrientes, como es el caso de las superficies pétreas. Otra de las características tenida en cuenta en la elección de estos géneros microbianos fue su morfología ya que, en ambos casos, se trata de cianobacterias de morfología filamentosa, protegidas del medio externo por una matriz polisacárida, mucilaginosa en el caso del género *Nostoc* y en forma de vaina en el caso del género *Scytonema*. Esta morfología les permite resistir condiciones extremas de temperatura y humedad y por lo tanto las hace muy adecuadas para la colonización de muros y fachadas, donde ambos parámetros medioambientales varían fuertemente dependiendo de la radiación solar y las precipitaciones. En concreto, se eligieron las cepas *Nostoc* sp. PCC 9104, *Nostoc* sp. PCC 9025 y *Scytonema* sp. CCC 9801 por ser cepas cianobacterianas aisladas por primera vez en Galicia y colonizadoras habituales de suelos y rocas de esta región (Acea *et al.*, 2001, 2003).

Siguiendo la metodología de trabajo planteada por Prieto *et al.* en 2002, se preparó un cultivo mixto de *Nostoc* sp. PCC 9104, *Nostoc* sp. PCC 9025 y *Scytonema* sp. CCC 9801 y a partir de él se extrajeron alícuotas de diferentes volúmenes que fueron filtradas a vacío a través de filtros de nitrocelulosa blancos (0,45 µm de tamaño de poro y 47 mm de diámetro) con el objetivo de depositar una capa homogénea de microorganismos en un área fija y circular de 9,62 cm^2 (35 mm de diámetro), simulando así la composición y características de un biofilm (Costerton, 2007). Puesto que el número de medidas mínimo necesario para caracterizar el color de una superficie heterogénea depende, entre otros factores, del tamaño del cabezal de medida (Capítulo 1), y que el contenido en humedad de las cianobacterias afecta a su caracterización colorimétrica (Prieto *et al.*, 2002), en el Capítulo 3 se analizó el número mínimo de medidas necesario para un tamaño de superficie determinado con respecto al tamaño del cabezal de medida, teniendo en cuenta el contenido en humedad de los microorganismos y su grado de cobertura, ya que cuanto mayor es éste más homogéneo será el color de la superficie (Prieto *et al.*, 2010b). Se demostró que el número mínimo de medidas necesario aumenta con la heterogeneidad del color de la superficie, por lo que para determinar el color del biofilm se recomienda medir en superficies completamente cubiertas por los microorganismos. Respecto al contenido en humedad, se observó que éste provoca cambios en los valores de claridad (L*), no afectando al resto de los parámetros de color CIELAB. Así, los valores de L* disminuyen exponencialmente con el contenido en humedad, volviéndose prácticamente estables en el

tramo de humedad del 50 al 100%, por lo que se estableció un contenido en humedad superior al 50% en el biofilm como condición para obtener una medida de color fiable. Por último y como era de esperar, el tamaño del cabezal de medida influyó en el número de medidas, decreciendo al aumentar éste. Así, para obtener resultados comparables, se propuso realizar un total de 10 medidas/9,62 cm^2 para cabezales de medida de 8 y 5 mm de diámetro y 8 medidas/9,62 cm^2 para un cabezal de medida de 10 mm de diámetro.

En lo que respecta al protocolo de medida de color para rocas pizarrosas (Capítulo 8), el número de medidas mínimo necesario se redujo substancialmente con respecto a las rocas graníticas y ligeramente con respecto a los biofilms. Además, mientras que en el caso de rocas graníticas si se emplean cabezales mayores de 10 mm es necesario disponer de un área de estudio de al menos 72 cm^2, para las rocas pizarrosas un área de 36 cm^2 es suficiente cualquiera que sea el tamaño del cabezal de medida. Estas diferencias son sin duda debidas a la mayor homogeneidad en cuanto a color de las rocas pizarrosas (Sanmartín *et al.*, 2010b). Así, en las rocas pizarrosas se recomiendan 3 medidas/36 cm^2 para un área de lectura o cabezal de 50 mm de diámetro, 6 medidas/36 cm^2 para los cabezales de 10 y 8 mm de diámetro y 7 medidas/36cm^2 para un cabezal de 5 mm de diámetro, y un área de 36 cm^2 resulta suficiente cualquiera que sea el tamaño del cabezal de medida.

El análisis conjunto de los resultados obtenidos en los tres trabajos de protocolo de medida del color (Capítulos 1, 3 y 8) pone de manifiesto la importancia que tiene el desarrollo de metodologías de estudio para superficies heterogéneas y permite concluir que el área de lectura o tamaño del cabezal de medida del espectrofotómetro o del colorímetro afecta al número de medidas requeridas para caracterizar el color de una superficie heterogénea. Así, el número de medidas mínimo necesario decrece cuanto mayor es la homogeneidad del color de la superficie. Respecto al área mínima de medida, que sólo fue considerada para las rocas ornamentales, ésta se ve afectada tanto por el tamaño del cabezal de medida como por el tipo de roca y acabado superficial. De manera concreta, un área de medida de 72 cm^2 es necesaria en el caso de rocas graníticas si se emplean cabezales mayores de 10 mm, mientras que para rocas pizarrosas un área de 36 cm^2 es suficiente cualquiera que sea el tamaño del cabezal de medida. En el caso de la medida del color en biopelículas, las propiedades de los microorganismos, como la concentración y el contenido en humedad, afectan al número mínimo de medidas requerido y, lo que es más importante, al color obtenido.

Una vez que se dispuso de los protocolos de medida fue posible delimitar las zonas tridimensionales del espacio de color CIELAB, teniendo en cuenta el grupo de coordenadas escalares (L*a*b*) y el grupo de coordenadas cilíndricas o polares ($L^*C^*_{ab}h_{ab}$), en las que se encuentran incluidas las rocas graníticas (Capítulo 2) y las rocas pizarrosas (Capítulo 8). La definición de estas regiones tridimensionales es muy importante ya que permite acotar el espacio CIELAB para la realización de estudios posteriores y construir una base de datos de

color para estas rocas ornamentales, necesaria cuando en la selección de materiales se emplea el criterio estético y cuando se quieran calibrar cámaras digitales para su uso como colorímetros en el Patrimonio monumental construido. Así, la zona del espacio CIELAB en la que se enmarcan las rocas graníticas tiene sus límites superiores en: L*= 74,9 ± 1,0; a*= 2,7 ± 0,5; b*= 7,4 ± 1,5; C^*_{ab}= 7,6 ± 1,1; y h_{ab}= 253,7º ± 6,1º con el modo SCI; y L*= 75,5 ± 3,5; a*= 3,3 ± 2,6; b*= 8,6 ± 3,6; C^*_{ab}= 9,3 ± 4,2; y h_{ab}= 237,2º ± 46,0º con el modo SCE y sus límites inferiores en: L*= 34,2 ± 0,5; a*= –0,9 ± 0,1; b*= –2,8 ± 0,3; C^*_{ab}= 1,1 ± 0,5; y h_{ab}= 71,8º ± 1,7º con el modo SCI; y L*= 30,7 ± 4,8; a*= –0,8 ± 0,3; b*= –1,4 ± 1,6; C^*_{ab}= 1,0 ± 0,6; y h_{ab}= 71,5º ± 4,9º con el modo SCE.

En el caso de las pizarras de techar de la Península Ibérica, los límites superiores son L*= 53,2 ± 0,2; a*= 0,0 ± 0,0; b*= 2,0 ± 0,1; C^*_{ab}= 4,6 ± 0,1; y h_{ab}= 271,9º ± 2,0º con el modo SCI; y de L*= 52,4 ± 0,7; a*= 0,1 ± 0,1; b*= 1,9 ± 0,3; C^*_{ab}= 4,5 ± 0,2; y h_{ab}= 273,3º ± 5,0º con el modo SCE, y los límites inferiores son L*= 33,7 ± 0,0; a*= –4,2 ± 0,1, b*= –1,4 ± 0,1; C^*_{ab}= 0,5 ± 0,1; y h_{ab}= 143,6º ± 17,9º con el modo SCI; y de L*= 33,5 ± 0,2; a*= –4,1 ± 0,1; b*= –1,8 ± 0,2; C^*_{ab}= 0,6 ± 0,3; y h_{ab}= 155,3º ± 2,6º con el modo SCE.

Tras definir los protocolos y delimitar las zonas tridimensionales de color de las rocas graníticas y pizarrosas en el espacio CIELAB, el siguiente paso fue analizar la influencia de los parámetros medioambientales, tales como la intensidad y la calidad de la luz, la disponibilidad de nitratos (fuente de nitrógeno asimilable) y la presencia de otros nutrientes, en la composición y/o abundancia de los pigmentos fotosintéticos y por tanto en el color del biofilm (Capítulo 4). El cambio de color en microorganismos fotoautotróficos debido a variaciones en los parámetros ambientales ya se había analizado previamente (Collier & Grossman, 1992; Sobczyk *et al.*, 1994; Grossman & Kehoe, 1997; Grossman *et al.*, 2001), observándose que las bajas y medias intensidades de luz generalmente estimulan la síntesis de clorofila-a y ficobiliproteínas en cianobacterias (Raven, 1984; Lonnenborg *et al.*, 1985; Fernández-Valiente & Leganés, 1989; Martín-Trillo, 1995; Jonte *et al.*, 2003; Loreto *et al.*, 2003), mientras que las altas intensidades estimulan la síntesis de carotenoides (Raps *et al.*, 1983). En lo que se refiere a limitaciones en los nutrientes, éstas provocan la disminución del contenido de clorofila-a (Stebvens *et al.*, 1981; Bartual *et al.*, 2002) y de ficobiliproteínas (Collier & Grossman, 1992), permaneciendo relativamente estable en tal situación el contenido de carotenoides (Duke & Allen, 1990). Diferentes términos cualitativos fueron empleados en estos estudios para describir las variaciones de color causadas por los cambios en pigmentos: blanqueo (*bleaching*), clorosis (*chlorosis*), palidez del color (*color paling*), decoloración (*color fading*), amarillamiento (*yellowing*), azulamiento (*blueing color*), etc. Sin embargo en ninguno de ellos se realizó una caracterización objetiva del color observado. En este trabajo de tesis por primera vez se cuantificó el color de forma objetiva (Capítulo 4) y se relacionaron los valores obtenidos con el contenido en pigmentos y los cambios producidos en ambos parámetros, color y pigmentos, con las variables medioambientales. Así, se estudió la variación del contenido en pigmentos

(clorofila-a, ficobiliproteínas ficocianinas y carotenoides totales) y de los parámetros de color CIELAB en dos cepas cianobacterianas, *Nostoc* sp. PCC 9104 y *Nostoc* sp. PCC 9025, mantenidas durante dos semanas en tres medios de cultivo (con nitrato, sin nitrato y sin nitrato y con baja concentración de nutrientes) sometidos a dos intensidades de luz (alta y baja). En ambas cepas las concentraciones de clorofila-a y ficocianinas fueron más altas en los cultivos que crecieron en presencia de nitrato (condiciones no-diazotróficas), aunque en condiciones de baja intensidad de luz para *Nostoc* sp. PCC 9104 y alta intensidad de luz para *Nostoc* sp. PCC 9025. Sin embargo, la concentración de carotenoides se vio afectada por diferentes factores en función de la cepa: para *Nostoc* sp. PCC 9104 la disponibilidad de nutrientes fue el factor determinante, mientras que para *Nostoc* sp. PCC 9025 la presencia de nitratos y la alta intensidad de luz afectaron en mayor medida a su concentración (Sanmartín *et al.*, 2010a).

Por otra parte, los resultados obtenidos revelaron que los valores de los parámetros de color CIELAB podrían ser empleados como indicadores de la concentración de pigmentos, ya que cada pigmento se correlacionó con cada parámetro de color CIELAB, excepto con h_{ab}. Se observó que un incremento en la concentración de pigmentos supone un incremento en los parámetros b*y C^*_{ab}, y un decremento de los parámetros L* y a*. Sin embargo, no todos los parámetros de color CIELAB son igualmente sensibles a los cambios en la concentración de pigmentos. Así, L* es el parámetro más informativo, por ser el más estrechamente correlacionado con cada uno de los pigmentos y el que mejor refleja los cambios en la concentración de pigmentos provocados por las diferentes condiciones ambientales consideradas en el estudio. Le sigue a*, que se mueve hacia valores más negativos a medida que el cultivo envejece y la concentración de pigmentos aumenta. Por su parte, b* y C^*_{ab} proporcionan información sobre la cantidad de ficocianinas en relación a la cantidad de los otros dos pigmentos estudiados, clorofila-a y carotenoides totales. En cuanto al parámetro h_{ab}, éste se correlaciona en una de las cepas, *Nostoc* sp. PCC 9025, con todos los pigmentos y en la otra, *Nostoc* sp. PCC 9104, sólo con la clorofila-a, pero en ambos casos los coeficientes de correlación son demasiado bajos para establecer una relación entre el contenido en pigmentos y este parámetro de color. A pesar de esto, tanto la observación a la que se sometieron los cultivos a lo largo del estudio, como el análisis de los valores de h_{ab}, permiten relacionar este parámetro de color con los cambios en la apariencia de los cultivos, ya que las alteraciones en la apariencia más importantes observadas a lo largo del experimento se vieron reflejadas en los valores de h_{ab}.

De la misma manera que para las rocas graníticas y pizarrosas (Capítulos 2 y 8), en el Capítulo 4 se recoge la delimitación de la zona del espacio CIELAB en la que se localiza el color de las cianobacterias estudiadas, cuyos valores máximos y mínimos son, L*= 92,39; a*= –2,28; b*= 35,22; C^*_{ab}= 41,00; y h_{ab}= 158,80º, y, L*= 36,85; a*= –23,92; b*= 1,30; C^*_{ab}= 2,94; y h_{ab}= 113,60º.

La relación color-pigmentos no sólo es informativa cuando los microorganismos se encuentran en condiciones óptimas de desarrollo, también lo es cuando se encuentran en condiciones de senescencia, como las que se derivan de la aplicación de productos biocidas o condiciones adversas. Así, en este proyecto de tesis se planteó el desarrollo de metodologías basadas en la medida del color para evaluar la eficacia de los biocidas analizando el estado fisiológico de los organismos después de un tratamiento, es decir métodos que permitan conocer si los organismos continúan desarrollándose o si, por el contrario, el tratamiento afectó a sus funciones vitales y se encuentran en fase de senescencia. La eficacia de un biocida en la eliminación de microorganismos fototróficos puede ser probada cuantificando la degradación de su contenido en clorofila a feopigmentos, *viz.* feofitina, clorofilida y feofórbido, (Underwood & Paterson, 1993; Silkina *et al.*, 2009). La relación entre la clorofila y sus productos de degradación se puede establecer mediante espectroscopía UV-Vis empleando los índices o cocientes de feofitinización: $A_{435/415}$, cociente entre las absorbancias registradas a 435 nm y 415 nm; y $A_{665/665a}$ cociente entre las absorbancias registradas a 665 nm antes y después de acidificar la muestra. En ambos casos, una disminución del cociente indica un incremento en la degradación de clorofila a feopigmentos (*e.g.* Barnes *et al.*, 1992; López *et al.*, 1997; Louda *et al.*, 1998). En el Capítulo 5 se demostró que la feofitinización puede ser estimada mediante el análisis del color de los microorganismos ya que, los parámetros de color CIELAB registrados con un colorímetro portátil se correlacionan con los índices de feofitinización, lo que permite analizar la actividad biocida y el estado fisiológico de los microorganismos a través de la caracterización de su color. De los parámetros de color CIELAB, L* resultó ser el más informativo correlacionándose con ambos índices de feofitinización en los modos de crecimiento (forma planctónica y biofilm), seguido de a* y C^*_{ab} que se correlacionaron con uno de los índices de feofitinización en ambos modos de crecimiento (Sanmartín *et al.*, 2011b).

En la puesta a punto de cualquier método es preciso contar con un método de referencia que permita establecer en qué medida el nuevo método permite obtener valores exactos. En el caso que nos ocupa, la cuantificación de la colonización epilítica fototrófica sobre construcciones graníticas a través de la cuantificación de su color, el método de referencia es la cuantificación espectrofotométrica de la clorofila-a. Sin embargo, si bien este método no presenta problemas cuando se analiza biomasa de algas y cianobacterias en medios líquidos y en suelos, cuando se trata de analizar biomasa fototrófica en sustratos rocosos presenta ciertas limitaciones derivadas del proceso de extracción de la clorofila-a (Prieto *et al.*, 2004). Por tanto, fue necesario mejorar dicho método de extracción antes de analizar los aspectos relativos al color de las rocas graníticas colonizadas. Con este objetivo, en el Capítulo 6 de la presente tesis doctoral se llevó a cabo una optimización del método de extracción de clorofila-a sobre roca granítica usando la metodología de superficie de respuesta de un diseño

factorial incompleto de 3er orden, que predice las condiciones experimentales óptimas para la máxima extracción de clorofila-a (Fernández-Silva *et al.*, 2011).

Se evaluaron tres pretratamientos mecánicos para determinar el procedimiento más eficaz en la extracción de clorofila-a con dimetil sulfóxido (empleado como solvente) en bloques de granito inoculados con un cultivo mixto de tres cepas cianobacterianas que forman biofilms sobre rocas graníticas, *Nostoc* sp. PCC 9104, *Nostoc* sp. PCC 9025 y *Scytonema* sp. CCC 9801. Dos de ellos, A y B, incluían la trituración de la probeta de granito seguida, en el caso del pretratamiento B, de una sonicación de los fragmentos de roca y extractante en un baño de ultrasonidos. En el tercer pretratamiento, C, se sustituía la trituración de la probeta por la aplicación de una sonda de ultrasonidos (sonicador) al extractante que baña los bloques enteros. Para cada pretratamiento se utilizó un diseño de Box-Behnken para 3 factores experimentales o variables de optimización: (1) relación volumen de extractante/volumen de muestra, (2) temperatura durante la extracción y (3) tiempo de extracción, siendo la variable dependiente o de respuesta, la clorofila-a extraída. Tras la incubación en DMSO con sus correspondientes condiciones experimentales, la concentración de clorofila-a fue determinada usando el método de espectrofotometría UV-Vis.

El análisis de los resultados determinó que: (i) la aplicación de ultrasonidos mejora la extracción de clorofila-a de los biofilms desarrollados sobre sustratos rocosos; (ii) la precisión de la medida usando el método de espectrofotometría UV-Vis para el cálculo de la concentración de clorofila-a disminuye cuando las muestras están altamente diluidas, por lo que son más convenientes los métodos que requieren un menor volumen de extractante, y, (iii) la temperatura de extracción es el factor experimental más importante (comparado con los otros dos analizados) en la extracción de clorofila-a de los biofilms desarrollados sobre sustratos rocosos. Por todo ello, se propone un método que implica la aplicación de ultrasonidos a la muestra intacta sin triturar (con lo que el método de extracción de clorofila-a deja de ser un método destructivo y pasa a ser un método meramente invasivo) seguido de una incubación en 0,43 ml de DMSO/cm^2 de muestra, a 63ºC durante 40 minutos. Esta mejora fue empleada en un experimento de confirmación en el que se consiguió la recuperación del 90% de la cantidad real (*i.e.* inocludada) de clorofila-a, un incremento sustancial frente al 68% que era el máximo de recuperación en trabajos anteriores (Fernández-Silva *et al.*, 2011).

Después de los experimentos de laboratorio, se pudo llevar a cabo la aplicación de la metodología desarrollada *in situ* en monumentos y edificaciones de granito que presentaban una problemática real relacionada con la colonización fototrófica y epilítica. De este modo, se realizó un estudio (que se presenta en el Capítulo 7) de detección y monitorización del crecimiento de biofilms fototróficos y epilíticos en la fachada de granito de un edificio institucional de Santiago de Compostela, el Centro de Supercomputación de Galicia (CESGA).

Se trata de un caso real orientado a la conservación preventiva que proporciona una base para el establecimiento de criterios de detección precoz del verdín y monitorización de su desarrollo en tiempo real, utilizando las variaciones de color registradas mediante un espectrofotómetro portátil.

Varios autores ya habían empleado colorímetros y espectrofotómetros portátiles en la cuantificación del color generado por los microorganismos fototróficos que se desarrollan de forma epilítica sobre los sustratos pétreos. Así, Urzì & Realini (1998) correlacionaron el color gris o naranja, determinado instrumentalmente, de las pátinas biológicas sobre roca calcárea con los microorganismos responsables, hongos o algas y bacterias respectivamente; Prieto *et al.* (2005) monitorizaron la evolución del color en un frente de cantera de cuarzo a cielo abierto tras la inducción de biofilms, los cuales enmascaraban el color blanco brillante del mineral reduciendo así el impacto visual. Más recientemente, Muynck *et al.* (2009) por medio de un análisis colorimétrico utilizando un colorímetro portátil, examinaron la efectividad de diferentes tratamientos hidrofugantes y/o biocidas para la prevención de la colonización por algas en dos tipos de hormigón con diferente biorreceptividad, y Tanaca *et al.* (2011) evaluaron la biorreceptividad de tres nuevas formulaciones de cemento expuestas en ambientes urbanos, rurales y costeros, mediante el cambio de color provocado por la colonización de hongos. Sin embargo, en ninguno de esos estudios, excepto en Prieto *et al.* (2005), se había empleado una metodología de determinación del color contrastada, y ésta fue la primera vez que la medida de color empleando un aparato de medida por contacto era utilizada para estudiar la evolución de la colonización fototrófica (verdín) sobre fachadas de granito (Sanmartín *et al.*, 2012).

Asimismo este trabajo permitió determinar los límites de percepción de la colonización fototrófica sobre rocas graníticas basándose en un trabajo previo llevado a cabo por Prieto *et al.* (2006), en el que a partir de un estudio psicofísico se definieron los términos cualitativos que indicaban el grado de colonización: inapreciable, ligera, apreciable, evidente, notable, intensa o muy intensa, relacionándolos con la diferencia total de color (ΔE^*_{ab}). En el Capítulo 7, tomando en cuenta aquel trabajo se realizó un experimento psicofísico con el que se determinó el límite entre la imperceptible y la perceptible colonización biológica, que provoca el enverdecimiento (*greening*) en términos de incremento de los parámetros de color L* (ΔL^*), a* (Δa^*) y b* (Δb^*), biomasa fotoautotrófica (en peso seco) y clorofila-a extraída.

Los resultados mostraron que los cambios registrados en b* permiten la detección temprana y la monitorización a tiempo real del desarrollo de biofilms en fachadas de granito, incluso cuando éstos son imperceptibles al ojo humano. El parámetro b* es el que proporciona mayor información, porque es el que detecta la colonización más temprana y porque es el que varía en mayor magnitud con el tiempo de manera que es el que condiciona en mayor medida el cambio de color total (ΔE^*_{ab}). Este resultado está en concordancia con resultados previos en otros sustratos como cuarzo (Prieto *et al.*, 2005) y cemento (Muynck *et al.*, 2009). Así, el límite

de percepción del enverdecimiento (*greening*) sobre una superficie de granito fue establecido en Δb* = + 0.59 unidades CIELAB, que corresponden a 6.3 μg biomasa fotoautotrófica en peso seco/cm^2 y (8.43 ± 0.24) x 10^{-3} μg de clorofila-a extraída/cm^2.

Los resultados alcanzados presentan utilidad práctica en la gestión y mantenimiento de edificaciones con problemas de biodeterioro, al incluir indicaciones sobre el momento en que se deben realizar labores de limpieza y/o aplicación de tratamientos para detener o revertir la aparición perceptible del verdín en las fachadas. De este modo, se establece que para mantener la superficie en un estado de apariencia muy cercano al original dichas tareas deben realizarse cuando la colonización existe pero aún no se percibe visualmente, ambos momentos fácilmente identificables empleando un espectrofotómetro portátil. En este sentido, la monitorización de los cambios en b* (Δb*) de la fachada del CESGA justo después de su limpieza revelaron que la recolonización por microorganismos fototróficos no tardó más de 129 días en producirse (un poco más de 4 meses), siendo necesarios menos de 178 días (prácticamente 6 meses) para ver un perceptible enverdecimiento en la fachada. Se constató así la rapidez con que ocurre la recolonización por verdín en Galicia, aspecto ya apuntado por Silva *et al.* en 1997.

En lo que se refiere a la información ofrecida por los distintos parámetros de color CIELAB, no se puede establecer un solo parámetro CIELAB como el único relevante, aunque debe subrayarse la importancia de L* en la caracterización del color de las rocas graníticas y de los microorganismos fototróficos (cianobacterias), puesto que L* resultó el parámetro que más varía entre los distintos acabados de las rocas graníticas (Capítulo 2), también el único que influye en la diferencia de color entre biofilms con diferente contenido en humedad (Capítulo 3), el que mejor se correlaciona con el contenido en pigmentos cuando éste varía debido a diferentes condiciones medioambientales (Capítulo 4) y el que mejor se ajusta a los cocientes de feofitinización que marcan la degradación de la clorofila-a y con ello el estado fisiológico de los microorganismos cianobacterianos (Capítulo 5). Sin embargo, cuando rocas graníticas y cianobacterias son analizadas en conjunto (Capítulo 7), es b* el parámetro que resulta más informativo para el estudio de la detección y monitorización del crecimiento de los microorganismos fototróficos sobre una fachada de granito.

El trabajo desarrollado en el núcleo central de tesis (Capítulos 1-7) ha posibilitado la posterior implementación del método colorimétrico a otros sustratos inorgánicos naturales como son rocas pizarrosas, suelos y sedimentos. Los objetivos planteados en esta serie de trabajos fueron diversos, mostrando como nexo de unión la aplicación práctica de la medida de color. Así, la medida instrumental del color es útil como criterio de selección de pizarras de techar para su sustitución en trabajos de restauración de edificios históricos (Capítulo 8), para lo que previamente fue planteado un protocolo de medida del color para rocas pizarrosas (Prieto *et al.*, 2011). En ese trabajo se analizó un total de cincuenta variedades de pizarra de techar

(todas las existentes en la Península Ibérica); el tono angular (h_{ab}) resultó el parámetro de color CIELAB más informativo en cuanto a la formación de grupos de pizarra colorimétricamente similares, y el componente especular excluido (SCE) el modo más sensible para la detección de diferencias de color (ΔE^*_{ab}) entre dos variedades de pizarra. Además, se establecieron las similitudes y diferencias en el color y la microestructura de las diferentes variedades comerciales, así como el grado de aceptación para la sustitución de un tipo de pizarra por otro. Así, cinco variedades de pizarra pueden reemplazar a y ser reemplazadas por prácticamente el resto de las cincuenta variedades y una única variedad no puede reemplazar ni ser reemplazada por ninguna otra pizarra.

Por otra parte y a pesar de que el impacto de los incendios sobre los suelos forestales gallegos es bien conocido (Soto & Díaz-Fierros, 1993; Soto *et al.*, 1997) y han sido muchos los casos en los que se han descrito variaciones apreciables en el color del suelo tras un incendio (como el ennegrecimiento debido a carbonización parcial o total de la materia orgánica y el enrojecimiento debido a la deshidratación de los óxidos de hierro), la variación de los parámetros de color y su relación con la intensidad del fuego no habían sido hasta ahora analizados en el contexto de los suelos gallegos. Así, el objetivo del Capítulo 9 fue el de analizar qué parámetros colorimétricos registrados mediante un colorímetro portátil pueden ser empleados como indicadores de la intensidad de un incendio a partir de experimentos de laboratorio con muestras de suelo inalteradas recogidas en campo. Considerando que el color de un suelo tras sufrir un incendio está principalmente influenciado por el tipo y la cantidad de materia orgánica (Shields *et al.*, 1968; Schulze *et al.*, 1993) y por los óxidos de hierro (Bigham *et al.*, 1978; Schwertmann, 1993), en este estudio (Capítulo 9) también se supusieron cambios químicos y mineralógicos que pudieran dar lugar a los cambios de color registrados (Sanmartín *et al.*, 2010c).

Los resultados obtenidos mostraron un descenso de la claridad en las muestras quemadas con respecto a las sin quemar, reflejado en los valores de *Value* Munsell y L* CIELAB, y un descenso del croma, marcado por el *Chroma* Munsell y C^*_{ab} CIELAB, probablemente debidos a la carbonización de la materia orgánica. Además, se produjo un empardecimiento-enrojecimiento del suelo reflejado en los valores de *Hue* Munsell, el descenso de h_{ab}, el aumento de a* y el descenso de b*, que podrían atribuirse simplemente a la desaparición de los componentes orgánicos del suelo que enmascaraban el color de los componentes inorgánicos, principalmente óxidos de hierro.

La comparación entre el color de los suelos quemados a una intensidad ligera y moderada, muestra que los únicos parámetros que establecen diferencias significativas son aquellos que se refieren al *Hue* Munsell y h_{ab} CIELAB, indicando que será el tono el parámetro a tener en cuenta en el uso del color como indicador de la intensidad de incendios en suelos de Galicia. Las diferencias pueden ser asignadas principalmente a variaciones en el estado de

deshidratación de los compuestos de hierro como la transformación de goethita, de un color anaranjado, a hematite, de color rojo sangre.

Para finalizar, en el Capítulo 10 de esta tesis doctoral se demostró la validez de las coordenadas de color CIELAB, registradas con un espectrofotómetro portátil, en la estimación de los fitopigmentos contenidos en los sedimentos de río recogidos a lo largo del cauce del río Anllóns (A Coruña) (Sanmartín *et al.*, 2011c). Aunque recientemente, se habían aplicado medidas instrumentales de color expresadas en coordenadas CIELAB a sedimentos en suspensión y en el cauce de ríos para aplicaciones forenses (Guedes *et al.*, 2009) y para determinar el origen de sedimentos en suspensión (Martínez-Carrera *et al.*, 2010a, 2010b), esta es la primera vez que la medida de color se utilizó para la cuantificación de los fitopigmentos (clorofila-a, clorofila-b, feopigmentos y carotenoides totales) presentes en sedimentos de río. La cuantificación de fitopigmentos en los sedimentos de río recibe la atención de los especialistas porque proporciona información sobre el efecto sinérgico que provocan los nutrientes, en especial nitrógeno y fósforo, en el crecimiento de las algas y por tanto sobre la eutrofización del río, un descriptor válido del estado trófico y de la calidad de las aguas y sedimentos (*e.g.* Biggs & Close, 1989; Dodds *et al.*, 2002; Chételat *et al.*, 2006; Muylaert *et al.*, 2009). Así, el desarrollo de una técnica no-destructiva, rápida, sencilla y económica para la cuantificación del contenido de fitopigmentos en los sedimentos de río basada en la cuantificación del color sería de gran interés ya que evitaría la extracción y análisis químico de los mismos.

Los resultados recogidos en el Capítulo 10 demostraron la validez del método ya que los parámetros de color CIELAB se correlacionan significativamente con el contenido en fitopigmentos permitiendo así el desarrollo de ecuaciones de predicción para el contenido en clorofila-a, clorofila-b, carotenoides totales y contenido total en fitopigmentos a partir del parámetro a* y del parámetro C^*_{ab} (Sanmartín *et al.*, 2011c). De esta forma, el mejor ajuste se alcanzó en la predicción de la clorofila-a, con las ecuaciones de predicción siguientes: Clorofila-a = $46{,}4–70{,}6\log_{10}(a^*)$ y Clorofila-a = $–15{,}7+238{,}1(1/C^*_{ab})$ con un valor ajustado de R^2 muy próximo a 0,9.

General Discussion

Cleaning is an important aspect of the maintenance and rehabilitation of stone buildings and structures. Colonizing microorganisms contribute substantially to the fouling of buildings, which causes aesthetic as well as physical and chemical damage to the building materials (Seaward, 1979; Grant, 1982). As biological colonization of outdoor-exposed surfaces is inevitable, it is important to detect the moment at which the colonization begins, so that it can be dealt with as early as possible to avoid irreparable damage. In the case of maintenance work, in which the elimination of biological colonization is almost always necessary, a suitable methodology for monitoring the efficiency of cleaning is required. To date, this has been done either visually, which may produce misleading results, or by use of traditional methods of microbiological analysis, which involve sampling (often impossible to perform because of the historical and artistic value of the object) and arduous and costly laboratory work. Therefore, this thesis proposes a color measurement-based method for quantifying the colonization of stone structures by phototrophic microorganisms such as algae, cyanobacteria and lichens (all colored microorganisms that commonly colonize buildings); the method is rapid, cost-effective, non-destructive and can be applied directly to buildings and structures.

Thus, the main purpose of this doctoral research project was to develop a new methodology for quantifying and studying the growth of epilithic phototrophic biofilms on granite constructions by use of using instrumental color measurements, focusing on those cases in which sampling would be difficult or even impossible to carry out. To achieve this main objective, specific research objectives related to the measurement, representation and discussion of the color data were established in relation to the two elements involved in the study - granite rocks and phototrophic microorganisms (cyanobacteria) - and the interactions between these. The best conditions for measuring color in this context were determined during the development of a methodology for color measurement and characterization of the granitic rocks (Chapters 1 and 2) and cyanobacteria (Chapters 3-5), and fine-tuning of the method of extracting chlorophyll-a, a biomarker for quantifying phototrophic biomass, from rocky substrates (Chapter 6). The methods have been successfully applied to real cases of biological colonization (epilithic phototrophic biofilms) on granite buildings (Chapter 7). Moreover, the work developed in the context of granite structures of historical and artistic importance has led to the implementation of

the colorimetric method to natural structures, and the method has been applied to other natural inorganic substrates: to determine the color of roofing slates as a replacement criterion in restoration work (Chapter 8), to characterize the color of burned soil as an indicator of fire intensity (Chapter 9), and to measure the color of riverbed sediments to estimate their phytopigment content (Chapter 10).

The underlying hypothesis of this doctoral study - the existence of a direct relationship between the quantity and physiological state of phototrophic organisms and the color change generated when they are deposited on a surface - was previously demonstrated by Prieto *et al.* (2002) in laboratory experiments. The reliability of color measurements as an estimator of the biomass of phototrophic organisms on stone surfaces was also demonstrated by Prieto *et al.* (2004) by comparison of the most common methods of quantification of phototrophic biomass on rocky substrates. Prior to development of the approach used in this doctoral research, several studies had applied the objective measurement of the color of ornamental stone with contact color measuring devices, such as tristimulus colorimeters and portable spectrophotometers (*e.g.* Durán-Suárez *et al.*, 1995; García-Talegón *et al.*, 1998; Iñigo *et al.*, 2004; Grossi *et al.*, 2007). However, no standardized protocol for characterizing the color of ornamental stone, which would enable comparison of the results obtained by different authors and instruments, had yet been established. In this regard, it should be noted that the geometry or optical design of the measuring instrument, whether a colorimeter or a spectrophotometer, enables a spatially-averaged reading of the reflected light from a fixed area, which is always circular and of a size determined by the diameter of the measurement head (ranging between 3 and 60 mm). Thus, the device records an integrated color, which is the result of the reflectance or transmittance caused by the different colors captured on the reading area. This supposes an important advantage in the case of surfaces of relatively homogeneous color, but implies the need for prior determination of the minimum area of measurement and the minimum number of measurements that must be made when the measurement surface is heterogeneous in color and texture, as in the case of granite. Lack of knowledge of these parameters leads to a loss of colorimetric information, and the importance of this will depend on the heterogeneity of the color.

In response to this situation, a procedure for measuring the color of ornamental granite is proposed in this doctoral thesis (Chapter 1); fin-tuning of the method involved determining the minimum area of measurement and the minimum number of measurements required with two contact color-measuring instruments, a portable tristimulus colorimeter and a spectrophotometer for solids (Prieto *et al.*, 2010a). Granite can be considered as one of the most complicated cases as far as determining the color of ornamental stone is concerned, because of the high heterogeneity of the color and texture of the surface as a result of the complexity of the mineral distribution. For this study, careful selection from among ornamental granites was carried out to obtain the widest range in color and texture from within the types of granite most commonly

used in buildings and heritage structures. The following varieties of ornamental granite were selected: *Labrador Claro*, a bluish-black, coarse-grained granite; *Grissal*, a grey, medium-grained granite; *Rosa Porriño*, a pinkish, coarse-grained granite; *Blanco Cristal*, a white, fine-grained granite (these granites comprised the reference samples and were referred to as the Granite Training group); and *Silvestre*, a fine-grained, lightly weathered granite, which has a brownish-gold color due to weathering of its minerals (this granite forms the Granite Test group used to validate the results achieved with the Granite Training group). Considering that all ornamental stone in built structures has a certain type of surface finish that can affect the color, samples of all of the varieties were prepared with four different types of commercial finish: polished (smoothest finish), honed, sawn, and flamed (roughest finish), except in *Labrador Claro* in which a flamed finish is not easy to achieve. Likewise, flamed and polished finishes cannot be achieved in the *Silvestre* variety of granite, so that these were substituted with bush hammered and polished without glow finishes, respectively. Three parameters were considered as variable factors: the type of granite (*Labrador Claro*, *Grissal*, *Rosa Porriño*, and *Blanco Cristal*), surface finish (polished, honed, sawn, and flamed), and target area (circular apertures of diameter 5, 8, 10, and 50 mm). The color measurements were analyzed by use of the CIELAB color space, with the L*a*b* group of scalar coordinates. Development of the methodology established to determine the influence of these factors on the color parameters is an important novel aspect of the work reported in this chapter. The importance of analyzing the color data from both colorimetric and statistical points of view was highlighted, as neither method alone enabled conclusions to be reached. The combination of both types of analysis demonstrated that the variability of granite in terms of color, texture and surface finish must be taken into account in standardizing the methodology for color measurement because all of these parameters affect the minimum number of measurements required. It was also found that for granite, the minimum number of measurements per surface measurement is affected by the field of view or measurement target area of the device, which is determined by the diameter of the measurement head. Thus, the number of measurements required is 6[†]/36 cm^2 surface area for a 50 mm diameter measurement head, 14/36 cm^2 for 8 and 10 mm diameter measurement heads, and 17/36 cm^2 for a 5 mm measurement head. As regards the minimum measuring area, the results showed that an area of 36 cm^2 is sufficient when measurement heads of diameter 10 mm or less are used. A surface area equal to or larger than 72 cm^2 is required for measurement heads of larger diameters. The differences in the L*, a*, b* color parameters obtained with the different measuring heads were statistically significant, although not at the level of a rigorous color tolerance (*i.e.* less than ΔE^*_{ab}: 3 CIELAB units), so that in practice they may be ignored (Prieto *et al.*, 2010a).

[†] In all cases the measurements were made consecutively by replacement at different points selected at random by the operator.

After publication of the results of the research reported in Chapter 1 of this thesis, Sousa & Gonçalves (2011) carried out a similar study to evaluate the factors (such as grain size and texture) affecting the assessment of the color of granite and to propose a methodology for this task that would reduce the margin of error associated with the procedure. In comparison with the study reported in Chapter 1, these authors used a colorimeter to analyze granite samples with only one type of surface finish (polished finish), a smaller range of measuring head size (4-, 8- and 16-mm diameter apertures), and larger samples (blocks of 100 cm^2 and 30,000 cm^2). These differences may explain the differences in the results obtained in both studies since, according to Sousa & Gonçalves (2011), color parameters did not differ significantly with different measurement head sizes (although the standard deviation of the mean values obtained with the 16-mm aperture was lower), and thus, the minimum number of measurements required was 40/100 cm^2 and 60/30,000 cm^2, with any size of measurement head. Another important aspect to consider is that Sousa & Gonçalves (2011) used the classical CIELAB formula to calculate differences in color, rather than the newer and improved CIEDE2000 and CIE94 color-difference formulae, which are more appropriate for assessing samples with low chroma values (Johnson & Fairchild, 2003). Furthermore, these authors did not take into account the suprathreshold color-difference, which is approximately 1.75 CIELAB units (Melgosa *et al.*, 1997).

Once the minimum requirements in terms of number of measurements and surface measurement area were established, the influence of the type of commercial finish (polished or polished without glow, honed, sawn, and flamed or bush hammered) on the appearance of ornamental granite was analyzed by means of roughness, color, and gloss measurements; the relationship between these three aesthetic parameters was also analyzed (Chapter 2). Studies of the relationships between color, gloss and roughness in heterogeneous samples are particularly scarce (Benavente *et al.*, 2003), in contrast with the large number of studies considering homogeneous samples (Barnett, 1973; Thomas, 1999; Dalal & Natale-Hoffman, 1999; Simonot & Elias, 2003; Keyf & Etikan, 2004; Eliades *et al.*, 2004; Ariño *et al.*, 2005; Briones *et al.*, 2006; Shih *et al.*, 2008; Ignell *et al.*, 2009).

When the surface of a smooth, colored object becomes rough, the apparent color of the object usually changes (Simonot & Elias, 2003). In the case of ornamental granite, the results demonstrated that different surface finishes produce differences in color (in most cases perceptible), especially in the lightness parameter (L*); the magnitude of these differences depends on the color of the ornamental granite, and is greatest in dark-colored stone. Thus, the greatest color variation due to different surface finishes was observed in *Labrador Claro*. This is consistent with the findings reported by Ignell *et al.* (2009) for polymeric surfaces in which the lightness L* increased most in the darkest (*i.e.* roughest) surfaces; it is also consistent with the results obtained by Benavente *et al.* (2003) in different types of marble and limestone, as in specimens with a high chroma value (C^*_{ab}), the changes in total color (ΔE_{94}) were affected by

surface finish to a greater degree than specimens with low chroma value, which scarcely showed any change in color in relation to finish.

These statistically significant and perceptible color changes, caused by the different commercial finishes on the surface of the granite, were observed in both the specular component included (SCI) and specular component excluded (SCE) measurement modes, unlike in other materials such as dental porcelain (Kim *et al.*, 2003) and injection-moulded plastics (Ariño *et al.*, 2007), in which color variations owing to differences in surface roughness were only observed in the SCE mode. However, it should be noted that for determining the color of granite, the SCE mode provided greater magnification of the differences in color produced by various commercial finishes. These results are of the great interest because they constitute valuable information regarding the methodology of measuring the color.

The color parameters ($L^*a^*b^*C^*_{ab}h_{ab}$) did not vary in proportion to the roughness generated by the different surface finishes, although the values of these parameters were different for each finish. Gloss depends on the refractive index of the various minerals that compose granite and is affected by the color of ornamental granite, but in a different way than in polished and rough finishes. Many authors have reported an inverse relationship between roughness and gloss in surfaces that are homogeneous in color and composition (Hunter & Harold, 1987; Thomas, 1999; Wang *et al.*, 2000; Ariño *et al.*, 2005; Briones *et al.*, 2006). In ornamental granite, gloss is not a function of roughness for the entire measurement range, and gloss and roughness are inversely related only within the range of low values of roughness. Although there are several possible explanations for this, perhaps the most important is that the treatments used to achieve the rough finishes (*viz.* flamed and bush hammered) break the surface minerals, which mostly tend to fracture along well-defined cleavage planes (López-Arce *et al.*, 2010), thus creating small areas of new smooth surfaces and causing an increase in surface gloss (Sanmartín *et al.*, 2011a).

The study methodology described in Chapter 1 was successfully used to define a color measurement protocol for biofilms (Chapter 3) and roofing slates (Chapter 8), which validates its use for other types of heterogeneous surfaces. In the case of biofilms, cyanobacteria were selected as the colonizing microorganisms under study, because they are the main constituent in a phenomenon often referred to as greening when developed on the surfaces of natural stone (Ortega-Morales *et al.*, 2000; Gaylarde *et al.*, 2001). In particular, the cyanobacteria used belong to the genera *Nostoc* and *Scytonema* (order Nostocales). The choice of these genera of cyanobacteria was performed in response to metabolic and morphological characteristics. Specifically, the selected microorganisms are nitrogen-fixing microorganisms, *i.e.* diazotrophs able to satisfy their metabolic requirements mainly through the compounds in the atmosphere, allowing them to act as pioneers in colonizing nutrient-poor surfaces, such as stone surfaces. Another characteristic taken into account in choosing these microbial genera was their

morphology, since both of these filamentous cyanobacteria are protected from the external medium - by a matrix of polysaccharide mucilage in the case of *Nostoc*, and by a mucilaginous sheath made of complex polysaccharides in the case of *Scytonema*. This morphology allows these microorganisms to withstand extreme temperatures and humidity, and therefore makes them well suited to colonizing walls and façades, where both environmental parameters vary greatly depending on solar radiation and precipitation. The strains selected were *Nostoc* sp. PCC 9104, *Nostoc* sp. PCC 9025 and *Scytonema* sp.CCC 9801. These cyanobacterial strains are common colonizers of soil and rocks in Galicia (Acea *et al.*, 2001, 2003).

Following the working methodology designed by Prieto *et al.* in 2002, a mixed culture of *Nostoc* sp. PCC 9104, *Nostoc* sp. PCC 9025 and *Scytonema* sp. CCC 9801 was prepared. Aliquots of different volumes were filtered under vacuum through white nitrocellulose filter discs (0.45 µm pore size and 47 mm in diameter) in order to deposit a uniform layer of microorganisms in a circular fixed area of 9.62 cm^2 (35 mm in diameter), to simulate the composition and characteristics of a biofilm (Costerton, 2007). The minimum number of measurements required to characterize the color of a heterogeneous surface depends, among other factors, on the size of the measuring head (Chapter 1). Moreover, the moisture content of cyanobacteria affects their colorimetric characterization (Prieto *et al.*, 2002). Therefore, the minimum number of measurements required for a given surface size with respect to the size of the measurement head was analyzed (Chapter 3) by taking into account moisture content of microorganisms and their degree of cover, which generate a heterogeneous surface color (Prieto *et al.*, 2010b). The findings demonstrated that the minimum number of measurements required increased with increasing heterogeneity of the color of the area measured, which depended on the concentration of the microorganisms and decreased with the diameter of the measuring head. To control for the influence of the heterogeneity of the color of the area measured, the color of the cyanobacteria should be measured on filters that are completely covered by the microorganisms, so that the color of the filter is totally obscured. With regard to the moisture content of the microorganisms, it was observed that this causes changes in the values of lightness (L*), but does not affect the other CIELAB color parameters. Thus, the L* values decreased exponentially with moisture contents of up to 50%, and become virtually stable at moisture contents between 50 - 100%, so that a moisture content above 50% in the biofilm was established as a condition for obtaining reliable color measurements. Finally, as expected, the size of the measuring head influenced the number of measurements required; the latter decreased as the former increased. Thus, in order to obtain comparable results, it was proposed to make a total of 10 measurements/9.62 cm^2 for measuring heads of 8 and 5 mm in diameter and 8 measurements/9.62 cm^2 for a measuring head of 10 mm diameter. Regardless of the dimensions of the measuring head of the device, 10 measurements/9.62 cm^2 are sufficient for characterizing the color of cyanobacteria.

In regard to the color measurement protocol for roofing slates (Chapter 8), the minimum number of measurements required was much lower than for granite and slightly lower than for biofilms. Furthermore, although in the case of granite, a study area of at least 72 cm^2 is required when heads larger than 10 mm are used, a surface area of 36 cm^2 is sufficient for slate, regardless of the size of the measurement head. These differences are undoubtedly due to greater uniformity in color of the roofing slate (Sanmartín *et al.*, 2010b). Thus, for roofing slate, 3 measurements/36 cm^2 are recommended for a reading area or measuring head area of 50 mm in diameter, 6 measurements/36 cm^2 for 10 and 8 mm diameter measuring heads, and 7 measurements/36cm^2 for a measuring head of diameter 5 mm. An area of 36 cm^2 is also sufficient, regardless of the size of the measuring head.

Joint analysis of the results obtained in the three studies in which protocols for color measurements were developed (Chapters 1, 3 and 8) highlights the importance of developing methodologies to study heterogeneous surfaces, and also indicates that the reading area or measuring head size of the spectrophotometer or colorimeter affects the number of measurements required to characterize the color of a heterogeneous surface. Thus, the minimum number of measurements required decreases with increasing homogeneity of the colored surface. The minimum measurement area, which was considered only for ornamental stone, was affected both by the size of the measuring head and the type of stone and surface finish. Specifically, a measurement area of 72 cm^2 is necessary in the case of granite when measuring heads larger than 10 mm are used, while for roofing slates an area of 36 cm^2 is sufficient, irrespective of the size of the measuring head. In the case of color measurement in biofilms, the properties of microorganisms, such as concentration and moisture content, affect the minimum number of measurements required, and, more importantly, they affect the color obtained.

Once the measurement protocols were established, it was possible to identify the regions of the CIELAB color space by taking into account the set of Cartesian coordinates (L*a*b*) and the set of polar or cylindrical coordinates ($L^*C^*_{ab}h_{ab}$) that include granite (Chapter 2) and roofing slate (Chapter 8). As three-dimensional color areas delimit the CIELAB space for the construction of color databases for ornamental stone, it is very important to define them correctly. The 3D color areas may be used in further studies within the framework of research in which selection of materials is performed by use of aesthetic criteria, and they can also be applied in characterizing trichromatic digital cameras as colorimeters for use with cultural heritage monuments. Therefore, for the area within the CIELAB color space that defines the ornamental granites under study, the limits were as follows: $L^*= 74.9 \pm 1.0$; $a^*= 2.7 \pm 0.5$; $b^*= 7.4 \pm 1.5$; $C^*_{ab}= 7.6 \pm 1.1$; $h_{ab}= 253.7º \pm 6.1º$ (upper limits) and $L^*= 34.2 \pm 0.5$; $a^*= -0.9 \pm 0.1$; $b^*= -2.8 \pm 0.3$; $C^*_{ab}= 1.1 \pm 0.5$; $h_{ab}= 71.8º \pm 1.7º$ (lower limits) in the specular component included (SCI) mode. In the specular component excluded (SCE) mode, the limits were as follows: $L^*= 75.5 \pm$

3.5; a*= 3.3 ± 2.6; b*= 8.6 ± 3.6; C^*_{ab}= 9.3 ± 4.2; h_{ab}= 237.2º ± 46.0º (upper limits) and L*= 30.7 ± 4.8; a*= –0.8 ± 0.3; b*= –1.4 ± 1.6; C^*_{ab}= 1.0 ± 0.6; and h_{ab}= 71.5º ± 4.9º (lower limits).

In the case of the fifty commercial varieties of roofing slate extracted from the twelve different slate mining districts in the Iberian Peninsula, the limits of the three-dimensional color area of the CIELAB space were as follows: L*= 53.2 ± 0.2; a*= 0.0 ± 0.0; b*= 2.0 ± 0.1; C^*_{ab}= 4.6 ± 0.1; and, h_{ab}= 271.9º ± 2.0º (upper limits) and L*= 33.7 ± 0.0; a*= –4.2 ± 0.1; b*= –1.4 ± 0.1; C^*_{ab}= 0.5 ± 0.1; h_{ab}= 143.6º ± 17.9º (lower limits) in the SCI mode. In the SCE mode, the limits were as follows: L*= 52.4 ± 0.7; a*= 0.1 ± 0.1; b*= 1.9 ± 0.3; C^*_{ab}= 4.5 ± 0.2; h_{ab}= 273.3º ± 5.0º (upper limits) and: L*= 33.5 ± 0.2; a*= –4.1 ± 0.1; b*= –1.8 ± 0.2; C^*_{ab}= 0.6 ± 0.3; h_{ab}= 155.3º ± 2.6º (lower limits).

After establishing the measurement protocols and defining the three-dimensional color areas of ornamental granite and roofing slates within the CIELAB color space, the next step in this research was to analyze the influence of environmental parameters such as light quality and light intensity, presence or absence of assimilable combined nitrogen sources, and presence or absence of other nutrients on the composition and/or abundance of photosynthetic pigments and hence on the color of biofilms (Chapter 4). Modifications in the color of photoautotrophic microorganisms due to pigmentary changes in response to variations in environmental parameters have been analyzed in previous studies (Collier & Grossman, 1992; Sobczyk *et al.*, 1994; Grossman & Kehoe, 1997; Grossman *et al.*, 2001). Thus, although different microorganisms and different strains of a microorganism are characterized by specific physiological changes in response to environmental stimuli, in most studies with cyanobacteria it was observed that low and intermediate light intensities generally stimulate synthesis of chlorophyll-a and phycobiliproteins (Raven, 1984; Lonnenborg *et al.*, 1985; Fernández-Valiente & Leganés, 1989; Martín-Trillo, 1995; Jonte *et al.*, 2003; Loreto *et al.*, 2003), while high light intensities stimulate synthesis of carotenoids (Raps *et al.*, 1983). Nutrient limitations lead to a decrease in the content of chlorophyll-a (Stebvens *et al.*, 1981; Bartual *et al.*, 2002) and phycobiliproteins (Collier & Grossman, 1992), although in such situations the carotenoid content remains relatively stable (Duke & Allen, 1990). Different terms were used in these studies to describe the color variations caused by these pigmentary changes: bleaching, chlorosis, color paling, color fading, yellowing, dark-green color, light-yellow color and blueing color. However, none of the above studies quantified the color objectively.

The color of cyanobacteria was objectively quantified (expressed in the CIELAB coordinates L*a*b*$C^*_{ab}h_{ab}$) for first time in this study (Chapter 4) and related to the pigment content; the variations in both color and pigments were also related to environmental parameters. For this purpose, two stone biofilm-forming cyanobacteria (*Nostoc* sp. PCC 9104 and *Nostoc* sp. PCC 9025) were acclimated in aerated batch cultures for two weeks, to three different culture conditions: non-diazotrophic, diazotrophic and “low nutrient” diazotrophic, and exposed at high

or low light intensity. Throughout the experiment, the cyanobacteria color was measured and represented in the CIELAB color space; the pigment contents (chlorophyll-a, phycocyanins (phycobiliproteins) and total carotenoids) were also quantified. The results confirmed the efficiency of color measurements in evaluating the extent to which pigment production is affected by environmental parameters (Sanmartín *et al.*, 2010a).

The results revealed that, for both strains, the concentrations of chlorophyll-a and phycocyanins (phycobiliproteins) were higher in cultures grown in the presence of nitrate (non-diazotrophic conditions) - in low light intensity for *Nostoc* sp. PCC 9104 and in high light intensity for *Nostoc* sp. PCC 9025. However, the concentration of carotenoids was affected by different parameters, depending on the strain: for *Nostoc* sp. PCC 9104 the availability of nutrients was the main factor affecting carotenoid concentration, whereas the presence of nitrates together with the high light intensity affected *Nostoc* sp. PCC 9025 to a greater extent (Sanmartín *et al.*, 2010a). Moreover, the findings showed that values of CIELAB color parameters may have been used for the same purpose as the pigment content because the concentration of each pigment was closely correlated with each CIELAB color parameter, except h_{ab}; thus, when the pigment content increased, b* and C^*_{ab} increased, and L* and a* decreased. However, not all CIELAB color parameters are equally sensitive to changes in pigment concentrations. Thus, L* appears to be most informative parameter because, as well as being the CIELAB color parameter most closely related to each pigment studied, it reflects the changes in pigment concentrations due to the different environmental conditions considered. Is followed by a*, which moved to negative values (the culture became greener) as the culture aged and pigment content increased. For their part, b* and C^*_{ab} provide information about the amount of phycocyanins (phycobiliproteins) in relation to the amount of the other two pigments studied, chlorophyll-a and total carotenoids. The parameter h_{ab} was correlated with each pigment in *Nostoc* sp. PCC 9025 and with chlorophyll-a concentration in *Nostoc* sp. PCC 9104; however, in both cases the correlation coefficients were too low to establish any relationship between pigments and this CIELAB color parameter. Nonetheless, the constant surveillance to which cultures were subjected, together with analysis of the h_{ab} values, allowed this parameter to be related to changes in the appearance of the cultures (color and density) because the most important changes in appearance that occurred through the experiment are clearly reflected in the h_{ab} values. Finally, in the same way as for the granite and roofing slate (Chapters 2 and 8), Chapter 4 reports the thresholds of the three-dimensional color area within the CIELAB color space in which the color of the cyanobacteria under study is located, the maximum and minimum values of which are L*= 92.39; a*= –2.28; b*= 35.22; C^*_{ab}= 41.00; h_{ab}= 158.80º, and L*= 36.85; a*= –23.92; b*= 1.30; C^*_{ab}= 2.94; h_{ab}= 113.60º, respectively.

The color-pigment relationship is not only useful when the microorganisms are actively growing, but also when they are senescent, *e.g.* after the application of biocidal products or conditions. Thus, this research aimed to develop working methods based on color measurement in order to

assess the effectiveness of biocides, by analyzing the physiological state of the microorganisms after treatment, *i.e.* colorimetric methods that reveal whether the microorganisms continue to develop or they are in the senescent phase. The effectiveness of biocides against phototrophic organisms can be tested as the degree of chlorophyll degradation (Underwood & Paterson, 1993; Silkina *et al.*, 2009). When chlorophyll degrades, it forms a series of degradation products, the nature of which depend on the part of the molecular structure of chlorophyll affected. These are called phaeopigments and include phaeophytin, chlorophyllide and phaeophorbide. The relationship between these pigments and chlorophyll can be established by UV-Vis spectroscopy, using phaeophytinization indexes or ratios: $A_{435/415}$, the ratio between the absorbances recorded at 435 nm and 415 nm, and the ratio of absorbances $A_{665/665a}$ registered at 665 nm before and after acidifying the sample with hydrochloric acid. In both cases, a decrease in the ratio indicates the start of the increase in the degradation of chlorophyll to phaeopigments (*e.g.* Barnes *et al.*, 1992; López *et al.*, 1997; Louda *et al.*, 1998). Chapter 5 of this thesis describes how the analysis of chlorophyll degradation in cyanobacteria by use of spectrophotometric methods can be replaced by instrumental color measurements because the CIELAB color parameters recorded with a portable colorimeter are correlated with the phaeophytinization indexes estimated by UV-Vis spectroscopy. On the basis of this result, both the effectiveness of the biocide and the physiological state of the microorganism can be determined by straightforward measurement of the color. Of all the CIELAB color parameters, L* was the most valuable for describing chlorophyll degradation as it is correlated with both phaeophytinization indexes ($A_{435/415}$ and $A_{665/665a}$) in both modes of growth (planktonic and biofilm), followed by a* and C^*_{ab}, which are correlated to the $A_{665/665a}$ index in both modes of growth (Sanmartín *et al.*, 2011b).

In the development and fine-tuning of any novel method, a reference method must be used to establish the reliability of the results obtained by the new method. In the present case (*i.e.* the quantification of epilithic phototrophic colonization on granite structures by color measurement), the reference method is the widely accepted spectrophotometric measurement of chlorophyll-a, one of the most commonly used biomarkers for quantifying microalgal and cyanobacterial biomass. However, although this method is valid for estimating photosynthetic growth in water, liquid media, and soil, its use in analyzing phototrophic biomass on rocky substrates associated with the process of chlorophyll-a extraction is limited (Prieto *et al.*, 2004). It was therefore necessary to improve the extraction method before analyzing the aspects of the color of the colonized granite. For this purpose, the method of extracting chlorophyll-a from biofilms developed on rocky substrata was optimized (Chapter 6), by use of a response surface methodology following a Box–Behnken third order design, which predicts the optimal experimental conditions for maximum extraction of chlorophyll-a (Fernandez-Silva *et al.*, 2011).

Three different mechanical pretreatments (A, B, C) were assayed to determine the best procedure for complete chlorophyll-a extraction with dimethyl sulfoxide (used as solvent) on

granite blocks inoculated with a mixed culture of three stone biofilm-forming cyanobacteria, *Nostoc* sp. PCC 9104, *Nostoc* sp. PCC 9025 and *Scytonema* sp. CCC 9801. In the two first methods, A and B, inoculated blocks were crushed, and in the case of pretreatment B, the blocks were subsequently placed in an ultrasonic bath filled with enough water to apply ultrasound to the whole of each sample. For pretreatment C, the crushing was replaced by sonication of intact inoculated blocks (without crushing) by inserting the narrow tip of an ultrasonic generator into the extractant.

For each pretreatment, a Box–Behnken design for three-variable optimization or experimental factors was used: (1) extractant-to-sample ratio, (2) temperature during the extraction, and (3) time of incubation, considering the recovery of chlorophyll-a as the dependent variable or response variable. After incubation in DMSO in their respective conditions, samples were filtered, and the concentration of chlorophyll-a in the filtrates was determined by UV-Vis spectrophotometry.

From the results obtained it can be concluded that: (i) the application of ultrasonic methods improved extraction of chlorophyll-a from biofilms developed on rocky substrata; (ii) the precision of the spectrophotometric method for calculation of the concentration of chlorophyll-a decreases with highly diluted samples, so that methods requiring a lower volume of extractant are more convenient; (iii) the temperature of extraction is the most important factor (compared with the other parameters analyzed) in chlorophyll-a extraction from biofilms on rocky substrata. Thus, we proposed the direct application of ultrasound to uncrushed rock samples (so that the method of extraction of chlorophyll-a ceases to be destructive and becomes merely an invasive method), followed by incubation in 0.43 ml DMSO/cm^2 sample (vol/surface) at 63ºC for 40 min, as an efficient method for chlorophyll-a extraction from stone material (Fernández-Silva *et al.*, 2011). Confirmatory experiments were performed at the predicted optimal conditions, allowing recovery of 90% of the chlorophyll-a, which implies a substantial improvement with respect to the recovery expected with previous methods (68%).

On completion of the laboratory experiments, the colorimetric method developed during the study was able to be applied *in situ* and on site in granite buildings or heritage structures affected by biological colonization and formation of epilithic phototrophic biofilms. Thus, Chapter 7 describes the detection and monitoring of the development of epilithic phototrophic biofilms on the granite façade of an institutional building, (*viz.* Supercomputing Centre of Galicia (CESGA), in Santiago de Compostela (Galicia, northwest Spain) (Sanmartín *et al.*, 2012). The research comprises a case study of preventive conservation and the results provide a basis for establishing criteria for the early detection of phototrophic colonization (greening) and for monitoring its development on granite buildings by the use of color changes recorded with a portable spectrophotometer and represented in the CIELAB color space.

Several authors have already used portable spectrophotometers or tristimulus colorimeters, and expressed the results in CIE-L*a*b* color system units for characterizing the color of stone, caused by the epilithical growth of phototrophic microorganisms. Thus, using this technique, Urzì & Realini (1998) correlated the orange or grey color of the patina on Noto's calcareous sandstone with the associated microflora; Prieto *et al.* (2005) quantified the development of biofilm induced on the open rock faces of quartz quarries to reduce the visual impact; De Muynck *et al.* (2009) evaluated strategies for preventing algal fouling on two types of concrete (man-made stone), and more recently, Tanaca *et al.* (2011) evaluated fungal colonization on three cement (man-made stone) formulations exposed to urban, rural and coastal environments. Nevertheless, none of these studies, except that of Prieto *et al.* (2005), used a previously established methodology for the color determination. Likewise, to our knowledge, the color measurement technique has not previously been used to study the phototrophic colonization (greening) of granite stone buildings naturally exposed to the outdoor environment (Sanmartín *et al.*, 2012).

In the present study (Chapter 7), the thresholds between imperceptible and perceptible greening were also determined, in terms of partial color differences (ΔL*, Δa* and Δb*), amount of phototrophic biomass (dry weight) and extracted chlorophyll-a content, taking into account the findings of a previous study carried out by Prieto *et al.* (2006). The following qualitative terms were defined by observers in the latter psychophysical study (Prieto *et al.* 2006): inappreciable, slight, appreciable, evident, notable, intense, or very intense, which indicated whether there was any perceptible difference in color between the granite blocks inoculated with cyanobacteria and the reference blocks. In the study performed by Sanmartín *et al.* (2012), the task of each observer was to decide whether the "greening" due to the presence of cyanobacteria in the granite blocks was perceptible or not. The observers provided "yes" or "no" responses.

Chapter 7 explains why measurement of color changes with a portable spectrophotometer is a reliable method for the early detection and real-time monitoring of phototrophic growth (greening) on granite façades, even before it is perceptible to the human eye. In this sense, changes in parameter b* were shown to provide the earliest indication of colonization and also varied most widely over time, so that this is the most important parameter for determining the total color change (ΔE^*_{ab}). This is consistent with previous observations for other stone materials such as quartz (Prieto *et al.*, 2005) and concrete (De Muynck *et al.*, 2009) and shows that parameter b* is the most informative for detecting phototrophic colonization. This finding suggests that the technique proposed here can be extrapolated to buildings other than granite buildings. Thus, Δb*: +0.59 CIELAB units, which correspond in this study to 6.3 mg biomass (dry weight) cm^{-2} and (8.43 + 0.24) x 10^{-3} μg extracted chlorophyll-a cm^{-2}, was established as the greening threshold.

The results reported in Chapter 7 are also of practical use for the management and maintenance of buildings affected by biodeterioration, as they show that greening can be detected when still imperceptible to the human eye, and also provide the basis for recommendations regarding the cleaning and/or application of treatments to halt or reverse the perceptible appearance of greening on building façades. According to our study, cleaning and/or treatment should be carried out by taking into account both the greening threshold in terms of Δb* and the moment at which the trend in the value of Δb* changes and becomes positive, *i.e.* when it indicates the presence of phototrophic colonization. In this sense, monitoring changes in b* on a cleaned granite façade exposed to the natural environment in Santiago de Compostela (NW Spain) revealed that recolonization by phototrophic microorganisms (greening) took no more than 129 days (just over 4 months), and greening was perceptible after approximately 178 days (almost 6 months). This rapid biological colonization was undoubtedly favoured by the mild wet climate of Santiago de Compostela, especially the microclimate affecting the most shaded walls of the buildings, as also occurs in other buildings in the city (Silva *et al.*, 1997).

On the other hand and in regard to the information provided by each CIELAB color parameter, no single CIELAB parameter could be used to achieve the specific aims and the overall aim of this doctoral study. Nevertheless, parameter L* was particularly important in the separate study of granite stone and phototrophic microorganisms (cyanobacteria) because L* was the color parameter that varied most widely among the different granite surface finishes (Chapter 2). This parameter also had the greatest influence on the color difference between biofilms with different moisture contents (Chapter 3), which is most closely correlated with the pigment content when it varies as a result different environmental conditions (Chapter 4). It was also the parameter that best fits the phaeophytinization indexes, which indicate the start of the increase in the degradation of chlorophyll to phaeopigments and thus indicate the physiological status of cyanobacterial organisms (Chapter 5). However, when granite and cyanobacteria were analyzed together (Chapter 7), parameter b * was the most informative as regards studying the detection and monitoring of the growth of phototrophic microorganisms on granite façade.

The information obtained in the core part of this doctoral research project (Chapters 1-7) was used to develop further research involving the application of the color method to other natural inorganic substrates, such as natural slate, soils and sediments, of interest in the field of environmental studies applied to natural heritage. The goals outlined in these studies (Chapters 8-10) were different, but were linked by the practical application of instrumental color measurements. Thus, instrumental color measurement was used as a criterion for selecting roofing slates from the Iberian Peninsula to replace damaged slates in stone restoration work in historic buildings (Chapter 8). In this sense, and with the purpose of determining the reproducible and comparable color of roofing slates, a measuring protocol, which takes into account the minimum number of measurements and the minimum area of measurement

required to quantify the color of roofing slate in relation to the dimensions of the measuring head, was carried out following the methodology proposed in the Chapter 1 for granite. Once the measuring protocol was defined, the color of fifty commercial varieties of roofing slate (all existing) mined in quarries from the twelve mining districts in the Iberian Peninsula was analyzed with a spectrophotometer device, by considering the CIELAB color space. The results of the study (Prieto *et al.*, 2011) were used to develop a protocol for characterizing the color of roofing slate and to define the color range of roofing slate from the Iberian Peninsula. In addition, the similarities and differences in the color and microstructure of the different commercial varieties of Iberian roofing slate were established and the limit of acceptability of replacement of one type of slate by another was determined. Thus, five commercial varieties of slate extracted from the twelve different slate mining districts in the Iberian Peninsula: *Itasi, Sigueya-Benuza* (ITA), *Canelas/Arouca* (ARO), *A Lastra* (LAS), *Os Vales* (PIV) and *Alto Bierzo* (ROC), can replace and be replaced by the most of the other fifty varieties, and only one variety: *Verde Lugo, Pol* (VLU), cannot replace or be replaced by any other slate. Parameter h_{ab} was found to be the most important CIELAB color coordinate as regards the formation of homogeneous color groups, and the specular component excluded (SCE) mode was most sensitive as regards detecting color differences (ΔE^*_{ab}) between two samples.

The impact of forest fires on soil degradation, which involves both physical loss (erosion) and a reduction in the quality of topsoil associated with nutrient decline and contamination, is well known in Galicia (NW Spain) (*e.g.* Soto & Díaz-Fierros, 1993; Soto *et al.*, 1997), and many studies have described appreciable variations in the color of the soil after fire (such as blackening due to partial or total destruction of organic matter and the redness due to dehydration of iron oxides). However, the objective variation in the color parameters and their relationship to the intensity of the fire had not been so far identified in the context of Galician soils. Thus, the purpose of the research outlined in Chapter 9 was to determine which parameters recorded with a colorimeter can be used as indicators of fire intensity: For this purpose, laboratory experiments were carried out with undisturbed soil samples collected in the field. Considering that the color of a soil after a fire is mainly influenced by the type and amount of organic matter (Shields *et al.*, 1968; Schulze *et al.*, 1993) and iron oxides (Bigham *et al.*, 1978; Schwertmann, 1993), it was also hypothesized that chemical and mineralogical changes might cause the color changes (Sanmartín *et al.*, 2010c).

The results showed a difference in lightness between the unburned (lighter) and burned soil samples (darker), reflected in the values of Munsell *Value* and CIELAB L*, and a decrease in chroma indicate by the Munsell *Chroma* and CIELAB C^*_{ab}; the change in color was probably due to carbonization of organic matter. In addition, there was a slight browning-reddening, which was reflected in the Munsell *Hue* values, a decrease in CIELAB h_{ab}, an increase in a * and a decrease in b*.This changes can be attributed simply to the disappearance of the soil organic components that masked the color of inorganic components, mainly iron oxides.

Comparison between the color values in soils in which different temperatures were reached (200ºC and 400ºC), shows that the parameters that establish significant differences are those that refer to the soil hue (Munsell *Hue* and CIELAB h_{ab}). In this case, differences can mainly be attributed to variations in the state of dehydration of the compounds of iron as goethite (orange color) is transformed to haematite (blood-red color). This suggests that the soil hue is the parameter that should be taken into account in the use of color as an indicator of fire intensity in Galician soils.

Finally, Chapter 10 describes the suitability of the CIELAB color coordinates, recorded with a portable spectrophotometer, for estimating the amounts of phytopigments in riverbed sediments collected along the Anllóns River (Galicia, NW Spain) (Sanmartín *et al.*, 2011c). Although CIELAB color measurements have recently been applied to suspended and riverbed sediments for forensic applications (Guedes *et al.*, 2009) and fingerprinting sediment sources (Martínez-Carreras *et al.*, 2010a, 2010b), to our knowledge, such measurements have not been used to study phytopigments in riverbed sediments as a proxy for the measurement of phototrophic microorganism content in phytoplankton and benthic algal communities.

There is considerable interest in quantifying phytopigments in order to assess the quality of freshwater bodies because this method considers the synergistic effect of nutrients such as nitrogen and phosphorus on algal growth and eutrophication. The concentration of phytopigments is a useful descriptor of the trophic state and environmental quality (*e.g.* Biggs & Close, 1989; Dodds *et al.*, 2002; Chételat *et al.*, 2006; Muylaert *et al.*, 2009). Thus, the development of a rapid, simple, cost-effective and non-destructive method of quantifying phytopigment contents in riverbed sediments on the basis of color measurements is of great interest because it would avoid the need for the extraction and chemical analysis of the pigments.

The results presented in Chapter 10 demonstrate the suitability of instrumental color measurements, since CIELAB color parameters were significantly correlated with the phytopigment content, which enabled the development of predictive equations for chlorophyll-a, chlorophyll-b, and total carotenoid contents, as well as the total pigment content from parameter a* and parameter C^*_{ab} (Sanmartín *et al.*, 2011c). Chlorophyll-a was the phytopigment most closely related to color parameters, which can therefore be estimated from the following equations: Chlorophyll-a = $46.4–70.6\log_{10}(a^*)$ and Chlorophyll-a = $–15.7+238.1(1/C^*_{ab})$, for which the adjusted R^2 value was close to 0.9.

Conclusiones

De los resultados obtenidos se extraen las siguientes conclusiones:

En lo que se refiere a la primera línea de trabajo de tesis: *Desarrollo de la metodología de medida y caracterización del color de las rocas graníticas*

1ª._ La metodología desarrollada para la caracterización del color de rocas graníticas mediante medidas de contacto es adecuada y fácilmente adaptable a otros materiales. Dicha metodología permitió determinar el número de medidas mínimo necesario y el área de medida mínima requerida para caracterizar objetivamente el color no-homogéneo de este tipo de rocas.

En relación con el número mínimo de medidas necesario, éste depende de la heterogeneidad de la roca en cuanto a color, textura y acabado superficial, y se ve afectado por el tamaño del cabezal del instrumento de medida, de modo que aumenta al disminuir el diámetro del cabezal de medida, o lo que es lo mismo el área de lectura. Así, el número mínimo de medidas es de 6 medidas/36 cm^2 para un área de lectura de 50 mm, 14 medidas/36 cm^2 para los cabezales de 10 y 8 mm y 17 medidas/36 cm^2 para un cabezal de 5 mm.

En cuanto al área de medida mínima, un área de 36 cm^2 es suficiente cuando se quiere caracterizar el color una roca granítica empleando cabezales con un diámetro ≤ 10 mm. En el caso de cabezales de mayor tamaño es necesario disponer de una superficie de 72 cm^2 o superior.

2ª._ La rugosidad inducida por los diferentes tipos de acabado comercial en la superficie de las rocas graníticas provoca cambios de color que son, por lo general, perceptibles (*i.e.*, con un valor de ΔE^*_{ab} de más de 3 unidades CIELAB) y que se deben principalmente a cambios en el parámetro claridad del color (L*). La magnitud del cambio de color asociado a la rugosidad depende del color del material, siendo mayor en las rocas más oscuras, *i.e.* aquéllas que presentan los valores más bajos de L*. Sin embargo, el color no varía proporcionalmente a la rugosidad generada por los diferentes acabados comerciales, por lo

que no se puede establecer ninguna regla general en cuanto a la influencia de la rugosidad en el color del granito ornamental.

Existe una relación inversa entre el brillo y la rugosidad en los granitos ornamentales pero sólo para los valores bajos de rugosidad. Los valores de brillo están afectados por el color de la roca granítica pero de diferente manera en las superficies lisas y en las rugosas. Así, brillo y claridad (L*) están inversamente relacionados en superficies lisas y directamente relacionados en superficies rugosas. Además, a este respecto se debe tener en cuenta la composición mineral de la roca, ya que ésta determina la topografía de la superficie rugosa y el índice de refracción.

3ª._ Se limitó la zona tridimensional dentro del espacio de color CIELAB que define el color de los granitos ornamentales estudiados. Ésta presenta sus límites superiores en: L*= 74,9 ± 1,0; a*= 2,7 ± 0,5; b*= 7,4 ± 1,5; C^*_{ab}= 7,6 ± 1,1; y h_{ab}= 253,7º ± 6,1º con el modo SCI; y L*= 75,5 ± 3,5; a*= 3,3 ± 2,6; b*= 8,6 ± 3,6; C^*_{ab}= 9,3 ± 4,2; y h_{ab}= 237,2º ± 46,0º con el modo SCE y sus límites inferiores en: L*= 34,2 ± 0,5; a*= –0,9 ± 0,1; b*= –2,8 ± 0,3; C^*_{ab}= 1,1 ± 0,5; y h_{ab}= 71,8º ± 1,7º con el modo SCI; y L*= 30,7 ± 4,8; a*= –0,8 ± 0,3; b*= –1,4 ± 1,6; C^*_{ab}= 1,0 ± 0,6; y h_{ab}= 71,5º ± 4,9º con el modo SCE. Esta información permitirá construir una base de datos de color para este tipo de rocas ornamentales, la cual es necesaria cuando en la selección de materiales se emplea el criterio estético, y también, para calibrar cámaras digitales para su uso como colorímetros en el marco del Patrimonio monumental construido.

En lo que se refiere a la segunda línea de trabajo de tesis: *Desarrollo de la metodología de medida y caracterización del color de las cianobacterias*

4ª._ La caracterización del color de las biopelículas cianobacterianas está influenciada tanto por características de los microorganismos como por características del instrumento de medida, ya que ambas van a determinar el número mínimo de medidas requerido.

El número mínimo de medidas aumenta con la heterogeneidad del color de la superficie, la cual depende de la concentración de microorganismos, y se reduce al aumentar el diámetro del cabezal de medida. Para controlar los efectos derivados de la heterogeneidad del color de la superficie se recomienda realizar las medidas en filtros completamente cubiertos por microorganismos. Así, para obtener resultados comparables, se propone realizar 10 medidas/9,62 cm^2 con cabezales de medida de 8 y 5 mm de diámetro y 8 medidas/9,62 cm^2 con un cabezal de medida de 10 mm de diámetro. Con el fin de estandarizar la medida del color de las cianobacterias independientemente de las dimensiones del cabezal de medida, se deben realizar 10 medidas/9,62 cm^2. Sin embargo, y cuando sea posible, se recomienda utilizar un cabezal de 10 mm, ya que el número de medidas requerido y el error derivado de la heterogeneidad son menores.

Los valores del parámetro claridad del color (L*) se encuentran afectados por el contenido en humedad de las muestras, mientras que los parámetros cromáticos a* y b* no se ven afectados. Dado que los valores de L* disminuyen exponencialmente con el contenido en humedad, haciéndose prácticamente estables en el tramo de humedad del 50 al 100%, se establece un contenido en humedad superior al 50% en la biopelícula como condición para obtener una medida de color reproducible y fiable.

5ª._ Se encontró una relación entre el color de las cianobacterias, la composición y/o abundancia de sus pigmentos fotosintéticos y las condiciones medioambientales a las que se sometieron. Las dos cepas estudiadas, *Nostoc* sp. PCC 9104 y *Nostoc* sp. PCC 9025, responden de manera diferente en términos de color y producción de pigmentos a condiciones ambientales tales como la intensidad de luz, la limitación de nutrientes y la disponibilidad de nitratos. Mientras PCC 9104 está más fuertemente afectada por la limitación de nutrientes, la presencia de nitratos y la alta intensidad de luz son los factores que determinan el estado de la cepa PCC 9025. El color de las cepas difiere a lo largo del experimento, alcanzando PCC 9104 un color más claro y cromático que PCC 9025.

Los parámetros de color CIELAB se correlacionaron con el contenido en pigmentos (clorofila-a, ficobiliproteínas ficocianinas y carotenoides totales), de manera que cada parámetro de color CIELAB refleja adecuadamente un aspecto específico del desarrollo de ambas cepas *Nostoc*. Así, L*, y en menor medida a*, se relacionan con las concentraciones de clorofila-a, ficocianinas y carotenoides totales, b* y C^*_{ab} se relacionan con las concentraciones de ficocianinas, y h_{ab}, parámetro que determina la longitud de onda dominante en un color dado, refleja los cambios en la apariencia de los cultivos y por tanto puede considerarse como el parámetro que mejor refleja la percepción del cambio.

6ª._ La medida del color es un método fiable para estimar la degradación de la clorofila a feopigmentos. Los índices o cocientes de feofitinización ($A_{435/415}$, cociente entre las absorbancias registradas a 435 nm y 415 nm; y $A_{665/665a}$ cociente entre las absorbancias registradas a 665 nm antes y después de acidificar la muestra), han resultado ser útiles para describir la degradación de la clorofila-a a feopigmentos en ensayos de susceptibilidad de la cepa *Nostoc* sp. PCC 9104 al biocida Biotin T® en ambos modos de crecimiento, forma planctónica y biofilm. Se demostró que la feofitinización puede ser estimada mediante el análisis del color de los microorganismos ya que, los parámetros de color CIELAB se correlacionan con los índices de feofitinización, lo que permite conocer la actividad biocida y el estado fisiológico de los microorganismos a través de la caracterización de su color. De los parámetros de color CIELAB, L* resultó ser el más informativo correlacionándose con ambos índices de feofitinización en ambos modos de crecimiento de los microorganismos.

En lo que se refiere a la tercera línea de trabajo de tesis: *Detección y cuantificación de los organismos sobre las construcciones*

7ª._ La aplicación de ultrasonidos mejora la extracción de clorofila-a de los biofilms desarrollados sobre sustratos rocosos. La aplicación de ultrasonidos directamente a las muestras intactas, sin triturar, seguida de una incubación en 0,43 ml de DMSO/cm^2 de muestra, a 63ºC durante 40 minutos es un método eficiente para la extracción de clorofila-a de los biofilms desarrollados sobre sustratos rocosos, permitiendo la detección de pequeñas cantidades de microorganismos fotosintéticos. Dicho procedimiento permite el uso de la cuantificación de clorofila-a como un método de control en el desarrollo de metodologías para la detección precoz de microorganismos fotosintéticos.

8ª._ La medida de los cambios en los parámetros de color, particularmente en el parámetro b* (Δb*), es un método fiable para la detección precoz y la monitorización en tiempo real del crecimiento fototrófico (verdín, *greening*) en las fachadas de granito. Así, se estableció el límite de percepción del enverdecimiento (*greening*) sobre una superficie de granito en $\Delta b^* = + 0.59$ unidades CIELAB, que corresponden en el estudio a 6.3 µg biomasa fotoautotrófica en peso seco/cm^2 y $(8.43 \pm 0.24) \times 10^{-3}$ µg de clorofila-a extraída/cm^2.

Las labores de limpieza y/o aplicación de tratamientos para detener el desarrollo de verdín en las fachadas deben realizarse cuando la colonización existe pero aún no se percibe, para lo cual se debe tener en cuenta el parámetro b*. En este sentido, la monitorización de los cambios en b* (Δb*) de la fachada del CESGA justo después de su limpieza revelaron que la recolonización por microorganismos fototróficos no tardó más de 129 días en producirse (un poco más de 4 meses), siendo necesarios menos de 178 días (prácticamente 6 meses) para ver un perceptible enverdecimiento en la fachada.

En lo que se refiere a la cuarta línea de trabajo de tesis: *Aplicación práctica de la medida del color a otros sustratos inorgánicos naturales*

9ª._ De entre los parámetros de color, son los que se refieren al tono (*Hue* Munsell y h_{ab} CIELAB) los que se deben emplear como indicadores de la intensidad de los incendios en suelos de Galicia.

10ª._ Es posible determinar el contenido de fitopigmentos en sedimentos de río por medio de las medidas de color representadas en el espacio de color CIELAB.

11ª._ Es necesario el desarrollo de un protocolo de medida para la caracterización del color de las pizarras de techar, al depender el número de medidas por unidad de superficie de la variedad comercial de pizarra y del tamaño del cabezal del instrumento de medida. En este sentido, las medidas de color en las pizarras de techar son reproducibles y comparables si se

llevan a cabo en un área de al menos 36 cm^2, realizándose 7, 6, 6 ó 3 medidas/36 cm^2 con cabezales de medida de 5, 8, 10 ó 50 mm de diámetro de apertura de lectura, respectivamente.

El color de las pizarras de techar de la Península Ibérica osciló entre los valores máximos de L*= 53,2 ± 0,2; a*= 0,0 ± 0,0; b*= 2,0 ± 0,1; C^*_{ab}= 4,6 ± 0,1; y h_{ab}= 271,9º ± 2,0º con el modo SCI; y de L*= 52,4 ± 0,7; a*= 0,1 ± 0,1; b*= 1,9 ± 0,3; C^*_{ab}= 4,5 ± 0,2; y h_{ab}= 273,3º ± 5,0º con el modo SCE, y los valores mínimos de L*= 33,7 ± 0,0; a*= –4,2 ± 0,1, b*= –1,4 ± 0,1; C^*_{ab}= 0,5 ± 0,1; y h_{ab}= 143,6º ± 17,9º con el modo SCI; y de L*= 33,5 ± 0,2; a*= –4,1 ± 0,1; b*= –1,8 ± 0,2; C^*_{ab}= 0,6 ± 0,3; y h_{ab}= 155,3º ± 2,6º con el modo SCE.

Teniendo en cuenta los límites de la percepción colorimétrica, las variedades comerciales *Itasi, Sigueya-Benuza* (ITA), *Canelas/Arouca* (ARO), *A Lastra* (LAS), *Os Vales* (PIV) y *Alto Bierzo* (ROC) pueden reemplazar a y ser reemplazadas por prácticamente el resto de las cincuenta variedades, y una única variedad, *Verde Lugo, Pol* (VLU), no puede reemplazar ni ser reemplazada por ninguna otra pizarra. Teniendo en cuenta la anisotropía estructural (lineación) de las pizarras de techar, *Itasi, Sigueya-Benuza* (ITA), *Canelas/Arouca* (ARO), *A Lastra* (LAS) y *Alto Bierzo* (ROC), serían apropiadas para la sustitución de las pizarras, con ninguna o sólo una ligera lineación, y *Os Vales* (PIV) sería apropiada para la sustitución de las pizarras con moderada o pronunciada lineación.

La **conclusión general** de esta tesis doctoral es que la determinación cuantitativa del color es un método adecuado para la detección precoz y la monitorización del crecimiento de biopelículas fototróficas y epilíticas en la superficie de los edificios y monumentos construidos en granito que presenta la importante ventaja de evitar la toma de muestra. Este método también puede ser aplicado a otros sustratos inorgánicos naturales, previo desarrollo de un protocolo de medida del color el cual es necesario para cualquier superficie heterogénea en color y/o textura, teniendo en cuenta en cada caso un parámetro de color diferente. Así, el parámetro asociado a la claridad del color (L*) es particularmente importante en el estudio de las rocas graníticas y de los microorganismos fototróficos, el parámetro b* es el más informativo para la detección y monitorización del crecimiento de los microorganismos fototróficos sobre una roca granítica, y el tono angular (h_{ab}) es la coordenada de color CIELAB que debe tenerse en cuenta para establecer grupos homogéneos de color, así como, en la investigación sobre la intensidad de un incendio en el suelo. Asimismo, el componente especular excluido (modo SCE) magnifica las diferencias en el color (ΔE^*_{ab}) frente al modo especular incluido (SCI).

Conclusions

From the results obtained, the following **particular conclusions** can be drawn:

In relation to the first subject addressed by this doctoral research: *Fine-tuning of the methodology for measuring and characterizing the color of granite surfaces*

1st._ An adaptable and affordable methodology of study supported by statistical analysis was developed. This was successful as regards examining the factors affecting color measurements on granite surfaces and demonstrating that color may be affected by properties of both the material and the instruments used. The methodology enabled determination of the minimum number of measurements and the minimum measuring area required to characterize the representative color of the non-homogeneous surface of granite.

In relation to the minimum number of measurements required to characterize the color of granite, it was found that this is affected by the type of stone, surface finish, and also by the diameter of the measurement head of the device. A wide variety of types of granite differing in terms of color, texture, and surface finish were examined, and it was found that the minimum number of measurements required to characterize the color of granite increases as the size of the measurement head decreases. Thus, the minimum number of measurements required is 6/36 cm^2 surface area for a 50 mm diameter measurement head, 14/36 cm^2 for 8 and 10 mm diameter measurement heads, and 17/36 cm^2 for a 5 mm measurement head.

As regards the minimum measuring area, an area of 36 cm^2 is sufficient for measurement heads of diameter ≤10 mm. A surface area equal to or larger than 72 cm^2 is required for larger diameter measurement heads.

2nd._ The roughness induced by different types of commercial surface finish on the granite surface causes a usually perceptible change in the color (*i.e.* more than ΔE^*_{ab}: 3 CIELAB units), primarily because of changes in the lightness parameter (CIELAB L*). The magnitude of the change in color associated with the roughness is governed by the color of the material and is higher in the stone with the lowest L* values. However, the color did not vary in proportion to the roughness generated by the different commercial finishes, and no general

conclusions could be drawn as regards the influence of roughness on the color of ornamental granite.

There is an inverse relationship between gloss and roughness only for low values of roughness in ornamental granite. Gloss values are affected by the color of the stone but in different ways in smooth and rough surfaces. Gloss and the lightness parameter (CIELAB L*) are inversely related in smooth surfaces and directly related in rough surfaces. The mineral composition of polymineral rocks must be taken into account as this determines the topography of the rough surface and also the refractive index.

3rd._ The three-dimensional color area of the CIELAB space that includes the color of the ornamental granites under study was defined. Thus, in the range of maximum values L*=74.9 ± 1.0; a*= 2.7 ± 0.5; b*= 7.4 ± 1.5; C^*_{ab}= 7.6 ± 1.1; and h_{ab}= 253.7º ± 6.1º in SCI mode; and L*= 75.5 ± 3.5; a*= 3.3 ± 2.6; b*= 8.6 ± 3.6; C^*_{ab}= 9.3 ± 4.2; and h_{ab}= 237.2º ± 46.0º in SCE mode. In the range of minimum values L*= 34.2 ± 0.5; a*= –0.9 ± 0.1; b*= –2.8 ± 0.3; C^*_{ab}= 1.1 ± 0.5; and h_{ab}= 71.8º ± 1.7º in SCI mode; and L*= 30.7 ± 4.8; a*= –0.8 ± 0.3; b*= –1.4 ± 1.6; C^*_{ab}= 1.0 ± 0.6; and h_{ab}= 71.5º ± 4.9º in SCE mode. This information should be taken into account when applying aesthetic criteria to the selection of ornamental granites for building and construction materials. It should also be used also when characterizing digital cameras for use as colorimeters in studies of cultural heritage monuments.

In relation to the second subject addressed by this doctoral research: *Fine-tuning of the methodology for measuring and characterizing the color of cyanobacteria*

4th._ Characterization of the color of cyanobacterial biofilms is influenced by both the microorganisms and the measuring instrument. Instrument properties, such as the diameter of the measurement head, affected the minimum number of measurements required to characterize the color. Properties of the microorganisms, such as concentration and moisture content, affected both the minimum number of measurements required and the color obtained.

The minimum number of measurements required increased with increasing heterogeneity of the color of the area measured, which depended on the concentration of the microorganisms, and decreased with the diameter of the measurement head. To control for the effects of the heterogeneity in the color of the area measured, the color of cyanobacteria should be measured on filters that are completely covered by the microorganisms. It was established that a total of 10 measurements/9.62 cm^2 are required for measurement heads of 8 and 5 mm diameter and 8 measurements/9.62 cm^2 for a measurement head of 10 mm diameter. Therefore, in order to standardize measurement of the color of cyanobacteria, 10 measurements/9.62 cm^2 are sufficient to characterize the color, regardless of the dimensions of the measurement head of the device. However, when possible, a 10 mm measurement

head should be used, as fewer measurements are required and the error derived from heterogeneity is reduced.

The L* values are greatly affected by the moisture content of the samples, whereas the chromatic parameters a* and b* are unaffected. Since the L*values decreased exponentially with moisture contents up to 50%, the color of the cyanobacteria should be characterized in samples with moisture contents of more than 50%.

5th._ There is a relationship between the color of the cyanobacteria, pigment production and the environmental conditions. *Nostoc* sp. strain PCC 9104 and *Nostoc* sp. strain PCC 9025 respond in different ways in terms of color and pigment production to environmental conditions such as light intensity, macronutrient limitation and availability of nitrates. While PCC 9104 is more strongly affected by nutrient limitations, the presence of nitrates and high light intensity are the factors that determine growth of strain PCC 9025. The color of the strains differed throughout the experiment; PCC 9104 was lighter and more chromatic than PCC 9025.

CIELAB color parameters were correlated with the chlorophyll-a, carotenoid and phycobiliprotein phycocyanin contents, so that variations in pigment contents were reflected by variations in color. Each CIELAB color parameter adequately described a specific aspect of the development of the *Nostoc* strains. Thus, L* and to a lesser extent a*, were related to the concentrations of chlorophyll-a, phycocyanin and carotenoid; b* and C^*_{ab} were related to the concentrations of phycocyanins, and h_{ab}, which refers to the dominant wavelength, reflected the changes in appearance of the cultures (*i.e.* changes in color and density); therefore, h_{ab} represents the major color perception attribute.

6th._ Color measurement is a reliable method of estimating the degradation of chlorophyll to phaeopigments. The phaeophytination indexes $A_{435/415}$ and $A_{665/665a}$ have been shown to be useful in describing degradation of chlorophyll-ato phaeopigments in both *Nostoc* sp. PCC 9104 planktonic and biofilm biocide susceptibility assays. However, determination of these indexes could be substituted by simpler color measurements as there is a close relation between the values of the indexes and of the color parameters. Among the CIELAB parameters, L* appeared to be the most informative parameter for describing the biocidal activity of Biotin T® against *Nostoc* sp. in both planktonic and biofilm mode of growth.

In relation to the third subject addressed by this doctoral research: *Detection and quantification of microorganisms colonizing the surface of buildings and monuments*

7th._ The application of ultrasonic methods improved extraction of chlorophyll-a from biofilms developed on rocky substrata. The direct application of ultrasound to uncrushed granite samples followed by incubation in 0.43 ml DMSO/cm^2 sample (vol/surface) at 63ºC for 40 min is an efficient method for chlorophyll-a extraction from stone materials and enables detection of

small amounts of photosynthetic microorganisms. This allows the use of chlorophyll-a quantification as a control method in the development of methodogies for early detection of photosynthetic micoorganisms.

8th._ Measurement of color changes is a reliable method for the early detection and real-time monitoring of phototrophic growth (greening) on granite façades, before it is perceptible to the human eye. Changes in parameter b* are the most informative. Thus, $\Delta b^* = + 0.59$ CIELAB units, which correspond to 6.3 µg biomass dry weight/cm^2 and $(8.43 \pm 0.24) \times 10^{-3}$ µg extracted chlorophyll-a/cm^2, was established as the greening threshold.

Cleaning and/or treatment should be carried out taking into account both the greening threshold in terms of Δb^* and the time that the trend in the value of Δb^* changes and becomes positive (*i.e.* indicates the occurrence of phototrophic colonization). In this sense, monitoring changes in b* of a cleaned granite façade exposed to the natural environment in Santiago de Compostela (NW Spain) revealed that recolonization by phototrophic microorganisms (greening) took no more than 129 days (just over 4 months) and that greening was perceptible after approximately 178 days (almost 6 months).

In relation to the fourth subject addressed by this doctoral research: *Practical application of color measurement on other naturally occurring inorganic substrates*

9th._ The parameters that refer to the soil hue (Munsell *Hue* and CIELAB h_{ab}) should be taken into account in the use of color as an indicator of fire intensity in Galician soils.

10th._ It is possible to determine phytopigment contents in riverbed sediments by means of a colorimetric method employing the CIELAB color parameters.

11th._ A protocol is required for the colorimetric characterization of roofing slate, as the number of measurements per unit of area will depend on the commercial variety and the size the measurement head of the measuring device. In this sense, color measurements on roofing slates are reproducible and comparable if they are carried out on an area of at least 36 cm^2, and 7, 6, 6 or 3 measurements/36cm^2 are made with measurement heads of 5, 8, 10 or 50 mm diameter viewing aperture, respectively.

The color of the roofing slates from the Iberian Peninsula ranged from maximum values of $L^* = 53.2 \pm 0.2$; $a^* = 0.0 \pm 0.0$; $b^* = 2.0 \pm 0.1$; $C^*_{ab} = 4.6 \pm 0.1$; and $h_{ab} = 271.9º \pm 2.0º$ to minimum values of $L^* = 33.7 \pm 0.0$; $a^* = -4.2 \pm 0.1$; $b^* = -1.4 \pm 0.1$; $C^*_{ab} = 0.5 \pm 0.1$; and $h_{ab} = 143.6º \pm 17.9º$ in the specular component included (SCI) mode, and from maximum values of $L^* = 52.4 \pm 0.7$; $a^* = 0.1 \pm 0.1$; $b^* = 1.9 \pm 0.3$; $C^*_{ab} = 4.5 \pm 0.2$; and $h_{ab} = 273.3º \pm 5.0º$ to minimum values of $L^* = 33.5 \pm 0.2$; $a^* = -4.1 \pm 0.1$; $b^* = -1.8 \pm 0.2$; $C^*_{ab} = 0.6 \pm 0.3$; and $h_{ab} = 155.3º \pm 2.6º$, in the specular component excluded (SCE) mode.

Considering the limits of colorimetric perception, the commercial varieties *Itasi, Sigueya-Benuza* (ITA), *Canelas/Arouca* (ARO), *A Lastra* (LAS), *Os Vales* (PIV) and *Alto Bierzo* (ROC) can be used to replace and can be replaced by most of the fifty commercial varieties of Iberian roofing slate, whereas *Verde Lugo, Pol* (VLU) cannot be replaced by any of the other types of slate. Considering the lineation, *Itasi, Sigueya-Benuza* (ITA), *Canelas/Arouca* (ARO), *A Lastra* (LAS), and *Alto Bierzo* (ROC) would be appropriate for replacing slates with no or only slight lineation, and *Os Vales* (PIV) would be appropriate for replacing slates with moderate or pronounce lineation.

The **general conclusion** of this thesis is that the quantitative determination of color is a suitable method for early detection and monitoring of epilithic phototrophic biofilm formation on the surface of granite buildings and monuments. This technique has many advantages; in particular it avoids the need for sampling. The method can also be applied to naturally occurring inorganic substrates. Since these surfaces are heterogeneous in color and/or texture, a protocol for measuring color must be developed by taking into account a different color parameter in each case. Thus, the lightness parameter (L*) is particularly important in the study of granite stone and in the study of phototrophic microorganisms (cyanobacteria), parameter b* is the most informative as regards the detection and monitoring of the growth of phototrophic microorganisms on granite rocks, and the hue angle (h_{ab}) is the CIELAB color coordinate that should be taken into account for establishing homogeneous color groups and in research on soil fire intensity. Moreover, the specular component excluded (SCE) mode magnifies the differences in color (ΔE^*_{ab}) relative to the specular component included (SCI) mode.

Referencias / *References*

Acea, M.J., Diz-Cid, N., Prieto-Fernández, A., 2001. Microbial populations in heated soils inoculated with cyanobacteria. *Biology and Fertility of Soils* 33(2), 118–125.

Acea, M.J., Prieto-Fernández, A., Diz-Cid, N., 2003. Cyanobacterial inoculation of heated soils: effect on microorganisms of C and N cycles and on chemical composition in soil surface. *Soil Biology and Biochemistry* 35(4), 513–524.

Aira, N., 2007. Pátinas oscuras sobre rocas graníticas: génesis y composición. PhD Thesis, Universidade de Santiago de Compostela, Spain.

Albertano, P., Moscone, D., Palleschi, G., Hermosin, B., Saiz-Jimenez, C., Sanchez-Moral, S., Hernandez-Marine, M., Urzì, C., Groth, I., Schroeckh, V., Saarela, M., Mattila-Sandholm, T., Gallon, J. R., Graziottin, F., Bisconti, F., Giuliani, R., 2003. Cyanobacteria attack rocks (CATS): Control and preventive strategies to avoid damage caused by cyanobacteria and associated microorganisms in Roman Hypogean Monuments. In: C. Saiz-Jimenez (ed.), *Molecular Biology and Cultural Heritage*, pp. 151–162, Swets & Zeitlinger, Lisse.

Amann, R.I., Ludwig, W., Schleifer, K.H., 1995. Phylogenetic identification and in situ detection of individual microbial cells without cultivation. *Microbiological Reviews* 59, 143–169.

Ariño, I., Kleist, U., Mattsson, L., Rigdahl, M., 2005. On the relation between surface texture and gloss of injection-molded pigmented plastics. *Polymer Engineering and Science* 45(10), 1343–1356.

Ariño, I., Johansson, S., Kleist, U., Liljenström-Leander, E., Rigdahl, M., 2007. The effect of texture on the pass/fail color tolerances of injection-molded plastics. *Color Research and Application* 32(1), 47–54.

Ariño, X., 1996. Estudio de la colonización, distribución e interacción de líquenes, algas y cianobacterias con materiales pétreos de los conjuntos arqueológicos de Baelo, Claudia y Carmona. PhD Thesis, Universidad de Barcelona and IRNA de Sevilla, Spain.

Artigas, J.M., Capilla, P., Pujol, J., 2002. Tecnología del color. Universitat de Valencia, Valencia, España (2002).

Ascaso, C., Wierzchos, J., Castello, R., 1998. Study of the biogenic weathering of calcareous litharenite stones caused by lichen and endolithic microorganisms. *International Biodeterioration and Biodegradation* 42, 29–38.

Ball, D.J., 1989. The soiling of buildings in Europe. In L.J. Brasser and W.C. Muller (Eds), Man and His Ecosystem, Prec. 8th World Clean Air Congr., The Hague, 11-15 September 1989, Elsevier Science Publishers, Amsterdam, 1989, Vol. 2, pp. 359–366.

Barberousse, H., Lombardo, R.J., Tell, G., Couté, A., 2006. Factors involved in the colonisation of building façades by algae and cyanobacteria in France. *Biofouling: The Journal of Bioadhesion and Biofilm Research* 22, 69–77.

Barnes, J.D., Balaguer, L., Manrique, E., Davison, A.W., 1992. A reappraisal of the use of DMSO for the extraction and determination of chlorophyll *a* and *b* in lichens and higher plants. *Environmental and Experimental Botany* 32, 85–90.

Barnett, S., 1973. Freezing of coffee extract to produce a dark colored freeze-dried product. Engineering of food preservation and biochemical processes, C.J. King, ed., AIChE Symp. Series, Vol. 69(132), 26–32.

Barranguet, C., Veuger, B., van Beusekom, S.A.M., Marvan, P., Sinke, J.J., Admiraal, W., 2005. Divergent composition of algal-bacterial biofilms developing under various external factors. *European Journal of Phycology* 40, 1–8.

Bartolini, M., Monte, M., 2000. Chemilithotrophic bacteria on stone monuments: cultural methods set up. In: Fassina V(ed) Proc. 9th Int Congr Deterioration and Conservation of Stone, Venice, Volume 1, pp 453–460.

Bartual, A., Lubian, L.M., Galvez, J.A., Niell, F.X., 2002. Effect of irradiance on growth, photosynthesis, pigment content and nutrient consumption in dense cultures of *Rhodomonas salina* (Wislouch) (Cryptophyceae). *Ciencias Marinas* 28, 381–392.

Bell, R.A., Sommerfeld, M.R., 1987. Algal biomass and primary production within a temperate zone sandstone. *American Journal of Botany* 74(2), 294–297.

Benavente, D., Martínez-Verdú, F., Bernabeu, A., Viqueira, V., Fort, R., García del Cura, M.A., Illueca, C., Ordóñez, S., 2003. Influence of surface roughness on color changes in building stones. *Color Research and Application* 28, 343–351.

Biggs, B., Close, M., 1989. Periphyton biomass dynamics in gravel bed rivers: the relative effects of flows and nutrients. *Freshwater Biology* 22, 209–231.

Bigham, J.M., Golden, D.C., Buol, S.W., Weed, S.B., Bowen, L.H., 1978. Iron oxide mineralogy of well-drained Ultisols and Oxisols: II. Influence on color, surface area and phosphate retention. *Soil Science Society of America Journal* 42, 825–830.

Boonaert, C.J.P., Dufrêne, Y.F., Derclaye, S.R., Rouxhet, P.G. 2001. Adhesion of *Lactococcus lactis* to model substrata: direct study of the interface. *Colloids and surfaces B: Biointerfaces* 22, 171–182.

Brechet, E., McStay, D., Wakefield, R., Sweet, M., Jones, M., 1996. In-situ monitoring of biological growth on stone. Proc. *SPIE-The International Society for Optical Engineering* 2835, 30.

Brechet, E., McStay, D., Wakefield, R., 1997. Detection of algae on stone using a novel low cost hand-held fluorimeter. In Sensors and Their Applications, Proceedings of the 8th Conference, ed. A. T. Augousi and N. M. White, pp. 3–8. Bristol: Institute of Physics.

Briones, V., Aguilera, V. J., Brown, C., 2006. Effect of surface topography on color and gloss of chocolate samples. *Journal of Food Engineering* 77(4), 776–783.

Campos Acosta, J., Rubiño López, M., Castillo Rubí, F., Pons Aglio, A., 2004. Comparación de instrumentos de medida del color / Colour measurement instruments comparison. *Óptica Pura y Aplicada* 37(1), 113–118.

Camuffo, D., 1995. Physical weathering of stones. *Science of the Total Environment* 167, 1–14.

Caneva, G., Nugari, M.P., 2005. Evaluation of Escobilla's mucilagino treatments in the archaeological site of Joya de Ceren (El Salvador). In ''LABS5. Biodegradation and Biodeterioration in Latin America'' (B. O. Ortega-Morales, C. C. Gaylarde, J. A. Narvaez-Zapata and P. M. Gaylarde, Eds.), pp. 59–64. Universidad de Campeche, Mexico.

Caneva, G., Nugari, M.P., Salvadori, O., 1991. Biology in the Conservation of Works of Art. International Centre for the Study of the Preservation and Restoration of Cultural Property (ICCROM), Rome.

Capilla, P., Artigas, J.M., Pujol, J., 2002. Tecnología del color. Universitat de Valencia, Valencia, España (2002).

Cappitelli, F., Principi, P., Sorlini, C., 2006. Biodeterioration of modern materials in contemporary collections: can biotechnology help? *Trends in Biotechnology* 24(8), 350–354.

Cappitelli, F., Principi, P., Pedrazzani, R., Toniolo, L., Sorlini, C., 2007. Bacterial and fungal deterioration of the Milan Cathedral marble treated with protective synthetic resins. *Science of the Total Environment* 385(1-3), 172–181.

Cappitelli, F., Abbruscato, P., Foladori, P., Zanardini, E., Ranalli, G., Principi, P., Villa, F., Polo, A., Sorlini, C., 2009. Detection and elimination of cyanobacteria from frescoes: the case of the St. Brizio Chapel (Orvieto Cathedral, Italy). *Microbial Ecology* 57(4), 633–639.

Carter, N.E.A., Viles, H.A., 2004. Lichen hotspots: Raised rock temperatures beneath *Verrucaria nigrescens* on limestone. *Geomorphology* 62, 1–16.

Cecchi, G., Pantani, L., Raimondi, V., Tomaselli, L., Lamenti, G., Tiano, P., Chiari, R., 2000. Fluorescence lidar technique for the remote sensing of stone monuments. *Journal of Cultural Heritage* 1(1), 29–36.

Chételat, J., Pick, F.R., Morin, A., 1999. Periphyton biomass and community composition in rivers of different nutrient status. *Canadian Journal of Fisheries and Aquatic Sciences* 56, 560–569.

CIE1932: Colorimétrie, Resolutions 1–4. Recueil des travaux et compte rendu des séances. Bureau Central de la Commission, The National Physical Laboratory Teddington, Cambridge University Press, 19–29.

CIE Publication 15-2. Colorimetry (1986) CIE Central Bureau, Vienna.

CIE Publication 116-1995: CIE Publication 116-1995, Industrial Color-Difference Evaluation, CIE Central Bureau, Vienna (1995).

CIE Publication 142-2001: CIE Publication 142-2001, Improvement to Industrial Color-Difference Evaluation, CIE Central Bureau, Vienna (2001).

Collier, J.L., Grossman, A.R., 1992. Chlorosis induced by nutrient deprivation in *Synechococcus* sp. strain PCC 7942: not all bleaching is the same. *Journal of Bacteriology* 174, 4718–4726.

Costerton, J.W., Geesey, G.G., Cheng, K.J., 1978. How bacteria stick. *Scientific American* 238, 86–95.

Costerton, J.W., Cheng, K.J., Geesey, G.G., Ladd, T.I., Nickel, J.C., Dasgupta, M., Marrie, T.J., 1987. Bacterial biofilms in nature and disease. *Annual Review of Microbiology* 41, 435–464.

Costerton, J.W., Lewandowski, Z., DeBeer, D., Caldwell, D.E., Korber, D., James, G., 1994. Biofilms, the customized microniche. *Journal of Bacteriology* 176(8), 2137–2142.

Costerton, J.W. 2007. The biofilm primer. Springer. Springer, Berlin-Germany (2007).

Crispim, C.A., Gaylarde, P.M., Gaylarde, C.C., 2003. Algal and cyanobacterial biofilms on calcareous historic buildings. *Current Microbiology* 46, 79–82.

Crispim, C.A., Gaylarde, C.C., 2005. Cyanobacteria and Biodeterioration of Cultural Heritage: A Review. *Microbial Ecology* 49, 1–9.

Cuzman, O.A., 2009. Biofilms on exposed monumental stones: mechanism of formation and development of new control methods. PhD Thesis, University of Bologna, Italy.

Dalal, E.N., Natale-Hoffman, K.M., 1999. The effect of gloss on color. *Color Research and Application* 24(5), 369–376.

Decho, A.W., 2000. Microbial biofilms in intertidal systems: an overview. *Continental Shelf Research* 20, 1257–1273.

Del Monte, M., Ausset, P., Forti, P., Lèfevre, R.A., Tolomelli, M., 2001. Air pollution records on selenite in the urban environment. *Atmospheric Environment* 35(22), 3885–3896.

De los Ríos, A., Cámara, J., Wierzchos, J., Ascaso, C., 2008. Diagnóstico de procesos de biodeterioro por combinación de microscopía *in situ* y técnicas de biología molecular. Red temática del CSIC de Patrimonio histórico y cultural.

De Muynck, W., Maury Ramirez, A., De Belie, N., Verstraete, W., 2009. Evaluation of strategies to prevent algal fouling on white architectural and cellular concrete. *International Biodeterioration and Biodegradation* 63, 679–689.

Di Pippo, F., Bohn, A., Congestri, R., De Philippis, R., Albertano, P., 2009. Capsular polysaccharides of cultured phototrophic biofilms. *Biofouling: The Journal of Bioadhesion and Biofilm Research* 25(6), 495–504.

Donlan, R.M., 2002. Biofilms: Microbial life on surfaces. *Emerging Infectious Diseases* 8(9), 881–890.

Dodds, W.K., Smith, V.H., Lohman, K., 2002. Nitrogen and phosphorus relationships to benthic algal biomass in temperate streams. *Canadian Journal of Fisheries and Aquatic Sciences* 59, 865–874.

Dornieden, T.H., Gorbushina, A.A., Krumbein, W.E., 2000. Patina: physical and chemical interactions of sub-aerial biofilms with objects of art. In: Ciferri, O., Tiano, P., Mastromei, G. (Eds.), *Microbes and Art*. Kluwer Academic Publishers, New York, pp. 105–119.

Duke, C.S., Allen, M.M., 1990. Effects of nitrogen starvation on polypeptide composition, ribulose-1,5-bisphosphate carboxylase/oxygenase, and thylakoid carotenoprotein content of *Synechocystis* sp. strain PCC 6308. *Plant Physiology* 94,752–759.

Durán-Suárez, J., García-Beltrán, A., Rodríguez-Gordillo, J., 1995. Colorimetric cataloguing of stone materials (biocalcarenite) and evaluation of the chromatic effects of different restoring agents. *Science of the Total Environment* 167(1-3), 171–180.

Eggert, A., Häubner, N., Klausch, S., Karsten, U., Schumann, R., 2006. Quantification of algal biofilms colonising building materials: chlorophyll *a* measured by PAM-fluorometry as a biomass parameter. *Biofouling: The Journal of Bioadhesion and Biofilm Research* 22(2), 79–90.

Eliades, T., Gioka, E., Heim, M., Eliades, G., Makou, M., 2004. Color stability of orthodontic adhesive resins. *The Angle Orthodontist* 74(3), 391–393.

Fernández-Silva, I., Sanmartín, P., Silva, B., Moldes, A., Prieto, B., 2011. Quantification of phototrophic biomass on rocks: optimization of chlorophyll-a extraction by response surface methodology. *Journal of Industrial Microbiology and Biotechnology* 38, 179–188.

Fernandez-Valiente, E., Leganés, F., 1989. Regulatory effect of pH and incident irradiance on the levels of nitrogenase activity in the cyanobacterium *Nostoc* UAM 205. *Journal of Plant Physiology* 135, 623–627.

Flemming, H.C., Wingender, J., 2001. Relevance of microbiol extracellular polymeric substances (EPSs). Part I: Structural and ecological aspects. *Water Science and Technology* 43, 1–8.

Friedmann, E.I., 1980. Endolithic microbial life in hot and cold deserts. *Origins of Life and Evolution of Biospheres* 10, 223–235.

Fuqua, W.C., Winans, S.C., Greenberg, E.P., 1994. Quorum sensing in bacteria: the LuxR-LuxI family of cell density-responsive transcriptional regulators. *Journal of Bacteriology* 176, 269–275.

García-Pichel, F., Castenholz, R.W., 1991. Characterization and biological implications of scytonemin, a cyanobacterial sheath pigment. *Journal of Phycology* 27, 395–409.

García-Talegón, J., Vicente, M.A., Vicente-Tavera, S., Molina-Ballesteros, E., 1998. Assessment of chromatic changes due to artificial ageing and/or conservation treatments of sandstones. *Color Research and Application* 23(1), 46–51.

Garty, J., 1990. Influence of epilithic microorganisms on the surface temperature of building walls. *Canadian Journal of Botany* 68(6), 1349–1353.

Gaylarde, C.C., Morton, L.H.G., 1999. Deteriogenic biofilms on buildings and their control: a review. *Biofouling: The Journal of Bioadhesion and Biofilm Research* 141, 59–74.

Gaylarde, P.M., Gaylarde, C.C., Guiamet, P.S., Gomez de Saravia, S.G., Videla, H.A., 2001. Biodeterioration of Mayan Buildings at Uxmal and Tulum, Mexico. *Biofouling: The Journal of Bioadhesion and Biofilm Research* 17, 41–45.

Gaylarde, P., Englert, G., Ortega-Morales, O., Gaylarde, C., 2006. Lichen-like colonies of pure *Trentepohlia* on limestone monuments. *International Biodeterioration and Biodegradation* 58, 248–253.

Gaylarde, C.C., Ortega-Morales, B.O., Bartolo-Pérez, P., 2007. Biogenic black crusts on buildings in unpolluted environments. *Current Microbiology* 54(2), 162–166.

Glazer, A.N., 1977. Structure and molecular organization of the photosynthetic accessory pigments of cyanobacteria and red algae. *Molecular and Cellular Biochemistry* 18, 125–140.

Golubic, S., Friedmann, I., Schneider, J., 1981. The lithobiontic ecological niche, with special reference to microorganisms. *Journal* of *Sedimentary Research* 51, 475–478.

Gorbushina, A.A., Krumbein, W.E., 2000. Microbial effects on subaerial rock surfaces. Subaerial microbial mats and their effects on soil and rock. In: R.E. Riding and S.M. Awramik (Eds.), *Microbial Sediments*, Springer, Berlin, pp: 161–170.

Gorbushina, A.A., 2007. Life on the rocks. *Environmental Microbiology* 9(7), 1613–1631.

Grant, C., 1982. Fouling of terrestrial substrates by algae and implications for control—a review. *International Biodeterioration Bulletin* 18, 57–65.

Grossi, C.M., Brimblecombe, P., Esbert, R.M., Alonso, F.J., 2007. Color changes in architectural limestones from pollution and cleaning. *Color Research and Application* 32, 320–331.

Grossman, A.R., Kehoe, D.M., 1997. Phosphorelay control of phycobilisome biogenesis during complementary chromatic adaptation. *Photosynthesis Research* 53, 95–108.

Grossman, A.R., Bhaya, D., He, Q., 2001. Tracking the light environment by cyanobacteria and the dynamic nature of light harvesting. *The Journal of Biological Chemistry* 276, 11449–11452

Guedes, A., Ribeiro, H., Valentim, B., Noronha, F., 2009. Quantitative colour analysis of beach and dune sediments for forensic applications: a Portuguese example. *Forensic Science International* 190, 42–51.

Guillite, O., 1995. Bioreceptivity: a new concept for building ecology studies. *Science of the Total Environment* 167, 215–220.

Guillite, O., Dreesen, R., 1995. Laboratory chamber studies and petrographical analysis as bioreceptivity assessment tools of building materials. *Science of the Total Environment* 167, 365–374.

Herrera, L.K., Videla, H.A., 2004. The importante of atmospheric effects on biodeterioration of cultural heritage constructional materials. *International Biodeterioration and Biodegradation* 54, 125–134.

Heukelekian, H., Heller, A., 1940. Relation between food concentration and surface for bacterial growth. *Journal of Bacteriology* 40, 547–558.

Hirsch, P., Eckhardt, F.E.W., Palmer Jr., R.J., 1995. Methods for the study of rock inhabiting microorganisms–A mini review. *Journal of Microbiological Methods* 23, 143–167.

Hoppert, M., Flies, C., Pohl, W., Günzl, B., Schneider, J., 2004. Colonization strategies of lithobiontic microorganisms on carbonate rocks. *Environmental Geology* 46, 421–428.

Hueck, H.J., 1965. The biodeterioration of materials as part of hylobiology. *Material und Organismen* 1(1), 5–34.

Hunter, R.S., Harold, R.W., 1987. The measurement of appearance, Wiley, New York (1987).

Hurley, M.A., Roscoe, M.E., 1983. Automated statistical analysis of microbial enumeration by dilution series. *Journal of Applied Bacteriology* 55, 159–164.

Hyvärinen, A., Meklin, T., Vepsäläinen, A., Nevalainen, A., 2002. Fungi and actinobacteria in moisture-damaged building materials — concentrations and diversity. *International Biodeterioration and Biodegradation* 49(1), 27–37.

ICOM-CC Preprints, 15th Triennial Meeting, New Delhi, 22-26 September 2008 (2 volumes), Ed. J. Bridgeland, ICOM-CC/Allied Publishers, New Delhi (2008).

ICR-CNR Istituto Centrale del Restauro-Commissione Normal (ICR-CNR).1988. Alterazioni dei Materiali Lapidei e Trattamenti Conservativi. Proposte per l' Unificazione dei Sperimentali di Studio e di Controlo, 1988. Micro flora autótrofa ed eterotrofa: Tecniche di isolamento in cultura. Doc Normal 9/88.

Ignell, S., Kleist, U., Rigdahl, M., 2009. On the relations between color, gloss, and surface texture in injection-molded plastics. *Color Research and Application* 34(4), 291–298.

Iñigo, A.C., Vicente-Tavera, S., Rives, V., 2004. MANOVA-Biplot statistical analysis of the effect of artificial ageing (freezing/thawing) on the colour of treated granite stones. *Color Research and Application* 29(2), 115–120.

Johnson, G., Fairchild, M.D., 2003. A top down description of S-CIELAB and CIEDE2000. *Color Research and Application* 28, 425–435.

Jonte, L., Rosales, N., Briceño, B., Morales, E., 2003. La irradiancia y la salinidad modulan el crecimiento de la cianobacteria *Synechocystis minuscula* en cultivos discontinuos. *Multiciencias* 3, 7–14.

Keyf, F., Etikan, I., 2004. Evaluation of gloss changes of two denture acrylic resin materials in four different beverages. *Dental Materials* 20(3), 244–251.

Kim, I.J., Lee, Y.K., Lim, B.S., Kim, C.W., 2003. Effect of surface topography on the color of dental porcelain. *Journal of Materials Science: Materials in Medicine* 14(5), 405–409.

Krumbein, W.E., 1988. Microbial interactions with mineral materials. D.R. Houghton, R.N. Smith, H.O.W. Eggins (Eds.), Biodeterioration, Vol. 7, Elsevier Applied Science, London, New York (1988), pp. 78–100

Krumbein, W.E., 1993. Colour changes of building stones and their direct and indirect biological causes. In: J. Delgado Rodrigues, F. Henriques and F. Telmo Jeremias, eds., Proceedings of the 7th International Congress on Deterioration and Conservation of Stone. Lisbon. Portugal. 1992. Lisbon: Laboratorio Nacional de Engenharia Civil. pp 443–452.

Krumbein, W.E., 1995. Gone with the wind—a second blow against spontaneous generation. In memoriam, Christian Gottfried Ehrenberg (1795–1876). *Aerobiologia* 11, 205–211.

Krumbein, W.E., Brehm, U., Gerdes, G., Gorbushina, A.A., Levit, G., Palinska, K. 2003. Biofilm, Biodictyon, and Biomat - Biolaminites, Oolites, Stromatolites - Geophysiology, Global mechanisms and Parahistology. En: Fossil and recent Biofilms A natural History of Life on Earth. Ed. Krumbein W.E., Paterson D.W., Zavarzin G.A., Kluwer Academic Press Publishers pp.1–28.

Kumar, R., Kumar, A.V., 1999. Biodeterioration of stone in tropical environments. An Overview. The Getty Conservation Institute, Los Angeles, EEUU (1999).

Lawrence, J.R., Korber, D.R., Hoyle, B.D., Costerton, J.W., Caldwell, D.E., 1991. Optical sectioning of microbial biofilms. *Journal of Bacteriology* 173, 6558–6567.

Liess, A., Francoeur, S.N., 2010. Substratum-associated microbiota. *Water Environment Research* 82(10), 1903–1944.

Lindsay, D., von Holy, A., 2006. Bacterial biofilms within the clinical setting: what healthcare professionals should know. *Journal of Hospital Infection* 64(4), 313–325.

Lognoli, D., Cecchi, G., Mochi, I., Pantani, L., Raimondi, V., Chiari, R., Johansson, T., Weibring, P., Edner, H., Svanberg, S., 2003. Fluorescence lidar imaging of the cathedral and baptistery of Parma. *Applied Physics B: Lasers and Optics* 76(4), 457–465.

Lonneborg, A., Lind, L.K., Kalla, S.R., Gustafsson, P., Oquist, G., 1985. Acclimation processes in the light-harvesting system of the cyanobacterium *Anacystis nidulans* following a light shift from white to red light. *Plant Physiology* 78,110–114.

Lopez, J., Retuerto, R., Carballeira, A., 1997. D665/D665a index *vs.* frequencies as indicators of bryophyte response to physicochemical gradients. *Ecology* 78(1):261–271. Ecological Society of America, USA.

López-Arce, P., Varas-Muriel, M.J., Fernández-Revuelta, B., Álvarez de Buergo, M., Fort, R., Pérez-Soba, C., 2010. Artificial weathering of Spanish granites subjected to salt crystallization tests: Surface roughness quantification. *Catena* 83(2-3), 170–185.

Loreto, C., Rosales, N., Bermúdez, J., Morales, E., 2003. Producción de pigmentos y proteínas de la cianobacteria *Anabaena* PCC 7120 en relación a la concentración de nitrógeno e irradiancia. *Gayana Botánica* 60, 83–90.

Louda, J.W., Li, J., Liu, L., Winfree, M.N., Baker, E.W., 1998. Chlorophyll-a degradation during cellular senescence and death. *Organic Geochemistry* 29(5–7), 1233–1251.

MacAdam, D.L., 1942. Visual sensitivities to color differences in daylight. *Journal of the Optical Society of America A* 32(5), 247–273.

Martín, A., 1990. Ensayos y experiencias de alteración en la conservación de obras de piedra de interés histórico artístico. Ed. Fundación Ramón Areces. Madrid, Spain(1990).

Martín-Trillo, M., 1995. Afloramientos masivos (blooms) de cianobacterias en los arrozales valencianos: seguimiento de su desarrollo y caracterización de dos estirpes formadoras. PhD Thesis, Universidad Autónoma de Madrid, Spain.

Martínez-Carreras, N., Krein, A., Gallart, F., Iffly, J.F., Pfister, L., Hoffmann, L., Owens, P.N., 2010a. Assessment of different colour parameters for discriminating potential suspended sediment sources and provenance: a multi-scale study in Luxembourg. *Geomorphology* 118, 118–129.

Martínez-Carreras, N., Udelhoven, T., Krein, A., Gallart, F., Iffly, J.F., Ziebel, J., Hoffmann, L., Pfister, L., Walling, D.E., 2010b. The use of sediment colour measured by diffuse reflectance spectrometry to determine sediment sources: application to the Attert River catchment (Luxembourg). *Journal of Hydrology* 382, 49–63.

Matthes-Sears, U., Gerrath, J.A., Larson, D.W., 1997. Abundance, biomass, and productivity of endolithic and epilithic lower plants on the temperate-zone cliffs of the Niagara Escarpment. *International Journal of Plant Sciences* 158, 451–460.

McNamara, C.J., Perry, T.D., Zinn, M., Breuker, M., Mitchell, R., 2003. Microbial processes in the deterioration of Mayan archaeological buildings in southern Mexico. In ‘‘Art, biology and conservation: Biodeterioration of works of art’’ (R. J. Koestler, V. H. Koestler, A. E. Charola and F. E. Nieto-Fernandez, eds.), pp. 248–265. The Metropolitan Museum of Art, New York.

McStay, D., Wakefield, R., Brechet, E., Prieto-Lamas, B., 2001. Nondestructive on site measurement of algal biofilms on historic surfaces. In “Sensors and their applications XI, Proc. of the XI Conference on Sensors and their Applications”, Held at City University, London, UK. September 2001, Ed K.T.V. Grattan and S.H. Khan. 377–382. Bristol: Institute of Physics.

Melgosa, M., Hita, E., Poza, A.J., Alman, D.H., Berns, R.S., 1997. Suprathreshold color-difference ellipsoids for surface colors. *Color Research and Application* 22, 148–155.

Melgosa, M., Huertas, R., Berns, R.S., 2004. Relative significance of the terms in the CIEDE2000 and CIE94 color-difference formulas. *Journal of the Optical Society of America A* 21(12), 2269–2275.

Miller, A.Z., Dionisio, A., Macedo, M.F., 2006. Primary bioreceptivity: a comparative study of different Portuguese lithotypes. *International Biodeterioration and Biodegradation* 57, 136–142.

Miller, A.Z., Rogerio-Candelera, M.A., Laiz, L., Wierzchos, J., Ascaso, C., Sequeira Braga, M.A., Hernández-Mariné, M., Maurício, A., Dionísio, A., Macedo, M.F., Saiz-Jimenez, C., 2010. Laboratory-induced endolithic growth in calcarenites: biodeteriorating potential assessment. *Microbial Ecology* 60(1), *5*5–68.

Miller, A.Z., Sanmartín, P., Pereira-Pardo, L., Saiz-Jimenez, C., Dionísio, A., Macedo, M.F., Prieto, B., 2012. Bioreceptivity of building stones: A review. *Science of the Total Environment*. DOI: 10.1016/j.scitotenv.2012.03.02.

Munsell, A.H., 1905. Una notación del color, Boston: G. H. Ellis Co.

Muylaert, K., Sánchez-Pérez, J.M., Teissier, S., Sauvage, S., Dauta, A., Vervier, P., 2009. Eutrophication and its effect on dissolved Si concentrations in the Garonne River (France). *Journal of Limnology* 68, 368–374.

Nagarkar, S., Williams, G.A., 1997. Comparative techniques to quantify cyanobacteria dominated epilithic biofilms on tropical rocky shores. *Marine Ecology Progress Series* 154, 281–291.

Newby, P.T., Mansfield, T.A., Hamilton, R.S., 1991. Sources and economic implications of building soiling in urban areas. *The Science of the Total Environment* 100, 347–365.

Ophir, T., Gutnick, D.L., 1994. A role for exopolysaccharides in the protection of microorganisms from desiccation. *Applied and Environmental Microbiology* 60, 740–745.

Ortega-Calvo, J.J., Hernández-Marine, M., Saiz-Jimenez, C., 1991a. Biodeterioration of buildings materials by cyanobacteria and algae. *International Biodeterioration* 28, 165–186.

Ortega-Calvo, J.J., Hernández-Marine, M., Saiz-Jimenez, C., 1991b. Mechanical deterioration of building stones by cyanobacteria and algae. *Biodeterioration and Biodegradation*, KW. Rossmoore (ed.), Elsevier, London, pp. 392–394.

Ortega-Calvo, J.J., Sanchez-Castillo, P.M., Hernandez-Marine, M., Saiz-Jimenez, C., 1993. Isolation and characterization of epilithic chlorophytes and cyanobacteria from two Spanish cathedrals (Salamanca and Toledo). *Nova Hedwigia* 57, 239–253.

Ortega-Morales, O., Guezennec, J., Hernandez-Duque, G., Gaylarde, C. C., Gaylarde, P.M., 2000. Phototrophic biofilms on ancient Mayan buildings in Yucatan, Mexico. *Current Microbiology* 40, 81–85.

Ortega-Morales, B.O., Narvaez-Zapata, J.A., Schmalenberger, A., Dousa-Lopez, A., Tebbe, C.C., 2004. Biofilms fouling ancient limestone Mayan monuments in Uxmal, Mexico: A cultivation-independent analysis. *Biofilms* 1, 79–90.

Otero, A., Muñoz, A., Benárdez, M.I., Fábregas, J. 2004. Quorum sensing: el lenguaje de las bacterias.Ed. Acribia, Zaragoza, España.

Otero, A., Romero, M., 2010. Interceptación de señales de comunicación bacteriana en bacterias aisladas del medio marino*. Revista Real Academia Galega de Ciencias. Vol. XXIX. Pp. 129–206. * Premio de Investigación 2010 de la Real Academia Gallega de Ciencias.

O'Toole, G., Kaplan, H.B., Kolter, R., 2000. Biofilm formation as microbiol development. *Annual Review of Microbiology* 54, 49–79.

Patent No. P200002956: Prieto B., Rivas T., Silva B., 2000. Patente No. P200002956. Determinación de biomasa y actividad biológica de organismos fototróficos en medio líquido y sobre materiales sólidos a partir de la medida del color. Universidad de Santiago de Compostela, Spain.

Pierres, A., Benoliel, A.M., Bongrand, P., 2002. Cell fitting to adhesive surfaces: a prerequisite to firm attachment and subsequent events. *European Cells and Materials* 3, 31–45.

Piñar, G., Ripka, K., Weber, J., Sterflinger, K., 2009. The microbiota of a subsurface monument the medieval chapel of St. Virgil (Vienna, Austria). *International Biodeterioration and Biodegradation* 63(7), 851–859.

Prieto, B., Silva, B., 2005. Estimation of the potential bioreceptivity of granitic rocks from their intrinsic properties. *International Biodeterioration and Biodegradation* 56, 206–215.

Prieto Lamas, B., Rivas Brea, M.T., Silva Hermo, B.M. 1995. Colonization by lichens of granite churches in Galicia (northwest Spain). *Science of the Total Environment* 167(1–3), 343–351.

Prieto, B., Silva, B., Rivas, T., Wierzchos, J., Ascaso, C., 1997. Mineralogical transformation and neoformation in granite caused by the lichens *Tephromela atra* and *Ochrolechia parella*. *International Biodeterioration and Biodegradation* 40, 191–199.

Prieto, B., Seaward, M.R.D., Edwards, H.G.M., Rivas, T., Silva, B., 1999. Biodeterioration of granite monuments by *Ochrolochia parella* (L.). Mass and F.T. Raman spectroscopy study. *Biospectroscopy* 5(1), 53–59.

Prieto, B., Edwards, H.G.M., Seaward, M.R.D., 2000. A fourier transform-Raman spectroscopic study of lichen strategies on granite monuments. *Geomicrobiology Journal* 17, 55–60.

Prieto, B., Rivas, T., Silva, B., 2002. Rapid quantification of phototrophic microorganisms and their physiological state through their colour. *Biofouling: The Journal of Bioadhesion and Biofilm Research* 18, 229–236.

Prieto, B., Silva, B., Lantes, O., 2004. Biofilm quantification on stone surfaces: comparison of various methods. *Science of the Total Environment* 333, 1–7.

Prieto, B., Silva, B., Aira, N., Laiz, L., 2005. Induction of biofilms on quartz surfaces as a means of reducing the visual impact of quartz quarries. *Biofouling: The Journal of Bioadhesion and Biofilm Research* 21, 237–246.

Prieto, B., Silva, B., Aira, N., 2006. Methodological aspects of the induction of biofilms for remediation of the visual impact generated by quartz mining. *Science of the Total Environment* 370, 254–261.

Prieto, B., Aira, N., Silva, B., 2007. Comparative study of dark patinas on granitic outcrops and buildings. *Science of the Total Environment* 381(1-3), 280–289.

Prieto, B., Sanmartín, P., Silva, B., Martínez-Verdú, F., 2010a. Measuring the color of granite rocks: a proposed procedure. *Color Research and Application* 35(5), 368–375.

Prieto, B., Sanmartín, P., Aira, N., Silva, B., 2010b. Color of cyanobacteria: some methodological aspects. *Applied Optics* 49(11), 2022–2029.

Prieto, B., Ferrer, P., Sanmartín, P., Cárdenes, V., Silva, B., 2011. Color characterization of roofing slates from the Iberian Peninsula for restoration purposes. *Journal of Cultural Heritage* 12(4), 420–430.

Proteau, P.J., Gerwick, W.H., Garcia-Pichel, F., Castenholz, R., 1993. The structure of scytonemin, an ultraviolet sunscreen pigment from the sheaths of cyanobacteria. *Experientia* 49(9), 825–829.

Ranalli, G., Pasini, P., Roda, A., 2000. Rapid diagnosis of microbial growth and biocide treatments on stone materials by bioluminescent low-light imaging technique. Fassina (Ed.), Proceedings of the 9th International Congress on Deterioration and Conservation of Stone, Venice, Elsevier, Amsterdam, pp. 499–505.

Raps, S., Wyman, K., Siegelman, H.W., Falkowski, P.G., 1983. Adaption of the cyanobacterium *Microcystis aeruginosa* to light intensity. *Plant Physiology* 72, 829–832.

Raven, J., 1984. A cost-benefit analysis of photon absorption by photosynthetic unicells. *New Phytologist* 98, 593–625.

Saiz-Jimenez, C., Garcia-Rowe, J., Garcia del Cura, M.A., Ortega-Calvo, J.J., Roekens, E., Van Grieten, R., 1990. Endolithic cyanobacteria in Maastricht limestone. *Science of the Total Environment* 94, 209–220.

Saiz-Jimenez, C., 1992. Biodeterioration of stone in historic buildings and monuments. In: *Biotoxins, Biodegradation, Biodeterioration Research* 4, Plenum, New York.

Saiz-Jimenez, C., Ariño, X., 1995. Colonización biológica y deterioro de morteros por organismos fotótrofos / Biological colonization and deterioration of mortars by phototrophic organisms. *Materiales de Construcción* 45(240), 5–16.

Saiz-Jimenez, C., Laiz, L., 2000. Occurrence of halotolerant/halophilic bacterial communities in deteriorated monuments. *International Biodeterioration and Biodegradation* 46, 319–326.

Sand, W., Jozsa, P.G., Mansch, R., 2002. Weathering, Microbiol. In Environmental Microbiolog (G. Britton, Ed.), Vol. 6, pp. 3364–3375. Wiley, New York.

Sanmartín, P., Aira, N., Devesa-Rey, R., Silva, B., Prieto, B., 2010a. Relationship between color and pigment production in two stone biofilm-forming cyanobacteria (*Nostoc* sp. PCC 9104 and *Nostoc* sp. PCC 9025). *Biofouling: The Journal of Bioadhesion and Biofilm Research* 26(5), 499–509.

Sanmartín, P., Ferrer, P., Cárdenes, V., Martínez-Verdú, F., Silva, B., Prieto, B., 2010b. El color de las rocas ornamentales: comparación de las metodologías de determinación en granitos y pizarras. In: *IX Congreso Nacional del Color*: Alicante, 29 y 30 de junio, 1 y 2 de julio de 2010. San Vicente del Raspeig: Publicaciones de la Universidad de Alicante, 2010. ISBN 978-84-9717-144-1, pp. 433–436.

Sanmartín, P., Cancelo-González, J., Rial, M.E., Silva, B., Díaz-Fierros, F., Prieto, B., 2010c. El color como indicador de la intensidad de los incendios en suelos de Galicia: Resultados preliminares / Color as an indicator of fire intensity on soils of Galicia, NW Spain: Preliminary results. *Óptica Pura y Aplicada* 43(3), 167–172.

Sanmartín, P., Silva, B., Prieto, B., 2011a. Effect of surface finish on roughness, color and gloss of ornamental granites. *Journal of Materials in Civil Engineering* 23(8), 1239–1248.

Sanmartín, P., Villa, F., Silva, B., Cappitelli, F., Prieto, B., 2011b. Color measurements as a reliable method for estimating chlorophyll degradation to phaeopigments. *Biodegradation* 22(4), 763–771.

Sanmartín, P., Devesa-Rey, R., Prieto, B., Barral, M.T., 2011c. Nondestructive assessment of phytopigments in riverbed sediments by use of instrumental color measurements. *Journal of Soils and Sediments* 11(5), 841–851.

Sanmartín, P., Vázquez-Nion, D., Silva, B., Prieto, B., 2012. Spectrophotometric color measurement for early detection and monitoring of greening on granite buildings. *Biofouling: The Journal of Bioadhesion and Biofilm Research*, 28(3), 329–338.

Scheerer, S., Ortega-Morales, O., Gaylarde, C., 2009. Microbial deterioration of stone monuments – an updated overview. *Advances in Applied Microbiology* 66, 97–139.

Schumann, R., Häubner, N., Klausch, S., Karsten, U., 2005. Chlorophyll extraction methods for the quantification of green microalgae colonizing building facades. *International Biodeterioration and Biodegradation* 55, 213–222.

Schwertmann, U., 1993. Relations between iron oxides, soil, color and soil formation. Soil Color. SSSA Special Publication. 31, 51–69.

Schwenzfeier, A., Wierenga, P.A., Gruppen, H., 2011. Isolation and characterization of soluble protein from the green microalgae *Tetraselmis* sp. *Bioresource Technology* 102(19), 9121–9127.

Seaward, M.R.D., 1979. Lower plants and the urban landscape. *Urban Ecology* 4, 217–225.

Shields, J.A., Paul, E.A., Arnaud, R.J.S., Head W.K., 1968. Spectrophotometric measurement of soil colour and its relationship to moisture and organic matter. *Canadian Journal of Soil Science* 48, 271–280.

Shih, T.-S., Wei, P.-S., Wu, C.-L., 2008. Effect of abrasives on the glossiness and reflectance of anodized aluminum alloys. *Journal of Materials Science* 43(6), 1851–1858.

Shirakawa, M.A., Beech, I.B., Tapper, R., Cincotto, M.A., Gambale, W., 2003. The development of a method to evaluate bioreceptivity of indoor mortar plastering to fungal growth. *International Biodeterioration and Biodegradation* 51, 83–92.

Schulze, D.G., Nagel, J.l., van Scoyoc, G.E., Henderson, T.L., Baumgardner, M.F., Stott, D.E., 1993. Significance of organic matter in determining soil colours. In: Bingham J.M., ciolcosz e.J. (eds.), Soil colours: 71–90. Soil Science Society of America, Madison, Wisconsin.

Silkina, A., Bazes, A., Vouve, F., Le Tilly, V., Douzenel, P., Mouget, J.L., Bourgougnon, N., 2009. Antifouling activity of macroalgal extracts on *Fragilaria pinnata* (Bacillariophyceae): A comparison with Diuron. *Aquatic Toxicology* 94(4), 245–254.

Silva, B., Prieto, B., 2004. Deteriorative effects of lichens on granite monuments. In: Clair LL, Mark RD, editors. Biodeterioration of stone surfaces: lichens and biofilms as weathering agents of rocks and cultural heritage. Dordrecht, The Netherlands: Kluwer Academic Publishers. p. 69–77.

Silva, B., Prieto, B., Rivas, T., Sanchez-Biezma, M.J., Paz, G., Carballal, R., 1997. Rapid biological colonization of a granitic building by lichens. *International Biodeterioration and Biodegradation* 4, 263–226.

Silva, B., Rivas, T., Prieto, B., 1999. Effects of lichens on the geochemical weathering of granitic Rocks. *Chemosphere* 39, 379–388.

Silva, B., Aira, N., Martínez-Cortizas, A., Prieto, B., 2009. Chemical composition and origin of black patinas on granite. *Science of the Total Environment* 408(1), 130–137.

Simonot, L., Elias, M., 2003. Color change due to surface state modification. *Color Research and Application* 28(1), 45–49.

Smith, B.J., McCabe, S., McAllister, D., Adamson, C., Viles, H.A., Curran, J.M., 2011. A commentary on climate change, stone decay dynamics and the 'greening' of natural stone buildings: new perspectives on 'deep wetting'. *Environmental Earth Sciences* 63, 1691–1700.

Sobczyk, A., Bely, A., Tandeau de Marsac, N., Houmard, J., 1994. A phosphorylated DNA-binding protein is specific for the red-light signal during complementary chromatic adaptation in cyanobacteria. *Molecular Microbiology* 13(5), 875–885.

Soltani, N., Khavari-Nejad, R., Tabatabaie, M., Shokravi, S.H., Valiente, E.F., 2006. Variation of nitrogenase activity, photosynthesis and pigmentation of cyanobacterium *Fischerella ambigua* strain FS18 under different irradiance and pH. *World Journal of Microbiology and Biotechnology* 22(6), 571–576.

Soto, B., Díaz-Fierros, F., 1993. Interactions between plants ash leachates and soil. *International Journal of Wildland Fire* 3, 207–216.

Soto, B., Basanta, R., Díaz-Fierros, F., 1997. Effects of burning on nutrient balance in an area of gorse (*Ulex europaeus* L.). *Science of the Total Environment* 204, 271–281.

Sousa, L.M.O., Gonçalves, B.M.M., 2011. Color assessment of granitic rocks and implications for their ornamental utilization. *Color Research and Application* doi: 10.1002/col.20681.

Stebvens, W.A., Spurdon, C., Onyon, L.J., Stirpe, F., 1981. Effect of inhibitors of protein synthesis from plants on tobacco mosaic virus infection. *Experientia* 37, 257–259.

Sterflinger, K., 2000. Fungi as geologic agents. *Geomicrobiology Journal* 17, 97–124.

Sterflinger, K., 2010. Fungi: their role in deterioration of Cultural Heritage. *Fungal Biology Reviews* 24(1-2), 47–55.

Stolz, J., 2000. Structure of microbial mats and bioflms. In: Riding R.E. & S.M. Awramik (Eds.). Microbial Sediments. Springer, Germany.

Stoodley, P., Sauer, K., Davies, D., Costerton, J., 2002. Biofilm as Complex Diferentiated Communities. *Annual Review of Microbiology* 56, 187–209.

Tanaca, H.K., Dias, C.M.R., Gaylarde, C.C., John, V.M., Shirakawa, M.A., 2011. Discoloration and fungal growth on three fiber cement formulations exposed in urban, rural and coastal zones. *Building and Environment* 46, 324–330.

Tandeau de Marsac, N., 1977. Ocurrence and nature of chromatic adaptation in cyanobacteria. 1977. *Journal of Bacteriology* 130, 82–91.

Tayler, S., May, E., 1991. The seasonality of heterotrophic bacteria on sandstones from ancient monuments. *International Biodeterioration* 28, 49–64.

Tayler, S., May, E., 2000. Investigations of the localisation of bacterial activity on sandstone from ancient monuments. *International Biodeterioration and Biodegradation* 46(4), 327–333.

Thomas, T.R., 1999. Rough surfaces, 2nd Ed., Imperial College Press, London.

Thornbush, M., Viles, H.A., 2004. Integrated digital photography and image processing for the quantification of colouration on soiled limestone surfaces in Oxford, England. *Journal of Cultural Heritage* 5, 285–290.

Thornbush, M., Viles, H.A., 2006. Changing patterns of soiling and microbial growth on building stone in Oxford, England after implementation of a major traffic scheme. *Science of the Total Environment* 367, 203–211.

Tiano, P., Tomaselli, L., Orlando, C., 1989. The ATP-bioluminescence method for a rapid evaluation of the microbial activity in the stone materials of monuments. *Journal of Bioluminescence and Chemiluminescence* 3(4), 213–216.

Tiano, P., 1993. Biodegradation of cultural heritage: decay mechanisms and control methods. In: *Conservation of stone and other materials*. Vol. 2. Prevention and treatment, Thiel MJ (ed), RILEM/UNESCO Paris, E & FN Spon Press, London, pp 573–580.

Tomaselli, L., Lamenti, G., Bosco, M., Tiano, P., 2000. Biodiversity of photosynthetic micro-organisms dwelling on stone monuments. *International Biodeterioration and Biodegradation* 46, 251–258.

Underwood, G.J.C., Paterson, D.M., 1993. Recovery of intertidal benthic diatoms after biocide treatment and associated sediment dynamics. *Journal of the Marine Biological Association of the United Kingdom* 73(1), 25–45.

Urquhart, D.C.M., Jones, M.S., Nicholson, K.A., Wakefield, R., Young, M.E., 1995. Biological growths, biocide treatment, soiling and decay of sandstone buildings and monuments. Report to Historic Scotland.

Urzì, C., Krumbein, W.E., Warscheid, T., 1992. On the question of biogenic colour changes of mediterranean monuments (coating – crust - microstromatolite - patina - scialbatura - skin - rock varnish) In: Decrouez, D., Chamay, J., Zezza, F. (Eds.), *Proceedings of the 2nd International Symposium on The conservations of the monuments in the Mediterranean Basin*, Musee d'Art et d'Histoire Naturelle: Genève, pp. 397–420.

Urzì, C., Realini, M., 1998. Colour changes of Noto's calcareous sandstone as related to its colonisation by microorganisms. *International Biodeterioration and Biodegradation* 42, 45–54.

Viles, H.A., Gorbushina, A.A., 2003. Soiling and microbial colonization on urban roadside limestone: A three year study in Oxford, England. *Building and Environment* 38, 1217–1224.

Viles, H.A., Taylor, M.P., Yates, T.J.S., Massey, S.W., 2002. Soiling and decay of NMEP limestone tablets. *Science of the Total Environment* 292, 215–229.

Wang, L., Huang, T., Kamal, M. R., Rey, A. D., 2000. The surface topography and gloss of polyolefin blown films. *Polymer Engineering and Science* 40(3), 747–760.

Ward, D.M., Weller, R., Bateson, M.M., 1990. 16S rRNA sequences reveal numerous uncultured microorganisms in a natural community. *Nature (London)* 345, 63–65.

Warke, P.A., Smith, B.J., Magee, R.W., 1996. Thermal response characteristics of stone: Implications for weathering of soiled surfaces in urban environments. *Earth Surface Processes and Landforms* 21, 295–306.

Warscheid, T., Oelting, M., Krumbein, W.E., 1991. Physico-chemical aspects of biodeterioration processes on rocks with special regard to organic pollutants. *International Biodeterioration* 28, 37–48.

Warscheid, T., Becker, T.W., Resende, M.A., 1996. Biodeterioration of Stone: A comparison of (sub-) tropical and moderate climate zones. In ''Biodegradation & biodeterioration in Latin America'' (C.C. Gaylarde, E.L.S. de Sá, and P.M. Gaylarde, Eds.), pp. 63–64. Mircen/UNEP/UNESCO/ICRO-FEPAGRO/UFRGS, Porto Alegre.

Warscheid, T., Braams, J., 2000. Biodeterioration of stone: a review. *International Biodeterioration and Biodegradation* 46, 343–368.

Webster, R.G.M., Andrew, C.A., Baxter, S., MacDonald, J., Rocha, M., Thomson, B.W., Tonge, K.H., Urquhart, D.C.M., Young, M.E.,1992. Stonecleaning in Scotland -Research Report to Historic Scotland and Scottish Enterprise by Masonry Conservation Research Group.

Wyszecki, G., Stiles, W.S., 1982. Color Science. Concepts and Methods, Quantitative Data and Formulae, John Wiley and Sons, New York.

Young, M.E. Wakefield, R.D., Urquhart, D.C.M., Nicholson, K., Tonge, K., 1995. Assessment in a field setting of the efficacy of various biocides on sandstone. In: Proceedings of the International Colloquium on Methods of Evaluating Products for the Conservation of Porous Building Materials in Monuments ICCROM, Roma pp: 93–99.

Young, M.E., 1997. Biological growths and their relationship to the physical and chemical characteristics of sandstones before and after cleaning. PhD Thesis. The Robert Gordon University, Aberdeen, UK.

Zobell, C.E., 1943. The effect of solid surfaces on bacterial activity. *Journal of Bacteriology* 46, 39–56.

Agradecimientos / *Acknowledgements*

A Beatriz Prieto Lamas por todo. Gracias por el pragmatismo, inteligencia y empatía que ha mostrado siempre en todo lo relativo a mi trabajo y que muestra siempre en general, lo que hace que sea una suerte poder trabajar con ella.

A Benita Silva Hermo, de la que una vez me dijeron que era buena investigadora y mejor persona, algo con lo que yo estoy muy de acuerdo. Gracias por toda la ayuda prestada y confianza depositada en mí.

A Francisco Miguel Martínez Verdú y todo su grupo de investigación, por todos los conocimientos transmitidos. Su ayuda ha sido importante en la elaboración de esta tesis doctoral.

To Francesca Cappitelli and her research group for giving me the freedom to plan and execute my research ideas while providing help and support.

A todos los compañeros y profesores del departamento de Edafología.

A todos los que quiero y me quieren.